AUBURN

SAMUEL GINN
COLLEGE OF ENGINEERING

Research Report

UPDATE OF BRIDGE DESIGN STANDARDS IN ALABAMA FOR AASHTO LRFD SEISMIC DESIGN REQUIREMENTS

Submitted to

The Alabama Department of Transportation

Prepared by

Justin D. Marshall, Ph.D., P.E.
J. Brian Anderson, Ph.D., P.E.
Jordan D. Law
Jordan L. Panzer
Kevin M. Kane

NOVEMBER 2013

Highway Research Center
Harbert Engineering Center
Auburn, Alabama 36849

www.eng.auburn.edu/research/centers/hrc.html

1. Report No. ALDOT 930-803	2. Government Accession No.	3. Recipient Catalog No.
4 Title and Subtitle UPDATE OF BRIDGE DESIGN STANDARDS IN ALABAMA FOR AASHTO LRFD SEISMIC DESIGN REQUIREMENTS		5 Report Date November 2013 6 Performing Organization Code
7. Author(s) Justin D. Marshall, J. Brian Anderson, Jordan D. Law, Jordan L. Panzer, Kevin M. Kane		8 Performing ALDOT 930-803
9 Performing Organization Name and Address Highway Research Center Department of Civil Engineering 238 Harbert Engineering Center Auburn, AL 36849		10 Work Unit No. (TRAIS) 11 Contract or Grant No.
12 Sponsoring Agency Name and Address Alabama Department of Transportation 1409 Coliseum Boulevard Montgomery, Alabama 36130-3050		13 Type of Report and Period Covered Technical Report 14 Sponsoring Agency Code
15 Supplementary Notes		

16 Abstract

The Alabama Department of Transportation (ALDOT) has been required to update their bridge design to the LRFD Bridge Design Specifications. This transition has resulted in changes to the seismic design standards of bridges in the state. Multiple bridges, provided by ALDOT, were re-designed so that they satisfied the requirements of the LRFD Specifications. New details were used to create standard drawings for bridges in SDC A and B. The superstructure-to-substructure connection was also investigated for the horizontal design forces. The original connection was recommended along with an extended longitudinal seat width. A new equation for determining the minimum seat width was recommended, and this new design philosophy was incorporated into the re-design of the bridges. Nonlinear response history analyses of bridge models resulted in the acceptance of the guide specification's design for use in Critical and Essential bridges. A comparison of the currently designed connection and an updated design was also performed, and indicated that the updated design could improve bridge behavior. Based on direct analysis of foundations, pile foundations were found to not be adequate to resist seismic loads in soft or liquefiable soils. Drilled shaft were sufficient regardless of soil type.

17 Key Words	18 Distribution Statement
Seismic Bridge Design, Displacement-Based Design, Soil-Foundation-Structure Interaction, Nonlinear Response History Analysis	No restrictions. This document is available to the public through the National Technical Information Service, Springfield, Virginia 22161

19 Security Classification (of this report)	20 Security Classification (of this page)	21 No. of pages	22 Price
Unclassified	Unclassified	323	

FORM DOT F 1700.7 (8-72)

Research Report

ALDOT Research Project #930-803

UPDATE OF BRIDGE DESIGN STANDARDS IN ALABAMA FOR AASHTO LRFD SEISMIC DESIGN REQUIREMENTS

Submitted to

The Alabama Department of Transportation

Prepared by

Justin D. Marshall
J. Brian Anderson
Jordan D. Law
Jordan L. Panzer
Kevin M. Kane

Highway Research Center

and

Department of Civil Engineering

at Auburn University

NOVEMBER 2013

DISCLAIMERS

The contents of this report reflect the views of the authors, who are responsible for the facts and the accuracy of the data presented herein. The contents do not necessarily reflect the official views or policies of Auburn University or the Federal Highway Administration. This report does not constitute a standard, specification, or regulation.

NOT INTENDED FOR CONSTRUCTION, BIDDING, OR PERMIT PURPOSES

Justin D. Marshall, Ph.D., P.E.
J. Brian Anderson, Ph.D., P.E.
Research Supervisors

ACKNOWLEDGEMENTS

Superstructure-to-substructure connections were obtained and studied from the following state DOTs: Alabama, Alaska, Georgia, Illinois, Missouri, North Carolina, Oregon, South Carolina, and Tennessee. Also, Volkert and Associates provided a restrainer detail that was studied.

Abstract

The Alabama Department of Transportation (ALDOT) has been required to update their bridge design specifications from the Standard Specifications for Highway Bridges to the LRFD Bridge Design Specifications. This transition has resulted in changes to the seismic design standards of bridges in the state. These changes, as well as their resulting effects on the design of bridges, have been researched and are discussed in this report. One of the goals was to determine if standard drawings and details for bridges in Seismic Design Categories A and B, which are low to moderate seismic regions, could be generated. Multiple bridges, provided by ALDOT, were re-designed so that they satisfied the requirements of the LRFD Specifications. These new design details were used to create standard drawings for bridges in SDC A and B. The superstructure-to-substructure connection was also investigated to determine if it was adequate to resist the expected horizontal design forces. It was determined to be inadequate, but instead of proposing a new connection design, the original connection was recommended along with supplying an extended seat width in the longitudinal direction. A new equation for determining the minimum seat width was recommended, and this new design philosophy was incorporated into the re-design of the bridges.

Nonlinear history analyses of nonlinear bridge models resulted in the acceptance of the guide specification's design for use in Critical and Essential bridges. Some additional design may be required for bridges with taller substructures due to p-delta effects. A comparison of the currently designed connection and an updated design was also performed, and indicated that the updated design could improve bridge behavior.

Based on direct analysis of the foundations of the bridges in the study, pile foundations were found to not be adequate to resist seismic loads in soft or liquefiable soils. Drilled shaft foundations were sufficient regardless of soil type. States surveyed allowed driven piles in seismic design with specific soil requirements.

Table of Contents

Acknowledgements iv
Abstract v
Table of Contents vii
List of Tables xiii
List of Figures xvi
Chapter 1: Introduction 1
1.1 Problem Statement 1
1.2 Problem Overview 2
1.3 Project Deliverables 3
1.4 Report Outline 4
Chapter 2: Literature Review 6
2.1 Introduction 6
2.2 Specification Comparison 6
2.2.1 Standard Specifications 9
2.2.2 LRFD Specifications 10
2.2.3 Guide Specifications 12
2.3 Liquefaction in Alabama 14
2.4 Soil Foundation Structure Interaction Analysis 19
2.4.1 Kinematic Interaction 19
2.4.2 Inertial Interaction 20
2.4.3 Seismic and Dynamic Response Analysis Methods 21
2.5 Software 25
2.5.1 Overview of FB-MultiPier 25
2.5.2 Dynamic Analysis Methods 27
2.5.3 FB-MultiPier Limitations 31
2.6 FHWA LRFD Seismic Analysis and Design of Bridge Foundations 32
2.7 Pile Failure Modes 33
2.8 Pile Performance under the combined Effect of Earthquake and Scour 36
2.9 Summary 38
Chapter 3: Superstructure-to-Substructure Connection 39

3.1 Introduction 39
3.2 Connection Study 40
3.2.1 Modified ALDOT Connection 41
3.2.2 Illinois DOT 41
3.2.3 North Carolina DOT 43
3.2.4 South Carolina DOT 45
3.2.5 Missouri DOT 45
3.2.6 Connection Recommendation 47
3.3 Extended Seat Width 48
3.4 Conclusion 51
Chapter 4: Bridge Design Standards 52
4.1 Introduction 52
4.2 SDC Determination 56
4.3 Guide Specification Design Process for SDC A1 60
4.3.1 Determine Vertical Reactions at Bent 61
4.3.2 Determine Design Forces 62
4.3.3 Determine Minimum Support Lengths 63
4.3.4 Minimum Column Detailing 64
4.4 Bridge Design Examples in SDC A1 66
4.4.1 County Road 39 Bridge 66
4.4.2 Stave Creek Bridge 71
4.4.3 Summary of Differences in SDC A1 75
4.5 Guide Specification Design Process for SDC A2 76
4.5.1 Determine Vertical Reactions at Bent 76
4.5.2 Determine Design Forces 77
4.5.3 Determine Minimum Support Lengths 78
4.5.4 Minimum Column Detailing 79
4.6 Bridge Design Examples in SDC A2 85
4.6.1 Stave Creek Bridge 85
4.6.2 Bent Creek Road Bridge 90
4.6.3 Bridge over Norfolk Southern Railroad 93
4.6.4 Oseligee Creek Bridge 96
4.6.5 Summary of Differences in SDC A2 101
4.7 Guide Specification Design Process for SDC B 103

4.7.1 Create a Design Response Spectrum 103
4.7.2 Create and Analyze Bridge Model 104
4.7.3 Bridge Capacity vs. Displacement 107
4.7.4 Column Seismic Detailing 109
4.8 SDC B Design Examples 118
4.8.1 Bent Creek Road over I-85 119
4.8.2 I-59 Bridge over Norfolk Southern Railroad 125
4.8.3 Oseligee Creek Bridge 130
4.8.4 Little Bear Creek Bridge 138
4.8.5 Scarham Creek Bridge 145
4.8.6 Summary of Differences in SDC B 154
4.9 Design Standards 156
4.9.1 Design Standards for SDC A1 156
4.9.2 Design Standards for SDC A2 159
4.9.3 Design Standards for SDC B 162
4.10 Conclusion 166
Chapter 5: Case Histories 171
5.1 Selection of Bridges 171
5.1.1 Seismic Hazard 172
5.1.2 Soil/Geologic Conditions 173
5.1.3 Bridge Geometry 174
5.2 Final Selection 174
5.3 Little Bear Creek Bridge 175
5.3.1 Background Information (Structural) 175
5.3.2 Background Information (Foundation) 176
5.4 Scarham Creek Bridge 176
5.4.1 Background Information (Structural) 176
5.4.2 Background Information (Foundation) 178
5.5 Norfolk Southern Railroad Bridge 179
5.5.1 Background Information (Structural) 179
5.5.2 Background Information (Foundation) 180
5.6 Oseligee Creek Bridge 181
5.6.1 Background Information (Structural) 181
5.6.2 Background Information (Foundation) 182

5.7 Bent Creek Road Bridge 183
5.7.1 Background Information (Structural) 183
5.7.2 Background Information (Foundation) 184
5.8 Summary 185
Chapter 6 Modeling 186
6.1 Selection of Ground Motions 186
6.1.1 Probable Seismic Hazard Analysis (PSHA) 186
6.2 Uniform Hazard Spectrum (UHS) 190
6.2.1 Ground Motion 192
6.3 Determination of Capacities 195
6.4 Selection of Modeling Elements 198
6.4.1 Superstructure Modeling 198
6.4.2 Substructure Model 200
6.4.3 Connection Modeling 204
6.5 FB Multipier 211
6.5.1 Lateral Interaction 211
6.5.2 Axial Interaction 211
6.5.3 Torsional Interaction 212
6.5.4 Structural Element Modeling 213
6.5.5 Pile Cap Modeling 214
6.5.6 Group Effects 215
6.6 Overview of Bridge Models 215
6.6.1 Little Bear Creek Bridge 216
6.6.2 Oseligee Creek Bridge 220
6.6.3 Norfolk Southern Railroad Bridge 223
6.6.4 Scarham Creek 228
6.6.5 Bent Creek Road 232
6.7 Summary 236
Chapter 7: Task 3 Results and Discussion 237
7.1 Introduction 237
7.1.1 Description of Results Presented 237
7.1.2 Limits of Bridge Behaviors 239
7.2 Bent Creek Road Bridge 240
7.2.1 Transverse Motion 240

7.2.2 Longitudinal Motion 243
7.3 Scarham Creek Bridge 246
7.3.1 Transverse Motion 247
7.3.2 Longitudinal Motion 250
7.4 Norfolk Southern Railroad Bridge 252
7.4.1 Transverse Motion 252
7.4.2 Longitudinal Motion 255
7.5 Oseligee Creek Bridge 258
7.5.1 Transverse Motion 259
7.5.2 Longitudinal Motion 262
7.6 Little Bear Creek Bridge 264
7.6.1 Transverse Motion 265
7.6.2 Longitudinal Motion 269
7.7 Summary of Results 271
Chapter 8: Task 4 Results and Discussion 274
8.1 FB Multipier Direct Analysis 274
8.1.1 Dynamic Analysis Method Used 274
8.1.2 Damping Analysis 274
8.2 Dead Load and Discrete Mass 276
8.3 Direct Analysis Results 277
8.4 Oseligee Creek Bridge 25% Scour Discussion 279
8.5 Oseligee Creek Bridge 100% Scour Discussion 283
8.6 Norfolk Southern Railroad Bridge Discussion 286
8.7 Little Bear Creek Bridge Discussion 290
8.8 Bent Creek Road Bridge Discussion 293
8.9 Scarham Creek Bridge Discussion 297
8.10 Direct Analysis Results Summary 301
Chapter 9: State DOT Survey 304
9.1 State DOT Survey 304
9.2 Arkansas Survey Response 305
9.3 Kentucky Survey Response 306
9.4 South Carolina Survey Response 307
9.5 State DOT Survey Summary 311
Chapter 10: Conclusion and Recommendations 313

10.1 Introduction 313
10.2 Superstructure-to-Substructure Connection 313
10.3 Bridge Design Standards 315
10.4 Task 3 Conclusions..... 317
10.5 Task 4 Conclusions..... 318
10.6 Overall Conclusions 319
10.7 Recommendations 320

Appendix A: Connection Design Calculations……..……Appendix-1

Appendix B: County Road 39 Bridge SDC A1……Appendix-11

Appendix C: Stave Creek Bridge SDC A1……..……...Appendix-28

Appendix D: Stave Creek Bridge SDC A2……...……...Appendix-40

Appendix E: Bent Creek Road Bridge SDC A2……..Appendix-56

Appendix F: I-59 Bridge over Norfolk Southern Railroad SDC A2……...Appendix-66

Appendix G: Oseligee Creek Bridge SDC A2…….Appendix-76

Appendix H: Bent Creek Road Bridge SDC B……Appendix-93

Appendix I: Bent Creek Road Moment-Interaction Diagrams……..……Appendix-121

Appendix J: I-59 Bridge over Norfolk Southern Railroad SDC B……Appendix-124

Appendix K: I-59 Bridge over Norfolk Southern Railroad

Moment-Interaction Diagrams.....Appendix-152

Appendix L: Oseligee Creek Bridge SDC B……..Appendix-155

Appendix M: Oseligee Creek Bridge Moment-Interaction Diagrams……...Appendix-195

Appendix N: Little Bear Creek Bridge SDC B……..Appendix-198

Appendix O: Little Bear Creek Bridge Moment-Interaction Diagrams…….Appendix-238

Appendix P: Scarham Creek Bridge SDC B……..Appendix-241

Appendix Q: Scarham Creek Bridge Moment-Interaction Diagrams……Appendix-30

List of Tables

Table 2.1 – Susceptibility of sedimentary deposits to liquefaction during strong shaking (Youd and Perkins 1978) 16
Table 2.2 – Liquefaction evaluation requirements for each SDC (AASHTO 2009)..... 18
Table 2.3 – Rayleigh damping factors used in Brown et al. (2001) 31
Table 3.1: Minimum Seat Width Calculations 50
Table 4.1: Bridge Locations..... 53
Table 4.2: SDC Category Determination..... 57
Table 4.3: Design Force Multiplier..... 63
Table 4.4: Mobile County Bridge Design Force Live Load Factor Comparison 68
Table 4.5: Mobile County Bridge Design Force Specification Comparison 68
Table 4.6: Mobile County Bridge Minimum Support Lengths..... 69
Table 4.7: Mobile County Bridge Design Summary 70
Table 4.8: Stave Creek Bridge Design Force Live Load Factor Comparison (SDC A1)..... 72
Table 4.9: Stave Creek Bridge Vertical Reactions and Design Forces Comparison (SDC A1)... 72
Table 4.10: Stave Creek Bridge Minimum Support Lengths Comparison (SDC A1)..... 72
Table 4.11: Stave Creek Bridge Design Summary (SDC A1)..... 73
Table 4.12: Stave Creek Bridge Design Force Live Load Factor Comparison (SDC A2)..... 86
Table 4.13: Stave Creek Bridge Vertical Reactions and Design Forces Comparison (SDC A2). 87
Table 4.14: Stave Creek Bridge Minimum Seat Width Comparison (SDC A2) 87
Table 4.15: Stave Creek Bridge Design Summary 88
Table 4.16: Stave Creek SDC A1 and A2 Design Comparison..... 89
Table 4.17: Bent Creek Road Bridge Design Force Live Load Factor Comparison (SDC A2)... 90
Table 4.18: Bent Creek Road Bridge Vertical Reaction and Design Forces (SDC A2)..... 91
Table 4.19: Bent Creek Road Bridge Minimum Seat Width Comparison (SDC A2) 91
Table 4.20: Bent Creek Road Bridge Design Summary (SDC A2)..... 92
Table 4.21: Norfolk Southern Bridge Design Force Live Load Factor Comparison (SDC A2) .. 94
Table 4.22: Norfolk Southern Bridge Design Force Comparison (SDC A2) 94
Table 4.23: Norfolk Southern Bridge Minimum Seat Width Comparison (SDC A2)..... 95
Table 4.24: Bridge over Norfolk Southern Railroad Design Summary (SDC A2) 95
Table 4.25: Oseligee Creek Bridge Design Force Live Load Factor Comparison (SDC A2)..... 97
Table 4.26: Oseligee Creek Bridge and Design Force Comparison (SDC A2)..... 98
Table 4.27: Oseligee Creek Bridge Minimum Support Lengths Comparison (SDC A2) 98
Table 4.28: Oseligee Creek Bridge Design Summary (SDC A2)..... 99
Table 4.29: Regular Bridge Requirements..... 105
Table 4.30: Analysis Results for Bent Creek Road Bent 2..... 121
Table 4.31: Capacity of the Steel Clip Angle 122
Table 4.32: Bent Creek Road Bridge Seat Width Specification Comparison (SDC B) 123
Table 4.33: Bent Creek Road Bent 2 Design Results (SDC B) 123
Table 4.34: Bent Creek Road SDC A2 and SDC B Design Comparison 125
Table 4.35: Analysis Results for Bridge over Norfolk Southern Railroad Bent 2 127
Table 4.36: Norfolk Southern Bridge Seat Width Specification Comparison (SDC B)..... 128

Table 4.37: Bridge over Norfolk Southern RR Bent 2 Design Results 129
Table 4.38: Bridge over Norfolk Southern Railroad SDC A2 and SDC B Comparison 130
Table 4.39: Displacement Results for Oseligee Creek Bridge 132
Table 4.40: Capacity of the Steel Clip Angle 134
Table 4.41: Oseligee Creek Bridge Seat Width Specification Comparison (SDC B) 134
Table 4.42: Oseligee Creek Plastic Hinge Length Comparison (SDC B) 135
Table 4.43: Oseligee Creek Final Design Comparison (SDC B)..... 136
Table 4.44: Oseligee Creek Bridge SDC A2 and SDC B Comparison 138
Table 4.45: Displacement Results for Little Bear Creek Bridge 140
Table 4.46: Capacity of the Steel Clip Angle 141
Table 4.47: Little Bear Creek Bridge Seat Width Specification Comparison 142
Table 4.48: Little Bear Creek Plastic Hinge Length Comparison (SDC B) 142
Table 4.49: Little Bear Creek Final Design Comparison (SDC B) 143
Table 4.50: Pushover Analysis Results for Scarham Creek Bridge..... 146
Table 4.51: Capacity of the Steel Clip Angle 148
Table 4.52: Scarham Creek Minimum Seat Width Comparison 148
Table 4.53: Scarham Creek Plastic Hinge Length Comparison 149
Table 4.54: Scarham Creek Final Column Design Summary..... 150
Table 4.55: Scarham Creek Final Strut Design Summary..... 151
Table 4.56: Maximum Spacing Requirements outside of Plastic Hinge Zone 158
Table 5.1: Bridge Locations..... 174
Table 6.1: Hazard Map Data..... 191
Table 6.2: Ground Motion Data..... 193
Table 6.3: Foundation Capacities 195
Table 6.4: Calculated Bolt Strengths 196
Table 6.5: Bent Displacement Limits 197
Table 7.1: Results Overview for Lower Limit Friction Bent Creek Transverse Model 241
Table 7.2: Results Overview for Upper Limit Friction Bent Creek Transverse Model 242
Table 7.3: MCE Level Results Overview for Lower Limit Friction Bent Creek Transverse Model 243
Table 7.4: MCE Level Results Overview for Upper Limit Friction Bent Creek Transverse Model 243
Table 7.5: Results Overview for Lower Limit Friction Bent Creek Longitudinal Model 244
Table 7.6: Results Overview for Upper Limit Friction Bent Creek Longitudinal Model 245
Table 7.7: MCE Level Results Overview for Lower Limit Friction Bent Creek Longitudinal Model 246
Table 7.8: MCE Level Results Overview for Upper Limit Friction Bent Creek Longitudinal Model 246
Table 7.9: Results Overview for Lower Limit Friction Scarham Creek Transverse Model..... 248
Table 7.10: Results Overview for Upper Limit Friction Scarham Creek Transverse Model 248
Table 7.11: MCE Level Results Overview for Lower Limit Friction Scarham Creek Transverse Model 249
Table 7.12: MCE Level Results Overview for Upper Limit Friction Scarham Creek Transverse Model 249
Table 7.13: Results Overview for Lower Limit Friction Scarham Creek Longitudinal Model . 250
Table 7.14: Results Overview for Upper Limit Friction Scarham Creek Longitudinal Model.. 251

Table 7.15: MCE Level Results Overview for Lower Limit Friction Scarham Creek Longitudinal Model 251
Table 7.16: MCE Level Results Overview for Upper Limit Friction Scarham Creek Longitudinal Model 252
Table 7.17: Results Overview for Lower Limit Friction Norfolk Southern Railroad Transverse Model 253
Table 7.18: Results Overview for Upper Limit Friction Norfolk Southern Railroad Transverse Model 254
Table 7.19: MCE Level Results Overview for Lower Limit Friction Norfolk Southern Railroad Transverse Model..... 255
Table 7.20: MCE Level Results Overview for Upper Limit Friction Norfolk Southern Railroad Transverse Model..... 255
Table 7.21: Results Overview for Lower Limit Friction Norfolk Southern Longitudinal Model 256
Table 7.22: Results Overview for Upper Limit Friction Norfolk Southern Longitudinal Model 257
Table 7.23: MCE Level Results Overview for Lower Limit Friction Norfolk Southern Longitudinal Model 258
Table 7.24: MCE Level Results Overview for Upper Limit Friction Norfolk Southern Longitudinal Model 258
Table 7.25: Results Overview for Lower Limit Friction Oseligee Creek Transverse Model..... 260
Table 7.26: Results Overview for Upper Limit Friction Oseligee Creek Transverse Model 260
Table 7.27: MCE Level Results Overview for Lower Limit Friction Oseligee Creek Transverse Model 261
Table 7.28: MCE Level Results Overview for Upper Limit Friction Oseligee Creek Transverse Model 261
Table 7.29: Results Overview for Lower Limit Friction Oseligee Creek Longitudinal Model . 262
Table 7.30: Results Overview for Upper Limit Friction Oseligee Creek Longitudinal Model .. 263
Table 7.31: MCE Level Results Overview for Lower Limit Friction Oseligee Creek Longitudinal Model 263
Table 7.32: MCE Level Results Overview for Upper Limit Friction Oseligee Creek Longitudinal Model 264
Table 7.33: Results Overview for Lower Limit Friction Little Bear Creek Transverse Model . 266
Table 7.34: Results Overview for Upper Limit Friction Little Bear Creek Transverse Model .. 266
Table 7.35: Results Overview for Upper Limit Friction Little Bear Creek Transverse Model with Old Bolts 267
Table 7.36: MCE Level Results Overview for Lower Limit Friction Little Bear Creek Transverse Model 268
Table 7.37: MCE Level Results Overview for Upper Limit Friction Little Bear Creek Transverse Model 268
Table 7.38: MCE Level Results Overview for Upper Limit Friction Little Bear Creek Transverse Model with Old Bolts..... 268
Table 7.39: Results Overview for Lower Limit Friction Little Bear Creek Longitudinal Model 270
Table 7.40: Results Overview for Upper Limit Friction Little Bear Creek Longitudinal Model270

Table 7.41: MCE Level Results Overview for Lower Limit Friction Little Bear Creek Longitudinal Model 271
Table 7.42: MCE Level Results Overview for Upper Limit Friction Little Bear Creek Longitudinal Model 271
Table 7.43: Summary of Critical Design Level Analysis Behaviors 273
Table 7.44: Summary of Critical MCE Level Analysis Behaviors 273
Table 8.1 – Frequency, structural period, and calculated average damping ratios for each bridge 276
Table 8.2 – Dead loads and discrete masses used for each case study 277
Table 8.3 – Results overview for Chambers 25% scour longitudinal models 281
Table 8.4 – Results overview for Oseligee Creek Bridge 25% scour transverse models 282
Table 8.5 – Results overview for Oseligee Creek Bridge 100% scour longitudinal models 284
Table 8.6 – Results overview for Oseligee Creek Bridge 100% Scour transverse models 285
Table 8.7 – Assumptions used in buckling analysis for Norfolk Southern Railroad Bridge 286
Table 8.8 – Norfolk Southern Railroad Bridge P_{des}/P_{cr} and L_{eff}/r_{min} results 287
Table 8.9 – Results overview for Norfolk Southern Railroad Bridge longitudinal models 288
Table 8.10 – Results overview for Norfolk Southern Railroad Bridge transverse models 289
Table 8.11 – Results overview for Little Bear Creek Bridge longitudinal models 291
Table 8.12 – Results overview for Little Bear Creek Bridge transverse models 292
Table 8.13 – Assumptions used in buckling analysis for Bent Creek Road Bridge 293
Table 8.14 – Bent Creek Road Bridge P_{des}/P_{cr} and L_{eff}/r_{min} results 294
Table 8.15 – Results overview for Bent Creek Road Bridge longitudinal models 295
Table 8.16 – Results overview for Bent Creek Road Bridge transverse models 296
Table 8.17 – Results overview for Scarham Creek Bridge longitudinal models 299
Table 8.18 – Results overview for Scarham Creek Bridge transverse models 300
Table 9.1 – South Carolina's Typical Pile Types and Sizes 309

List of Figures

Figure 2.1: Displacement Based Design 8
Figure 2.2: Force-Based Design 9
Figure 2.3. Liquefaction susceptibility of Alabama based on Youd and Perkins 1978 (Ebersole and Perry 2008). 17
Figure 2.4. Inertial interaction model for deep foundations (Kavazanjian et al. 2011) 21
Figure 2.5. Foundation substructure model for kinematic analysis (Kavazanjian et al. 2011) 23
Figure 2.6. Example of a foundation stiffness curve 24
Figure 2.7. Direct (or Total) soil-foundation-structure kinematic interaction model (Kavazanjian et al. 2011) 25
Figure 2.8. Modal analysis process for a bridge pier within FB-MultiPier (Fernandes 1999) 30
Figure 3.1: Alabama DOT Connection 40
Figure 3.2: Previously Modified ALDOT Connection 41
Figure 3.3: Illinois Connection 43
Figure 3.4: North Carolina DOT Connection 44
Figure 3.5: North Carolina DOT Connection Detail "A" 44

Figure 3.6: South Carolina DOT Connection 45
Figure 3.7: Missouri DOT Connection 46
Figure 3.8: ALDOT Welded Connection..... 47
Figure 3.9: Proposed Weld Connection 48
Figure 4.1: Bridge Locations 54
Figure 4.2: Alabama SDC Map for Soil Site Class B..... 58
Figure 4.3: Alabama SDC Map for Soil Site Class C..... 59
Figure 4.4: Alabama SDC Map for Soil Site Class D..... 60
Figure 4.5: Mobile County Bridge Bent 2 Final Design Details 70
Figure 4.6: Stave Creek Bridge Bent 2 Final Design Details (SDC A1)..... 74
Figure 4.7: Stave Creek Bridge Bent 3 Final Design Details (SDC A1)..... 74
Figure 4.8: Stave Creek Bridge Bent 2 Final Design Details (SDC A2)..... 88
Figure 4.9: Stave Creek Bridge Bent 3 Final Design Details (SDC A2)..... 89
Figure 4.10: Bent Creek Road Bridge Bent 2 Final Design Details (SDC A2)..... 93
Figure 4.11: Bridge over Norfolk Southern Railroad Final Design Details (SDC A2)..... 96
Figure 4.12: Oseligee Creek Bridge Bent 2 Final Design Details (SDC A2)..... 100
Figure 4.13: Oseligee Creek Bridge Bent 3 Final Design Details (SDC A2)..... 101
Figure 4.14: Design Response Spectrum, Construction Using Three-Point Method 104
Figure 4.15: SAP2000 3D Model of Bent Creek Road Bridge..... 120
Figure 4.16: Static Pushover Curve for Bent Creek Road Bridge Bent 2..... 121
Figure 4.17: Bent Creek Road Bridge Bent 2 Final Design Details (SDC B)..... 124
Figure 4.18: SAP2000 3D Model of Bridge over Norfolk Southern RR..... 126
Figure 4.19: Static Pushover Curve for the Bridge over Norfolk Southern Railroad Bent 2 127
Figure 4.20: Bridge over Norfolk Southern Railroad Final Design Details (SDC B) 129
Figure 4.21: SAP2000 3D Model of Oseligee Creek Bridge..... 131
Figure 4.22: Static Pushover Curve for Oseligee Creek Bridge Bent 3..... 133
Figure 4.23: Oseligee Creek Bent 2 Final Design Details (SDC B)..... 136
Figure 4.24: Oseligee Creek Bent 3 Final Design Details (SDC B)..... 137
Figure 4.25: SAP2000 3D Model of Little Bear Creek Bridge 139
Figure 4.26: Static Pushover Curve for Little Bear Creek Bridge Bent 3 140
Figure 4.27: Little Bear Creek Bridge Bent 2 Final Design Details..... 144
Figure 4.28: Little Bear Creek Bridge Bent 3 Final Design Details..... 145
Figure 4.29: SAP2000 3D Model of Scarham Creek Bridge..... 146
Figure 4.30: Static Pushover Curve for Scarham Creek Bridge Bent 3..... 147
Figure 4.31: Scarham Creek Bridge Bent 2 Final Design Details 152
Figure 4.32: Scarham Creek Bridge Bent 3 Final Design Details 153
Figure 4.33: Scarham Creek Bridge Bent 4 Final Design Details 154
Figure 4.34: Maximum Spacing Requirements outside of Plastic Hinge Zone..... 158
Figure 4.35: Standard Details for Circular Columns in SDC A2 161
Figure 4.36: Standard Details for Rectangular Columns in SDC A2 162
Figure 4.37: Standard Details for Circular Columns in SDC B..... 165

Figure 4.38: Standard Details for Rectangular Columns in SDC B 166
Figure 5.1. Map of Alabama Counties with bridge locations (modified after Yellow Maps 2010) 172
Figure 5.2: Little Bear Creek Bridge Model 176
Figure 5.3: Scarham Creek Bridge Model 178
Figure 5.4: Norfolk Southern Bridge Model 180
Figure 5.5: Oseligee Creek Bridge Model 182
Figure 5.6: Bent Creek Bridge Model 184
Figure 6.1: Deaggregation Plot for Muscle Shoals, AL 188
Figure 6.2: Deaggregation Plot for Bridgeport, AL 189
Figure 6.3: Targeted Design Spectrum 191
Figure 6.4: Design Level Response Spectra 194
Figure 6.5: Idealized Caltrans Hinge 202
Figure 6.6: Fiber Analysis Backbone Curve 203
Figure 6.7: Example Bearing Pad Configuration (Alabama DOT 2012) 205
Figure 6.8: Example Bearing Pad Force-Displacement Relationship 206
Figure 6.9: Clip Angle Connection Detail 208
Figure 6.10. Example p-y curves for sand (O'Neil and Murchison 1983) and limestone (McVay and Niraula 2004) 211
Figure 6.11. Axial t-z curves for driven piles (McVay et al. 1989) and 212
drilled shafts in sand and Reese and O'Neill (1988). 212
Figure 6.12. Axial Q-z curves for driven piles (BSI 2013(b)) and drilled shaft end bearing in sand O'Neill and Reese (1999) 212
Figure 6.13 Hyperbolic representation of T-q curve (BSI 2013(b)) 213
Figure 6.14 Hognestad model for concrete (Hognestad et al. 1955) 214
Figure 6.15 Default stress-strain curve for 60 ksi steel (BSI 2013(b)) 214
Figure 6.16. Little Bear Creek Bridge model 219
Figure 6.17. Little Bear Creek Bridge idealized soil profile 219
Figure 6.18. Oseligee Creek Bridge model 222
Figure 6.19. Oseligee Creek Bridge idealized soil profile for Bent 3 223
Figure 6.20. Norfolk Southern Railroad Bridge model 226
Figure 6.21. Norfolk Southern Railroad Bridge idealized soil profile 227
Figure 6.22. Scarham Creek Bridge model 231
Figure 6.23. Scarham Creek Bridge idealized soil profile 232
Figure 6.24. Bent Creek Road Bridge model 235
Figure 6.25. Bent Creek Road Bridge idealized soil profile 236

Chapter 1: Introduction

1.1 Problem Statement

The Alabama Department of Transportation (ALDOT) currently designs precast prestressed concrete bridges in the state of Alabama using the latest edition (17th) of the American Association of State Highway and Transportation (AASHTO) Standard Specification (Standard Specifications for Highway Bridges, 2002). This specification, which was originally based on allowable stress design (ASD) theory and since updated to include Load and Resistance Factor (LRFD) principles, has not been updated since 2002. Recently, ALDOT has been required to update their bridge design specifications to the AASHTO LRFD Design Specifications (LRFD Bridge Design Specifications, 2009). This specification is based on LRFD principles and is updated every few years by AASHTO. Some of the major changes in the new specification have been in the area of seismic design, which prompted ALDOT to update their seismic design criteria. A previous study by Coulston and Marshall (2011) concluded that the AASHTO Guide Specifications for LRFD Seismic Bridge Design (Guide Specifications for LRFD Seismic Bridge Design, 2009) is an acceptable alternative to the seismic design criteria in the LRFD Specification. The differences between the Guide Specifications and the Standards Specifications are expected to have a major impact on the seismic design procedures for bridges in the state. To address these impacts, the following tasks were performed:

- Developed design standards for concrete bridges in low seismic regions (SDC A and B)
- Investigated the current superstructure-to-substructure connection
- Evaluated whether the Guide Specifications are suitable for critical and essential bridges in a moderate seismic hazard

- Evaluated the effect of significant seismic loads on driven pile foundations

Once these tasks were studied, the results were used to develop training modules for ALDOT personnel to assist with future bridge design.

1.2 Problem Overview

During an earthquake, inertial forces are generated by the bridge in response to the ground accelerations. The larger the ground accelerations, the larger the inertial forces in the bridge. During the design process for low seismic regions, such as Seismic Design Category (SDC) B, these expected forces are typically applied as static lateral loads on the bridge. The bridge must maintain a complete load path from the point of load application to the foundation, with each element being able to resist the loads acting on the bridge. Since bridge design is focused on preventing collapse and ensuring that bridges remain open to at least emergency vehicles after a design earthquake, the desirable behavior for a bridge experiencing extreme loading conditions is for the substructure of the bridge to receive damage without loss of span. This allows the superstructure of the bridge, the roadway deck and girders, to be passable. Therefore, the superstructure of the bridge is designed to remain elastic during a seismic event, while the substructure of the bridge is designed to dissipate energy through inelastic response. This is accomplished by designing for plastic hinging to occur in the columns and/or foundations, which allows the substructure to dissipate energy through cracking of the concrete and yielding of steel. Plastic hinges form when reinforcement in one cross section yields, without failure, and allows the element to redistribute moments from additional loads to cross sections that have not yielded (Wight & MacGregor, 2009). In order for these plastic hinges to occur in the columns, the columns must be designed as ductile elements. Ductility is defined as

the ability of the structure to absorb and dissipate energy without significant strength loss. Research following the 1994 Northridge and 1995 Kobe earthquakes showed the importance of having ductile substructures to prevent failure of a bridge. If the substructure is not ductile, it will not be able to dissipate all the energy from the earthquake and the entire bridge will be at risk of collapse. Specific reinforcement detailing is required to allow for plastic hinging to occur in bridge columns. Both the Standard Specification and the Guide Specification address the importance of detailing for ductility in SDC B. However, the Standard Specification results in most of the state being classified as SDC A, for which no minimum detailing is required. This occurs because the seismic hazard maps used in the Standard Specification were last updated in 1988 and are based on a return period of 475 years. The research that has been incorporated into new seismic hazard maps is included in the Guide Specifications, which uses maps from 2007. They are based on a design earthquake of 1000 years that has been determined by seismological research. These maps result in the classification of many more bridges in the state as SDC B. Therefore, the Standard Specification does not require bridges in the state to be designed as having ductile substructures, while the Guide Specification does.

1.3 Project Deliverables

This final task of this report is the development of training materials to assist ALDOT with the transition to the LRFD Specifications. The first deliverable is the recommendation for a new superstructure to substructure connection. It was assumed that the current connection would not allow for a complete load path during an earthquake. One of the first steps was studying already established connections used by other state DOTs. These different options were analyzed based on safety, constructability and economy. Once a final recommendation

concerning the connection was approved by the ALDOT Bridge Bureau, it was included in the new bridge designs.

The second deliverable was a refinement of design standards for those bridges classified as SDC B and the development of standard drawings and design sheets for bridges in SDC A. Some design standards had been developed in a previous project by Coulston and Marshall (2011); these were refined by using two additional case studies to show the differences between the two specifications. Computer aided design sheets were created for each of the bridges studied in SDC B, and each of the bridges studied in SDC A. Also, two additional bridge models were created for the two additional bridges studied.

The third deliverable was a Displacement-based analysis and evaluation of bridges classified as “Critical” or “Essential” that have been designed using the procedures of the Guide Specification. Any design recommendations will be included in this analysis in addition to the design specification procedures.

The fourth deliverable was the evaluation of the performance of typical deep foundations utilized by ALDOT. This originally began as pile foundations only, but came to include drilled shafts as the project progressed. The complete substructures (from pier/bent cap down) of five ALDOT bridges were modeled using FB-Multipier to demonstrate their behavior under earthquakes generated in Task three.

1.4 Report Outline

This report is organized into seven chapters and multiple appendices. The first chapter is an introduction to the problem and description of the report. The second chapter is a literature review, including a discussion on the differences between the two design specifications. The third chapter describes an analysis of the current superstructure-to-substructure connection and

recommends a new design. The fourth chapter reviews the seismic design process for bridges in SDC A and B and provides detailed procedures used for the design of each bridge. The fifth chapter discusses the effect the Guide Specifications will have on Critical and Essential bridges in the state. The sixth chapter discusses the evaluation of driven pile foundations with significant seismic loads. The seventh chapter concludes the report and presents the final design recommendations. The appendices contain the design sheets for each of the bridges studied, moment-axial load interaction diagrams for bridges (where appropriate) and the connection design calculations.

Chapter 2: Literature Review

2.1 Introduction

For each task in this report, background research was performed. This research, presented below, is intended to provide the necessary information so that the results of the study can be understood. Research concerning the first two tasks will be discussed first, followed by task three and four.

2.2 Specification Comparison

One task of this report was to develop standard details for bridges in SDC A and B. In order to accomplish this task, the design specifications needed to be compared. The Standard Specification and the LRFD Specification express different design philosophies, which control the design procedure of the bridge. Research is constantly completed in the area of seismic design that results in a better understanding of bridge behavior during an earthquake and, consequently, better design procedures to mitigate poor behavior. The Standard Specification was first compiled in 1921 using allowable stress design (ASD) standards. ASD uses elastic analysis to determine the stresses in an element. It requires that these calculated stresses be less than the allowable stress the material can withstand divided by a factor of safety. Only one factor of safety is used, incorporating uncertainties in both the load and material resistance. However, this factor of safety does not recognize that some loads are more variable than others. In the 1970s, load factor design (LFD) was introduced to the Standard Specifications. It requires the nominal strength to be greater than the factored load demand and uses two factors of safety, one for the load and one for strength reduction, which allow more efficient structures to be designed. The load factors are calibrated for specific loads because LFD recognizes that

some loads are more variable than others. In 1994, the first edition of the LRFD Specifications, on which the AASHTO Guide Specifications for LRFD Seismic Bridge Design are based, was published. It uses load and resistance factor (LRFD) design and both elastic and plastic analysis to determine the nominal strength. It also requires the factored nominal strength to be greater than the factored load. LRFD is an extension of LFD, but uses various load and resistance factors that are specifically analyzed for each limit state to account for variability in both resistance and load while achieving a uniform level of safety (Caltrans, 2011). In 2000, the Federal Highway Administration decided to stop updating the Standard Specifications and only maintain the LRFD Specifications. In 2007, states were required to adopt the new LRFD Specification for all bridge design. Any new research in the area of bridge seismic design, such as return periods for design earthquakes, has been addressed in the LRFD Specifications but not in the Standard Specifications. Therefore, the differences in the seismic design of the two specifications is due mainly to continuing research, which has been included in the LRFD Specifications, but not in the Standard Specifications. Another alternative to the LRFD Specifications, in the area of seismic bridge design, is the Guide Specifications. These specifications use a displacement-based design, while the LRFD Specifications use a force-based design. A displacement-based design requires a bridge to meet certain displacement criteria, determined by estimating the inelastic displacement of the bridge using a model that represents the first mode of vibration. The forces are determined from this displacement demand. For example, in Figure 2.1 the actual force at an expected displacement of 6 inches would be about 300 kips, while the elastic force would be 600 kips.

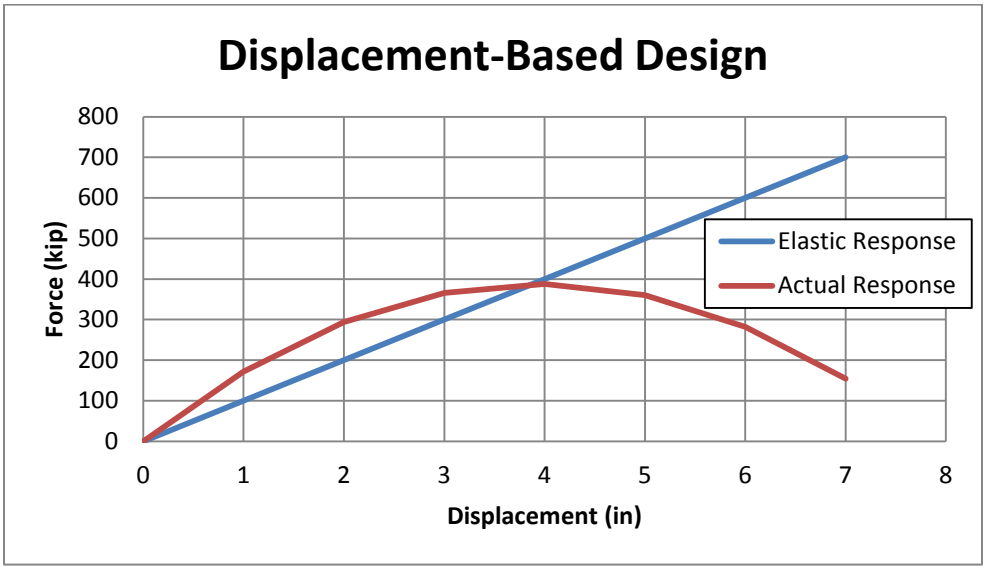

Figure 2.1: Displacement Based Design

A force based design determines the design loads by dividing the elastic force by a response modification factor. The bridge is designed for this lower force, but still expected to achieve the same lateral displacement from the elastic force. For example, in Figure 2.2, the elastic force is 800 kips, but the design force is 200 kips. Both are expected to reach the ultimate displacement of 8 inches, but the elasto-plastic response allows for smaller design forces. In order to achieve this displacement, the structure must be designed to be ductile so that it can dissipate the additional energy expected from the inelastic response.

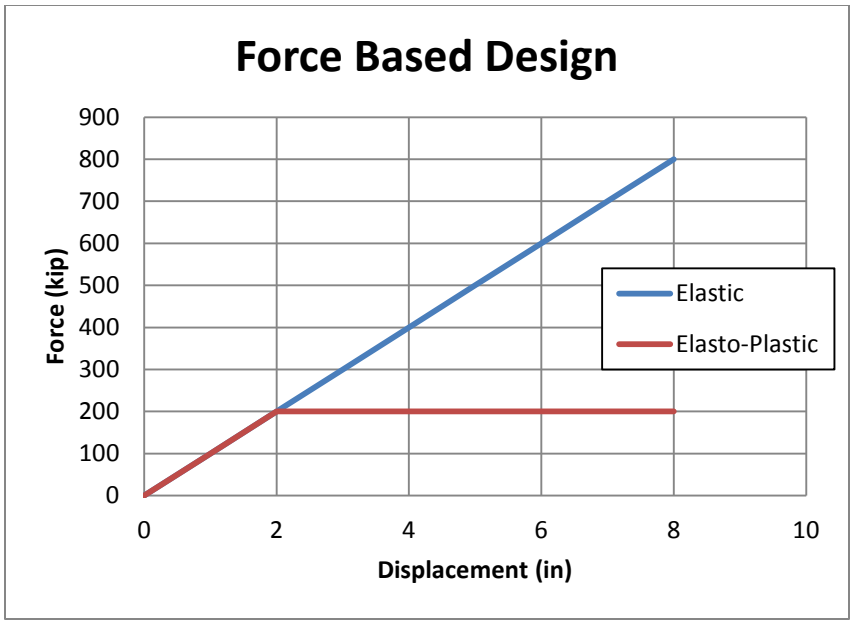

Figure 2.2: Force-Based Design

While most of the current design codes feature a force-based design, recent research has suggested that a displacement-based design better estimates the true response of a bridge. This is one of the reasons why the Guide Specifications are recommended for design instead of the LRFD Specifications. These two design specifications are compared later in this chapter. In order to understand how changes in research have influenced bridge design, the Standard Specifications are discussed first.

2.2.1 Standard Specifications

Like the LRFD Specifications, the Standard Specifications are a force based design. They are applicable only for conventional bridges, meaning those of steel or concrete girder construction with spans less than 500 feet. Bridge sites are classified as one of four Seismic Performance Categories (SPC) based on the acceleration coefficient at the site and importance classification of the bridge. The importance classification comes from the bridge being classified as either “Essential” or “Other.” Bridges

classified as “Essential” must remain functional during and after a design earthquake, and “Other” encompasses all other bridges. The acceleration coefficient is determined from the seismic hazard maps, which were last updated in 1988. These maps are based on an estimated return period of 475 years with the soil assumed to be rock. Once the bridge SPC has been classified, the response coefficient is determined based on the acceleration coefficient, soil profile type and bridge period. The soil profiles are based on the type of soil present at the bridge site or by a shear wave velocity test or “other appropriate means of classification” (AASHTO, 2002). Applying these procedures to bridge sites in Alabama results in most bridges in the state being classified as SPC A.

For SPC A, no structural analysis is required to determine the design forces. The horizontal design forces are determined to be 20% of the tributary weight resisted by the substructure. The only other requirement is for the minimum seat width to be provided.

For SPC B, the design forces are determined from an elastic structural analysis and are divided by a response modification factor. The minimum seat width is also required to be provided. One additional requirement in this SPC is minimum detailing requirements in the top and bottom of a column. These minimum details are intended to provide a limited measure of ductility to the column.

2.2.2 LRFD Specifications

The LRFD Specification uses a force based design and is applicable to bridges with conventional construction only. Bridges are classified as one of four Seismic Design Categories (SDC) that are roughly equivalent to the SPC in the Standard Specification. The SDC of a bridge is based on the soil site class and 1.0-second spectral

response acceleration coefficient. The soil site classes are divided into six categories, determined using the shear wave velocity, undrained shear strength, or average blow count of the soil. Whereas in the Standard Specifications the soil profile affects the forces after the SPC was determined, in the LRFD Specifications the soil profile is used to determine the SDC and not the design forces. One key difference is the seismic hazard maps used in the LRFD Specifications. Three maps are used to determine the peak ground acceleration, 0.2-second spectral response acceleration, and 1.0-second spectral response acceleration. These maps were updated in 2007 and based on an estimated return period of 1000 years. This results in the ground accelerations in the LRFD Specifications being much larger than those in the Standard Specifications. Also, bridges are classified into three categories: "Critical," "Essential," and "Other." Both "Critical" and "Essential" bridges must remain open after a design earthquake, but "Essential" bridges are designed for earthquakes with 1000-year return period, and "Critical" bridges for earthquakes with 2500-year return period. The LRFD Specifications result in many more bridges in the state of Alabama classified as "Essential" or "Other" to be SDC B. So the biggest difference between the two specifications is the change in the seismic design classification of a bridge, which has a significant effect on its design.

For SDC A, only the horizontal connection forces and minimum seat width are designed. The horizontal connection force is either 15% or 25% of the vertical reaction due to the tributary load depending on the acceleration coefficient at the site. For sites with an acceleration coefficient of less than 0.05g, the connection force is 15% of the vertical reaction, otherwise it is 25%. The Standard Specifications do not allow for a reduction at sites with smaller expected accelerations. The minimum seat width in this

design category is calculated using the same equation as the Standard Specification, but is also allowed to be reduced by 25% if the expected acceleration is less than 0.05g.

For SDC B, a structural analysis is required to determine the elastic forces. These elastic forces are then divided by a response modification factor to determine the seismic forces. In this SDC, the minimum seat width is still calculated with the same equation, but the supplied seat width is required to be 150% of the minimum seat width equation to accommodate the full capacity of the plastic hinging mechanism. The major difference in this category compared to the Standard Specifications is the more extensive detailing requirements. These requirements are the same as those required for SDC C and D, with the exception of a larger maximum longitudinal reinforcement ratio limit. These details include designing a plastic hinge zone at the top and bottom of the column that adheres to specific transverse reinforcement spacing requirements, maximum and minimum longitudinal reinforcement ratio limits, and splicing requirements. These design requirements are the result of research in earthquake engineering that has been incorporated into the LRFD Specifications, but not the Standard Specifications.

2.2.3 Guide Specifications

The differences between the Guide Specifications and Standard Specifications are the same as those between the Standard Specifications and LRFD Specifications. For this reason, this section will focus on the differences between the Guide and LRFD Specifications. The Guide Specifications are not applicable for use of “Critical” or “Essential” bridges. They are only for conventional bridges, which fall into the “Other” category in the LRFD Specifications. The largest difference is that the Guide

Specifications use a displacement based design, meaning the bridge must satisfy displacement demands at each of the bents and abutments. This makes sure the bridge is capable of transmitting the maximum force effects developed by the plastic hinges into the foundation. The calculation of the horizontal design forces will be discussed next.

The calculation of the horizontal design force in SDC A is the same as in the LRFD Specifications, where it is equal to either 15% or 25% of the vertical reaction. The one difference in this design category is the requirement of bridges to satisfy the minimum detailing requirements of SDC B if they are within 0.05g of the SDC B classification.

A structural analysis is still required for SDC B, but the design forces are not divided by a response modification factor. Once the bridge is determined to have satisfied the displacement demand, the design forces that result from the displacement analysis are used unless the plastic forces are greater. The minimum detailing requirements are similar, with two exceptions. The maximum spacing of the transverse reinforcement in the plastic hinge zone is 6 inches, whereas in the LRFD Specification it is 4 inches. And there is no requirement of an extension of the plastic hinge zone into the bent cap or foundation in the Guide Specifications. The largest difference is the determination of the design forces. The previous study by Coulston and Marshall (2011) determined the Guide Specifications to be an acceptable and more economical alternate for seismic bridge design. These specifications will be used to design the remainder of the bridges, except where they specifically require the LRFD Specifications.

2.3 Liquefaction in Alabama

During an earthquake, insitu soils may be susceptible to liquefaction. Liquefaction typically occurs when saturated cohesionless soil undergoes undrained loading conditions which generate excess pore water pressures (Kramer, 1996). This increase in pore water pressure subsequently decreases soil shear strength and stability; the soil then mobilizes until it reaches a state of equilibrium. There are two general modes of liquefaction that can occur: (A) flow liquefaction and (B) cyclic mobility (lateral spreading) (Kramer, 1996).

Flow liquefaction produces the most dramatic effects of the two, flow failures (or landslides), which occur on sloping ground. Flow liquefaction occurs when the shear stress required for static equilibrium is greater than the shear strength of the soil (Kramer, 1996). The soil then "flows" under the influence of gravity until it reaches a stable condition. These can often be catastrophic, destroying structures and killing people in its path.

Lateral Spreading, on the other hand, occurs on gently sloping ground or flat ground near water when the static shear stress is less than the shear strength of the liquefied soil (Kramer 1996). These deformations can occur well after ground shaking has ceased, depending on the length of time required to reach static equilibrium (Kramer 1996). This mode can be destructive as well, causing bridges to collapse and excessive settlement of structures. Because both modes of liquefaction can cause significant structural damage to existing structures, an evaluation of liquefaction susceptibility is an important aspect of seismic design. Both modes of liquefaction can cause axial and lateral resistance of foundations to decrease significantly.

In a recent study (Ebersole and Perry 2008), liquefaction potential was mapped based on geologic age and origin using the Youd and Perkins (1978) method, which is shown in Table 2.1. This method is based on geologic conditions. Some geologic formations are inherently more susceptible to liquefaction than others. Figure 2.3 shows liquefaction susceptibility for Alabama. This map clearly indicates the relatively low potential for the northern part of the state. However, almost all of the areas that have a high potential for liquefaction are located near stream or river beds where alluvial cohesionless deposits generally make up the soil stratigraphy and the soils have a high degree of saturation. This is important because many bridges are built to cross waterways.

Type of deposit (1)	General distribution of cohesionless sediments in deposits (2)	Likelihood that Cohesionless Sediments, When Saturated, Would Be Susceptible to Liquefaction (by age of Deposit)			
		<500 yr (3)	Holocene (4)	Pleistocene (5)	Pre-Pleistocene (6)
(a) Continental Deposits					
River channel	Locally variable	Very high	High	Low	Very low
Flood plain	Locally variable	High	Moderate	Low	Very low
Alluvial fan and plain	Widespread	Moderate	Low	Low	Very low
Marine terraces and plains	Widespread	----	Low	Very low	Very low
Delta and fan-delta	Widespread	High	Moderate	Low	Very low
Lacustrine and playa	Variable High	Moderate	Low	Very low	
Colluvium	Variable High	Moderate	Low	Very low	
Talus	Widespread	Low	Low	Very low	Very low
Dunes	Widespread	High	Moderate	Low	Very low
Loess	Variable High	High	High	Unknown	
Glacial till	Variable Low	Low	Very low	Very low	
Tuff	Rare	Low	Low	Very low	Very low
Tephra	Widespread	High	High	?	?
Residual soils	Rare	Low	Low	Very low	Very low
Sebka	Locally variable	High	Moderate	Low	Very low
(b) Coastal Zone					
Delta	Widespread	Very high	High	Low	Very low
Esturine	Locally variable	High	Moderate	Low	Very low
Beach					
High wave energy	Widespread	Moderate	Low	Very low	Very low
Low wave energy	Widespread	High	Moderate	Low	Very low
Lagoonal	Locally variable	High	Moderate	Low	Very low
Fore shore	Locally variable	High	Moderate	Low	Very low
(c) Artificial					
Uncompacted fill	Variable	Very high	----	----	----
Compacted fill	Variable	Low	----	----	----

Table 2.1 – Susceptibility of sedimentary deposits to liquefaction during strong shaking (Youd and

Perkins 1978)

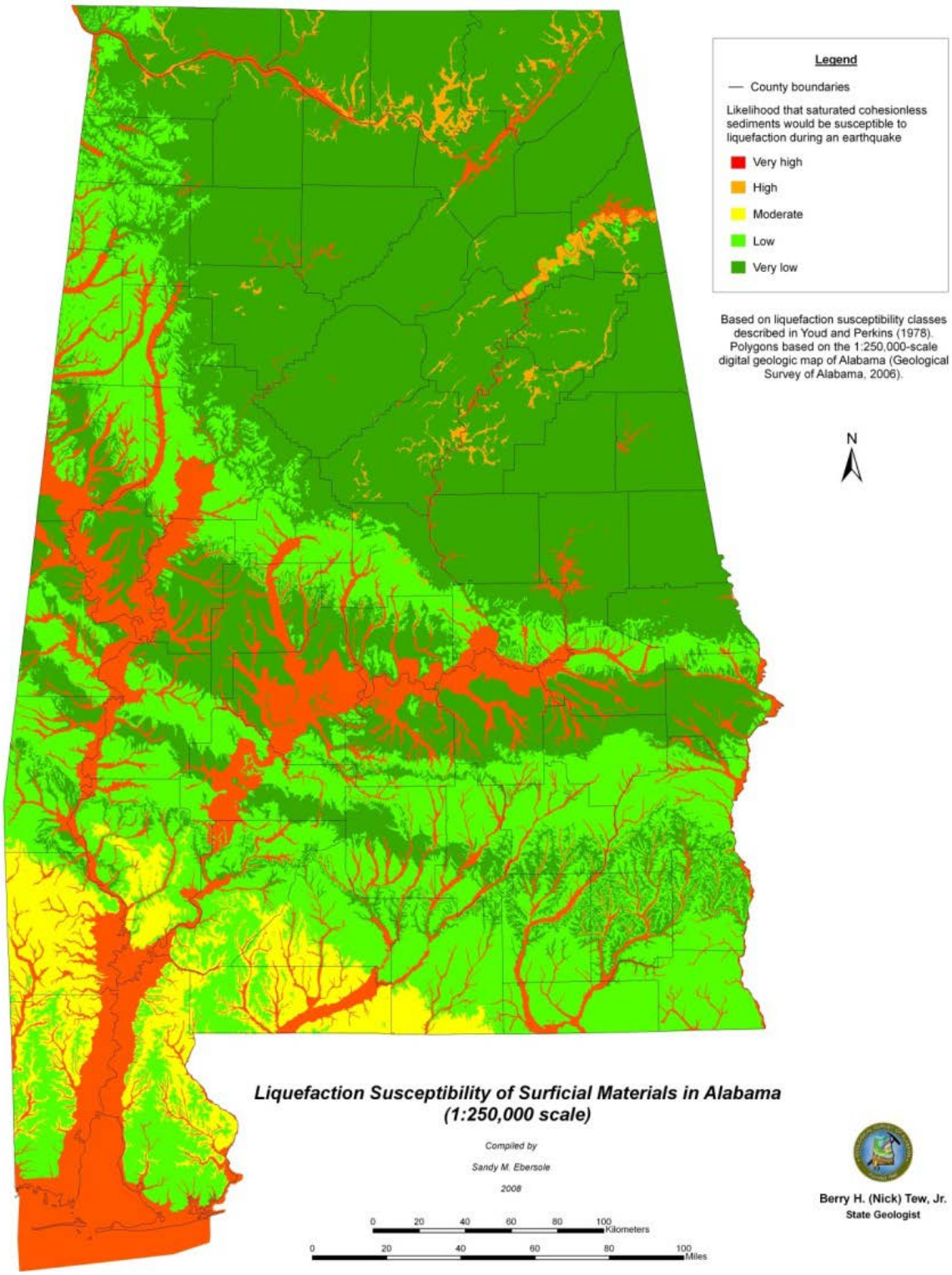

Figure 2.3. Liquefaction susceptibility of Alabama based on Youd and Perkins 1978 (Ebersole and Perry 2008).

Table 2.2 presents the Guide Specification requirements for liquefaction for each SDC. It should be noted that Kavazanjian et al. (2011) recommended that a liquefaction evaluation for SDC B was not necessary.

Table 2.2 – Liquefaction evaluation requirements for each SDC (AASHTO 2009)

Value of SA_1	**SDC**	**Liquefaction Evaluation Required?**
$SA_1 < 0.15$	A	No
$0.15 < SA_1 < 0.30$	B	Should be considered for certain conditions
$0.30 < SA_1 < 0.50$	C	Yes
$0.50 < SA_1$	D	Yes
Where: SA_1 = Spectral acceleration at a period of 1 second		

If the site is deemed to have a high potential for liquefaction, a formal liquefaction evaluation should be done in most cases. Referring to Figure 2.3, most of the areas that have a high potential for liquefaction are located in the southern part of the state, which has a low sesmic hazard (SDC A). However, the potential for liquefaction should always be considered in a SDC B, especially in regard to bridges near waterways in the northern part of the state. The Simplified Procedure, originally developed by Seed and Idris (1982) is one of the most common method used to evaluate liquefaction potential and is recommended to use should the engineer deem it necessary. It has been revised since its initial development and is presented in Kavazanjian et al. (2011). It should be noted that the Simplified Procedure should be primarily used for sites with moderate to strong ground motions ($0.2\ g < a_{max} < 0.5\ g$) (Kavazanjian et al. 2011).

2.4 Soil Foundation Structure Interaction Analysis

Understanding how the global system of any problem works is an important step in analysis and design of systems and structures. In this case, the global system is the bridge pier and surrounding elements, which can be broken into two main components: the soil and structure. The presence of a constructed facility modifies the free-field ground motion at the base of the structure and typically reduces it (Kavazanjian et al. 2011). Free-field ground motion is the natural ground motion one would feel standing on undisturbed earth during an earthquake event. The interaction between the soil and the structure is commonly referred to as soil-structure interaction (SSI). The structure can be further broken down into two separate components: foundation and above-ground structure. The above-ground structure in the case of the type of bridge under consideration is the pier column(s) and cap, and the bridge deck. The interaction of the system is more properly described as soil-foundation-structure interaction (SFSI) which will be used throughout this document (Kavazanjian et al. 2011). There are two sources of SFSI: kinematic interaction and inertial interaction. Both interactions occur during an earthquake event and are complex. The foundation is loaded kinematically by the earthquake, and then the structure begins to move, causing inertial forces to be transferred from the structure to the foundation.

2.4.1 Kinematic Interaction

Kinematic interaction directly interplays both the soil and foundation system, making this interaction the more complex of the two (Bhattacharya 2003). Before the superstructure begins to oscillate, the piles may be forced, by the soil, to displace

depending on the flexural stiffness (EI) of the pile (Bhattacharya 2003). The motion difference between the pile and the free-field motion can induce bending moments in the pile (Bhattacharya 2003). Kinematic interaction is often ignored in analysis because it is negligible for flexible piles in competent soils and tends to reduce the above-ground structural motion for stiff piles (Kavazanjian et al. 2011). In most applications, kinematic interaction response analysis is not feasible because it leads to large numerical models (Kavazanjian et al. 2011). However, it can prove to limit conservatism, and could reduce costs associated with constructing the bridge.

2.4.2 Inertial Interaction

Inertial interaction takes place as the structure begins to move, and the magnitude of the inertial forces depends upon the fundamental period of the structure and the frequency content of the ground motions (Kavazanjian et al. 2011). These inertia forces of the structure are transferred to the foundation system as lateral forces, vertical forces and bending moments. To model inertial interaction for deep foundations, an equivalent cantilever or spring-dashpot model is used to represent the foundation (Kavazanjian et al. 2011). Figure 2.4 shows a generalized form of the inertial interaction model for deep foundations. This is a simple approach and is done often. However, it cannot account for the bending moment distribution in the pile, and, for each of the five relevant degrees of freedom (DOF) (2 translational and 3 rotational), the length of the equivalent cantilever (or point of fixity) may be different (Kavazanjian et al. 2011).

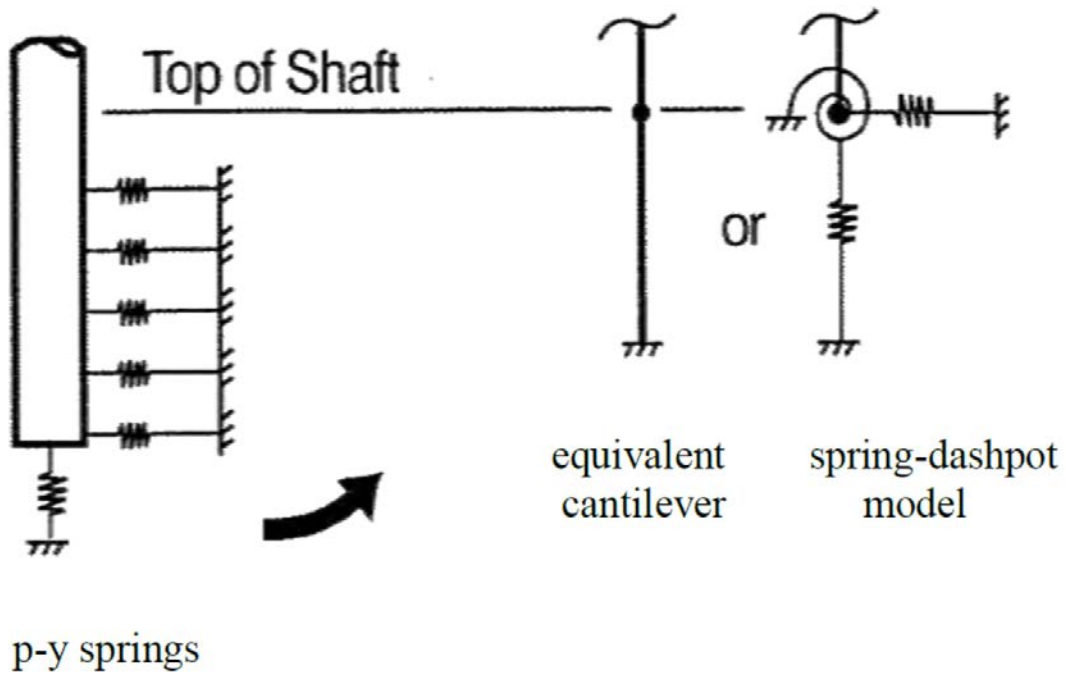

Figure 2.4. Inertial interaction model for deep foundations (Kavazanjian et al. 2011)

2.4.3 Seismic and Dynamic Response Analysis Methods

The two most common methods that are used to analyze the seismic response of bridge foundations are substructure analysis and direct analysis. For both methods, several factors must be considered: soil stratigraphy and strength parameters, water table elevation, foundation types and lengths, pile cap design (if applicable), and different geotechnical hazards such as scour and liquefaction. Each project is different and the analysis may or may not need to include consideration for other geotechnical hazards besides an earthquake. Thoughtful consideration must be given to all possibilities before implementing an analysis program.

Depending on what type of abutment is present, there are different resisting mechanisms, including mobilization of the abutment back-wall, that contribute to the resistance of a bridge to an earthquake event. For further detail, see Kavazanjian et al. (2011).

2.4.3.1 Substructure Analysis

Substructure modeling is the simpler and the more common method of the two. The most common way to determine the foundation stiffness is by using a computer program, such as LPILE or FB-MultiPier, that uses the p-y method to determine soil response, then extrapolate the stiffness so that it represents a group stiffness (if necessary). Since the extrapolation method was not used in this project, it is not covered. See Kavazanjian et al. (2011), for a more detailed discussion. While this is widely accepted, there is software capable of modeling pile groups more accurately such as GROUP and FB-MultiPier (which was used for this research project). Greater detail about FB-MultiPier and the p-y method is covered in Section 2.6 of this chapter.

There are six DOF for a foundation system and the stiffness of the foundation for each degree must be known or estimated. The DOF are axial and bi-lateral translation (u, v, and w) and rotation (Θ_X, Θ_Y, and Θ_Z) about each of the three axes. Sometimes, it may be appropriate to assume some DOF are fixed, and therefore, they do not need to be evaluated, such as axial translation or torsional rotation. To determine the response of the foundation, a static response analysis is done at the pile head or pile cap head. See Figure 2.5 for a representation of substructure modeling. In this case, it was assumed the pile head was fixed within the cap, therefore they were modeled together. One question that is usually asked when determining the response is whether the axial dead load should be included in the lateral and rotational push-over analysis. Lam and Martin (1986) concluded the following:

> *For convenience in design or analysis, the axial soil support characteristics are assumed to be independent of the lateral soil support*

characteristics. This is justified because lateral soil reactions are usually concentrated along the top 5 or 10 pile diameters whereas almost all of the axial soil resistance is developed at greater depths. Therefore, the axial and lateral soil support behavior can be studied and analyzed separately.

The end result of a static foundation response analysis is a family of force/moment versus displacement/rotation response curves that represent the pile head or the top of a pile group in a structural model. These curves are almost always nonlinear. The structural and geotechnical engineer must communicate effectively as where to properly apply the springs and in what fashion. Figure 2.6 shows an example of a foundation stiffness curve.

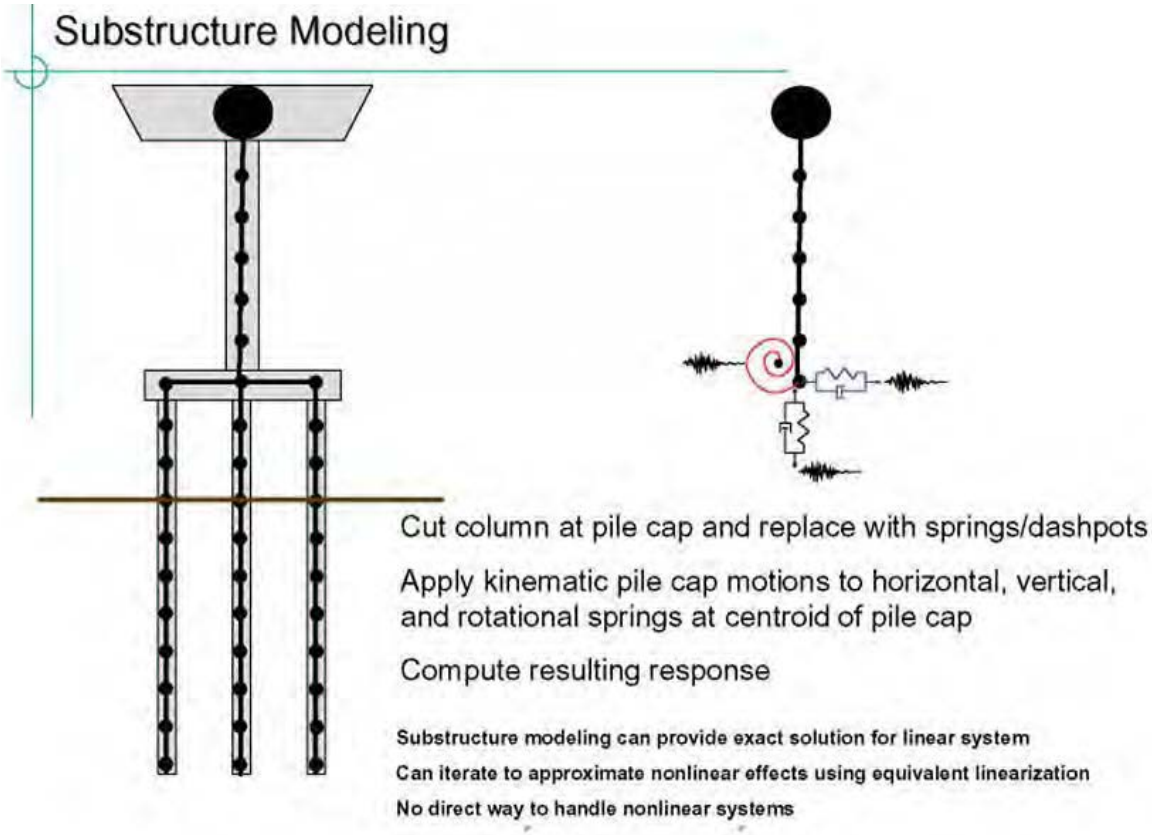

Figure 2.5. Foundation substructure model for kinematic analysis (Kavazanjian et al. 2011)

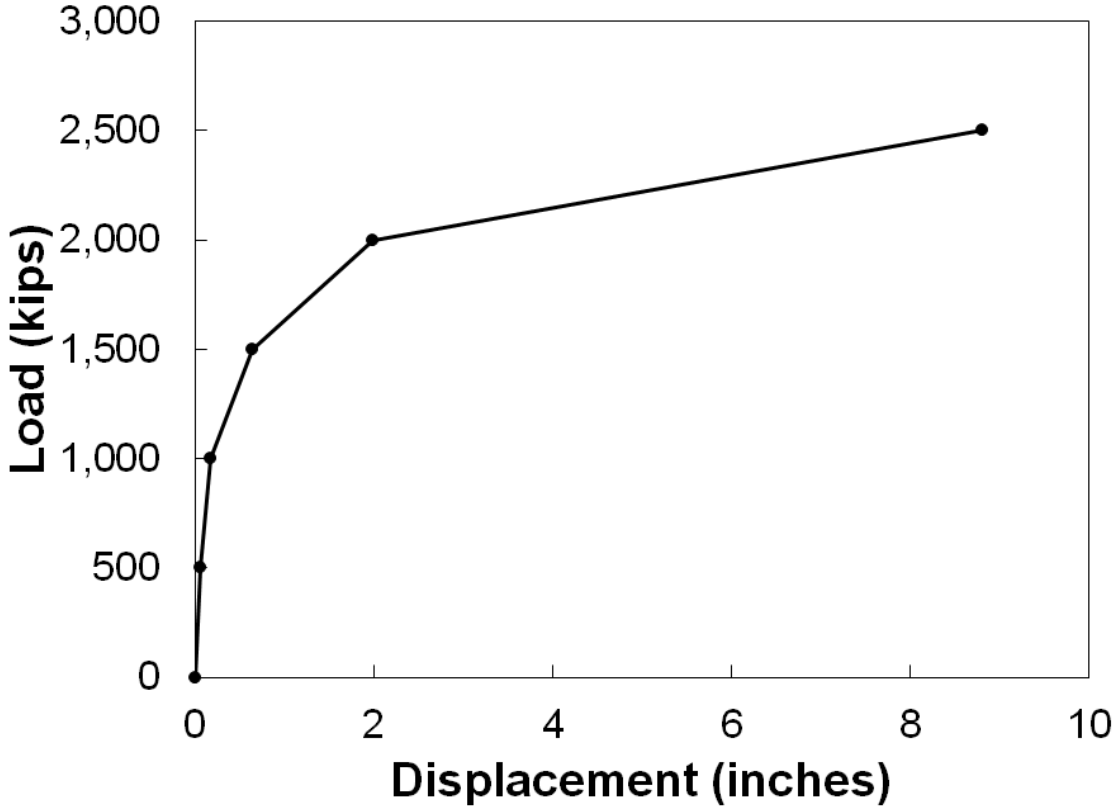

Figure 2.6. Example of a foundation stiffness curve

2.4.3.2 Direct Analysis

Direct analysis is not done in most applications. It is simply too time consuming and complicated to be used for every project, and most institutions or companies cannot afford the type of software that is best suited to run this method of analysis. Direct analysis builds on that of substructure modeling. However, time-history or response spectrum functions, structure configuration, and dead loads must also be input into the program. See section 2.6 for more detail on these topics. Figure 2.7 shows a detailed representation of direct analysis.

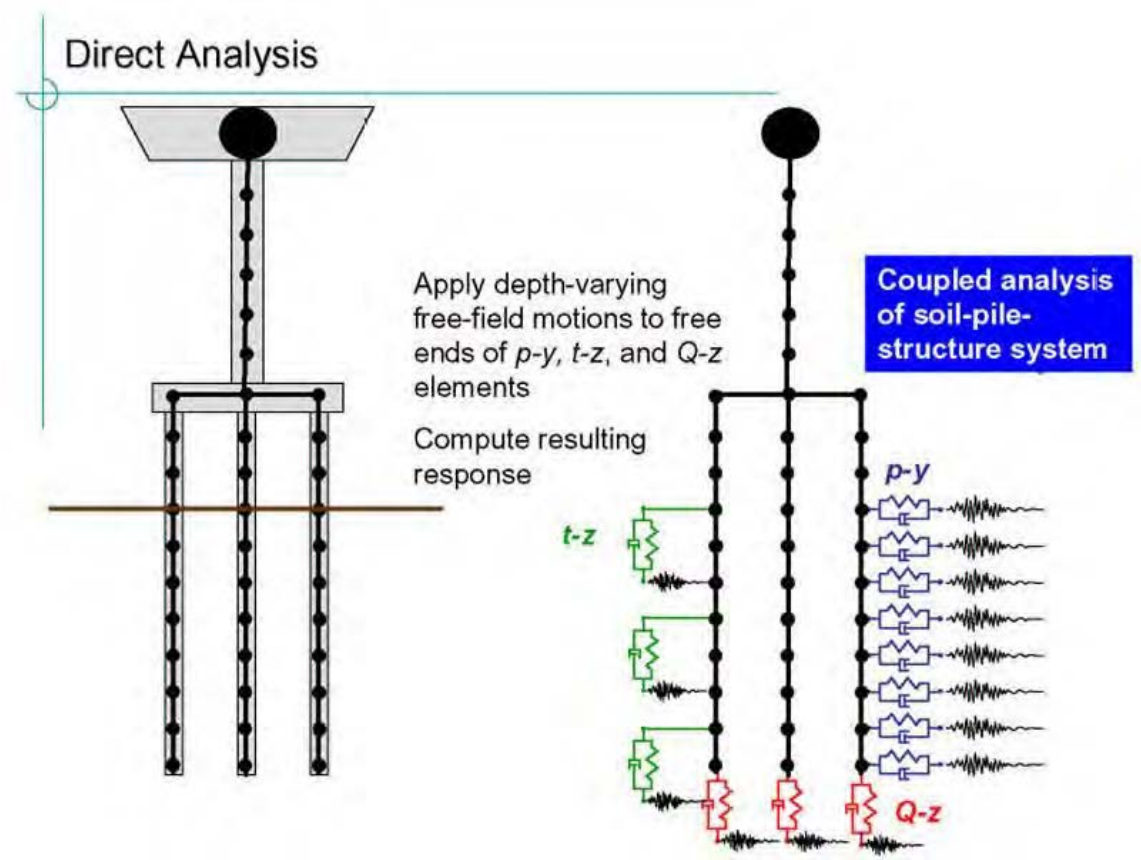

Figure 2.7. Direct (or Total) soil-foundation-structure kinematic interaction model (Kavazanjian et al. 2011)

2.5 Software

The leading software packages used in the simulation of deep foundation soil structure interaction are LPile (Ensoft 2013(b)), GROUP (Ensoft 2013(a)), and FB-MultiPier (BSI 2013(b)). FB-Multipier can be used to perform both the substructure and direct analysis. FB-Multipier was used for this task.

2.5.1 Overview of FB-MultiPier

FB-MultiPier is a hybrid finite element analysis program developed by the Bridge Software Institute (BSI), which is headquartered at the University of Florida in Gainesville, FL. It is capable of modeling multiple bridge pier structures that are interconnected by single representative bridge spans. The full structure can be subjected

to a full array of AASHTO load types in a static analysis or time varying load functions in a dynamic analysis (BSI 2013(b)).

The structural elements that it is capable of simulating include foundation element(s) (piles and drilled shafts), pile cap(s), column, and pier cap. All of the structural elements can be uniquely modeled by the user. The program also provides standard sections for many common foundation elements (H-pile, drilled shaft, prestressed concrete pile, pipe pile, etc.). For the soil-foundation interaction, FB-MultiPier uses axial (t-z, Q-z), lateral (p-y), and torsional (T-θ) nonlinear spring functions (soil springs). It uses 2-node finite elements below the ground surface to model the pile, placing the corresponding axial, lateral, and torsional soil springs at each element. The number of 2-node finite elements can be varied from five to fifty below the ground and for the free length of the pile (if any). FB-MultiPier employs several soil spring functions to characterize the soil stiffness as well as the capability to enter a customized set of ten curve points if none of the default soil springs are suitable.

FB-MultiPier uses an iterative solution method to solve for the structural displacements. This method follows a secant approach where FB-MultiPier finds the stiffness of the soil and structure for a computed set of displacements, assembles a stiffness matrix, and then solves for a new set of displacements. Convergence is achieved when the system is in static equilibrium. This is determined by comparison of the magnitude of the highest out-of-balance nodal force and the tolerance defined by the user in the input file. If the highest out-of-balance force is lower than the tolerance, the system is in static equilibrium and the program terminates. If the program did not converge, it is likely due to one of three reasons: (1) structural failure, (2) soil failure, or

(3) numerical instability. Structural failure occurs when a plastic hinge develops within the model and the shaft/column/pile cannot distribute the load any longer and subsequently, does not converge to a solution. Soil failure occurs when the displacements of the soil springs are large enough that the soil cannot absorb any more load. This leads to large out-of-balance forces. Numerical instability can occur from a combination of things within the model such as secondary moment effects, time stepping issues, corrupt input data, etc. The output files are a good indication of what causes the model to fail (especially the last time-step) and should always be reviewed.

The following sections provide a brief introduction to the system processes and various models employed by FB-MultiPier and are taken (in most part) from the FB-MultiPier User's Manual (user's manual) (BSI 2013(b)). Refer to the user's manual for further details and relevant information.

2.5.2 Dynamic Analysis Methods

There are two methods that FB-MultiPier employs to predict the dynamic response of a system: transient dynamic (time-history) analysis and modal response analysis. Both dynamic analysis options are briefly discussed herein. For more detail on either analysis type, see Fernandes (1999).

2.5.2.1 Time-History Analysis

FB-MultiPier uses time-history analysis to simulate the structural response under an earthquake event. This is done by loading an earthquake record into the program. FB-MultiPier has built in functions and also allows the user to upload their own. The functions can be either applied as load versus time or acceleration versus time. The "load versus time" functions are generally for impact analysis such as a barge impact.

Time-history analysis allows significant inertial and damping effects to be considered when determining the structural response. This done by using implicit time integration algorithms to obtain a numerical solution to the equation of motion.

FB-MultiPier has the option of using either the Newmark or Wilson-Θ method to determine the numerical solution of the equation of motion by using discrete time increments specified by the user. Typically, the same time step is used in that of the time function. It is possible, however, to use a larger time step to reduce analysis time if the time-history event is long. This skips over some time steps and may miss a few peaks, but generally it is not significant in the overall response of the structure. For more detail regarding time-history analysis, see Fernandes (1999).

2.5.2.2 Modal Response Analysis

Modal response analysis performs a response spectrum analysis of the structure in its equilibrium position (BSI 2013(b)). The equilibrium position being the response of the system after it was statically loaded. Figure 2.8 shows the cycle for how modal analysis is conducted within FB-MultiPier. To perform modal analysis, FB-MultiPier requires the number of modes in which to run and a spectral acceleration function (acceleration versus frequency). Global damping factors can be applied if applicable. Fernandes (1999) describes the modal analysis process within FB-MultiPier:

> *In the first cycle the earthquake is applied to the structure and the initial forces at the base of the piers are computed. Initially the springs that represent the foundation are considered very stiff, to simulate fixed supports. Then for each column a vector of six forces is generated, the three forces F_x, F_y, and F_z in the x, y and z directions, and the three*

respective moments. Then each of these forces is applied to the foundation, one at a time, like in a regular static analysis. This will produce three displacements, d_X, d_Y, and d_Z, in the x, y, and z directions, and three respective rotations, θ_X, θ_Y, and θ_Z, at the base of each column.... After all six forces are applied we have the six by six flexibility matrix for the foundation, one (flexibility matrix) for each column. Inverting this matrix we obtain the new stiffness for the foundation, which becomes the foundation springs for the base of each pier for the next cycle.

Note that the force vectors generated represent the foundation response. Once two consecutive forces are within the user defined tolerance, the program terminates. Note that in this analysis, the structure is considered linear, but the springs generated for each cycle will have characteristics of nonlinear behavior (Fernandes 1999).

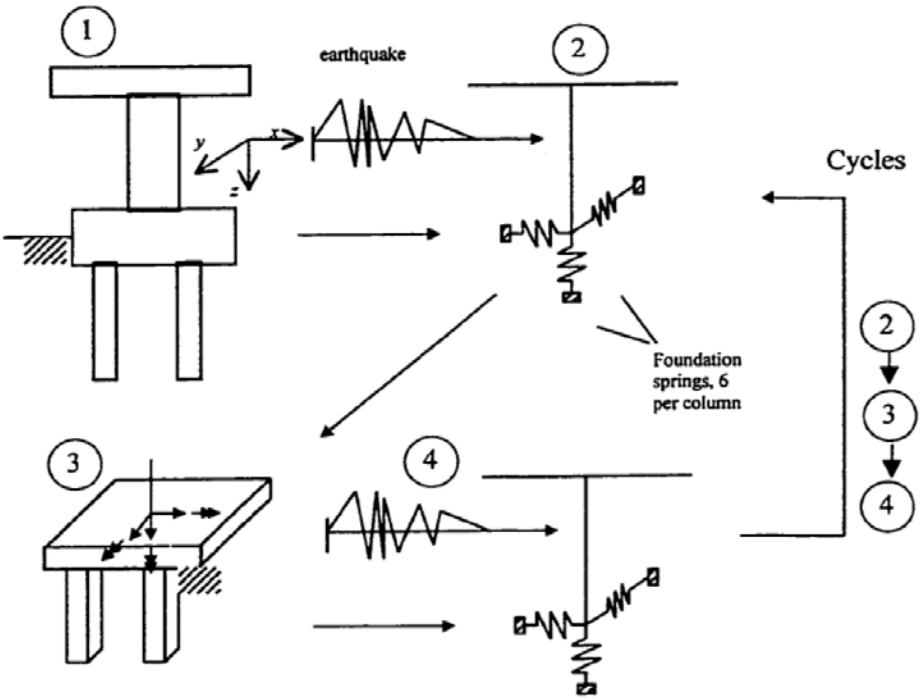

Figure 2.8. Modal analysis process for a bridge pier within FB-MultiPier (Fernandes 1999)

2.5.2.3 Damping

Damping is a complex and important part of structural response during dynamic loading. It reduces the free motion vibrations in an oscillatory system. Damping effects in a real system, such as a bridge, are due to friction, air resistance, or other external or internal (within the damped system) physical mechanisms. FB-MultiPier employs Rayleigh mass and stiffness damping factors in time-history analysis. In the initial development of the dynamic analysis option in FB-MultiPier (Brown et al. 2001), Rayleigh mass and stiffness damping factors for the pier, piles, and soil were determined based on field tests correlated to the program results. The Rayleigh damping factors used in Brown et al. (2001) are presented in Table 2.3.

Table 2.3 – Rayleigh damping factors used in Brown et al. **(2001)**

	Mass (α)	Stiffness (β)
Pier	0.04	0.01
Piles	0.001 (steel)	0.001 (steel)
Soil	0.015	0.015

2.5.2.4 Dynamic Relaxation

Dynamic relaxation within FB-MultiPier accounts for a static dead load before the transient dynamic load is applied. Static analysis of the structure is conducted before the dynamic load is applied and a new stiffness matrix and nodal displacement vector are obtained through the static analysis once the system is in equilibrium (BSI 2013(b)). This new initial stiffness and nodal displacement vector is then used in the dynamic time-history analysis. If this option is not used, it will apply the dead load as an impact load simultaneously with the dynamic load (BSI 2013(b)). This can exaggerate the dynamic structural response, and therefore, any assessment made based on that response is unreliable (BSI 2013(b)).

2.5.3 FB-MultiPier Limitations

While FB-MultiPier is a very powerful program, there are several limitations that the user should be aware of. These limitations can affect the quality of the output. Therefore, it is important to understand them to properly interpret the output generated. Most of these limitations directly affect the dynamic analysis.

- FB-MultiPier can only apply 100 percent of the ground motion in the X, Y or Z direction (or a combination of the three). It cannot apply, for example, 30 percent in the X direction and 70 percent in the Y direction.

- There is an apparent limitation in the number of decimal places the time and acceleration values can be in the ".acc" input files. If the time step was originally 0.005 seconds, duplicating numbers would be read by the program due to rounding by the program. Also, if the time step was 0.01 seconds and the time history function is over 100 seconds long, the program would only recognize numbers to the accuracy of 0.1. For example, the program would read 100 until 100.05, and then read 100.05 as 100.1 and so forth until it reached 101.05. This can cause numerical error within the program.
- FB-MultiPier has a memory restriction of 4GB. This is too low for a dynamic model with many piles and structural members, and causes the program to crash due to insufficient memory capacity. Increasing the time step was an option to lower the amount of memory needed for analysis. BSI is currently in the process of correcting this memory restriction.
- Batch mode cannot be used when using the dynamic relaxation option. The program will not start the dynamic analysis after the static analysis is completed to use the new stiffness matrix and displacements. BSI is currently in the process of correcting this issue.

2.6 FHWA LRFD Seismic Analysis and Design of Bridge Foundations

Recently, the FHWA sponsored the revision of GEC-3 (Kavazanjian et al. 2011), to include the LRFD guidelines developed by AASHTO. Along with Kavazanjian et al. (2011), a course was developed (Kavazanjian et al. 2012) that aims to illustrate the principles and methodologies for LRFD seismic analysis and

design of geotechnical features and structural foundations for bridges (Kavazanjian et al. 2012). Three design examples were presented to show the procedures that need to be addressed in the seismic design process in accordance with AASHTO specifications for LRFD seismic design (Kavazanjian et al. 2012). There are several points of emphasis pertaining to geotechnical considerations that were addressed in Kavazanjian et al. (2012) document:

1. Development of the acceleration response spectrum for use in structural design, including adjustment for local site conditions.
2. Deaggregation of the seismic hazard to get the earthquake magnitude for seismic stability analysis.
3. Evaluation of lateral pile stiffness (p-y behavior) for the piles for both the abutments and the central piers (substructure analysis)
4. Evaluation of vertical pile capacity (including uplift) and spring stiffness for both abutment and central pier piles (substructure analysis).
5. Evaluation of the seismic stability of the abutment slope.
6. Evaluate the seismic passive resistance and spring stiffness of the abutment wall.
7. Evaluate liquefaction and lateral spreading potential of slopes at the abutments.
8. Evaluation of the bearing capacity, sliding resistance and spring stiffness of the pier and abutment footings (if applicable).

All of these points of emphasis are discussed in detail in Kavazanjian et al. (2011).

2.7 Pile Failure Modes

During an earthquake, deep foundations have the capacity to perform well and maintain overall stability. However, it is important to understand the different failure modes a pile can

undergo during an earthquake. This allows the engineer to design the proper foundation while accounting for the different failure modes that could occur. Pile failure can occur in several different ways. The mechanisms of pile failure are shear force and flexure failure, and excessive settlement, all of which can be induced by several different modes. There are two primary categories of pile failure during an earthquake: (a) pile failure without liquefaction-induced phenomena and (b) pile failure with liquefaction-induced phenomena (Wei et al. 2008). A brief description of each category is presented:

A) Pile failure with no liquefaction-induced phenomena

1) Failure due to the inertial force of the superstructure

   Ishihara (1997) described this as the 'top down effect' because the inertial force exerted by the superstructure is transferred down to the upper portion of the pile, inducing large bending moments at the pile cap and pile head(s). Therefore, most of the damage and pile failure is located at joints between the pile cap and pile head or at the top of the pile (Wei et al. 2008).

2) Failure at the interface of soft and hard soil layers (Wei et al. 2008)

   Excessive bending moment and shear force can also develop at the interface of two distinct soil layers of differing strength (i.e. a large deposit of soft clay over very dense sand). Wei et al. (2008) also states that the p-y curve method, which is commonly used to determine the response of deep foundations, cannot reflect the actual situation that occurs between the two soil layers; therefore, careful consideration and proper engineering judgment should be used to determine the most representative response of a deep foundation system in this situation.

3) Pile settlement due to thixotropy

Thixotropy is a unique phenomenon that generally occurs in flocculated clayey soil. Thixotropy is a time-dependent process that occurs when the soil is softened due to remolding of the soil skeleton that is induced by a dynamic loading; it then returns to its original, harder state after the loading is over and the particles realign (McCarthy 2007). Thixotropy of soft soil can occur during an earthquake, therefore, the axial resistance of the soil can be greatly reduced which could cause excessive settlement.

4) Retaining wall or embankment near pile foundations (Wei et al. 2008)

Earthquakes can cause retaining wall or embankment failures without the soil liquefying (i.e. tension cracks, etc.) during and after the event. The soil could induce large passive pressures on the pile foundation should the soil mobilize, which could lead to excessive bending moment and ultimately structural failure of the pile.

B) Pile failure with liquefaction-induced phenomena (Wei et al. 2008)

1) Failure without lateral spreading

If the soil liquefies, but does not undergo lateral spreading, it can create non-uniform distributions in liquefied strength and thickness of the soil (Wei et al. 2008). The load distribution of the structure can become eccentric which could lead to differential settlement. However, if the distribution of soil strength and thickness are uniform, the pile could still fail at the liquefied and non-liquefied soil interface due to the inertial loading of the structure (Wei et al. 2008).

2) Failure with lateral spreading

Bridges often span rivers. The soil profile of these areas often includes liquefiable sand and silt layers sloping towards the river (Wei et al. 2008). If the liquefied soil is present below the ground surface, the non-liquefiable soil (crust) above the liquefied layer can

place a significant amount of passive pressure on the pile foundations as the liquefied soil displaces the top layer during liquefaction (Berrill et al. 2001). This results in increased shear and bending at the pile head and cap. The lateral and axial resistance of the soil also drastically decreases, and the pile can become unstable. The main cause for pile failure during an earthquake is thought to be due to lateral spreading around the pile according to a report published by National Research Council (NRC) Committee on Earthquake Engineering (1985). They go on to claim that lateral spreading is responsible for more damage during an earthquake than any other mode of ground failure due to liquefaction. This failure mechanism is widely accepted and has been used as the explanation for pile failure in many earthquakes (Bhattacharya 2003).

Another failure mechanism that can develop during an earthquake that does not necessarily lie within the two categories previously described is pile buckling. Typically, buckling is accounted for in design by considering: (a) piles in very soft clay, (b) during installation by driving, and (c) partially exposed piles such as offshore platforms or jetties (Fleming et al., 1992) Recently there has been research (Bhattacharya et al. (2004), Knappett and Madabhushi (2005), Kimura and Tokimatsu (2005), and Shanker et al. (2007)) suggesting that this is an important aspect of pile foundation design for earthquake loading and should be accounted for (Bhattacharya et al. 2008).

2.8 Pile Performance under the combined Effect of Earthquake and Scour

The combined effect of flood-induced scour and earthquake hazards is a complex problem. There are three components of scour that should be considered: (a) long-term aggradation and degradation, (b) contraction scour, and (c) local scour (Ghosn et al. 2003). Aggradation and degradation is long-term elevation change due to deposition or erosion of the

streambed of the waterway. Contraction scour is often due to the bridge embankments constricting the main channel (causes water to accelerate). Local scour occurs when the water around the bridge piers accelerates in concurrence with rising water levels (Ghosn et al. 2003).

Because of the uncertainty of when an earthquake will occur, it is possible that the soil could scour around a bridge before or even during an earthquake. One of the major questions is how much scour to account for during the design process. If the insitu soil is susceptible to scour, the lateral stiffness of the foundation can be significantly reduced by the lack of soil resistance. However, scour can possibly reduce the applied inertial forces, which could also reduce the demand for lateral capacity (Ghosn et al. 2003). This means that scour has the potential to be both harmful and beneficial to bridge response during an earthquake; therefore, it is important to check different scenarios.

In Ghosn et al. (2003), the authors suggest using a scour factor of 0.25 (25% of the maximum anticipated scour depth be used in design) when combining scour and earthquake events. This was based on the fact that the inertial forces are partially offset by the reduction in soil resistance capacity due to scour. They presented the following load combination:

$$\text{Extreme Event VI:} \quad 1.25\,DC + 1.00\,EQ; \; 0.25\,SC$$

where:

DC	=	Dead Load
EQ	=	Earthquake Load
SC	=	Design Scour Depth

The second recommendation they provide is to design the foundations so that they are twice the length of the scour depth. This recommendation attempts to ensure that the resistance capacity needed to resist an earthquake event will not be reduced below the demand. However, some instances may necessitate longer foundation lengths, and this recommendation should be a

minimum controlling factor when considering scour in design. It should be noted that the design scour depth used in the Ghosn et al. (2003) is based on Richardson and Davis (1995).

2.9 Summary

This chapter has reviewed the reasons why new design standards are necessary for bridges in Alabama. Changes in the seismic hazard maps and research in earthquake engineering have been included in the LRFD and Guide Specifications, but not in the Standard Specifications. These changes have resulted in the bridges in Alabama being classified in higher seismic design categories, which requires different design procedures and has significant impacts on the design requirements for a bridge. The old standards are not based on the new design requirements, and therefore must be updated. The horizontal design forces have also changed, and the superstructure to substructure connection needs to be updated to ensure it can resist these new forces and maintain the load path.

Chapter 3: Superstructure-to-Substructure Connection

3.1 Introduction

The first task to be studied in this report is the investigation of the superstructure-to-substructure connection, because the results of this task will be included in the development of new design standards. One of the most important aspects of bridge engineering is ensuring a complete load path exists. If there is any element of the bridge that is unable to provide a complete load path, the bridge will not behave as designed and may suffer unexpected failure. The superstructure should be able to resist all of the forces and transfer them to the ductile substructure. Thus, the connection between the superstructure and substructure is very important to ensuring the ductility of the bridge. It must be able to resist the loads in each orthogonal direction and transfer them to the substructure. ALDOT had expressed concern about the current connection and wanted to find another option that is simple to construct, cost effective, and structurally safe. So the first step was to analyze the current ALDOT connection and determine if it was adequate to transfer the loads. Once the problem areas of the connection were identified, other connections from state DOTs were studied to determine if they could be used to design a new connection that addressed the design issues as well as be constructible and economical. This chapter will detail the steps that were taken to design the new connection. Only the connections used to develop new designs will be shown. All design checks and calculations for this chapter can be found in Appendix A.

3.2 Connection Study

The first step was to review the current connection used by ALDOT, seen below in Figure 3.1. The precast beam rests on the bearing pad and is connected to the bent cap by two steel angles. A 3-inch cap screw with a diameter of 0.875 inches is attached to the side of the beam and an anchor bolt is attached to the bent cap (Alabama DOT, 2012). The two directions of movement are transverse and longitudinal. In the transverse direction, the angles are expected to transfer the loads into the anchor bolts, and in the longitudinal direction, the cap screws would transfer the loads into the anchor bolts. However, after discussion with the Bridge Bureau, it was determined that the cap screw inserts were not adequate to resist the longitudinal forces and a new design in the longitudinal direction was necessary. With this in mind, the other connections from other state DOTs were studied. The clip angles that resist loads in the transverse direction were assumed to be adequate, but this assumption is discussed in Chapter 4.

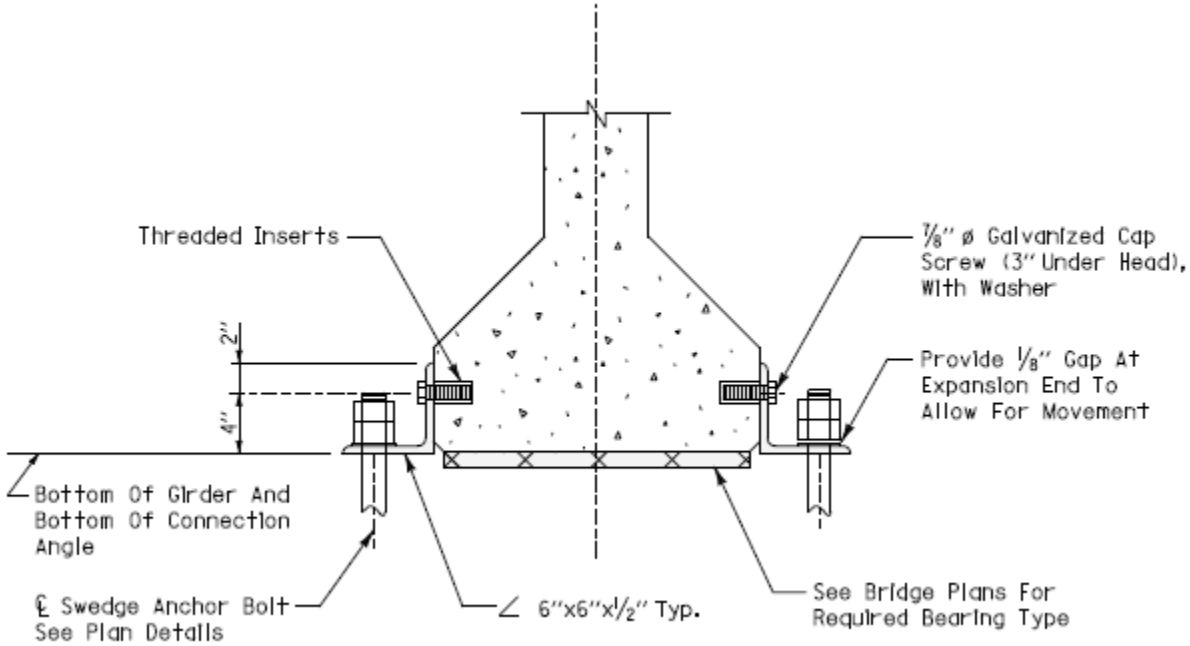

Figure 3.1: Alabama DOT Connection

3.2.1 Modified ALDOT Connection

In a previous study conducted at Auburn University, a modified connection was proposed. This connection is seen in Figure 3.2. By placing a bolt through the bottom of the girder, the longitudinal restraint of the connection was achieved by increasing the bearing area of the concrete which would allow the forces to be transferred into the anchor bolts. The rest of the connection stayed the same, so this design allowed the connection to transfer the forces into the bent cap. However, this bolt interferes with the prestressing strands in the concrete girder. Since these strands in the girder could not be moved without sacrificing strength and ductility, it was determined that the modified connection would not be acceptable (Coulston & Marshall, 2011).

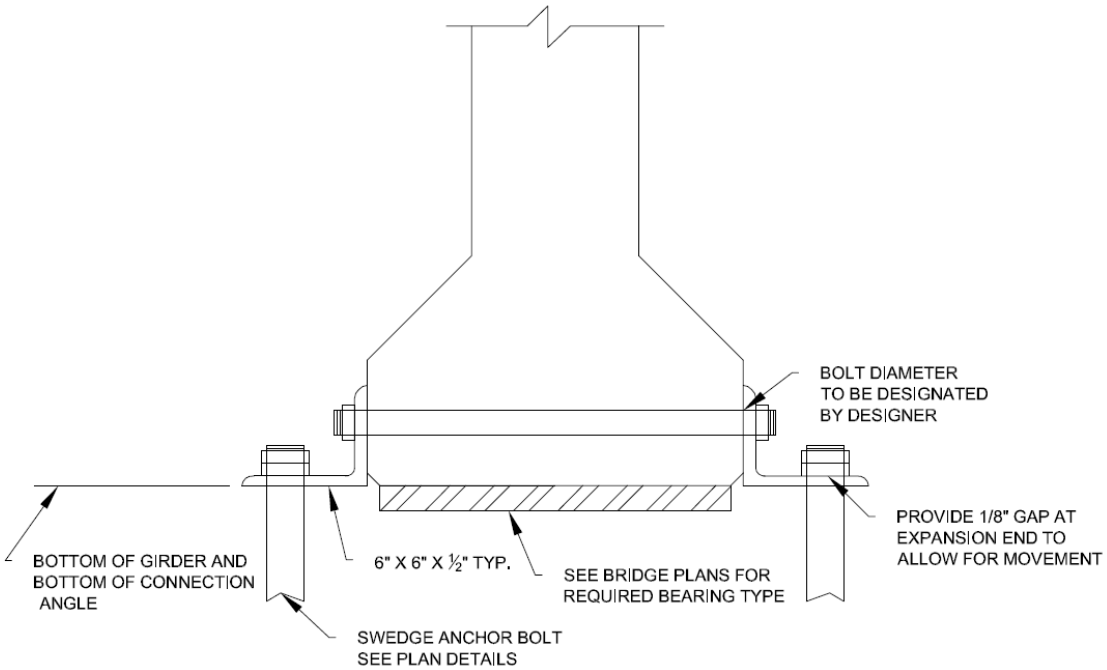

Figure 3.2: Previously Modified ALDOT Connection

3.2.2 Illinois DOT

The connection used by the Illinois DOT was also studied. This connection was designed after Illinois conducted research into its earthquake resisting system (ERS). Their new ERS

utilizes three tiers to prevent span loss. The first tier is the connection between the superstructure and substructure, seen in Figure 3.3. This connection is designed to provide resistance in the transverse direction. In the longitudinal direction, no restraint is provided, as is evident in the figure. This will result in the connection slipping during a design earthquake, which will dissipate energy. However, the seat width must be large enough to allow the superstructure to "ride out" the remainder of the earthquake since it will not be restrained in the longitudinal direction. The second tier of the ERS is to provide additional seat length. This seat length, calculated using Equation 3.1, is larger than the seat length as calculated in the LRFD Specifications. The third tier includes plastic hinging of columns and foundation elements. The connection has a steel plate cast with the bottom of the concrete girder. The bearing pad assembly is then connected to the girder by pintles. The assembly resists transverse movement by side retainers connected to the bent cap by two anchor bolts (Tobias, Anderson, Hodel, Kramer, Wahab, & Chaput, 2008). This connection has the same problem of the current ALDOT connection, which is a lack of restraint in the longitudinal direction. For this reason, it was not studied further. Other aspects of the Illinois ERS, however, were studied and will be discussed later in this chapter.

$$N = \left(0.10 + 0.0017L + 0.007H + 0.05\sqrt{H}\sqrt{1 + (2\frac{B}{L})^2}\right) * \left(\frac{1+1.25F_vS_1}{\cos(\alpha)}\right) \qquad \text{Equation 3.1}$$

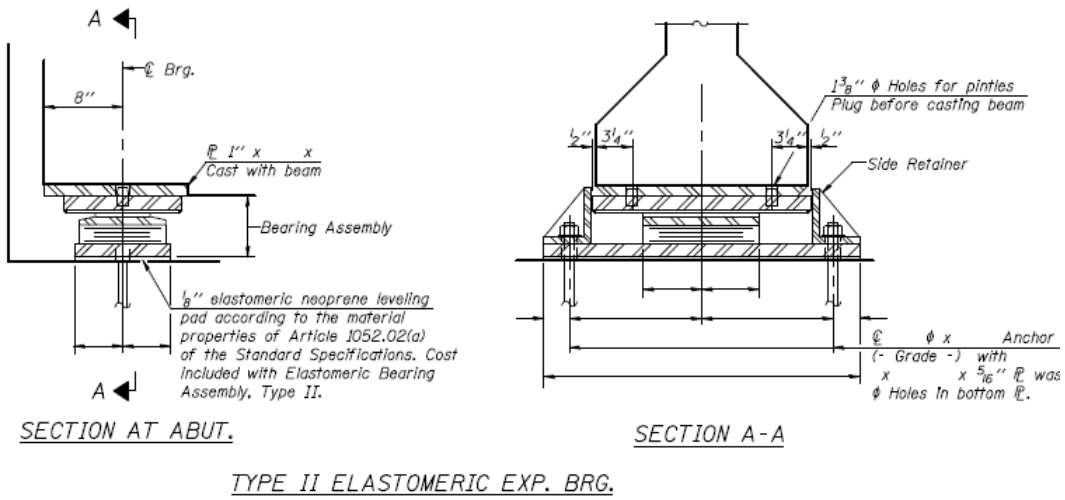

Figure 3.3: Illinois Connection

3.2.3 North Carolina DOT

The next connection that was studied can be seen in Figure 3.4 and is the North Carolina DOT connection. A steel plate is cast on the bottom of the concrete girder. This plate is welded to the sole plate in accordance with detail "A" (Figure 3.5). The sole plate is placed on top of an elastomeric bearing pad, and the entire assembly is connected to the bent cap through two anchor bolts. The sole plate and bearing pad can be slotted to accommodate an expansion joint. The weld and the anchor bolts are designed to resist the horizontal forces in both the transverse and longitudinal directions (North Carolina DOT, 2012). This connection is very similar to the next two connections to be studied, the South Carolina DOT connection and Missouri DOT connection. Because of their similarity, the other two connections will be discussed before a specific analysis is performed.

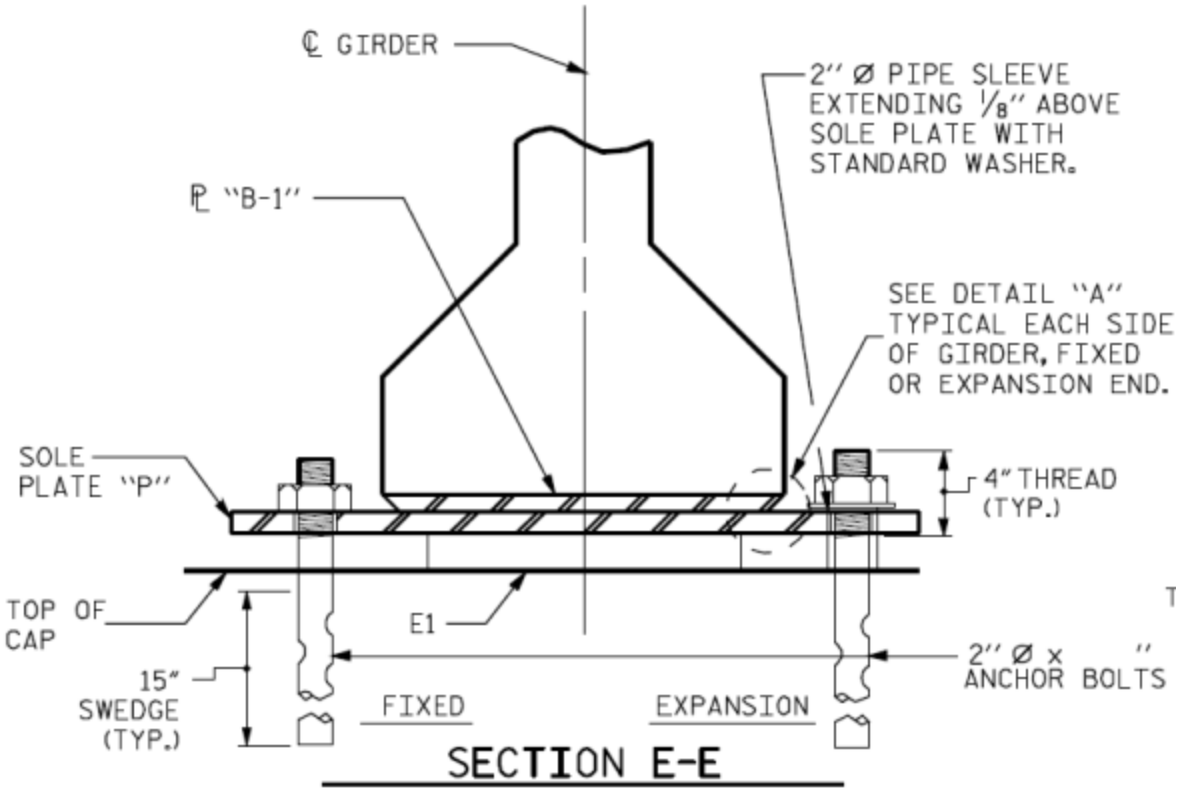

Figure 3.4: North Carolina DOT Connection

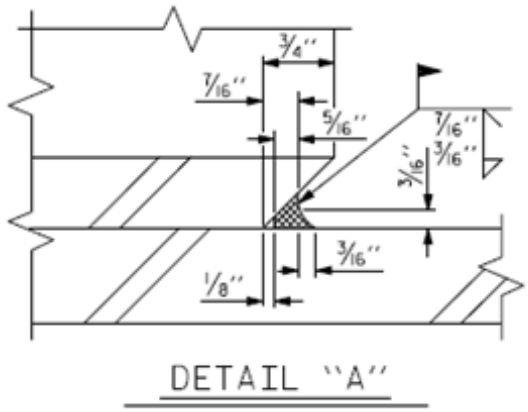

Figure 3.5: North Carolina DOT Connection Detail "A"

3.2.4 South Carolina DOT

The South Carolina DOT connection, seen in Figure 3.6, is used for both expansion and non-expansion bearings. A sole plate is cast with the precast beam and welded to the bearing plate. Two anchor bolts connect the entire assembly to the bent cap. The welds and anchor bolts are designed for the horizontal forces in each direction. For expansion bearings, the bearing plate is slotted to allow for movement (South Carolina DOT, South Carolina Bridge Design Manual, 2006). This connection is very similar to the North Carolina connection because it uses an embedded sole plate welded to a bearing plate that transfers the forces into the bent cap. The Missouri connection will be discussed next, and then the results of an analysis will be presented.

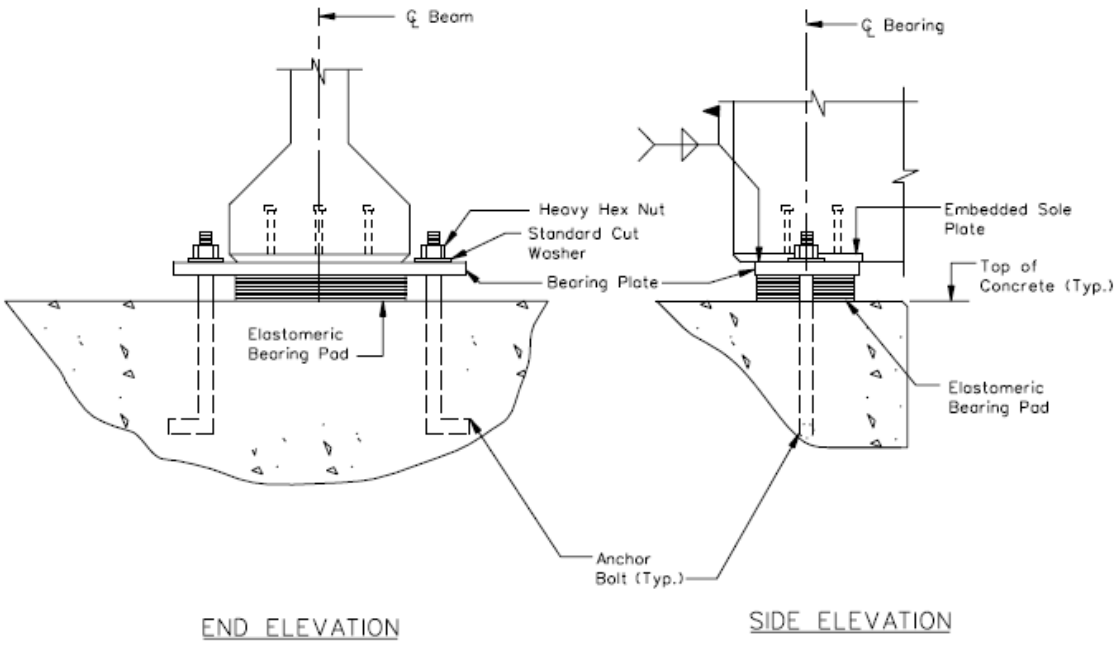

Figure 3.6: South Carolina DOT Connection

3.2.5 Missouri DOT

The Missouri DOT Connection is detailed in Figure 3.7. An anchor plate is cast at the bottom of the girder and welded to a steel plate on top of the elastomeric bearing. This steel plate is bolted to the bent cap with two anchor bolts, which transfer the loads to the bent cap.

The anchor bolts are placed above the bearing pad to reduce the deformations in the pad. The weld and anchor bolts provide the resistance for the longitudinal and transverse horizontal forces (Missouri DOT, Bridge Standard Drawings - Bearings, 2009). As mentioned earlier, this connection is very similar to the North Carolina and South Carolina connections. The weld resists the forces in both directions and allows the anchor bolts to transfer the forces into the bent cap. ALDOT has a welded connection design in its standard drawings, seen in Figure 3.8, so it was assumed that the contractors would be familiar with it and be able to construct it. The weld could be designed to resist the appropriate horizontal design force for a specific bridge and also would eliminate the need for cap screws, which were assumed not to transfer any load. For these reasons, a welded design was chosen to be used as the basis for a new connection design. This design will be discussed below.

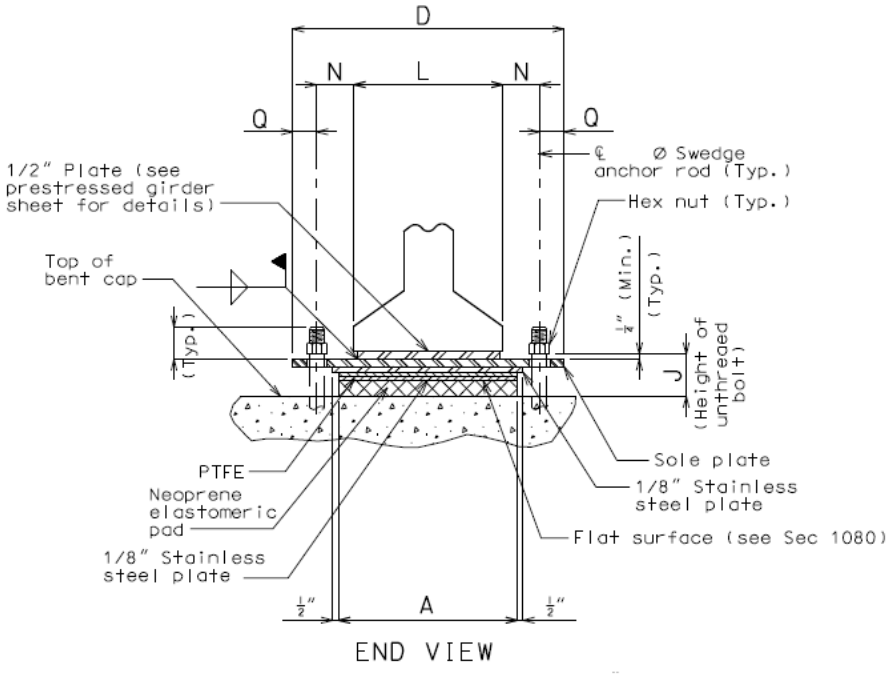

Figure 3.7: Missouri DOT Connection

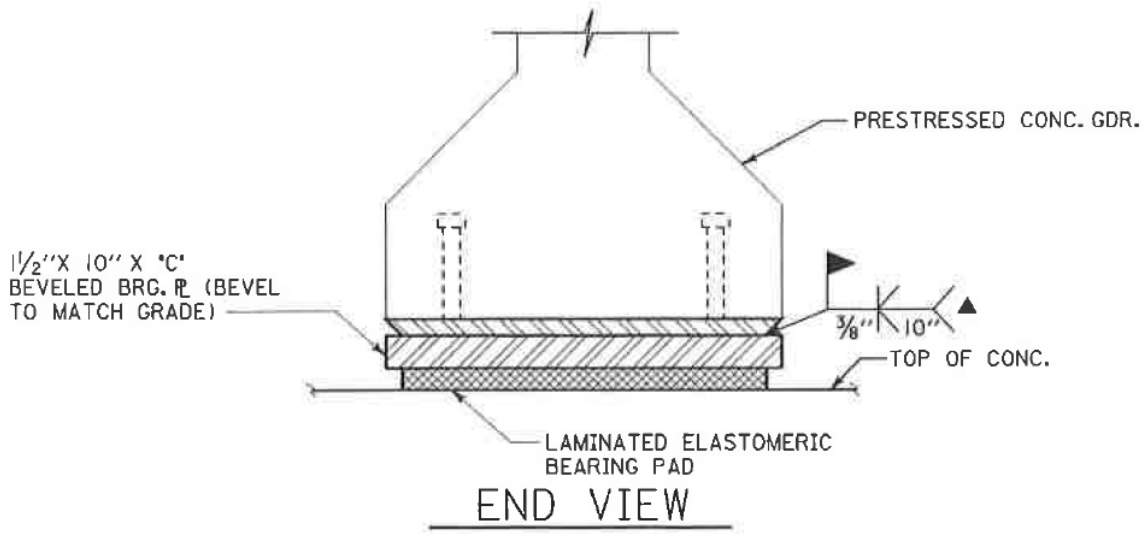

Figure 3.8: ALDOT Welded Connection

3.2.6 Connection Recommendation

The welded plate connection used by ALDOT was used as the backbone for the new design connection. The new connection can be seen in Figure 3.9 and has a sole plate that is cast with the bottom of the concrete girder. Shear studs protrude from the plate into the girder to transfer the forces from the girder. The sole plate would be welded to another plate that rested on the bearing and anchor bolts would connect the assembly with the bent cap. The weld would provide sufficient restraint in both directions, and the anchor bolts would transfer the loads into the bent cap. Another option would be to have the anchor bolts cast with the sole plate, eliminating the need for a weld. However, after discussion with ALDOT, it was decided to keep the current connection because there was concern about the ability of their contractors to be able to transition to a new connection design. Instead, it was decided to allow the connection to move in the longitudinal direction. In order to prevent span loss, either the displacements would be decreased by using longitudinal restrainers, or the seat width would be increased. After discussion with ALDOT, it was decided to use an extended seat width to prevent span loss.

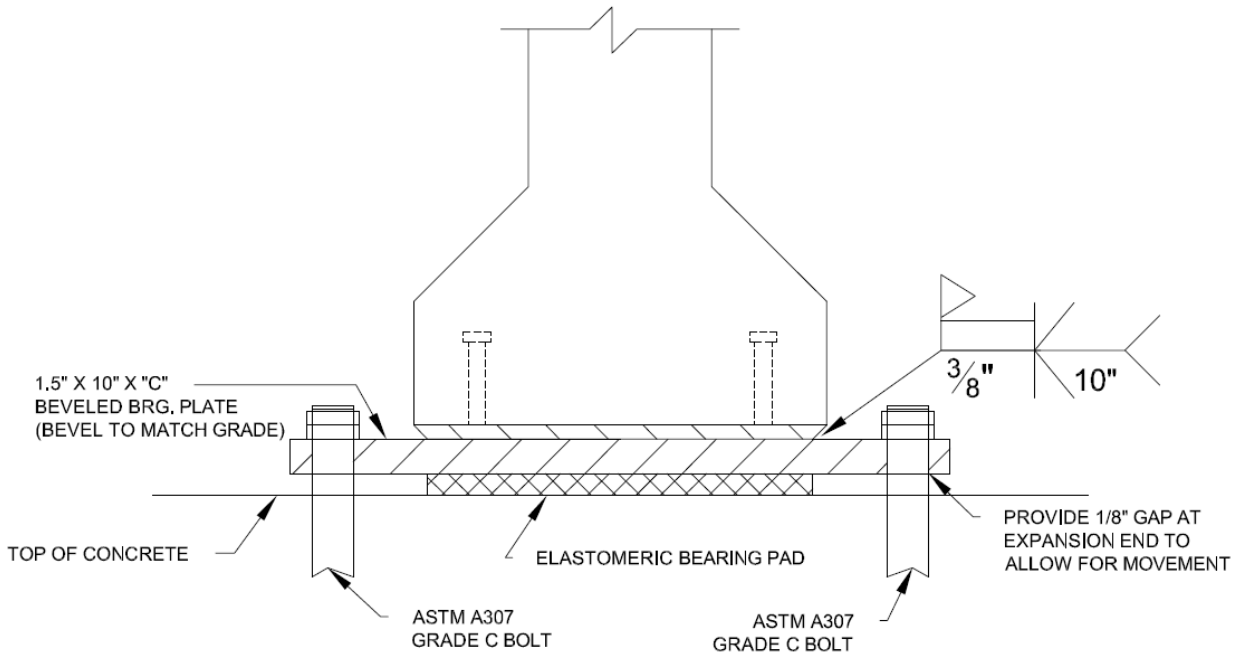

Figure 3.9: Proposed Weld Connection

3.3 Extended Seat Width

As discussed earlier, a second option exists to prevent span loss. By extending the minimum seat width for the girders, more room can be provided for the girders to displace once the connection slips to prevent unseating. This technique is utilized by Illinois DOT as discussed earlier. The equation used by Illinois was one of two alternate equations that was compared with the current seat width calculations in the Guide Specifications to determine if they provided more seat width for the bridges studied.

The current method of calculating the seat width uses Equation 3.3 from the Guide Specifications in Article 4.12.2. It is based on the span length, column height, and skew of the bridge. 100% of this equation is required to be supplied in SDC A and 150% is required to be supplied for SDC B, C, and D.

$$N = (8 + 0.02L + 0.08H) * (1 + 0.000125S^2) \qquad \text{Equation 3.3}$$

The first alternative was Equation 3.1 which is used by the Illinois DOT as shown earlier in the chapter. This equation was selected because the Illinois earthquake resisting system design strategy, which is to allow the girders to "ride out" the design earthquake, is similar to the desire strategy presented in this report. This equation is based on research performed by the Applied Technology Council (ATC) and the Multidisciplinary Center for Earthquake Engineering Research (MCEER) in 2003. It gives a better estimation of the expected displacements and deformations that occur at the seat (ATC/MCEER Joint Venture, 2003). Instead of multiplying the seat width by 1.5 for SDC B, which is the procedure found in the Guide Specifications, the multiplier is based on the expected spectral acceleration coefficient at a 1-second period, S_{D1}. As such, the seat width can vary for different sites in SDC B. The largest and lowest values of S_{D1} (0.15 and 0.30) will be used to find the seat width using this method and compared to the results from the other methods. The equation was converted from metric units into English units in Equation 3.4.

$$N = \left(0.10 + 0.0017L + 0.007H + 0.05\sqrt{H}\sqrt{1 + (2\frac{B}{L})^2}\right) * \left(\frac{1+1.25F_v S_1}{\cos(\alpha)}\right) \qquad \text{Equation 3.1}$$

$$N = \left(4 + 0.02L + 0.08H + 1.09\sqrt{H}\sqrt{1 + (2\frac{B}{L})^2}\right) * \left(\frac{1+1.25S_{D1}}{\cos(\alpha)}\right) \qquad \text{Equation 3.4}$$

The second alternative would be to perform a rigorous analysis that is required for SDC D. Article 4.12.3 in the Guide Specifications provides a minimum seat width equation, represented as Equation 3.5, for SDC D that uses the expected displacement demand instead of the column height and span length. The expected displacement demand was calculated for each bridge in SDC B using the structural analysis and computer bridge models in Chapter 4. The calculated seat width from this equation is not allowed to be less than 24 inches.

$$N = \left(4 + 1.65 * \Delta_{EQ}\right) * (1 + .00025 * S^2) \geq 24 \qquad \text{Equation 3.5}$$

Seat widths for each bent of each bridge studied in SDC B were calculated using each of the three equations. These seat widths were compared to determine which provided the greatest seat length. The results in Table 3.1 show that the maximum seat width depended on the S_{D1} coefficient for that particular site. In SDC B, it can range from 0.15 to 0.30. At 0.15, Equation 3.3 in the Guide Specification controls. But at 0.30, the Equation 3.4 from the ATC/MCEER study controls. This is because the multiplier for the Guide Specification equation is 1.5 for all sites in SDC B, and the multiplier for the ATC 49 Equation varies based on S_{D1}. The equation for SDC D did not control because all the calculated longitudinal displacements for these bridges were less than 1 inch (with one exception), so only small seat widths were determined. Technically these cannot be less than 24 inches, but in order to show the effect of the small displacements, values less than 24 inches were shown.

Table 3.1: Minimum Seat Width Calculations

Equation	Minimum Seat Lengths (in)								
	Bent Creek Road	Norfolk Southern Railroad	Little Bear Creek Bent 2	Little Bear Creek Bent 3	Oseligee Creek Bent 2	Oseligee Creek Bent 3	Scarham Creek Bent 2	Scarham Creek Bent 3	Scarham Creek Bent 4
Guide Spec SDC B	18.5	19.2	17.3	17.9	16.5	17.5	20.0	23.0	19.8
Guide Spec SDC D	5.7	5.7	5.7	5.7	6.1	6.3	5.7	5.7	5.7
ATC 49 (S_{D1} = 0.15)	17.1	18.2	14.3	15.8	15.2	17.4	19.9	25.1	19.5
ATC 49 (S_{D1} = 0.30)	19.8	21.1	16.6	18.3	17.6	20.1	23.1	29.1	22.6

As the table shows, for all but one of the bents, assuming S_{D1} equals 0.30 gave the most conservative value for minimum seat width. The current Guide Specification controlled the minimum seat width for bent 2 of Little Bear Creek bridge. This is a result of the small column

heights at this bent. But, because the ATC 49 equation is designed to give a better estimation of the seat displacement, and because the minimum seat width obtained from this equation is only one inch less than the current specifications, this anomaly was not considered important. Equation 3.4 was selected to be recommended assuming S_{D1} equals 0.30 because it would be the upper limit for SDC B and result in a larger value than the Guide Specifications equation. Since the equation has been researched by ATC and MCEER and designed to give a better estimation of the deformations and displacements at the seat and is currently in use by Illinois DOT, it is reasonable to assume that this equation will provide enough seat width to prevent the girders from unseating during a design earthquake.

3.4 Conclusion

This task was necessary because it was unknown if the current superstructure-to-substructure connection was adequate to resist the calculated horizontal design forces. After analysis, it was determined that it was adequate in the transverse direction, but not in the longitudinal direction, so a complete load path did not exist between the superstructure and substructure and a new connection design was necessary. Several options were investigated and designed, but ALDOT chose to keep the original connection design and allow the girders to move in the longitudinal direction after the connection slipped. This would be accomplished by providing additional seat width in the longitudinal direction using Equation 3.4 described above. Since the original connection design will continue to be used, the clip angles and anchor bolts will also have to be checked to ensure they can withstand the horizontal design forces. They will be checked in Chapter 4 for each bridge in SDC B to show if the connection is adequate.

Chapter 4: Bridge Design Standards

4.1 Introduction

The first task of this project was to determine if standard design details and drawings could be created for bridges in Seismic Design Categories (SDC) A and B. As discussed in chapter 2, the Guide Specifications contain updated seismic hazard maps that have higher expected ground motions than the maps in the Standard Specifications. These greater accelerations, along with changes to the bridge design resulting from additional research in earthquake engineering, have resulted in changes in the minimum details and seismic design procedures for bridges. By redesigning multiple bridges in each SDC that had previously been designed under the Standard Specifications and comparing the column details, the change in the design details could be shown and standard details could be developed. Along with the standard details, design sheets for each bridge were developed to provide examples of the new seismic design procedures. In the previous study by Coulston and Marshall (2011), design sheets and standards for three bridges in SDC B were created. These design sheets were updated to include changes in the Guide Specification from the 2009 edition to the revised 2011 edition, and design sheets for two additional bridges in SDC B were created. Design sheets for SDC A, which has two subclasses, were developed using the same revised 2011 edition. ALDOT supplied the design drawings for each bridge designed using the Standard Specifications, as well as a foundation report. While the expected ground accelerations a bridge would be expected to experience is typically determined from the Guide Specifications seismic hazard maps, this values were used that allowed different bridges to be placed in the SDC of choice. This allowed some bridges to be designed in multiple SDCs in order to show the difference in the details

resulting from the two design categories. The procedure for determining the SDC as well as the differences between the categories will be discussed further in this chapter.

Seven different bridges were chosen to be re-designed using the Guide Specifications in order to create new bridge standards. These bridge locations can be seen below in Figure 4.1, and are listed in Table 4.1. These bridges were supplied by ALDOT and were chosen because they are representative of many different bridges throughout the state. The two bridges in the southern part of the state, Stave Creek and County Road 39, are in low seismic hazard zones but assumed to be in poor soil conditions. The three bridges in the northern part of the state, Little Bear Creek, Scarham Creek, and Norfolk Southern Railroad, are in the highest seismic zones of the state but are assumed to be over rock. The three remaining bridges are a combination of the two. Having bridges in different locations allowed the standards to be applicable for bridges not just in high seismic zones, but throughout the state.

Table 4.1: Bridge Locations

Number	Bridge	Location
1	Little Bear Creek	Russellville
2	Scarham Creek	Albertville
3	Norfolk Southern RR	Gadsden
4	Oseligee Creek	Lanett
5	Bent Creek Road	Auburn
6	Stave Creek	Jackson
7	County Road 39	Mobile

Figure 4.1: Bridge Locations

The first subclass of SDC A, termed SDC A1 throughout this report, classifies bridges in seismic regions that are not likely to experience substantial ground accelerations and do not require minimum details. The two bridges designed in SDC A1 include the following: County Road 39 Bridge over CSX in Mobile County and Stave Creek Bridge in Clarke County. The design calculations and design sheets can be found in Appendices B and C**.**

The second subclass of SDC A, termed SDC A2, classifies bridges in low seismic regions that are not likely to experience plastic forces, but still require minimum detailing. The following four bridges were designed in SDC A2: Bent Creek Road Bridge in Lee County,

Bridge over Norfolk Southern Railroad in Etowah County, Oseligee Creek Bridge in Etowah County, and Stave Creek Bridge in Clarke County. The Stave Creek Bridge was also designed in the SDC A1 category. All of the calculations for these details can be found in Appendices D-G**.**

Finally, five bridges were redesigned in SDC B, including the three designed under the previous study. SDC B bridges are in a moderate seismic hazard and must be designed using additional analysis techniques and must also satisfy minimum detailing. The analysis of all five of the bridges was completed using computer software, with the results recorded in the design sheets. The design sheets and supplemental design data for these five bridges can be found in Appendices H-Q. The five bridges include the following: Bridge over Little Bear Creek in Franklin County, Bent Creek Road Bridge over I-85 in Lee County, Oseligee Creek Bridge in Chambers County, Bridge over Norfolk Southern Railroad in Etowah County, and Scarham Creek Bridge in Marshall County. Bent Creek Road Bridge, Oseligee Creek Bridge and Bridge over Norfolk Southern Railroad had also been designed as SDC A2 so their design details could be compared.

All bridge design sheets can be found in the Appendices and were created using Mathcad (PTC, 2007). The first step was to input the given bridge information at the beginning of the sheet, including the length of the bridge, span lengths, deck thickness and widths, girder cross sectional areas, etc. Other information needed for specific articles or bridge components, such as reinforcement type and spacing, were input at that location in the sheet. All of the input variables were notated with a green background and all output information necessary for design was notated with a yellow background. This allows the variables to be quickly located and changed during the design. The steps in the design sheets were laid out in the same order as the design charts in the Guide Specification. Each specific article used either in the Guide

Specifications or LRFD Specifications was cited. Each step of the design process will be discussed below.

4.2 SDC Determination

The first step in the design process is to determine the Seismic Design Category (SDC) of the bridge. The SDC will determine what type of analysis and detailing is necessary for the bridge. Chapter 3 of the Guide Specifications lists the steps involved in determining the design category. The soil site class is determined first. The site class plays a large role in the determination of the SDC, as a change from one class to the other can result in a change in the SDC. Site classes range from A (hard rock) to F (poor soil such as stiff clay) and are determined using either soil shear wave velocity, uncorrected blow counts, or undrained shear strengths. However, it should be noted that site classes A and B cannot be verified without performing a shear wave velocity test. Table 3.4.2.1-1 in the Guide Specifications is used to determine the appropriate site class.

The next step is to determine the response spectra from national ground motion maps. The AASHTO Ground Motion Calculator (AASHTO, 2007) was used to determine these ground accelerations. The latitude and longitude of the bridge site, along with the site class of the soil, is input into the program and the acceleration coefficient, A_s, design spectral acceleration coefficient at 1-sec period, S_{D1}, and design spectral acceleration coefficient at 0.2-sec period, S_{DS}, is output. If the longitude and latitude are not known, the zip code of the area can be used, but the spectral coefficients will not be as precise. Once S_{D1} is known, the seismic design category can be determined according to Table 4.2.

Table 4.2: SDC Category Determination

Value of S_{D1}	SDC
$S_{D1} < 0.10g$	A1
$0.10g \leq S_{D1} < 0.15g$	A2
$0.15g \leq S_{D1} < 0.30g$	B
$0.30g \leq S_{D1} < 0.50g$	C
$0.50g < S_{D1}$	D

In order to show the significance of the site class, the following three maps were created for Alabama. The AASHTO Ground Motion Calculator program (2007) was used to find the highest spectral accelerations for each county in Alabama. The SDC was determined for each county using three different site classes. The maximum spectral acceleration for each county in the northern half of the state was assumed to occur at either the northeast or northwest corner of the county since the maximum accelerations in the state are in the northeast and northwest corners. For the southern counties, the maximum spectral acceleration was assumed to occur at the northernmost point of the county. The results can be seen in Figure 4.2., Figure 4.3, and Figure 4.4. The entire state is classified as SDC A1 for soil site class B. This would also mean that soil site class A would result in the entire state being classified as SDC A1. For soil site class C, the northern part of the state is classified as SDC A2, with one county being in SDC B. Finally, for soil site class D, the majority of the state is at least SDC A2, with the northern part of the state being SDC B and the southern part of the state still in SDC A1. The changes in the soil site class can have a significant effect on the determination of the SDC, which affects the design of a bridge. It is recommended to use the soil shear wave velocity test to verify soil site class A or B at the site because it would result in the bridge being in SDC A1, generating a more

economical design. It should be noted that these maps are only an estimation of the spectral accelerations in each county. Certain sites may have higher values than the average value assumed over the county.

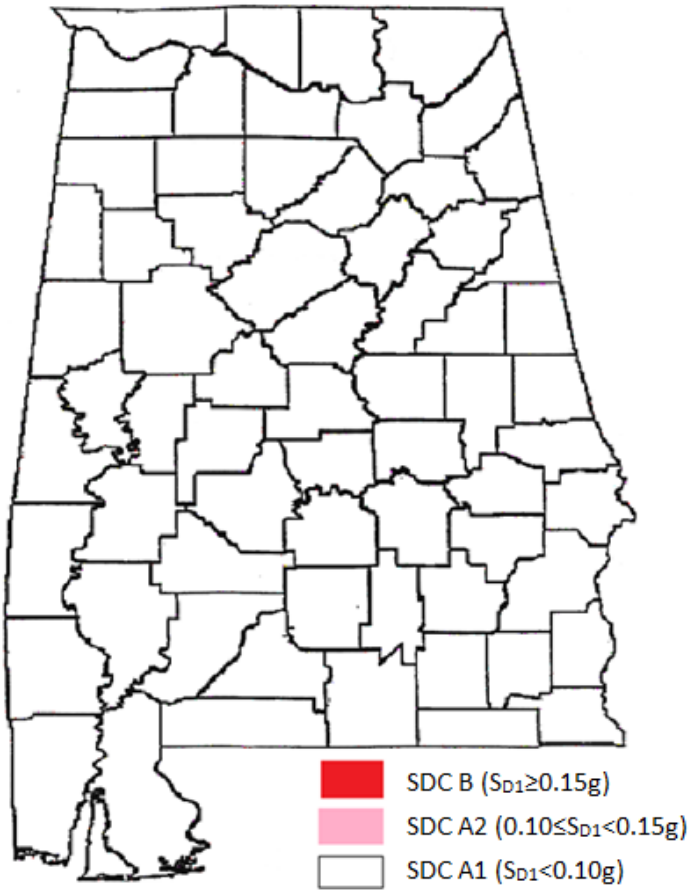

Figure 4.2: Alabama SDC Map for Soil Site Class B

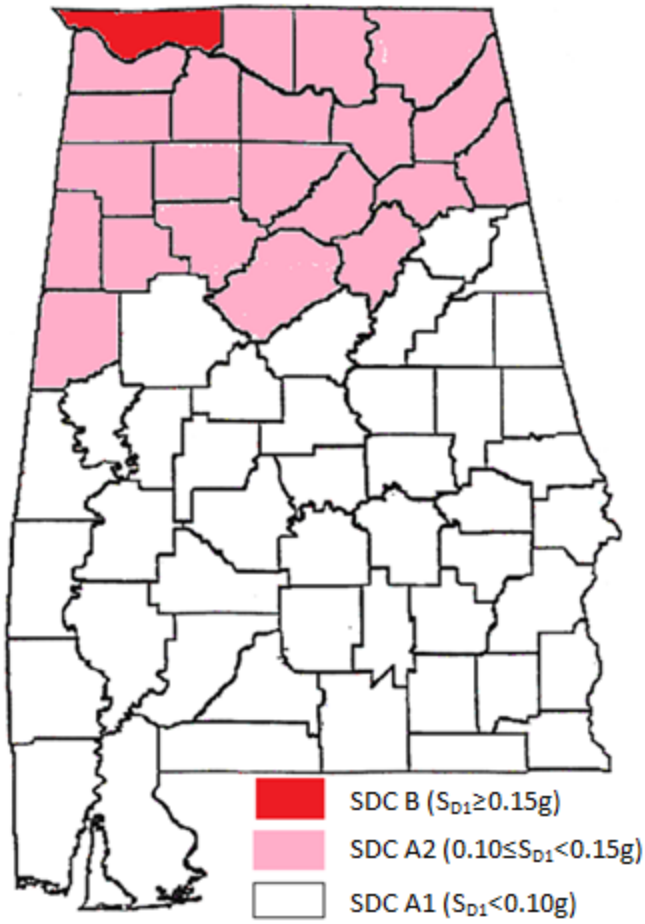

Figure 4.3: Alabama SDC Map for Soil Site Class C

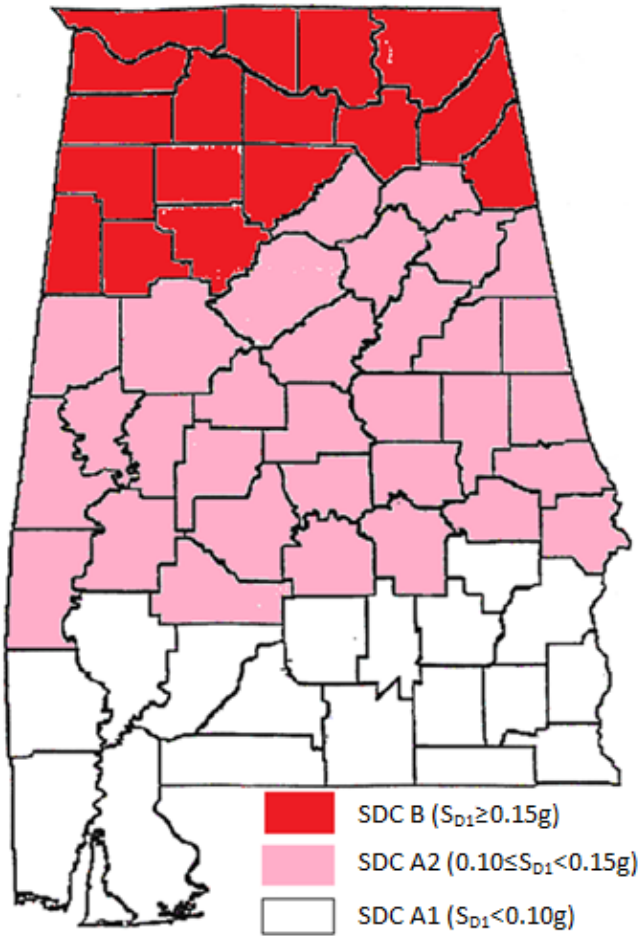

Figure 4.4: Alabama SDC Map for Soil Site Class D

4.3 Guide Specification Design Process for SDC A1

The design process for SDC A1 will be discussed first. SDC A1 is the lowest design category in the Guide Specifications, and bridges in this category are expected to experience low seismic forces. It does not require additional structural analysis or minimum detailing. The expected horizontal design forces are minimal and used only for designing the superstructure-to-substructure connection and the column for shear. These design forces are calculated as a percentage of the total tributary weight resisted at a bent. The minimum support length is also

calculated as a part of the design. The steps involved with this design category will be discussed next.

4.3.1 Determine Vertical Reactions at Bent

The first step in calculating the horizontal design force is to determine the vertical reaction at the bent. This is accomplished by finding the tributary area of the bent, the total dead weight of the bridge in that tributary area, and the uniform live load acting on the area. The dead weight of the bridge includes the weight of the deck, girders, piers, columns, and guard rails. The uniform live load consists of a 0.64 kip per linear foot per lane load that is applied simultaneously with the dead load. The LRFD Specifications, in Article C3.4.1, recommends including 50% of this live load in the vertical reaction calculations, but does not require it. It does require the bridge owner to determine the live load factor, γ_{EQ}, on a project specific basis. This live load factor determines what percentage of the live load is to be included in the weight calculations. For bridges in high traffic areas, such as major highways in large city centers, it is recommended to include at least half of the live load, because it is possible for that bridge to experience live loads during a seismic event. Once the live load is determined, it is multiplied by the number of design lanes and the tributary length of the bent. The total vertical reaction is the sum of the dead and live load resisted by the bent. Two horizontal design forces will be calculated for all bridges in SDC A, one that includes the 0.50 live load factor and one that includes a factor of zero, so that no live load is considered. A comparison between these two design forces will show if the live load factor has a significant effect.

4.3.2 Determine Design Forces

Using the vertical reaction at the bent, the horizontal design forces are calculated using Article 4.6 of the Guide Specifications. This article details the seismic design requirements for bridges in SDC A. The horizontal design force is used to design the columns for shear as well as the connection between the superstructure and substructure. For column shear, the vertical reaction is divided by the number of columns at the bent to represent the amount of load each column will resist. For the connection, the vertical reaction is divided among the number of connections, which is equal to the number of girders at the bent. The horizontal design forces presented in this report will be the connection design forces. The design force is then multiplied by either 0.15 or 0.25 times the vertical reaction at the bent depending on the acceleration coefficient at the site. The acceleration coefficient (A_s) is calculated when the SDC is determined, as discussed earlier. For sites with an acceleration coefficient less than 0.05g, the design force is 0.15 times the tributary weight. For all other sites, the design force is 0.25 times the vertical reaction. This difference in design forces is only possible in SDC A1 because the ground accelerations in SDC A2 will be above 0.05g. The reason for the difference is the Guide Specifications recognize that since seismic forces in some parts of the country are very small, the seismic design forces will also be small (AASHTO, 2011). All the design forces are multiplied by a factor of 1.0 in accordance with the load combinations found in the LRFD Specification. Table 4.3 shows the relationship between the acceleration coefficient and horizontal design force. The Standard Specifications require 0.20 times the vertical reactions for all sites in SDC A. It does not allow for a different force in low seismic regions.

Table 4.3: Design Force Multiplier

A_s	Force
<0.05g	15%
≥0.05g	25%

4.3.3 Determine Minimum Support Lengths

Support lengths are the length of overlap between the girder and pier or abutment seat. The minimum support length must be provided to accommodate differential movement between the superstructure and the substructure. These displacements occur during a design earthquake and are typically conservative. However, providing the minimum support length alone does not guarantee the girder will remain seated during an earthquake, especially if it is larger than the design earthquake. Providing seat widths larger than the minimum or using restrainer bars and cables can limit the displacement if unseating is a concern. Article 4.12 in the Guide Specifications uses Equation 4.1 to determine the minimum support length. Currently, ALDOT uses this equation to determine the minimum support lengths, but in chapter 3 of this report, it was recommended to use Equation 4.2 from the ATC-49 study (ATC/MCEER Joint Venture, 2003) to determine the minimum seat length because it will give a larger seat width. The Standard Specification uses Equation 4.1 in both SDC A and B. To develop design standards, the minimum seat lengths for bridges in SDC A1 will be calculated using Equation 4.2 and compared with the results from Equation 4.1, which represent the minimum seat length from the Standard Specifications.

$$N = (8 + 0.02L + 0.08H) * (1 + 0.000125S^2) \qquad \text{Equation 4.1}$$

$$N = \left(4 + 0.02L + 0.08H + 1.09\sqrt{H}\sqrt{1 + (2\frac{B}{L})^2}\right) * \left(\frac{1+1.25S_{D1}}{\cos(\alpha)}\right) \qquad \text{Equation 4.2}$$

4.3.4 Minimum Column Detailing

Once the design forces and minimum support lengths are determined, no further analysis is required for SDC A1. For bridges in this category, the bridge is not expected to experience forces that will result in the formation of plastic hinges. Therefore, the minimum design details are not required. The design force is used to design the superstructure to substructure connection and the remainder of the substructure. Article 8.6.1 of the Guide Specifications allows for the use of the LRFD Specifications to design the column for the areas outside of the plastic hinge region. For SDC A1, there is no plastic hinge region, so the LRFD Specifications are used to design the transverse reinforcement for the column.

4.3.4.1 Design of Reinforcement outside Plastic Hinge Region

The detailing for transverse reinforcement outside of the plastic hinge region is not mentioned in the Guide Specifications because the equations for determining concrete capacity used in the Guide Specification are not meant to be used outside of the plastic hinge region. They include the expected concrete behavior as the hinge region becomes plastic, which will not occur outside of the plastic hinge zone. Therefore, the LRFD Specifications are used to design the shear reinforcement outside of the plastic hinge region. The shear reinforcement must be checked to ensure that it provides greater resistance than the expected horizontal design force in the column. Equations 4.3 and 4.4 from Article 5.8.3.3 in the LRFD Specifications are used to determine the shear capacity of the transverse reinforcement and the concrete. Once the design is satisfied for strength, three spacing requirements are checked. These spacing requirements could control the design and must be checked. The first requirement can be found in Article 5.8.2.5 of the LRFD Specifications and is a minimum amount of transverse reinforcement. It is

only required when the factored load is greater than half of the factored resistance by the concrete section and prestressing steel (if present). It is intended to provide reinforcement in regions where there is a significant chance of diagonal cracking (AASHTO, 2009). If it is determined that this minimum reinforcement is required, then Equation 4.5 is used to determine the minimum area of transverse reinforcement. This equation in the LRFD Specifications is different than the equation found in the Standard Specifications. It results in a larger minimum area of transverse steel in the column. Article 8.19.1.2 of the Standard Specification uses Equation 4.6 to find the minimum area. The value is a constant, 0.05 ksi. Article 5.8.2.5 in the LRFD Specifications uses Equation 4.5, and the coefficient is a function of the compressive strength of concrete. For 4,000 psi concrete, the value is 0.0632 ksi.

The second check is the maximum spacing check found in LRFD article 5.8.2.7. This check addresses the need for tighter spacing if the section experiences very high shear stress. Most sections will not experience very high shear stress, so this requirement will not typically control the design. The final check is an ALDOT standard maximum spacing of 12 inches. In the event that the column is not required to meet the minimum area of transverse reinforcement requirement, this 12 inch maximum spacing will likely control.

$$V_c = 0.0316 * \beta * \sqrt{f_c'} * b_v * d_v \qquad \text{Equation 4.3}$$

$$V_s = \frac{A_v * f_y * d_v * \cot(\theta)}{s} \qquad \text{Equation 4.4}$$

$$A_{v,min} = 0.0316 * \sqrt{f_c'} * \frac{b_v * s}{f_y} \qquad \text{Equation 4.5}$$

$$A_{v,min} = 0.05 * \frac{b * s}{f_y} \qquad \text{Equation 4.6}$$

Another factor that would affect the spacing of the reinforcement would be the requirement of cross-ties. LRFD Article 5.10.6.3 requires the use of cross-ties in rectangular

columns to ensure that no longitudinal bar is more than 2 feet from a restrained bar. However, for all of the bridges in this study, no columns were large enough for this requirement to be necessary. Therefore, this requirement did not control the design.

4.4 Bridge Design Examples in SDC A1

The design procedure in the Guide Specifications for SDC A1 was used to redesign two bridges previously designed under the Standard Specifications. These bridges were supplied by ALDOT and are conventional bridges in the "other" category as described in Chapter 2, making them applicable to the Guide Specifications. One bridge was designed with an acceleration coefficient less than 0.05g and the other with an acceleration coefficient greater than 0.05g to show how the lower accelerations affect the design of the bridge, as well as highlight the differences between the Standard Specifications and Guide Specifications for bridges in each. For each bridge, design sheets were created with references to specific articles in the Guide Specifications or LRFD Specifications and can be seen in Appendix B and C. Notes and other information necessary to the understanding of a certain variable were also noted. Since the purpose of these designs is to determine if a standard set of drawings and details can be identified for these bridges, design data is established for each bent of a bridge. This information will be summarized for each bridge. The two bridges include County Road 39 Bridge over CSX in Mobile County and Stave Creek Bridge in Clarke County.

4.4.1 County Road 39 Bridge

County Road 39 crosses over CSX railroad and US Highway 90 in Mobile County. The overpass has two bridges designed to carry traffic in both the northbound and southbound

directions. Each bridge is similarly designed, but the deck of the southbound bridge flares from a width of 54.75 feet at the second pier to 66 feet at the north abutment. The northbound bridge deck remains constant at a width of 54.75 feet. Because the northbound bridge is closest to the conventional bridge definition, it was chosen to be redesigned instead of the southbound bridge. It is a four span bridge with three equal spans of 135 feet and one unequal span of 80 feet at the north end of the bridge. The three equal spans support the 7-inch concrete deck with 9 BT-72 Girders. The unequal span supports the deck with 9 Type III girders. The three bridge piers are 53’ x 4’ x 4.5’ and are supported by three rectangular columns 3.75 feet in diameter with 2 inches of concrete cover. The columns are longitudinally reinforced with 16 #11 bars and transversely with #4 ties uniformly spaced at 12 inches from the bottom of the pier cap to the top of the foundation. The average clear height of each bent was measured from the bottom of the pier cap to the top of the pile cap foundation. The average clear height is 23.6 feet for Bent 2, 28.84 feet for Bent 3, and 26.6 feet for Bent 4. All columns are supported on pile caps with dimensions of 8.6’ x 8’ x4.5’ and each pile cap is supported by nine HP 12x53 driven steel piles. All design calculations can be found in Appendix B.

The first step is finding the vertical reaction at each of the bridge bents. The uniform live load on the bridge, discussed in LRFD 3.6.1.2.4, over the 4 design lanes was 1.28 kips per linear foot. The dead weight included the deck, girders, pier, columns, and guard rails. The total loads were determined using the tributary area of the bents. Table 4.4 compares the design forces when the 0.5 live load factor is used. It shows that using the 0.5 live load factor increases the design forces by 10%.

Table 4.4: Mobile County Bridge Design Force Live Load Factor Comparison

Bent	Design Force with γ_{EQ} (kips)	Design Force without γ_{EQ} (kips)	Percent Difference
2	32.0	29.1	9.9%
3	32.0	29.1	9.9%
4	25.4	23.1	10.0%

Once the vertical reactions were calculated, the design forces for each column were calculated. The acceleration coefficient for this bridge was 0.045g. Since it was less than the 0.05g limit found in Article 4.6, the horizontal design forces were 15% of the vertical reactions. The design forces using the Standard Specifications were 20% of the vertical reactions. As seen in Table 4.5, the design forces are reduced by 25% in the Guide Specifications.

Table 4.5: Mobile County Bridge Design Force Specification Comparison

Bent	Vertical Reaction (kips)	Guide Spec Design Force (kips)	Standard Spec Design Force (kips)	Percent Difference
2	1948	32.0	42.6	-25.0%
3	1948	32.0	42.6	-25.0%
4	1400	25.4	33.9	-25.0%

The minimum support lengths were calculated next. They were different for each bridge bent because of the difference in heights of each bent. Equation 4.2 was used to calculate the new minimum seat lengths and Equation 4.1 was used to calculate the Standard Specifications seat lengths. At each bent, the new lengths were 31-36% greater than those required by the Standard Specifications. Table 4.6 shows the minimum lengths for each bent.

Table 4.6: Mobile County Bridge Minimum Support Lengths

Bent	New Design Minimum Support Length (in)	Standard Spec Minimum Support Length (in)	Percent Difference
2	16.6	12.6	31.7%
3	17.8	13.1	35.9%
4	16.7	12.3	35.8%

For SDC A1, no structural analysis is necessary and the detailing requirements of SDC A2 and B do not apply. The design of the column outside of the plastic hinge zone is accomplished using the LRFD Specifications. #4 ties were used to remain consistent with the previous design. The tie spacing was controlled by 12 inch ALDOT standard. Since the calculated shear was less than half of the nominal shear resistance of the concrete, the minimum area of transverse reinforcement was not required to be satisfied for any of the bents. This resulted in the same amount of transverse reinforcement being required for the designs since the Standard Specifications design also used ties spaced at 12 inches. The results from the redesign of the column can be seen in Table 4.7. Figure 4.5 compares the final design details from the Guide Specifications and Standard Specifications at bent 2. The details for bents 3 and 4 will be similar, except for a different column height, so they are not shown. The only changes in this design were the decrease in the horizontal design force and the increase in the minimum seat width.

Table 4.7: Mobile County Bridge Design Summary

	Bent 2		Bent 3		Bent 4	
	Standard Specification	Guide Specification	Standard Specification	Guide Specification	Standard Specification	Guide Specification
Column Height (in)	283	283	346	346	319	319
Tie Size	#4	#4	#4	#4	#4	#4
Tie Spacing (in)	12	12	12	12	12	12
Number of Ties	24	24	29	29	27	27
Area of Steel (in^2)	4.8	4.8	5.8	5.8	5.4	5.4
Percent Difference	0%		0%		0%	

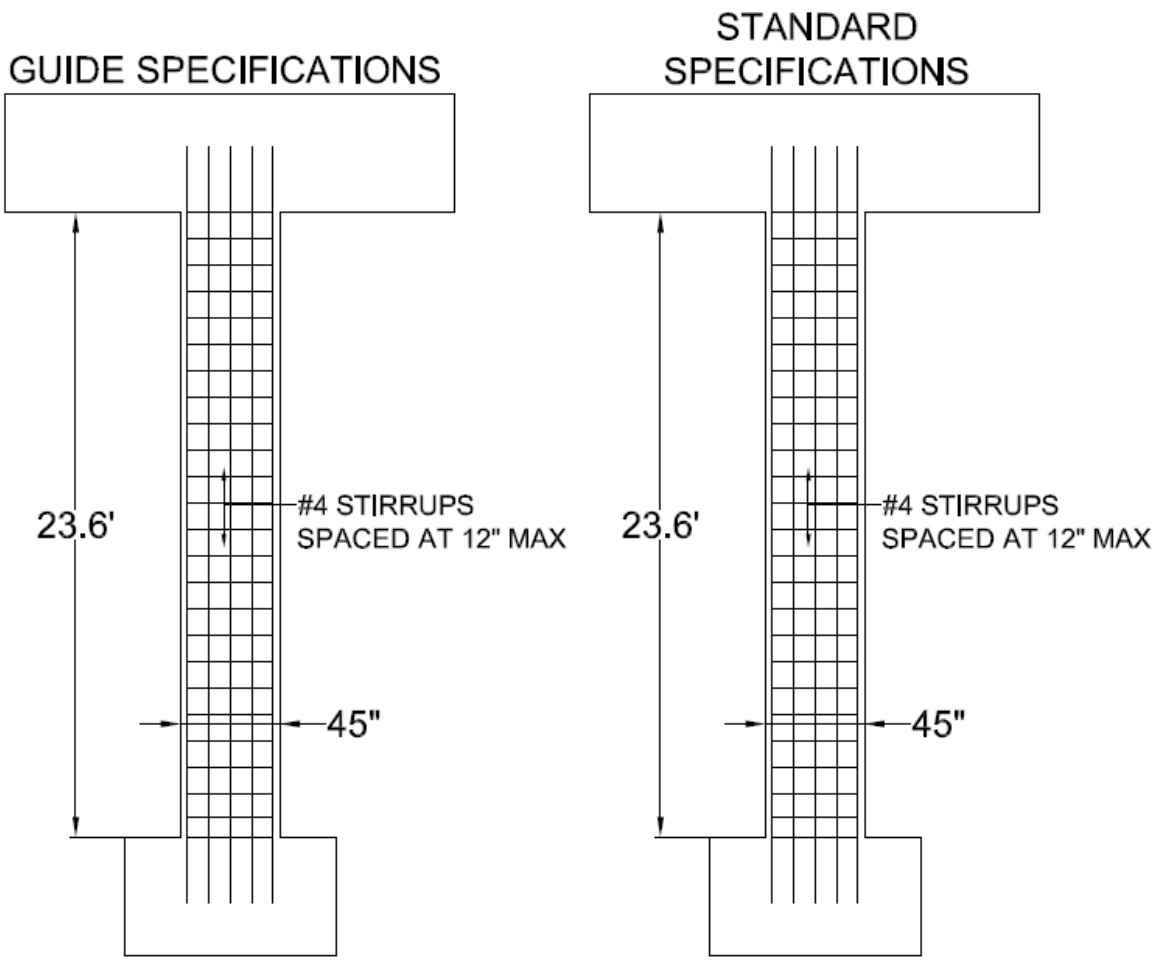

Figure 4.5: Mobile County Bridge Bent 2 Final Design Details

4.4.2 Stave Creek Bridge

State Road 69 crosses over Stave Creek in Clarke County. The overpass has two bridges designed to carry traffic in both the northbound and southbound directions. It is a three span bridge with the two end spans 40 feet long and middle span 85 feet long. The 7-inch concrete deck is a constant 42.75 feet in width and supported by 6 Type I girders in the end spans and 6 Type III girders in the middle span. The two bridge piers are not rectangular because of the different girder types. They are 40 feet long, 4 feet wide, and have depths of 3.75 feet and 5.4 feet. The depths change at approximately 2 feet of width. The piers are supported by two square columns 3 feet in width with 2 inches of concrete cover. The columns are reinforced longitudinally with twelve #11 bars and transversely with #4 ties spaced uniformly at 12 inches from the bottom of the pier cap to the top of the foundation. The average clear height of the columns in Bent 2 is 10.2 feet and for the columns in Bent 3 is 14.34 feet. All columns are supported on 7’ x 6.5’ x 4.5’ pile caps and the pile caps are supported on five HP 12x53 driven steel piles. All design calculations can be found in Appendix C.

The first step is determining the vertical reaction at each of the bridge bents. The uniform live load on the bridge, discussed in LRFD 3.6.1.2.4, over the 3 design lanes was 0.96 kips per linear foot. The dead weight included the deck, girders, pier, columns, and guard rails. The total loads were determined using the tributary area of the bents. Because the bridge was symmetric, the vertical reactions of the bents were equal. Table 4.8 compares the connection design forces when the live load factor is considered and not considered. As the table shows, the design forces increased by 11% when the live load factor of 0.5 was included.

Table 4.8: Stave Creek Bridge Design Force Live Load Factor Comparison (SDC A1)

Bent	Design Force with γ_{EQ} (kips)	Design Force without γ_{EQ} (kips)	Percent Difference
2	25.2	22.7	11.0%
3	25.2	22.7	11.0%

Once the vertical reactions were calculated, the horizontal design forces were calculated for each column. The acceleration coefficient for this bridge was 0.086g, greater than the 0.05g limit found in Article 4.6, so the horizontal design forces were 25% of the vertical reactions. The design forces from the Standard Specification were 20% of the vertical reactions. The design forces can also be found in Table 4.9, displaying the design forces, shows that the Guide Specifications resulted in a 25% increase in the horizontal design forces.

Table 4.9: Stave Creek Bridge Vertical Reactions and Design Forces Comparison (SDC A1)

Bent	Vertical Reaction (kips)	Guide Spec Design Force (kips)	Standard Spec Design Force (kips)	Percent Difference
2	604	25.2	20.1	25.0%
3	604	25.2	20.1	25.0%

The minimum support lengths were calculated next. They were different for each bridge bent because of the difference in clear heights of each bent. The support lengths from the Standard Specifications were calculated using Equation 4.1 and the recommended design support lengths were calculated using Equation 4.2. The new support lengths are greater than the Standard Specifications support lengths by 14-23%, as seen in Table 4.10.

Table 4.10: Stave Creek Bridge Minimum Support Lengths Comparison (SDC A1)

Bent	New Design Minimum Support Length (in)	Standard Spec Minimum Support Length (in)	Percent Difference
2	11.5	10.1	13.9%
3	12.8	10.4	23.1%

For SDC A1, the detailing requirements of SDC A2 and B do not apply. The LRFD Specifications were used to design the transverse reinforcement in the columns since there is no plastic hinge zone. #4 ties were used to remain consistent with the current design. The tie spacing was controlled by the minimum area of transverse reinforcement requirements instead of the shear capacity of the ties, which decreased the maximum spacing to 10 inches. This spacing decrease resulted in a 20% increase in the number of ties at each bent compared to the Standard Specification design. The results from the redesign of the column can be seen in Table 4.11. Figure 4.6 and Figure 4.7 compare the final design details from the Guide Specifications and the Standard Specifications.

Table 4.11: Stave Creek Bridge Design Summary (SDC A1)

	Bent 2		Bent 3	
	Standard Specification	Guide Specification	Standard Specification	Guide Specification
Column Height (in)	120	120	168	168
Tie Size	#4	#4	#4	#4
Tie Spacing (in)	12	10	12	10
Number of Ties	10	12	14	17
Area of Steel (in^2)	2	2.4	2.8	3.4
Percent Difference	20.0%		21.4%	

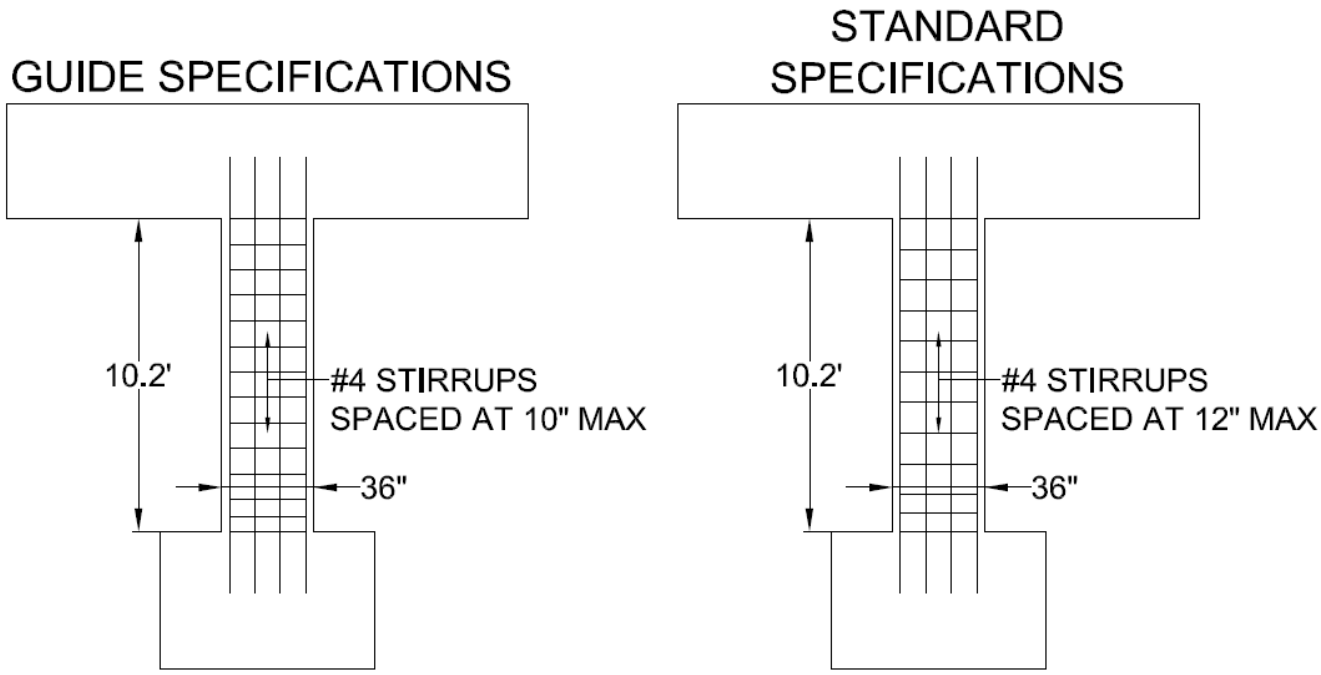

Figure 4.6: Stave Creek Bridge Bent 2 Final Design Details (SDC A1)

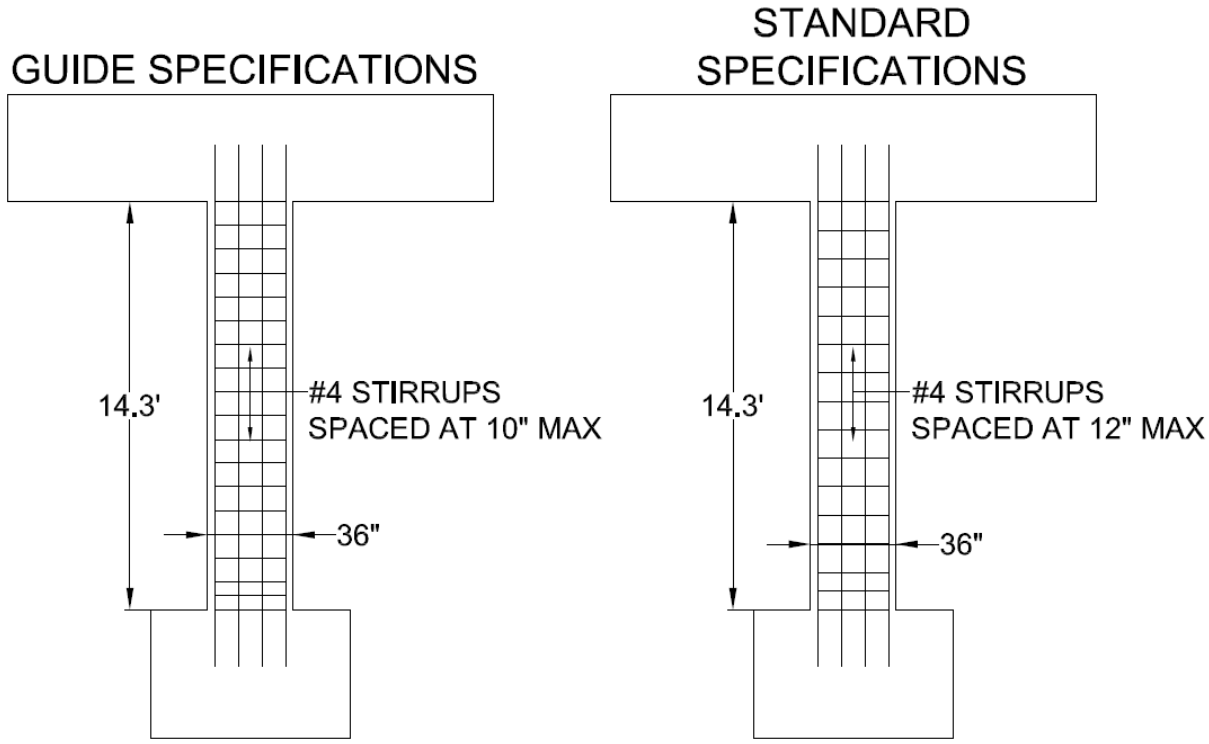

Figure 4.7: Stave Creek Bridge Bent 3 Final Design Details (SDC A1)

4.4.3 Summary of Differences in SDC A1

The changes in bridge design from the Standard Specification to the Guide Specification in SDC A1 were different for lower and higher seismic regions. For very low seismic regions ($A_S < 0.05g$), the design forces decreased by 25%. For other regions in SDC A1 ($A_S \geq 0.05g$), the design forces were increased by 25%. The design forces increased because the changes in the seismic hazard maps resulted in higher ground accelerations than those used in the Standard Specifications. However, the Guide Specifications recognizes that bridges in areas of low seismicity will not experience very high seismic design forces and reduces them accordingly. Another change was that the new seat width equation resulted in greater seat widths for both bridges studied, which was expected since it was designed to give larger seat widths than the equation used in the Standard Specifications and Guide Specifications.

The other change between the two specifications was not related to seismic design. The amount of transverse reinforcement was the same for Mobile County Bridge but different for Stave Creek Bridge. When it did change, it was the result of the minimum area of transverse reinforcement equation in the LRFD Specifications requiring a tighter spacing than that required by a similar equation in the Standard Specifications. This equation was not required for the Mobile County Bridge because the nominal shear resistance of the concrete was twice as large as the expected shear. Though it only affected one of the bridges, this minimum area check is still an important change because it could control the spacing of the ties in the columns. Therefore, it is possible that the transverse reinforcement spacing requirements outside of the plastic hinge zone for bridges designed using the LRFD Specifications will be tighter than the Standard Specifications. However, there are some options that can be used to increase the spacing to 12

inches. Using cross-ties will increase the area of shear reinforcement at each tie level, which would allow the spacing to be increased. Similarly, using a larger size reinforcing bar would also increase the area and spacing of reinforcement. These options could be used if 12 inch spacing was more desirable.

4.5 Guide Specification Design Process for SDC A2

Bridges in SDC A that are expected to experience moderate seismic forces are classified as SDC A2. The possibility exists that these bridges will experience seismic forces that result in plastic hinging and, therefore, require the same minimum detailing from SDC B so that the hinges form at the top and bottom of the column in the transverse direction, and at the bottom in the longitudinal direction. However, there is no structural analysis required. Like SDC A1, the design forces are determined using simplified relationships between the vertical reaction at a bent and the expected ground acceleration. The design steps for SDC A2 bridges will be discussed next.

4.5.1 Determine Vertical Reactions at Bent

Like SDC A1, the first step in calculating the horizontal design force is to determine the vertical reaction at the bent. This is accomplished by finding the tributary area of the bent, the total dead weight of the bridge in that tributary area, and the uniform live load acting on the area. The dead weight of the bridge includes the weight of the deck, girders, piers, columns, and guard rails. The uniform live load consists of a 0.64 kip per linear foot per lane load that is applied simultaneously with the dead load. The LRFD Specifications, in Article C3.4.1, recommends including 50% of this live load in the vertical reaction calculations, but does not require it. It

does require the bridge owner to determine the live load factor, γ_{EQ}, on a project specific basis. This live load factor determines what percentage of the live load is to be included in the weight calculations. For bridges in high traffic areas, such as major highways in large city centers, it is recommended to include at least half of the live load, because it is possible for that bridge to experience live loads during a seismic event. Once the live load is determined, it is multiplied by the number of design lanes and the tributary length of the bent. The total vertical reaction is the sum of the dead and live load resisted by the bent. Two horizontal design forces will be calculated for all bridges in SDC A, one that includes the 0.50 live load factor and one that does not. A comparison between these two design forces will show if the live load factor has a significant effect.

4.5.2 Determine Design Forces

Using the vertical reaction at the bent, the horizontal design forces are calculated using Article 4.6 of the Guide Specifications. This article details the seismic design requirements for bridges in SDC A. The design force is used to design the column for shear and the connection between the superstructure and substructure. For column shear, the vertical reaction is divided by the number of columns at the bent to represent the amount of load each column will resist. For the connection, the vertical reaction is divided by the number of connections, which is equal to the number of girders at the bent. The design force is then multiplied by 0.25 times the vertical reaction at the bent. Unlike SDC A1, it is not possible for the design force to be 0.15 times the vertical reaction at the bent because A_S will not be below 0.05g, which is the limit for the lower design force in Article 4.6. The Standard Specifications require 0.20 times the vertical reactions for all sites in SDC A.

4.5.3 Determine Minimum Support Lengths

Support lengths are the length of overlap between the girder and pier or abutment seat. The minimum support length must be provided to accommodate differential movement between the superstructure and the substructure. These displacements occur during a design earthquake and are typically conservative. However, providing the minimum support length alone does not guarantee the girder will remain seated during an earthquake, especially if it is larger than the design earthquake. Providing seat widths larger than the minimum or using restrainer bars and cables can limit the displacement if unseating is a concern. Article 4.12 in the Guide Specifications uses Equation 4.1 to determine the minimum support length. Currently, ALDOT uses this equation to determine the minimum support lengths, but in chapter 3 of this report, it was recommended to use Equation 4.2 from the ATC-49 study (ATC/MCEER Joint Venture, 2003) to determine the minimum seat length because it will give a larger seat width. The Standard Specification uses Equation 4.1 in both SDC A and B. To determine design standards, the minimum seat lengths for bridges in SDC A1 will be calculated using Equation 4.2 and compared with the results from Equation 4.1, which represent the minimum seat length from the Standard Specifications. Because the new equation uses the spectral acceleration, S_{D1}, in the multiplier factor, for SDC A2 greater seat widths can be expected since these bridges will have higher accelerations than those in SDC A1.

$$N = (8 + 0.02L + 0.08H) * (1 + 0.000125S^2) \qquad \text{Equation 4.1}$$

$$N = \left(4 + 0.02L + 0.08H + 1.09\sqrt{H}\sqrt{1 + (2\frac{B}{L})^2}\right) * \left(\frac{1+1.25S_{D1}}{\cos(\alpha)}\right) \qquad \text{Equation 4.2}$$

4.5.4 Minimum Column Detailing

Once the minimum seat widths and horizontal design forces are calculated, the minimum detailing requirements of SDC B must be met, according to Article 8.2. These include the minimum shear reinforcement of Article 8.6.5 and the minimum requirements for lateral reinforcement in Article 8.8.9. This shear reinforcement is to extend over the entire plastic hinge length determined in Article 4.11.7. These details will allow the column to be ductile and form plastic hinges in the high moment regions if the bridge experiences high seismic forces.

4.5.4.1 Plastic Hinge Length

The plastic hinge length (PHL) is the assumed length of the column where the plastic hinge will form and is designed to be at the top of the column and the bottom of the column for bending in the transverse direction and at the bottom of the column for bending in the longitudinal direction, where the column meets the foundation, although the location of the plastic hinge at the bottom can vary depending on the soil and foundation type. For the bridges in SDC A2, the plastic hinge was assumed to form at the connection between the column and foundation element. These locations occur at the point of maximum moment and shear in the column. These flexural areas allow the bridge to dissipate energy. The shear reinforcement helps confine the concrete and prevent buckling of the longitudinal reinforcement, as well as increase the shear resistance of the section, which decreases the possibility of a brittle failure that will not allow the column to dissipate energy and remove vertical capacity. Article 4.11.7 in the Guide Specification defines the PHL to be the largest of three lengths (AASHTO, 2011):

- 1.5 times the largest cross-sectional dimension in the direction of bending

- The region of the column where the moment demand exceeds 75% of the maximum plastic moment
- The analytical plastic hinge length, L_p

The largest cross-sectional dimension will be either the diameter of a circular column or the width in the direction of bending of a rectangular column. The maximum plastic moment is determined by a moment-axial load interaction diagram. For this project, the software program spColumn was used (StructurePoint, 2012). The dimensions of the column and the reinforcement layout are input into the program, and the maximum moment is determined from the resulting moment interaction diagram. Once the maximum plastic moment is determined, the moment diagram from the computer analysis software can be used to determine the length of the column where the moment exceeds 75% of the plastic moment. The analytical plastic hinge length is determined in Article 4.11.6 using Equation 4.7. This equation is specifically for reinforced concrete columns framing into a footing, integral bent cap, oversized shaft, and cased shaft, which meets the criteria for this project.

$$L_p = 0.08 * L + 0.15 * f_{ye} * d_{bl} \geq 0.3 * f_{ye} * d_{bl} \qquad \text{Equation 4.7}$$

In most cases, the PHL is controlled by the 1.5 times the gross cross-sectional dimension. This can result in a large PHL for large columns and since the PHL is at the top and bottom of the column, the entire column could be considered to be within the plastic hinge. This makes it difficult to satisfy the lap splicing requirements found in Article 8.8.3 for the longitudinal column reinforcement. The splicing is required to be outside of the plastic hinge length. Failure to do so could lead to undesirable seismic performance because the splice would be subject to plastic forces and deformations, which could lead to a reduced effective plastic hinge length and severe local curvature demand (AASHTO, 2011). While this article only applies to SDC C and

D, the commentary recommends that they also be applied to SDC B. While these splicing requirements are not required in SDC A2, the designer should consider their effects.

An alternative to this PHL is given in Article 8.2 of the Guide Specifications. This article allows the use of Article 5.10.11.4.1e in the LRFD Specifications to calculate the length. These requirements are easier to determine and do not require any computer software. The maximum of three limits is taken as the PHL (AASHTO, 2007):

- The largest cross-sectional dimension
- One-sixth the clear height of the column
- 18 inches

The largest cross-sectional dimension will be either the diameter of a circular column or the largest width of a rectangular column. The clear height of the column depends on the foundation type and geometry. For three of the bridges, driven piles were used as the foundations. It was assumed the plastic hinge would form at the column to pile cap connection, and the column height was taken from the bottom of the pier cap to the top of the pile cap. However, one of the bridges used drilled shafts as the foundation. The drilled shaft was the same diameter as the column, so because of the similar geometry and relatively small amount of soil able to resist flexure of the column and drilled shaft, it was conservatively assumed that the point of fixity of the column to be at the rock line. It is important to understand how the column and foundation will interact in order to determine where the plastic hinge is likely to form. Using the maximum of these three values will typically result in a smaller PHL than that found in the Guide Specifications. This will allow for a greater length of column for splicing. For the bridges in SDC A2, both values will be checked.

The LRFD Specifications, in Article 5.10.11.4.3, discuss an extension of the plastic hinge length into the cap beam or the foundation (pile cap or drilled shaft). The extension length is an extra length over which the ties from the plastic hinge zone span. The spacing of these ties is the same required in the plastic hinge zone. This is an extra measure to ensure the plastic hinge forms at the top or bottom of the column. Article 5.10.11.4.1e in the LRFD Specifications requires the extension length to be the maximum of the following:

- One-half of the column diameter
- 15 inches

This extension is only required in SDC C and D, but it is recommended in SDC B. This extension length is not found in the Guide Specifications, but since the plastic hinge zone requirements for SDC A2 include the same detailing from SDC B, the extension length will be calculated for all four bridges, but will not be provided in the design drawings.

4.5.4.2 Transverse Reinforcement inside the Plastic Hinge Zone

Once the plastic hinge length is determined, the size and spacing of the transverse reinforcement within the PHL can be determined. For SDC A2, the minimum ratios of transverse reinforcement in Article 8.6.5 and the requirements of Article 8.8.9 must be met. The ratios are calculated in Article 8.6.2, and must be greater than or equal to 0.003 for spirals in circular columns and greater than or equal to 0.002 for rectangular columns. Article 8.8.9 lists standard tie requirements that will ensure the lateral support is supplied to the longitudinal reinforcement. These requirements will not be discussed, with the exception of the maximum spacing requirements inside the plastic hinge regions. The maximum spacing is to be the smaller of the following:

- One-fifth the least dimension of the cross-section for columns
- Six times the nominal diameter of the longitudinal reinforcement
- 6 inches

If the longitudinal reinforcement is at least a #9 bar and the column size is at least 30 inches, as all of the bridges in this study are, then the 6 inch maximum spacing controls. However, the spacing must still satisfy the minimum ratios. Once this ratio and all the requirements of Article 8.8.9 have been satisfied, the detailing within the PHL is finished.

4.5.4.3 Transverse Reinforcement outside the Plastic Hinge Zone

The detailing for transverse reinforcement outside of the plastic hinge region in SDC A2 is the same as SDC A1. The LRFD Specifications were used to design the shear reinforcement outside of the plastic hinge zone. The shear reinforcement must be checked to ensure that it provides greater resistance than the expected horizontal design force in the column. Equations 4.3 and 4.4 from Article 5.8.3.3 in the LRFD Specifications are used to determine the shear capacity of the transverse reinforcement and the concrete. Once the design is satisfied for strength, three spacing requirements are checked. These spacing requirements could control the design and must be checked. The first requirement can be found in Article 5.8.2.5 of the LRFD Specifications and is a minimum amount of transverse reinforcement. It is only required when the factored load is greater than half of the factored resistance by the concrete section and prestressing steel (if present). It is intended to provide reinforcement in regions where there is a significant chance of diagonal cracking (AASHTO, 2009). If it is determined that this minimum reinforcement is required, then Equation 4.5 is used to determine the minimum area of transverse reinforcement. This equation in the LRFD Specifications is different than the equation found in

the Standard Specifications. It results in a larger minimum area of transverse steel in the column. Article 8.19.1.2 of the Standard Specification uses Equation 4.6 to find the minimum area. The value is a constant, 0.05 ksi. Article 5.8.2.5 in the LRFD Specifications uses Equation 4.5, and the coefficient is a function of the compressive strength of concrete. For 4,000 psi concrete, the value is 0.0632 ksi. The difference between the values shows that the LRFD Specifications will result in a higher minimum area of reinforcement compared to the Standard Specifications.

The second check is the maximum spacing check found in LRFD article 5.8.2.7. This check addresses the need for tighter spacing if the section experiences very high shear stress. Most sections will not experience very high shear stress, so this requirement will not typically control the design. The final check is an ALDOT standard maximum spacing of 12 inches. In the event that the column is not required to meet the minimum area of transverse reinforcement requirement, this 12 inch maximum spacing will likely control.

$$V_c = 0.0316 * \beta * \sqrt{f_c'} * b_v * d_v \qquad \text{Equation 4.3}$$

$$V_s = \frac{A_v * f_y * d_v * \cot(\theta)}{s} \qquad \text{Equation 4.4}$$

$$A_{v,min} = 0.0316 * \sqrt{f_c'} * \frac{b_v * s}{f_y} \qquad \text{Equation 4.5}$$

$$A_{v,min} = 0.05 * \frac{b * s}{f_y} \qquad \text{Equation 4.6}$$

Another factor that would affect the spacing of the reinforcement would be the requirement of cross-ties. LRFD Article 5.10.6.3 requires the use of cross-ties in rectangular columns to ensure that no longitudinal bar is more than 2 feet from a restrained bar. However, for all of the bridges in this study, no columns were large enough for this requirement to be necessary. Therefore, this requirement did not control the design.

4.6 Bridge Design Examples in SDC A2

Four bridges in SDC A2 were redesigned using the Guide Specifications. These bridges were supplied by ALDOT and are conventional bridges in the "other" category as described earlier, making them applicable to the Guide Specifications. One of the bridges was also redesigned in the SDC A1 category. The differences between the two designs will be discussed to show how SDC A1 and SDC A2 are different. Three other bridges will be redesigned as SDC B bridges for similar purposes, but comparisons will not be mentioned in this section. For those comparisons, refer to the "Bridge Design Examples in SDC B" section of this chapter. For each bridge, design sheets were created with references to specific articles in the Guide Specifications or LRFD Specifications. Notes and other information necessary to the understanding of a certain variable were also recorded. Since the purpose of these redesigns is to determine if a standard set of drawings and details can be identified for these bridges, design data is established for each bent of a bridge. This information will be summarized for each bridge. The four bridges to be redesigned include the following: Stave Creek Bridge in Clarke County, Bent Creek Road Bridge in Lee County, Bridge over Norfolk Southern Railroad in Etowah County, and Oseligee Creek Bridge in Etowah County.

4.6.1 Stave Creek Bridge

This bridge has been previously designed in the SDC A1 section and will be compared to it in order to determine the differences in design. The designs from the Standard Specification to the Guide Specification will also be compared. Stave Creek Bridge is in Clarke County and carries State Road 69 over Stave Creek. The overpass has two bridges designed to carry traffic in both the northbound and southbound directions. It is a three span bridge with the two end

spans 40 feet long and middle span 85 feet long. The 7 inch concrete deck is a constant 42.75 feet in width and supported by 6 Type I girders in the end spans and 6 Type III girders in the middle span. The two bridge piers are not rectangular because of the different girder types. They are 40 feet long, 4 feet wide, and have depths of 3.75 feet and 5.4 feet. The depths change at approximately 2 feet of width. The piers are supported by two square columns 3 feet in width with 2 inches of concrete cover. The columns are reinforced longitudinally with 12 #11 bars and transversely with #4 ties spaced uniformly at 12 inches from the bottom of the pier cap to the top of the foundation. The average clear height of the columns in Bent 2 is 10.2 feet and for the columns in Bent 3 is 14.34 feet. All columns are supported on 7' x 6.5' x 4.5' pile caps and the pile caps are supported on five HP 12x53 driven steel piles. All design calculations for this bridge can be found in Appendix D.

The first step is determining the vertical reaction at each of the bridge bents. The uniform live load on the bridge, discussed in LRFD 3.6.1.2.4, over the 3 design lanes was 0.96 kips per linear foot. Since the tributary area of the bents was equal, the vertical reactions at each bent will be equal. Since the horizontal design force is 25% of the vertical reaction, these design forces are equal to the design forces from SDC A1. As Table 4.12 shows, including the 0.50 live load factor increases the design forces by 11%.

Table 4.12: Stave Creek Bridge Design Force Live Load Factor Comparison (SDC A2)

Bent	Design Force with γ_{EQ} (kips)	Design Force without γ_{EQ} (kips)	Percent Difference
2	25.2	22.7	11.0%
3	25.2	22.7	11.0%

Once the vertical reactions were calculated, the horizontal design forces were calculated. For SDC A2, the design forces are 25% of the vertical reaction. The design forces in the

Standard Specification are 20% of the vertical reaction, meaning the Guide Specification results in a 25% increase in the horizontal design forces, as seen in found in Table 4.13.

Table 4.13: Stave Creek Bridge Vertical Reactions and Design Forces Comparison (SDC A2)

Bent	Vertical Reaction (kips)	Guide Spec Design Force (kips)	Standard Spec Design Force (kips)	Percent Difference
2	604	25.2	20.1	25.0%
3	604	25.2	20.1	25.0%

The minimum support lengths were determined next. They were different for each bridge bent because of their difference in clear heights. The support lengths from the Standard Specifications were calculated using Equation 4.1 and the recommended design support lengths were calculated using Equation 4.2. Table 4.14 shows the minimum support lengths for each bent required by each specification. The seat length increases by 16-26%. The new design seat length is greater for the Stave Creek Bridge bents designed in SDC A2 (compared to SDC A1) because the spectral acceleration values are slightly greater.

Table 4.14: Stave Creek Bridge Minimum Seat Width Comparison (SDC A2)

Bent	New Design Minimum Support Length (in)	Standard Spec Minimum Support Length (in)	Percent Difference
2	11.8	10.1	16.8%
3	13.1	10.4	25.9%

Once the design forces and seat widths were calculated, the transverse reinforcement was designed. Table 4.15 shows the results from the design. Both bents had the same plastic hinge lengths, tie sizes, and tie spacing. The plastic hinge length was determined to be 36 inches for each bent. The width of the columns controlled the plastic hinge length since the columns were relatively short. The spacing inside the plastic hinge zones was controlled by the reinforcement ratio, and a maximum spacing of 5 inches was determined to satisfy the ratio. The spacing

outside of the plastic hinge zone was 10 inches, controlled by the minimum area of transverse reinforcement, which was required for these columns. A 12 inch maximum spacing throughout the entire column was required by the Standard Specifications. So, the tighter spacing resulted in a 40-45% increase in the number of ties required. Figure 4.8 and Figure 4.9 compare the final design details from the Standard Specifications and the Guide Specifications.

Table 4.15: Stave Creek Bridge Design Summary

	Bent 2		Bent 3	
	Standard Specification	Guide Specification	Standard Specification	Guide Specification
Column Height (in)	122	122	172	172
Tie Size	#4	#4	#4	#4
Plastic Hinge Length (in)	-	36	-	36
PHL Spacing (in)	-	5	-	5
Spacing outside PHL (in)	12	10	12	10
Number of Ties	11	16	15	21
Area of Steel (in^2)	2.2	3.2	3	4.2
Percent Difference	45.5%		40.0%	

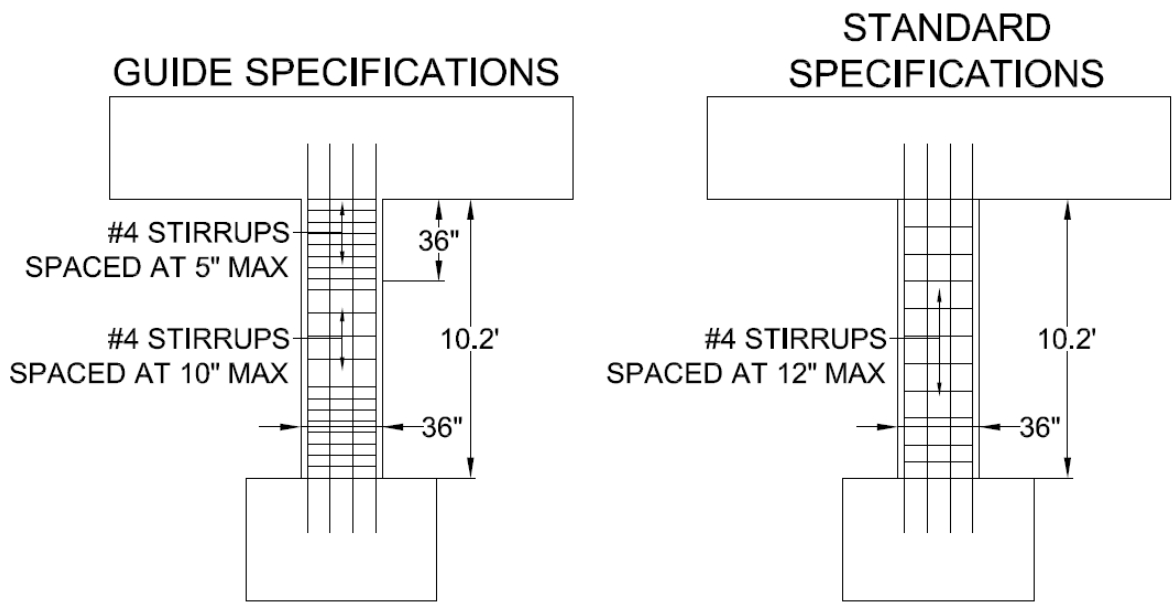

Figure 4.8: Stave Creek Bridge Bent 2 Final Design Details (SDC A2)

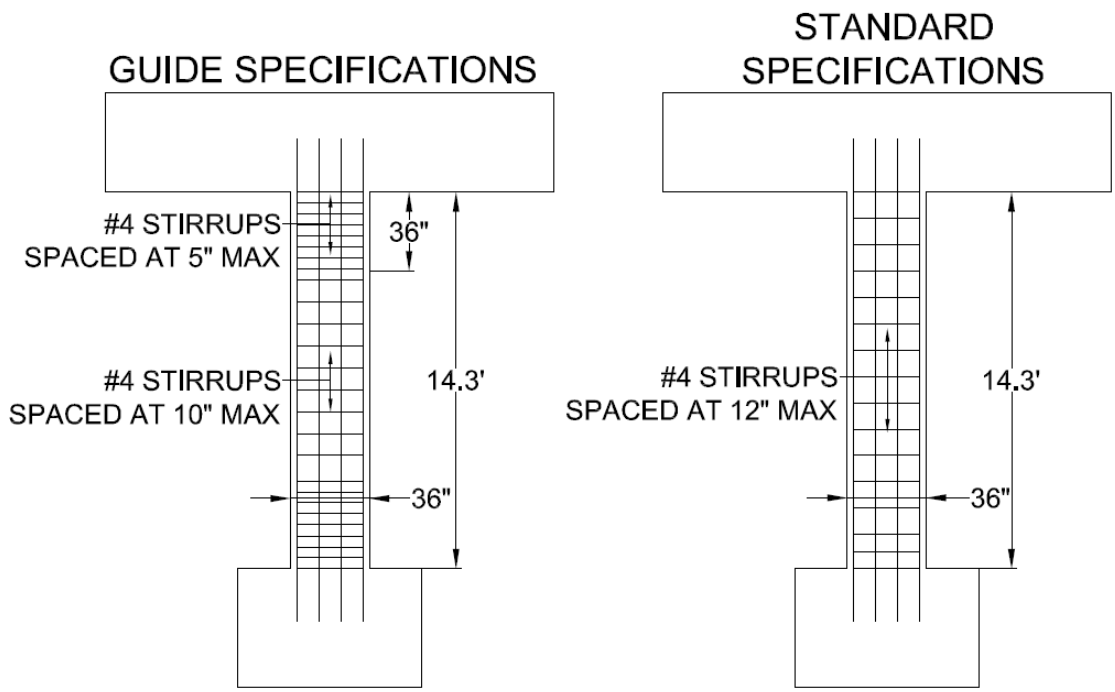

Figure 4.9: Stave Creek Bridge Bent 3 Final Design Details (SDC A2)

One change from SDC A1 to SDC A2 was the addition of the plastic hinge zone. As Table 4.16 shows, requiring tighter tie spacing over a portion of the column results in a 25-30% increase in the number of ties. The design forces stayed the same, but the minimum seat widths as determined by the recommended equation increased slightly as a result of higher expected spectral accelerations.

Table 4.16: Stave Creek SDC A1 and A2 Design Comparison

	Bent 2		Bent 3	
	Guide SDC A1	Guide SDC A2	Guide SDC A1	Guide SDC A2
Number of Ties	12	16	17	21
Area of Steel (in^2)	2.4	3.2	3.4	4.2
Percent Difference	33.3%		23.5%	

4.6.2 Bent Creek Road Bridge

The next bridge to be designed was Bent Creek Road Bridge in Lee County. It is a five-lane bridge that crosses over Interstate 85 with two spans of 135 feet. Each span is comprised of 15 modified BT-54 girders spaced approximately 5.33 feet apart that support a 6 inch concrete deck that is 80.75 feet wide. The only bridge pier is 79' x 4' x 4.5' and supported by five square columns 3.5 feet in width. The columns are reinforced longitudinally with 12 #11 bars and transversely with #4 ties uniformly spaced at 12 inches from the bottom of the bent to the top of the pile cap foundation. The average clear height of the columns is 20.1 feet. The bridge is supported on driven piles. The pile cap is 8.5' x 8' x 4.5' and each pile cap is supported by 9 HP 12x52 steel piles. The design calculations for this bridge can be found in Appendix E.

The first step is determining the vertical reaction at the bridge bent. The uniform live load on the bridge, discussed in LRFD 3.6.1.2.4, over the 6 design lanes was 1.92 kips per linear foot. The total loads were determined using the tributary area of the bent. The horizontal design forces including the live load factor of 0.50 were compared with the design forces with no live load considered. As Table 4.17 shows, the design forces increased by 10% with the addition of the live load.

Table 4.17: Bent Creek Road Bridge Design Force Live Load Factor Comparison (SDC A2)

Bent	Design Force with γ_{EQ} (kips)	Design Force without γ_{EQ} (kips)	Percent Difference
2	47.5	43.2	9.9%

Once the vertical reaction was found, the horizontal design forces were calculated. For SDC A2, the vertical reactions are 25% of the vertical reactions. These forces were 25% greater than those calculated using the Standard Specification, where the design force is 20% of the vertical reaction. Table 4.18 compares the two design forces.

Table 4.18: Bent Creek Road Bridge Vertical Reaction and Design Forces (SDC A2)

Bent	Vertical Reaction (kips)	Guide Spec Design Force (kips)	Standard Spec Design Force (kips)	Percent Difference
2	2852.2	47.5	38.0	25.0%

The next step was to calculate the minimum seat widths. Equation 4.1 and Equation 4.2 were used to calculate the seat widths according to the Standard Specifications and the new design recommendation, respectively. The new design equation resulted in a 30% longer seat width, as seen in Table 4.19.

Table 4.19: Bent Creek Road Bridge Minimum Seat Width Comparison (SDC A2)

Bent	New Design Minimum Support Length (in)	Standard Spec Minimum Support Length (in)	Percent Difference
2	16.4	12.3	30.1%

The design of the transverse reinforcement in the columns was completed next. Table 4.20 summarizes the results from the design. The plastic hinge length was controlled by the width of the column and determined to be 42 inches. The spacing inside the plastic hinge zones was controlled by the reinforcement ratio, and a maximum spacing of 4 inches was determined to satisfy this ratio. The spacing outside of the plastic hinge zone was 9 inches. The minimum area of transverse reinforcement check in the LRFD Specifications controlled this spacing. The Standard Specifications design only required 12 inch spacing. Using the Guide Specification resulted in an 85% increase in the number of ties required, both from the tighter spacing of ties in the plastic hinge zone and the tighter spacing of ties outside of the plastic hinge zone.

Table 4.20: Bent Creek Road Bridge Design Summary (SDC A2)

	Bent 2	
	Standard Specification	**Guide Specification**
Column Height (in)	240	240
Tie Size	#4	#4
Plastic Hinge Length (in)	-	36
PHL Spacing (in)	-	4
Spacing outside PHL (in)	12	9
Number of Ties	20	37
Area of Steel (in^2)	4	7.4
Percent Difference	85.0%	

The major differences between the two design specifications were the design forces and spacing of ties. The design forces increased by 25% and required approximately 85% more ties because of the tighter spacing requirements. This was due to the addition of the plastic hinge zone, which requires tight spacing, and the increase in spacing outside of the plastic hinge zone from the minimum area requirements. The only thing not affected was the minimum seat width, which was the same. Figure 4.10 shows the design details from each specification. While this design used #4 ties to maintain consistency with the Standard Specifications design, another option that would increase the spacing would be to use cross-ties or a larger bar size. This would maintain the same amount of reinforcing steel, but allow for larger spacing between ties.

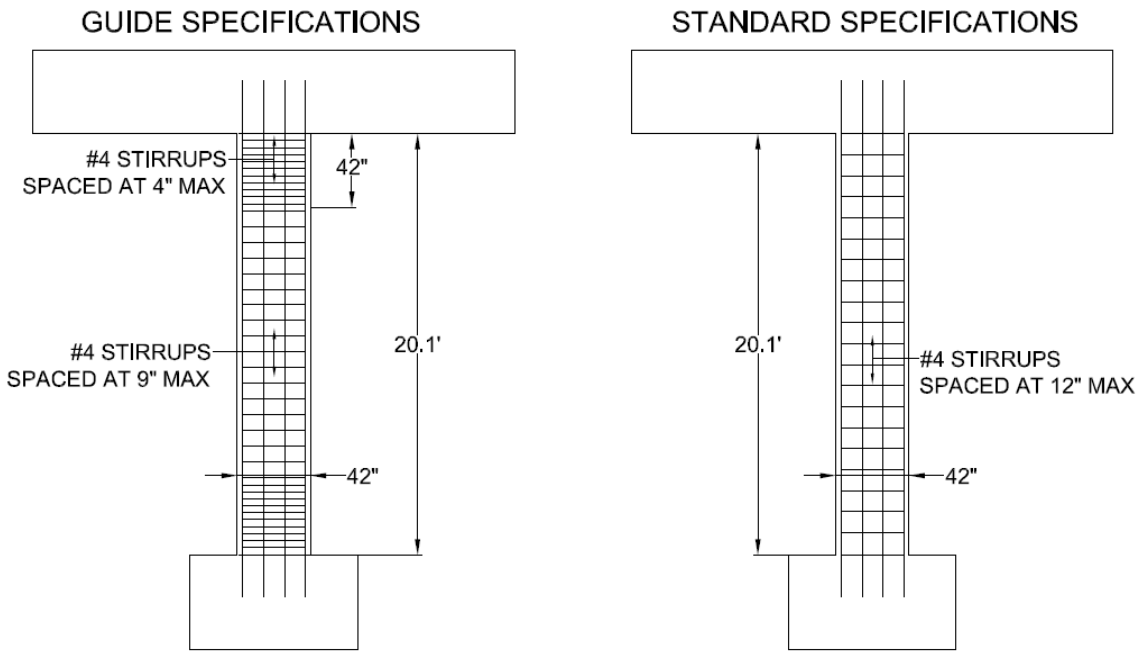

Figure 4.10: Bent Creek Road Bridge Bent 2 Final Design Details (SDC A2)

4.6.3 Bridge over Norfolk Southern Railroad

The third bridge to be designed in SDC A2 was the Bridge over Norfolk Southern Railroad. The southbound I-59 bridge in Etowah County is a two lane bridge that crosses over a Norfolk Southern railroad line and a state highway. It is a two span bridge with unequal span lengths of 125 feet and 140 feet. Nine modified BT-54 girders support a 6 inch concrete deck that is 46.75 feet wide. The only bridge pier is 53’ x 4.5’ x 4’ and supported by three square columns 3.5 feet in width. The columns are reinforced longitudinally with twelve #11 bars and transversely with #4 ties uniformly spaced at 12 inches from the bottom of the bent to the top of the pile cap foundation. The average clear height of the columns is 25.25 feet. The bridge is supported on driven piles. The pile cap is 8.5’ x 8’ x 4.5’ and each pile cap is supported by 7 HP 12x53 steel piles. Appendix F contains the design calculations for this bridge.

The first step was to determine the horizontal design forces at the bridge bent. This live load was calculated using 3 design lanes. The horizontal design forces were determined with and without the live load factor and are compared in Table 4.21. Including the live load increased the design forces by almost 8% for this bridge.

Table 4.21: Norfolk Southern Bridge Design Force Live Load Factor Comparison (SDC A2)

Bent	Design Force with γ_{EQ} (kips)	Design Force without γ_{EQ} (kips)	Percent Difference
2	49.1	45.5	7.9%

Once the vertical reaction was found, the horizontal design forces were calculated. For SDC A2, the design forces are 25% of the vertical reactions according to the Guide Specifications. In the Standard Specifications, the horizontal design forces are 20% of the vertical reaction. Table 4.22 shows that using the Guide Specifications increased the forces by 25%.

Table 4.22: Norfolk Southern Bridge Design Force Comparison (SDC A2)

Bent	Vertical Reaction (kips)	Guide Spec Design Force (kips)	Standard Spec Design Force (kips)	Percent Difference
2	1766	49.1	39.3	25.0%

The next step was to calculate the minimum seat width. Equation 4.1 was used to calculate the seat width for the Standard Specification and Equation 4.2 was used to calculate the new recommended seat width. As Table 4.23 shows, the new seat length is nearly 45% greater than the seat length provided by the Standard Specifications.

Table 4.23: Norfolk Southern Bridge Minimum Seat Width Comparison (SDC A2)

Bent	New Design Minimum Support Length (in)	Standard Specification Minimum Support Length (in)	Percent Difference
2	18.4	12.7	44.9%

Next, the design of the transverse reinforcement in the columns was completed. Table 4.24 summarizes the results from the design. The plastic hinge length was controlled by the height of the column and determined to be 50.5 inches. The spacing inside the plastic hinge zones was controlled by the reinforcement ratio, and a maximum spacing of 4 inches was determined to satisfy this ratio. The spacing outside of the plastic hinge zone was 9 inches. The minimum area of transverse reinforcement check in the LRFD Specifications was required for this bent and it controlled the spacing. Using the Guide Specification resulted in an 85% increase in the number of ties required because of the tighter spacing. An option that could be used to increase the spacing would be to use cross-ties or increase the tie size.

Table 4.24: Bridge over Norfolk Southern Railroad Design Summary (SDC A2)

	Bent 2	
	Standard Specification	Guide Specification
Column Height (in)	303	303
Tie Size	#4	#4
Plastic Hinge Length (in)	-	50.5
PHL Spacing (in)	-	4
Spacing outside PHL (in)	12	9
Number of Ties	26	48
Area of Steel (in^2)	5.2	9.6
Percent Difference	84.6%	

The major differences between the two design specifications were the design forces, minimum seat widths, and amount of transverse reinforcement. The design forces increased by 25% and the new design needed approximately 85% more ties. This was due to the addition of

the plastic hinge zone and the increase in spacing outside of the plastic hinge zone from the minimum area requirements. The minimum seat width increased because of the new equation that is used. Because the bent was very tall, the change in the seat length was greater than in any of the previously studied bridges. Figure 4.11 shows the design details from each specification.

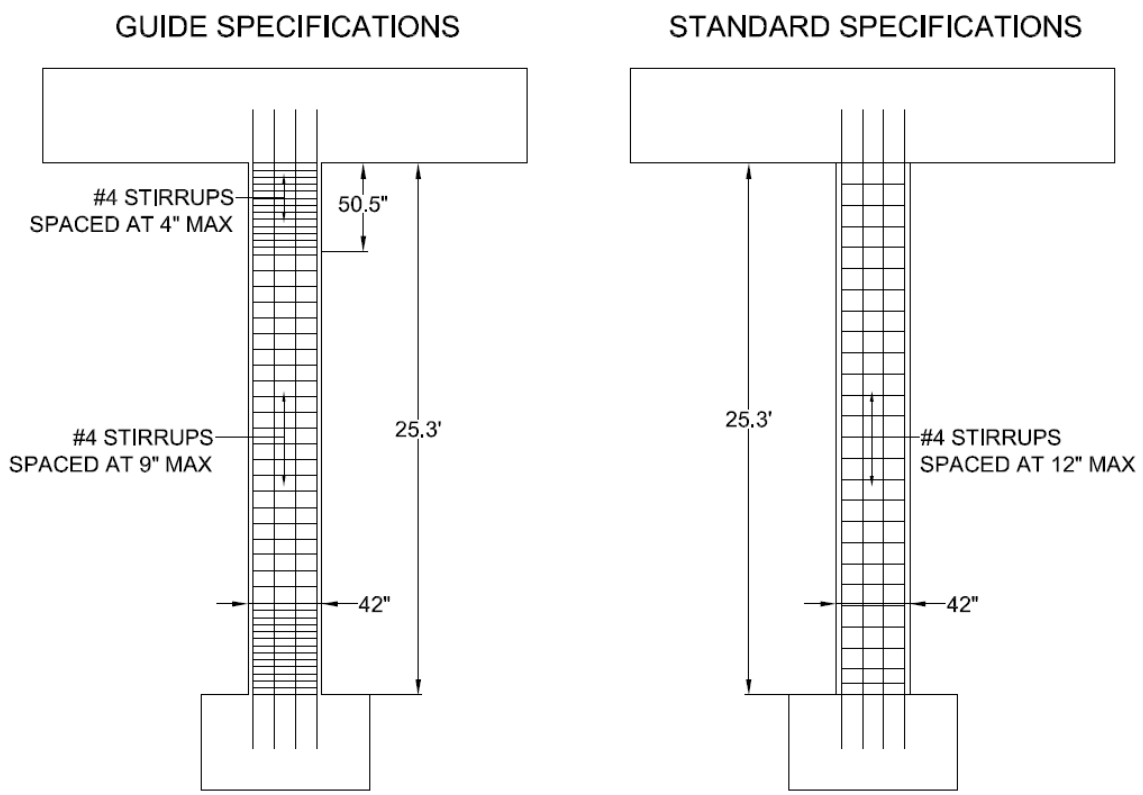

Figure 4.11: Bridge over Norfolk Southern Railroad Final Design Details (SDC A2)

4.6.4 Oseligee Creek Bridge

The final SDC A2 bridge to be re-designed was Oseligee Creek Bridge. This two lane bridge carries County Road 1289 over Oseligee Creek in Chambers County. It is a three span bridge with equal span lengths of 80 feet. The 7 inch concrete deck is supported by 4 Type III girders. The two bridge piers are 30’ x 4’ x 5’ and supported by two circular columns 3.5 feet in diameter with 3 inches of concrete cover. The columns are reinforced longitudinally with 12 #11

bars and transversely with #5 hoops uniformly spaced at 12 inches from the bottom of the pier cap to the rock line. The average clear height of Bent 2 is 17.93 feet and 25.83 feet for Bent 3. All columns are supported on drilled shafts 3.5 feet in diameter with concrete cover of 3 inches. Because the column and drilled shaft were the same diameter with no clear transition between them, it was unknown where the plastic hinge would form. It was assumed that the soil would not provide enough lateral reinforcement alone to force the plastic hinge to form at the ground line, so the plastic hinge was designed to form at the rock line. For this reason, the height of the columns used for the plastic hinge calculation was assumed to be from the bottom of the bent cap to the rock line. The design calculations for this bridge can be seen in Appendix G.

The first step in calculating the horizontal design force was determining the vertical reaction at each of the bridge bents. Each bent was similar, with the same dead weight and tributary area, so the vertical reactions were the same. The horizontal design forces including and excluding the live load factor were compared. As Table 4.25 shows, including the live load increased the design forces by 9%.

Table 4.25: Oseligee Creek Bridge Design Force Live Load Factor Comparison (SDC A2)

Bent	Design Force with γ_{EQ} (kips)	Design Force without γ_{EQ} (kips)	Percent Difference
2	38.8	35.6	8.9%
3	38.8	35.6	8.9%

Once the vertical reactions were found, the design forces were calculated. The Guide Specifications require the horizontal design forces to be 25% of the vertical reactions for bridges in SDC A2. The Standard Specifications requires the design forces to only be 20% of the vertical reactions. Table 4.26 shows that the design forces increased by 25% when the Guide Specification was used.

Table 4.26: Oseligee Creek Bridge and Design Force Comparison (SDC A2)

Bent	Vertical Reaction (kips)	Guide Spec Design Force (kips)	Standard Spec Design Force (kips)	Percent Difference
2	621	38.8	31.0	25.0%
3	621	38.8	31.0	25.0%

The next step was to calculate the minimum seat widths. Equation 4.1 and 4.2 were used to calculate the seat widths. As the results in Table 4.27 show, the new minimum seat lengths are 32-42% greater than those required by the Standard Specifications.

Table 4.27: Oseligee Creek Bridge Minimum Support Lengths Comparison (SDC A2)

Bent	New Design Minimum Support Length (in)	Standard Spec Minimum Support Length (in)	Percent Difference
2	14.6	11.0	32.7%
3	16.6	11.7	41.9%

The design of the transverse reinforcement in the columns was completed next. Table 4.28 summarizes the results from the design. The plastic hinge length for Bent 2 was 42 inches, controlled by the diameter of the column. Bent 3 was controlled by the height of the column and determined to be 51.7 inches. The design using the Standard Specifications used a #5 bar as the hoop size, but during the re-design, it was determined that a #4 hoop could be used at the maximum spacing, which inside the plastic hinge zones was controlled by the reinforcement ratio and was 6 inches. The spacing outside of the plastic hinge zone was 12 inches. The minimum area of transverse reinforcement check in the LRFD Specifications was not required because the shear resistance of the concrete was twice as large as the expected shear. Using a #4

hoop at the maximum spacing actually reduced the amount of transverse reinforcement by 11% for each of the bents.

Table 4.28: Oseligee Creek Bridge Design Summary (SDC A2)

	Bent 2		Bent 3	
	Standard Specification	Guide Specification	Standard Specification	Guide Specification
Column Height (in)	215	215	310	310
Hoop Size	#5	#4	#5	#4
Plastic Hinge Length (in)	-	42	-	51.7
PHL Spacing (in)	-	6	-	6
Spacing outside PHL (in)	12	12	12	12
Number of Hoops	18	25	26	36
Area of Steel (in^2)	5.6	5.0	8.1	7.2
Percent Difference	-10.7%		-11.1%	

There were three significant differences between the two designs: increase in design forces, increase in the minimum seat length, and decrease in the amount of transverse reinforcement. Interestingly, the design forces increased by 20% but the amount of transverse reinforcement was actually reduced by 11%, even with the addition of the plastic hinge zone. In the Standard Specifications design, #5 hoops were used. However, in the re-design it was determined #4 hoops could be used with the maximum spacing of the reinforcement. So even though the number of hoops increased, the area of the reinforcement decreased. Since only the seismic load condition was used in the re-design, it is possible that another load case resulting in a higher shear force controlled the original bridge design performed using the Standard Specifications, which required #5 hoops. The minimum seat width also increased, which is the result of the using the recommended minimum seat width equation. Figure 4.12 and Figure 4.13 show the design details from each specification.

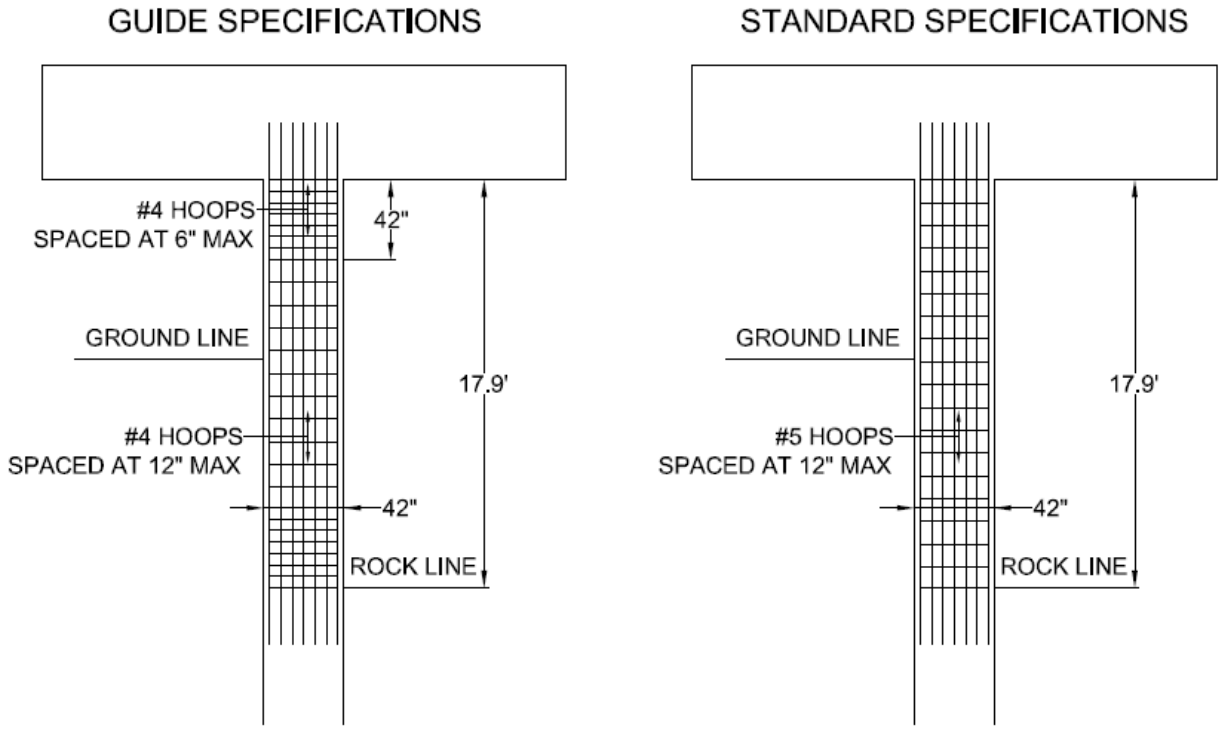

Figure 4.12: Oseligee Creek Bridge Bent 2 Final Design Details (SDC A2)

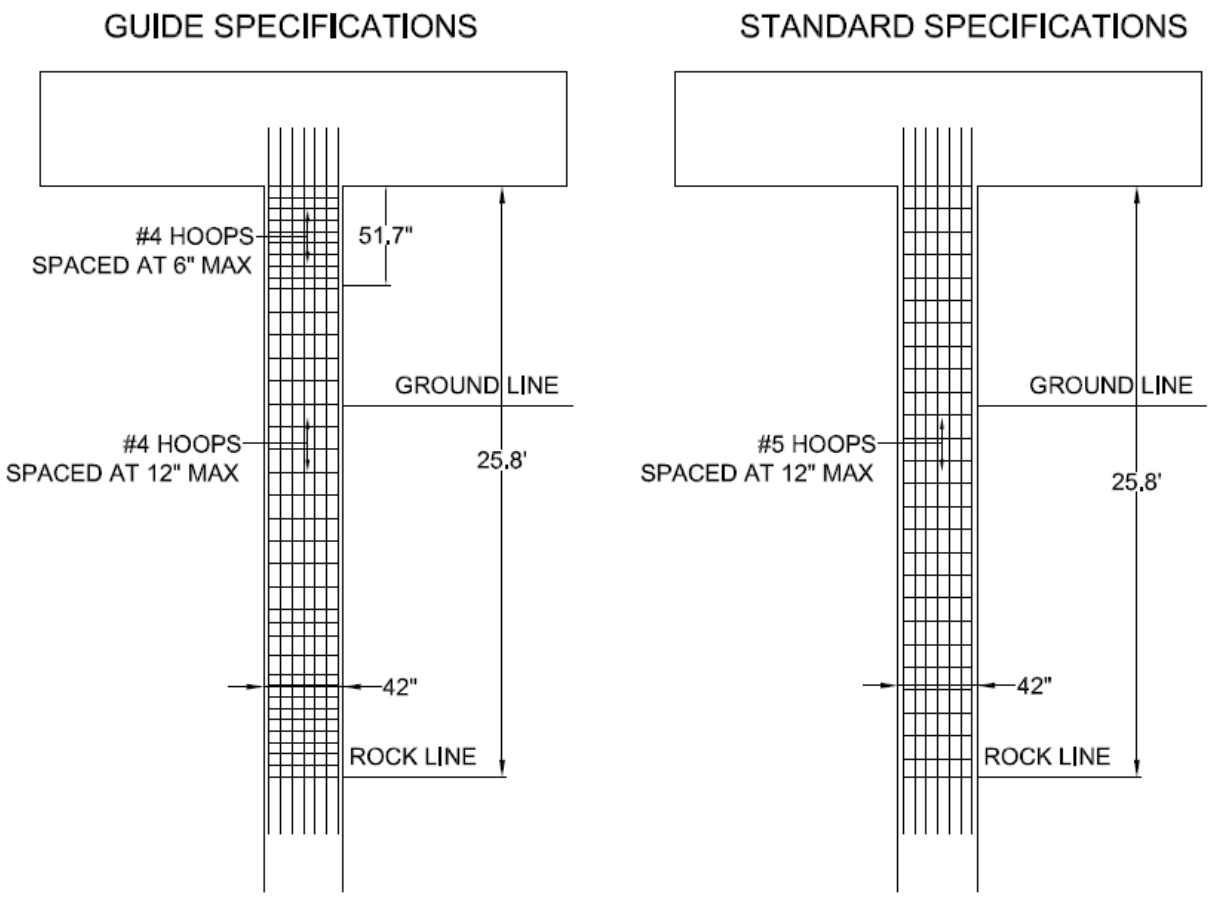

Figure 4.13: Oseligee Creek Bridge Bent 3 Final Design Details (SDC A2)

4.6.5 Summary of Differences in SDC A2

In SDC A2, the differences between the specifications are the increased horizontal design forces, change in the amount of transverse reinforcement, and the increased minimum seat length. The design force increased by 25% because SDC A2 requires the design force to be 25% of the vertical reaction, while the Standard Specification only requires 20%. The amount of transverse reinforcement increased by 40-85% for three of the bridges because the addition of the plastic hinge zone required more ties to satisfy the minimum ratios. The Standard Specification does not require a plastic hinge zone for bridges in SDC A, so the reinforcement is allowed to be spaced further apart. For all the bridges in this study, 12 inch uniform spacing was used for the

Standard Specification design and the Guide Specifications require a maximum spacing of 6 inches in the plastic hinge zone. The one exception came at Oseligee Creek Bridge, where #4 hoops were able to be used instead of #5 hoops as specified in the original design. And even with more hoops required because of the plastic hinge zone, the overall area of transverse reinforcement decreased. It is expected, however, that when the plastic hinge zone is required the amount of transverse reinforcement will increase because a larger number of ties or hoops will be needed. Taller columns will require more reinforcement because of the larger length over which the more tightly spaced ties or hoops will span. The minimum seat width increased in the range of 16-45%, depending on the height of the bridge and the expected spectral acceleration at the bridge site. This is a direct result of using the recommended ATC-49 equation, which gives a better estimation of the displacement of the girder during a seismic event.

There were three changes from SDC A1 to SDC A2. The first was the addition of the plastic hinge zone. This resulted in an increase in the amount of transverse reinforcement as mentioned earlier. The second was a slight increase in the minimum seat width. This is because the spectral accelerations for sites in SDC A2 are higher than sites in SDC A1. Since Equation 4.2 uses the spectral acceleration in the calculation of the minimum seat length, a higher value will give a higher minimum seat length. The third change was an increase in the horizontal design forces. They were required to be 25% of the vertical reaction because, unlike SDC A1 where they were 15% of the vertical reaction, bridges in SDC A2 will not experience low seismic forces ($A_S < 0.05g$).

4.7 Guide Specification Design Process for SDC B

SDC B bridges are expected to experience moderate seismic forces that will cause plastic hinges to form in the columns. These forces cannot be estimated using the simple relationships from SDC A. Additional structural analysis is required to determine the shear forces in the columns at individual bents during a design earthquake. These bents must be designed to resist the shear forces and moments. Minimum detailing is also required in this design category to ensure that the hinges form in the top and bottom of the column in the transverse direction and only in the bottom in the longitudinal direction. The design steps for this SDC are discussed below.

4.7.1 Create a Design Response Spectrum

Bridges in SDC B require a design response spectrum in order to calculate the horizontal design forces. The response spectrum is created from the three spectral accelerations, A_S, S_{D1}, and S_{DS}, calculated when determining the SDC. Article 3.4.1 in the Guide Specification outlines the steps to create the design spectrum. Figure 4.14 illustrates the three-point method found in the article, with T_o and T_S calculated from the three spectral acceleration values.

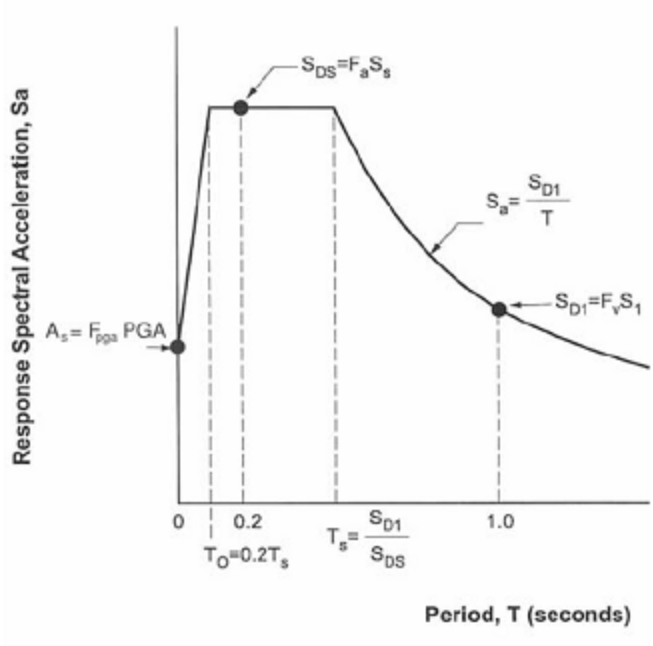

Figure 4.14: Design Response Spectrum, Construction Using Three-Point Method

4.7.2 Create and Analyze Bridge Model

The design forces will be the lesser the elastic forces and the plastic forces. The plastic forces will be determined at a later step. The elastic forces are determined from a bridge model and structural analysis. An equivalent static earthquake loading factor is determined from the structural analysis and design response spectrum. This factor is multiplied by the forces in the model to determine the elastic forces. Each of the five SDC B bridges in the project was modeled using the structural analysis software, CSI Bridge 15 (Computer and Structures Inc., 2012). The three bridges from the previous study, Little Bear Creek, Oseligee Creek, and Scarham Creek, had already been modeled so new models of those bridges were not necessary. Once the model is created, a structural analysis method is performed on the model to determine the displacements. The Guide Specifications allow for the use of either an Equivalent Static Analysis (ESA) or Elastic Dynamic Analysis (EDA). It recommends using the ESA if the bridge

is regular and EDA if it is not. Bridge regularity is defined as having fewer than 7 spans, no abrupt or unusual change in geometry and satisfying the requirements in Table 4.29 (Guide Specifications Table 4.2-3). Regular bridges typically respond in their fundamental mode of vibration, and the procedures in an ESA are calibrated for that specific response. For the bridges in this study, ESA methods were used because all of the bridges in this project were "regular" bridges. The EDA provides a much better model for inelastic behavior by better representing inelastic elements and secondary modal responses. However, if it is used, the bridge model should be based on cracked section properties for concrete components and secant stiffness coefficients for foundations and abutments (AASHTO, 2011).

Table 4.29: Regular Bridge Requirements

Parameter	Value				
Number of Spans	2	3	4	5	6
Maximum subtended angle (curved bridge)	30°	30°	30°	30°	30°
Maximum span length ratio from span-to-span	3	2	2	1.5	1.5
Maximum bent/pier stiffness ratio from span-to-span (excluding abutments)	-	4	4	3	2

Two different ESA options that are acceptable are the uniform load method and single-mode spectral method. The uniform load method is simpler, but it can overestimate the lateral forces in the abutment by as much as 100% (AASHTO, 2011). The uniform load method procedure is described in article C5.4.2 of the Guide Specification. This analysis should be completed in each direction (transverse and longitudinal) because the results will need to be combined. This method places a uniform load of 1 kip/in along the entire length of the bridge and determines the maximum displacement along the bridge length. The maximum

displacement is used to calculate the bridge lateral stiffness as seen in Equation 4.8. The period of the bridge is calculated using Equation 4.9. Using the bridge period and response spectrum, the equivalent static earthquake loading is calculated using Equation 4.10.

$$K = \frac{p_o * L}{v_{s,max}} \qquad \text{Equation 4.8}$$

$$T_m = 2 * \pi * \sqrt{\frac{W}{K * g}} \qquad \text{Equation 4.9}$$

$$\rho_e = \frac{S_a * W}{L} \qquad \text{Equation 4.10}$$

Another analysis procedure, the single-mode spectral method, is described in article 4.7.4.3.2b of the LRFD Specifications. This is a more complicated analysis, but can be used to determine more accurate design forces if the results from the uniform load method are too conservative. This analysis should also be done in both the transverse and longitudinal direction, just like the uniform load method. The procedures are similar, but generalized functions are used to describe the displacement instead of a maximum value. The first step is building a bridge model and applying a uniform load of 1 kip/in. The displacement of the bridge is calculated as a function along the entire length of the bridge. A program such as Microsoft Excel can be used to input the displacements along the length of the bridge and generate a function from a graph. Three factors are determined from this displacement function as seen in Equations 4.11, 4.12, and 4.13: α, generalized flexibility, β, generalized participation, and γ, generalized mass.

$$\alpha = \int_0^L v_s(x) * dx \qquad \text{Equation 4.11}$$

$$\beta = \int_0^L w(x) * v_s(x) * dx \qquad \text{Equation 4.12}$$

$$\gamma = \int_0^L w(x) * {v_s}^2(x) * dx \qquad \text{Equation 4.13}$$

The period of the bridge is determined using Equation 4.14 and the equivalent static earthquake load is determined using Equation 4.15. In the LRFD Specifications, the variable C_{sm} is equal to S_a used in the Guide Specifications.

$$T_m = 2 * \pi * \sqrt{\frac{\gamma}{p_o * g * \alpha}} \qquad \text{Equation 4.14}$$

$$p_e(x) = \frac{\beta * C_{sm}}{\gamma} * w(x) * v_s(x) \qquad \text{Equation 4.15}$$

The equivalent static earthquake loading factor, ρ_e, represents the response of the bridge in the primary mode of vibration. Both the transverse and longitudinal directions have their own factor since the response of the bridge is different in each direction. This factor is used to determine the bridge displacement demand as well as the design forces. The design forces are determined by multiplying the appropriate equivalent static earthquake loading by the forces from the model (either longitudinal or transverse). The displacement demand will be discussed in the next section.

4.7.3 Bridge Capacity vs. Displacement

Article 4.8 in the Guide Specification requires a capacity displacement check to be satisfied for bridges in SDCs B, C, and D. The bridge is required to have a larger displacement capacity than displacement demand at each of the bents. This ensures that the bridge can achieve its inelastic deformation capacity (AASHTO, 2011). Since the bridge is designed to be ductile, it is assumed that the bridge will be able to carry load without failure through the entire demand displacement. But the capacity of the bridge must be greater than the demand for this to be true. Equation 4.16 shown below is used to determine the capacity of the bridge based on the geometry and clear height of the columns for bridges in SDC B. It is only intended for determining displacement capacities of single and multiple reinforced concrete column bridges

with clear heights greater than 15 feet, plastic hinging occurring above ground, and where fusing of the superstructure and substructure during a design earthquake is not expected (AASHTO, 2011). The five bridges studied in SDC B were assumed to have the plastic hinging occur either where the column was connected to the foundation or where the foundation reached the rock line, which was below ground, and would violate the requirements for use of the equations. However, the Guide Specifications specifically allow for these equations to be used for bridges with a plastic hinge occurring below ground where the column connects with the foundation. Equation 4.17 requires a factor for column end restraint condition (Λ), which for this project was assumed to be fixed at the top and bottom for movement in the transverse direction and pinned at one end for movement in the longitudinal direction. The Guide Specifications provides guidance if a different end restraint condition exists. If a bridge does not satisfy the requirements for use of Equation 4.16, a Nonlinear Static Procedure or "pushover" analysis, mentioned in Article 4.8.2, is to be used. Also, if any of the bent displacements are greater than the capacities of Equation 4.16, a pushover analysis could be performed on the model using the computer software.

$$\Delta_C^L = 0.12 * H_o * (-1.27 \ln(x) - 0.32) \geq 0.12 * H_o \qquad \text{Equation 4.16}$$

$$x = \frac{\Lambda * B_o}{H_o} \qquad \text{Equation 4.17}$$

The demand displacement of the bridge is determined in each orthogonal direction at each bent from the bridge model and structural analysis. Once the static analysis is performed, the displacements of the bent in each orthogonal direction are recorded and multiplied by the equivalent static earthquake load and short period magnification factor. The short period magnification factor is determined in Article 4.3.3, and corrects the displacement determined from an elastic analysis for bridges in a short period range as determined from the response

spectrum. The expected displacement of the bents is determined using Equations 4.18 and 4.19. Article 4.4 in the Guide Specification requires the use of two unique load cases to capture the expected displacement of the bridge based on the uncertainty of earthquake motions and simultaneous earthquake forces in two perpendicular horizontal directions. Equations 4.18 and 4.19 determine the displacement by taking the square root sum of the squares of 100% of the absolute value of seismic displacements in one direction (either longitudinal or transverse) with 30% of the absolute value of seismic displacements in the other orthogonal direction. The larger of the two displacements is taken as the expected displacement of the bent. If all bents in a bridge have a higher capacity than demand, then detailing of the reinforcement in each column can begin. If a single bent does not satisfy the displacement demands, a pushover analysis can be performed, the capacity equations from SDC C can be used, or the dynamic characteristics of the bridge can be modified. If these equations for SDC C are used, the bridge must be designed according to SDC C requirements. This project did not deal with this method, instead using a pushover analysis if a bent did not meet the capacity requirements.

$$\Delta D = \sqrt{(1 * \Delta D_{LONG})^2 + (0.3 * \Delta D_{TRAN})^2} \qquad \text{Equation 4.18}$$

$$\Delta D = \sqrt{(1 * \Delta D_{TRAN})^2 + (0.3 * \Delta D_{LONG})^2} \qquad \text{Equation 4.19}$$

4.7.4 Column Seismic Detailing

Once the capacity of a bridge bent is confirmed, the reinforcement for each column can be detailed. For SDC B, there is minimum detailing that must be met within the plastic hinge region as well as detailing for reinforcement outside of the plastic hinge region. The first step is to determine the plastic hinge length (PHL) for each individual column.

4.7.4.1 Plastic Hinge Length

The plastic hinge length (PHL) is the assumed length of the column where the plastic hinge will form and is designed to be at the top of the column and the bottom of the column, where the column meets the foundation, although the location of the plastic hinge at the bottom can vary depending on the soil and foundation type. For the bridges in SDC B, the plastic hinge was assumed to form at the top of the column and at the bottom of the column, at the connection with the foundation element, in the transverse direction, but only at the bottom of the column in the longitudinal direction. The minimum detailing requirements increase the amount of shear reinforcement, which helps confine the concrete and prevent buckling of the longitudinal reinforcement, as well as give the section more shear resistance, decreasing the possibility of a brittle failure that will not allow the column to dissipate energy. Article 4.11.7 in the Guide Specification provides the PHL to be the largest of three lengths (AASHTO, 2011):

- 1.5 times the largest cross-sectional dimension in the direction of bending
- The region of the column where the moment demand exceeds 75% of the maximum plastic moment
- The analytical plastic hinge length, L_p

The largest cross-sectional dimension will be either the diameter of a circular column or the largest width of a rectangular column. The maximum plastic moment is determined by a moment-axial force interaction diagram. For this project, the software program spColumn was used (StructurePoint, 2012). The dimensions of the column and the reinforcement layout are input into the program, and the maximum moment is determined from the resulting moment interaction diagram. Once the maximum moment is determined, the moment diagram from the computer analysis software can be used to determine the length of the column where the moment

exceeds 75% of the plastic moment. The analytical plastic hinge length is determined in Article 4.11.6 using Equation 4.7. This equation is specifically for reinforced concrete columns framing into a footing, integral bent cap, oversized shaft, and cased shaft, which meets the criteria for this project.

$$L_p = 0.08 * L + 0.15 * f_{ye} * d_{bl} \geq 0.3 * f_{ye} * d_{bl} \qquad \text{Equation 4.7}$$

In most cases, the PHL is controlled by the 1.5 times the gross cross-sectional dimension. This can result in a large PHL for large columns and since the PHL is at the top and bottom of the column, the entire column could be considered to be within the plastic hinge. This makes it difficult to meet the splicing requirements found in Article 8.8.3 for the longitudinal column reinforcement. The splicing is required to be outside of the plastic hinge length. Failure to do so could lead to undesirable seismic performance because the splice would be subject to plastic forces and deformations, which could lead to a reduced effective plastic hinge length and severe local curvature demand (AASHTO, 2011). While this article only applies to SDC C and D, the commentary recommends that they also be applied to SDC B.

Article 8.8.9 in the Guide Specifications gives an alternative PHL that can be used in SDC B that is calculated using Article 5.10.11.4.1e of the LRFD Specification. These requirements are easier to determine and do not require any computer software. The maximum of three limits is taken as the PHL (AASHTO, 2007):

- The largest cross-sectional dimension
- One-sixth the clear height of the column
- 18 inches

The largest cross sectional dimension will be either the diameter of a circular column or the largest width of a rectangular column. The clear height of the column depends on the

foundation type and geometry. The foundations from the three bridges in the previous project were drilled shafts. For two of the bridges, Little Bear Creek Bridge and Scarham Creek Bridge, the drilled shafts were six inches wider than the columns, and the plastic hinge was assumed to form at the transition between the two. The clear height was taken from the bottom of the bent cap to this transition point. However, for Oseligee Creek Bridge, the drilled shaft was the same size as the columns, and it was unknown if the plastic hinge would form at the transition point because there was no change in stiffness between the two members. Therefore, it was assumed the plastic hinge would form at the rock line because below the drilled shaft would be unable to displace below the rock line. The clear height of these columns was measured from the bottom of the bent cap to the rock line. For the other two bridges, driven piles were used as the foundations. It was assumed the plastic hinge would form at the column to pile cap connection, and the column height was taken from the bottom of the pier cap to the top of the pile cap. It is important to understand how the column and foundation will interact in order to determine where the plastic hinge is likely to form. Using the plastic hinge length from the LRFD Specifications will typically result in a smaller PHL than that found in the Guide Specifications. This will allow for a greater length of column for splicing and fewer confinement ties. For the bridges in SDC B, both values will be checked.

The LRFD Specifications, in Article 5.10.11.4.3, discuss an extension of the plastic hinge length into the cap beam or the foundation (pile cap or drilled shaft). The Guide Specifications do not specifically mention this extension length, but since it is mentioned in the same article as the LRFD plastic hinge length, it will be considered appropriate for use. This extension is only required in SDC C and D, but it is recommended in SDC B. The extension length is an extra length over which the ties from the plastic hinge zone extend. The spacing of these ties is equal

to the spacing from the plastic hinge zone. This is an added measure to protect the elements adjacent to the plastic hinge. Article 5.10.11.4.1e in the LRFD Specifications requires the extension length to be the maximum of the following:

- One-half of the column diameter
- 15 inches

The extension length will be calculated and shown in the details for each bridge in SDC B, but it should be noted that the inclusion of this length in the design is at the Owner's discretion and not required.

4.7.4.2 Transverse Reinforcement inside Plastic Hinge Zone

Once the plastic hinge length is determined, the size and spacing of the transverse reinforcement within the plastic hinge length can be determined. Unlike SDC A2, the flexure and shear demands in the column are used, along with the minimum ratios, to determine the spacing. The column will be designed for the maximum expected forces in the plastic hinge, and the minimum ratios will be checked. In order to determine the design forces, Article 8.3.2 states that for SDC B "the design forces shall be the lesser of the forces resulting from the overstrength plastic hinging moment capacity or unreduced elastic seismic forces in columns or pier walls" (AASHTO, 2011). The elastic seismic forces come directly from the software analysis, multiplied by the equivalent static earthquake load factor. For SDC B, the plastic moment capacity comes from the moment-axial force interaction diagram computed earlier. The Guide Specifications allow for the use of the nominal plastic moment from the interaction diagram instead of the idealized capacity because the inelastic demands should be small (AASHTO, 2011). This plastic moment must still be multiplied by an overstrength factor to account for

material strength variations between the column and adjacent members. A shear force is calculated from this overstrength plastic moment, and the lesser of the plastic shear force and elastic shear force is used to design the transverse reinforcement. Article 8.6 recommends designing for the plastic force whenever possible, but does not require it. In this project, the lesser of the elastic forces and plastic forces will be used in the design.

Once the design forces have been determined, the concrete shear capacity and steel reinforcement shear capacities are determined according to Articles 8.6.2 through 8.6.4. These equations are based on the degradation of the concrete shear capacity within the plastic hinge region (AASHTO, 2011). To determine these capacities, column dimensions and reinforcement size and spacing must be known. A computer based design sheet can be used to easily allow for an iterative process. The Guide Specifications does give some guidance to the size of ties and the spacing of ties. Article 8.8.9 requires at least #4 bars to be used for transverse reinforcement if #9 bars or smaller are used as longitudinal reinforcement, and at least #5 bars for transverse reinforcement if #10 bars or greater are used as longitudinal reinforcement. The article also has maximum spacing requirements. These requirements indicate that the maximum spacing of transverse reinforcement cannot be greater than the smallest of the following:

- One-fifth the least dimension of the cross-section for columns
- Six times the nominal diameter of the longitudinal reinforcement
- 6 inches

If the longitudinal reinforcement is at least a #9 bar and the column size is at least 30 inches, as all of the bridges in this study are, then the 6 inch maximum spacing controls. Once the concrete and shear capacities are determined to be greater than the demand, the minimum ratio of transverse reinforcement in Article 8.6.5 must be checked. It requires a minimum ratio

of transverse reinforcement, as calculated in Article 8.6.2, of greater than or equal to 0.003 for spirals in circular columns and greater than or equal to 0.002 for rectangular columns. Once this minimum requirement has been satisfied and the transverse reinforcement is determined to provide sufficient capacity, the detailing within the PHL is finished.

4.7.4.3 Transverse Reinforcement outside Plastic Hinge Zone

The detailing requirements inside the plastic hinge region are specifically outlined in the Guide Specifications. However, the equations for determining concrete capacity used in the Guide Specification are not meant to be used outside of the plastic hinge region because they include the expected concrete behavior as the hinge region becomes plastic. Therefore, the LRFD Specifications are used to design the shear reinforcement outside of the plastic hinge region. The shear force to be used in the design is the same shear force calculated in the static analysis. Article 5.8.3.3 in the LRFD Specifications is used to determine the capacity of the column. Since these requirements are different than those used in the Guide Specifications they should not be used to calculate the concrete capacity within the plastic hinge zone. Equations 4.3 and 4.4 are used determine the shear capacity of the transverse reinforcement and the concrete. These equations are specific to the bridges studied and should be checked against the other methods for calculating shear capacity in the LRFD Specifications. Once the design is satisfied for strength, three spacing requirements are checked. The reinforcement size is already known from the plastic hinge zone calculations, but the spacing of reinforcement is determined from the capacity equations and the limit checks. The first requirement can be found in Article 5.8.2.5 of the LRFD Specifications and is a minimum amount of transverse reinforcement. It is only required when the factored load is greater than half of the factored resistance by the concrete

section and prestressing steel (if present). It is intended to provide reinforcement in regions where there is a significant chance of diagonal cracking (AASHTO, 2009). If it is determined that this minimum reinforcement is required, then Equation 4.5 is used to determine the minimum area of transverse reinforcement. This equation in the LRFD Specifications is different than the equation found in the Standard Specifications. It results in a larger minimum area of transverse steel in the column. Article 8.19.1.2 of the Standard Specification uses Equation 4.6 to find the minimum area. The value is a constant, 0.05 ksi. Article 5.8.2.5 in the LRFD Specifications uses Equation 4.5, and the coefficient is a function of the compressive strength of concrete. For 4,000 psi concrete, the value is 0.0632 ksi. The difference between the values shows that the LRFD Specifications will result in a higher minimum area of reinforcement compared to the Standard Specifications.

The second check is the maximum spacing check found in LRFD article 5.8.2.7. This check addresses the need for tighter spacing if the section experiences very high shear stress. Most sections will not experience very high shear stress, so this requirement will not typically control the design. The final check is an ALDOT standard maximum spacing of 12 inches. In the event that the column is not required to meet the minimum area of transverse reinforcement requirement, this 12 inch maximum spacing will likely control.

$$V_c = 0.0316 * \beta * \sqrt{f_c'} * b_v * d_v \qquad \text{Equation 4.3}$$

$$V_s = \frac{A_v * f_y * d_v * \cot(\theta)}{s} \qquad \text{Equation 4.4}$$

$$A_{v,min} = 0.0316 * \sqrt{f_c'} * \frac{b_v * s}{f_y} \qquad \text{Equation 4.5}$$

$$A_{v,min} = 0.05 * \frac{b * s}{f_y} \qquad \text{Equation 4.6}$$

Another factor that would affect the spacing of the reinforcement would be the requirement of cross-ties. LRFD Article 5.10.6.3 requires the use of cross ties in rectangular columns to ensure that no longitudinal bar is more than 2 feet from a restrained bar. However, for all of the bridges in this study, no columns were large enough for this requirement to be necessary. Therefore, this requirement did not control the design.

4.7.4.4 Longitudinal Reinforcement

The longitudinal reinforcement is designed using the moment-axial force interaction diagrams for the columns. For this project, the longitudinal reinforcement in the original designs was used in the new designs. This reinforcement was checked using the moment-axial force interaction diagrams to determine if the column capacity is greater than the load demand. The load demands are calculated from the bridge model and structural analysis. Multiple load cases need to be analyzed, as discussed in Article 4.4 of the Guide Specifications. The axial load is determined by taking the largest axial force from the dead load and adding it to the largest axial force from the combination of earthquake loads multiplied by the equivalent static earthquake load. In order to determine the maximum moment, the maximum and minimum dead load cases should be considered because the axial load can affect the moment capacity. The most severe axial loads and moments should be input into the spColumn software to determine if the column capacity is sufficient to resist the loads.

Once the capacity of the columns is ensured, a minimum and maximum ratio check is to be performed. Articles 8.8.1 and 8.8.2 detail these checks. The maximum check, found in Article 8.8.1, requires the area of longitudinal reinforcement to be equal to or less than 4% of the gross area of the column. Limiting the amount of longitudinal reinforcement increases the

ductility of the column. The minimum check in Article 8.8.2 requires that the longitudinal reinforcement area be greater than or equal to 0.7% of the gross area. This check is done to "avoid a sizable difference between the flexural cracking and yield moments" (AASHTO, 2011). Once these checks are satisfied, the longitudinal reinforcement design is finished.

4.8 SDC B Design Examples

The design procedure in the Guide Specifications for SDC B was used to redesign five bridges previously designed under the Standard Specifications. These bridges were supplied by ALDOT and are conventional bridges in the "other" category as described earlier, making them applicable to the Guide Specifications. For each bridge, design sheets were created with references to specific articles in the Guide Specifications or LRFD Specifications. Since the purpose of these redesigns is to determine if a standard set of drawings and details can be identified for these bridges, design data is established for each bent of a bridge. This information was summarized for each bridge. Under the previous study by Coulston and Marshall (2011), three bridges in SDC B were redesigned using both the Guide Specifications and the LRFD Specifications. These three bridges are included in the five bridges to be redesigned in this project so that all the bridges will have been designed using the most recent edition of the Guide Specifications. The two new bridges to be redesigned are Bent Creek Road Bridge over I-85 in Lee County and the Bridge over Norfolk Southern Railroad in Etowah County. The three bridges previously designed include Bridge over Little Bear Creek in Franklin County, Oseligee Creek Bridge in Chambers County, and Scarham Creek Bridge in Marshall County.

The superstructure-to-substructure connection must be investigated for bridges in this SDC. As discussed in chapter 3, the current connection is to be used for all bridges, and any

longitudinal forces will be dealt with by allowing the girders to move and "ride out" the earthquake without unseating. This is accomplished by providing greater seat widths than provided by the equations in the Guide Specifications. However, in the transverse direction, the connection needs to be checked to ensure it can transfer the loads into the substructure. Article 4.11 in the Guide Specifications requires those elements "not participating as part of the primary energy-dissipating system" to be capacity protected, meaning they must be designed for the maximum expected forces (AASHTO, 2011). These forces are determined from a pushover analysis. The clip angles and anchor bolts from this connection were designed for each bridge based on these forces. The results from the pushover analysis, as well as the design of the transverse connection, will be discussed for each bridge.

4.8.1 Bent Creek Road over I-85

This bridge was already designed in the SDC A2 category and will be re-designed in SDC B to compare the two designs determine if it is more economical to design the bridge as a SDC B bridge. Bent Creek Road bridge is a five-lane bridge that crosses over Interstate 85 in Lee County. It is a two span bridge with equal span lengths of 135 feet comprised of 15 modified BT-54 girders spaced approximately 5.33 feet apart and supports a 6 inch concrete deck that is 80.75 feet wide. The only bridge pier is 79' x 4' x 4.5' and supported by five rectangular square columns 3.5 feet in width. The columns are reinforced longitudinally with 12 #11 bars and transversely with #4 ties uniformly spaced at 12 inches from the bottom of the bent to the top of the pile cap foundation. The average clear height of the columns is 20.1 feet. The bridge is supported on driven piles. The pile cap is 8.5' x 8' x 4.5' and each pile cap is supported by 9 HP 12x53 steel piles. Figure 4.15 shows a 3D view of the bridge as modeled in SAP2000.

All design calculations can be seen in Appendix H and the moment-axial force interaction diagrams for the columns can be seen in Appendix I.

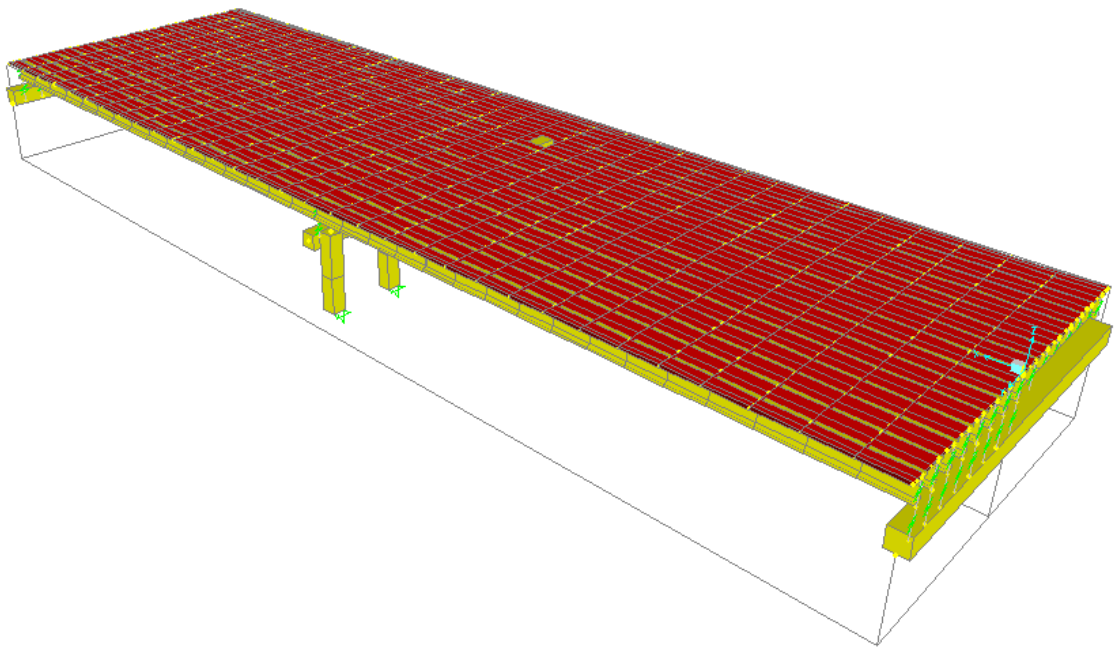

Figure 4.15: SAP2000 3D Model of Bent Creek Road Bridge

The first step was to determine if the bridge capacity was greater than the demand. Table 4.30 shows the results from this analysis. The bridge model was used to analyze the bridge and determine the displacements of the bents. The uniform load method was used to determine the equivalent static earthquake loading factor, which, along with the short period magnification factor, was multiplied by the bent displacements in each direction to determine the expected displacement at the bent. The capacity of the bridge bent was determined in each direction using Equations 4.16 and 4.17. The largest displacement from the square root sum of the squares (SRSS) of the two orthogonal displacements was compared to the smallest capacity. As the table

shows, the capacity was greater than demand, so this bent passed the demand/capacity check and could be designed.

Table 4.30: Analysis Results for Bent Creek Road Bent 2

	Transverse	Longitudinal
Displacement at Bent from Model	3.012"	0.052"
Expected Displacement at Bent	0.862”	0.078”
Bent Capacity	2.448”	4.567”
SRSS Displacement	0.863”	

A pushover analysis of the bridge was also performed. The design force for the connection was determined using the expected transverse displacement of the bent calculated in the structural analysis as described above. Figure 4.16 shows that, for this bridge, the base shear was 620 kips and since the bridge had 15 girder connections, the connection design force was 41.3 kips. This force was used to design the clip angles and anchor bolts, which will be discussed below.

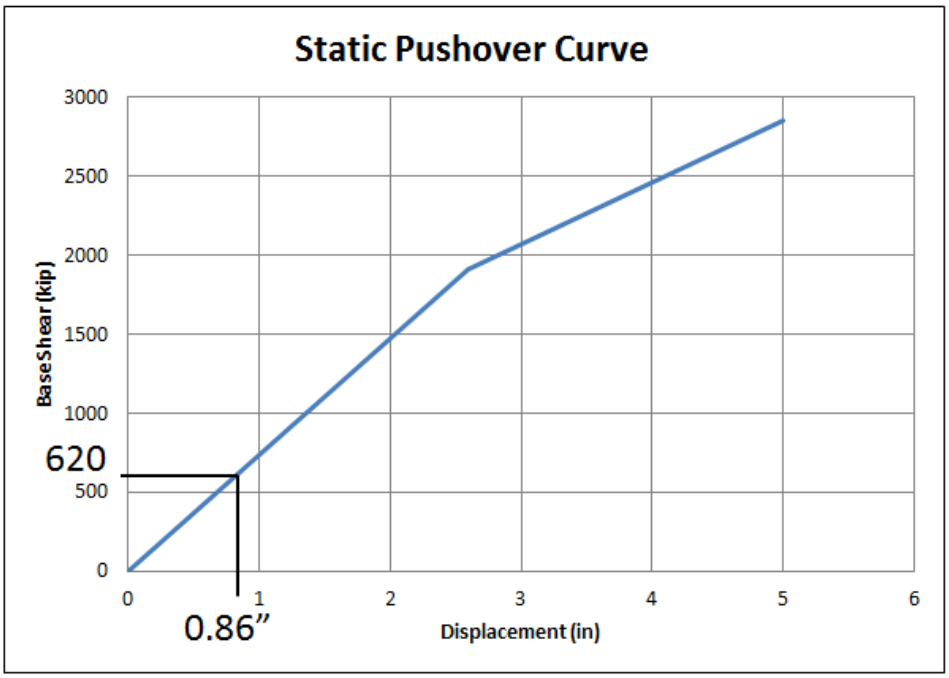

Figure 4.16: Static Pushover Curve for Bent Creek Road Bridge Bent 2

Using the design force from the pushover analysis, the transverse clip angles and anchor bolts were designed. The LRFD Specifications and AISC Specifications were used to design them. The specific articles are referenced in the design which can be seen in the appendices. The clip angle size was chosen from the original connection and block shear, tension and shear capacities of the angles were checked against the design force. It was assumed that one of the angles would have to resist the entire design force because the other angle would not be able to transfer a tensile force. Table 4.31 shows the capacity of the clip angle for these three limit states. For this design force, the clip angle was acceptable. The anchor bolt was designed for shear, bearing, tension, and combined tension and shear. Like the clip angle, only one anchor bolt was assumed to resist the load since only one clip angle would be able to transfer load. It was determined that an ASTM A307 Class C bolt with a diameter of 1.75 inches would be required for this connection.

Table 4.31: Capacity of the Steel Clip Angle

Limit State	Capacity (kips)
Block Shear	156
Tension	118
Shear	130

Once the capacity check was satisfied and the connection design completed, the minimum seat widths were calculated. The ATC-49 equation, Equation 4.2, was used to calculate the minimum seat widths and Equation 4.1 was used to find the Standard Specifications minimum seat width. As recommended in chapter 3, S_{D1} was taken to be 0.30 for all of the bridges in SDC B. This resulted in a 70% increase in the minimum seat length required, as seen in Table 4.32.

Table 4.32: Bent Creek Road Bridge Seat Width Specification Comparison (SDC B)

Specification	Standard	New Design
Minimum Seat Width (in)	12.3	19.8
Percent Difference	70.0%	

The column design was completed next. The longitudinal reinforcement satisfied both checks, and the column capacity was acceptable. Table 4.33 shows the results from this design analysis. The plastic hinge length from the LRFD Specifications was used, because it resulted in a 50% decrease of the plastic hinge length calculated using the Guide Specifications. The length was calculated to be 42 inches, with an extension length of 21 inches. The column length outside of the plastic hinge region that could be used for splicing was 156 inches or about 13 feet. Similar to SDC A2, the new design requires 95% more ties than the original design under the Standard Specifications. Figure 4.17 shows the differences between the two specifications using the design details.

Table 4.33: Bent Creek Road Bent 2 Design Results (SDC B)

	Bent 2	
Plastic Hinge Length (in)	42	
Extension Length (in)	21	
Available Splice Length (in)	156	
Tie Size	#4	
Specification	Standard	Guide
Spacing within PHL (in)	-	4
Spacing outside PHL (in)	12	9
Total Number of Ties	20	37
Area of Ties (in^2)	4	7.8
Percent Difference	95.0%	

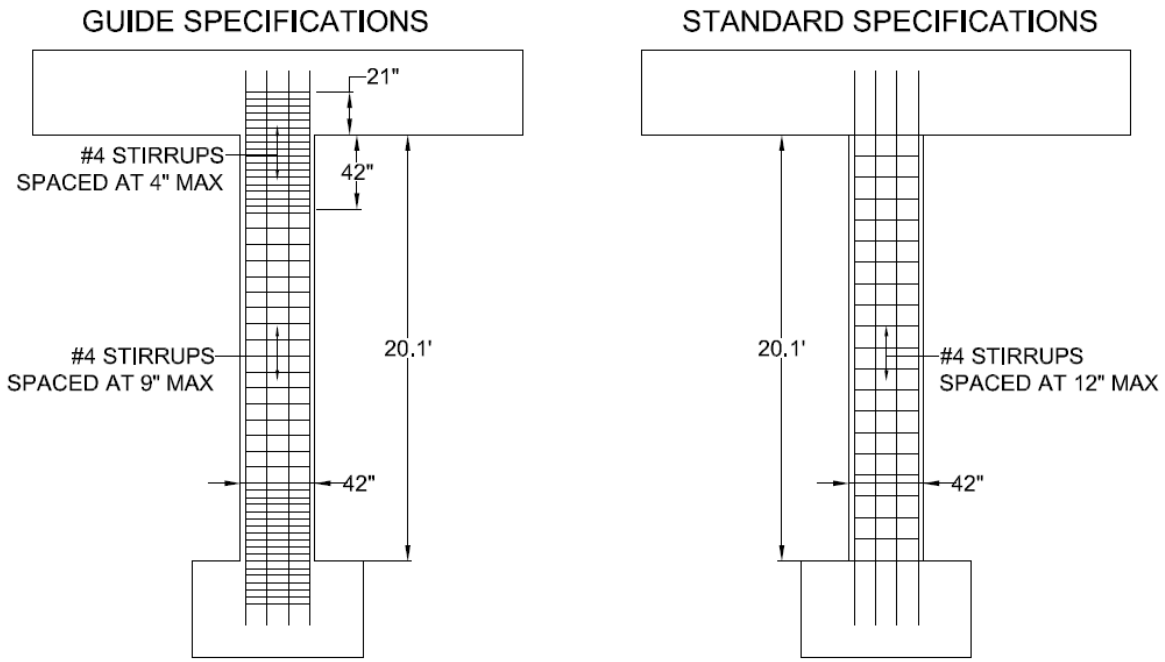

Figure 4.17: Bent Creek Road Bridge Bent 2 Final Design Details (SDC B)

When compared with the same design in SDC A2, the only differences are the horizontal design force and minimum seat width. With the exception of the extension length, which is not required for SDC B and therefore not included in the reinforcement calculation, the amount of transverse reinforcement was the same in both categories. The horizontal design force from SDC A2 that was compared did not include the live load because it resulted in the smaller force. As Table 4.34 shows, the horizontal design force was determined to be 4.4% less for SDC B than for SDC A2. For this bridge, it would be more economical to perform a structural analysis to determine the horizontal design forces for the connection. The minimum seat width is almost 21% greater in SDC B than in SDC A2, because the new equation increases the seat width for higher SDC because of the increase in expected spectral acceleration. The amount of transverse reinforcement did not change, because both categories satisfy the same minimum detailing requirements.

Table 4.34: Bent Creek Road SDC A2 and SDC B Design Comparison

	SDC A2	SDC B
Design Force (kip)	43.2	41.3
Percent Difference	-4.4%	
Minimum Seat Width (in)	16.4	19.8
Percent Difference	20.7%	
Number of Ties	37	37
Percent Difference	0.0%	

4.8.2 I-59 Bridge over Norfolk Southern Railroad

This bridge was the second SDC A2 bridge redesigned as an SDC B bridge. The designs will be compared to determine if it is more economical to design the bridge as a SDC B bridge. The southbound I-59 bridge in Etowah County is a two lane bridge that crosses over a Norfolk Southern railroad line and a state highway. It is a two span bridge with unequal span lengths of 125 feet and 140 feet. Nine modified BT-54 girders support a 6 inch concrete deck that is 46.75 feet wide. The only bridge pier is 53’ x 4.5’ x 4’ and supported by three square columns 3.5 feet in width. The columns are reinforced longitudinally with 12 #11 bars and transversely with #4 ties uniformly spaced at 12 inches from the bottom of the bent to the top of the pile cap foundation. The average clear height of the columns is 25.25 feet. The bridge is supported on driven piles. The pile cap is 8.5’ x 8’ x 4.5’ and each pile cap is supported by 7 HP 12x53 steel piles. Figure 4.18 shows the 3D model of the bridge used in the structural analysis. All design calculations can be found in Appendix J and the moment-axial force interaction diagrams can be seen in Appendix K.

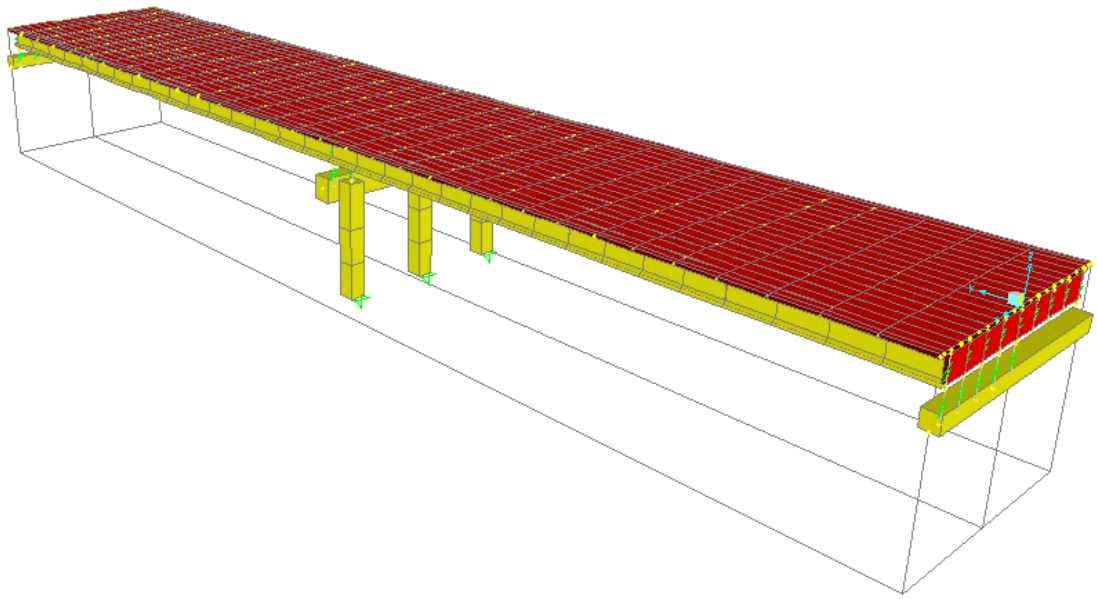

Figure 4.18: SAP2000 3D Model of Bridge over Norfolk Southern RR

The capacity of the bridge was checked first. All results from the capacity analysis can be found in Table 4.35. The bridge model was used to determine the demand displacements at each of the bents, as well as the equivalent static earthquake loading following the uniform load method. The equivalent static earthquake loading factor in each direction was multiplied by the short period magnification factor to determine the expected displacement at the bent. The capacity of the bridge bent was determined in each direction using Equations 4.16 and 4.17. The largest displacement from the square root sum of the squares (SRSS) of the two orthogonal displacements was compared to the smallest capacity. As the table shows, the capacity was greater than demand, so this bent passed the demand/capacity check and could be designed.

Table 4.35: Analysis Results for Bridge over Norfolk Southern Railroad Bent 2

	Transverse	Longitudinal
Displacement at Bent from Model	5.601”	0.042”
Expected Displacement at Bent	0.788”	0.241”
Bent Capacity	3.967”	6.634”
SRSS Displacement	0.788”	

A pushover analysis of the bridge was performed next. The static pushover curve can be seen in Figure 4.19. The design force for the connection was determined using the expected transverse displacement of the bent calculated in the structural analysis as described above. For this bridge, the base shear was 200 kips, and since the bridge had 9 girder connections, the connection design force was 22.2 kips. This force was used to design the clip angles and anchor bolts, which will be discussed below.

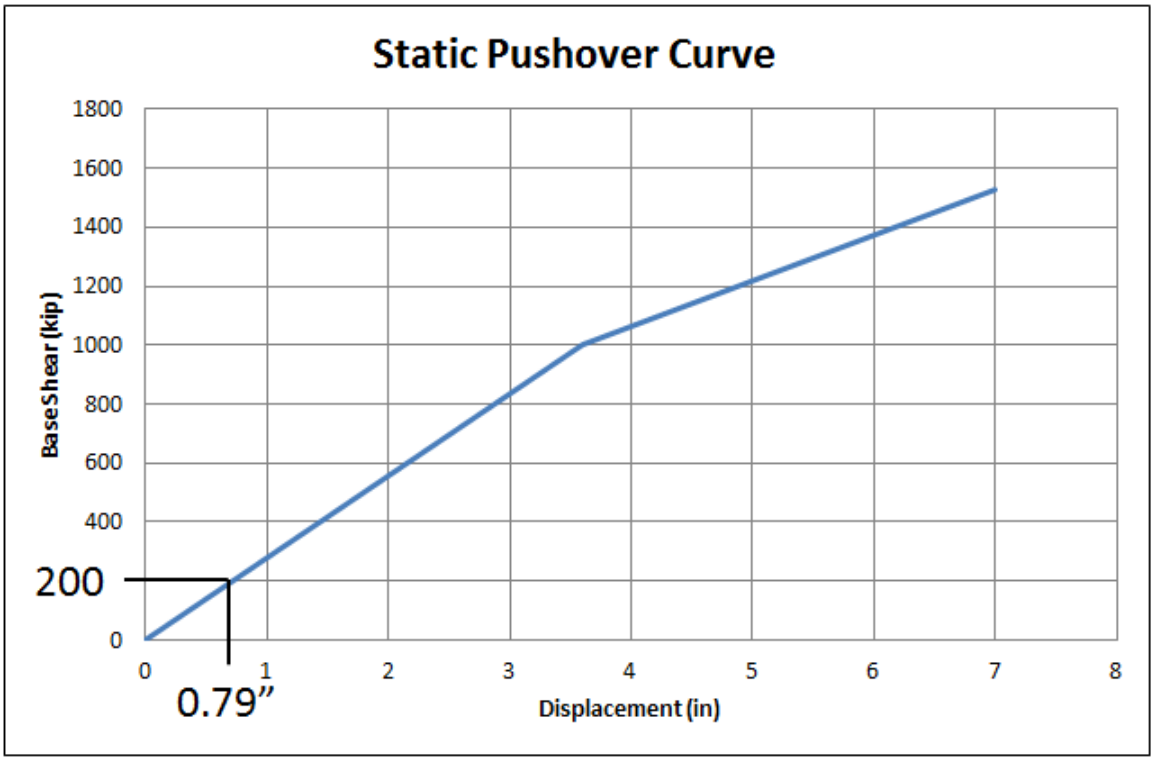

Figure 4.19: Static Pushover Curve for the Bridge over Norfolk Southern Railroad Bent 2

The design force from the pushover analysis was used to design the clip angles and anchor bolts. Since the clip angles were adequate for a force of 41.3 kips, used in the Bent Creek Road Bridge above, they would also be adequate for the force of 22.2 kips. ASTM A307 Class C anchor bolts were used in the design, and it was determined they would have to be 1.375 inches in diameter to resist the connection. This is smaller than the diameter determined above, and it can be seen that the anchor bolts should be designed for each bridge.

The minimum seat width was calculated once the capacity check and connection design were completed. The comparison can be seen in Table 4.36. The seat width is increased by 68% using the new equation.

Table 4.36: Norfolk Southern Bridge Seat Width Specification Comparison (SDC B)

Specification	Standard	New Design
Minimum Seat Width (in)	12.7	21.3
Percent Difference	67.7%	

The column design was completed next. The longitudinal reinforcement was sufficient for the expected loading, and both longitudinal checks were satisfied. Table 4.37 shows the final results from this design. The plastic hinge length was calculated to be 50.5 inches using the LRFD Specifications. For these columns, one-sixth of the column height controlled the hinge length instead of the width of the column. However, the length was still almost 25% less than that calculated by the Guide Specifications. The column length outside of the plastic hinge zone available for splicing was approximately 202 inches or 16.5 feet. The extension length was 21 inches, controlled by one-half of the column width. When compared to the original design using the Standard Specifications, the main difference is the increase in the amount of transverse reinforcement. Like SDC A2, more ties are required because of the plastic hinge zone and the stricter minimum area requirements. The seat width is also required to be 68% larger than the

Standard Specification seat width. Figure 4.20 compares the design details between the two specifications.

Table 4.37: Bridge over Norfolk Southern RR Bent 2 Design Results

	Bent 2	
Plastic Hinge Length (in)	50.5	
Extension Length (in)	21	
Available Splice Length (in)	202	
Specification	Standard	Guide
Spacing within PHL (in)	-	4
Spacing outside PHL (in)	12	9
Total Number of Ties	26	48
Area of Ties (in^2)	5.2	9.6
Percent Difference	84.6%	

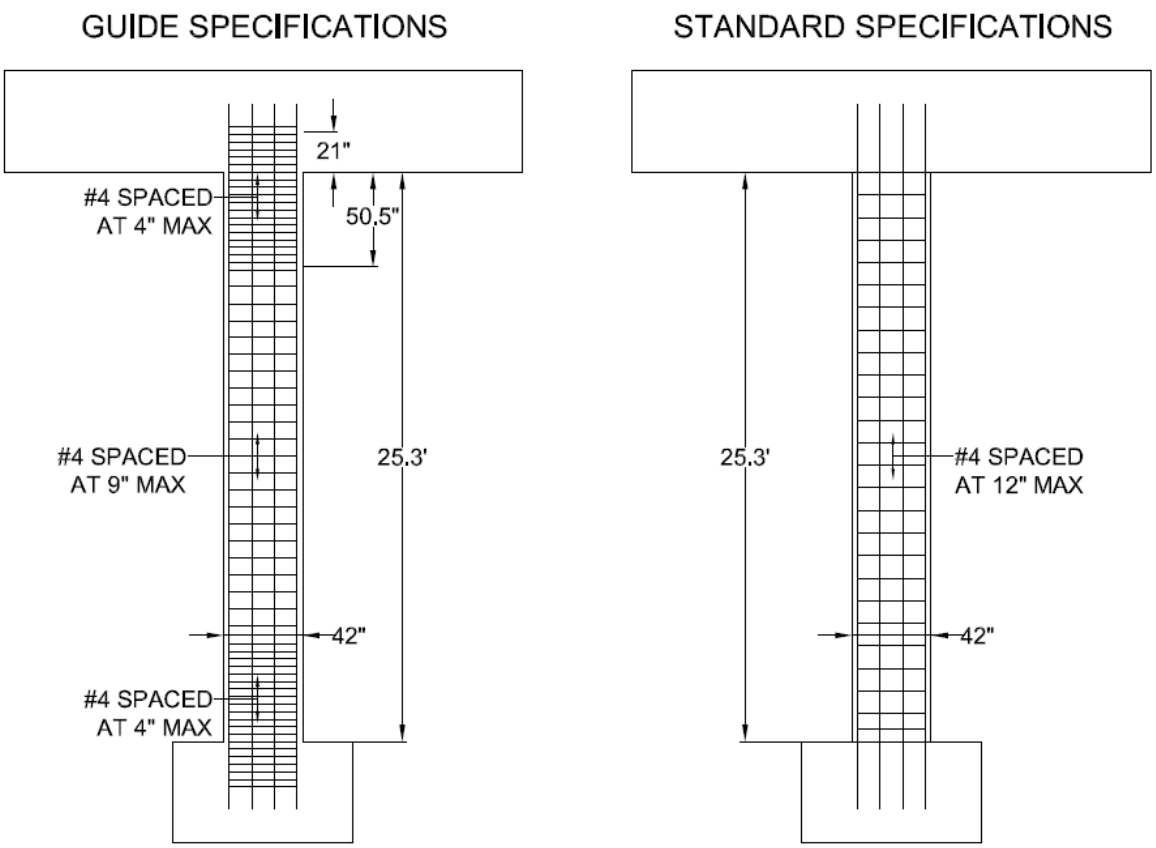

Figure 4.20: Bridge over Norfolk Southern Railroad Final Design Details (SDC B)

Table 4.38 compares the designs in SDC A2 and SDC B, and it can be seen that the horizontal design force for the connection is 50% smaller than the design force in SDC A2 that does not use the live load factor. For this bridge, it is more economical to perform a structural analysis to determine the horizontal design forces. The minimum seat width is larger in the SDC B design because the spectral acceleration value is higher in SDC B than in SDC A2. Even though the SDC B design force is half of the SDC A design force, the amount of transverse reinforcement does not change because the same minimum requirements still apply.

Table 4.38: Bridge over Norfolk Southern Railroad SDC A2 and SDC B Comparison

	SDC A2	SDC B
Design Force (kip)	45.5	22.2
Percent Difference	-51.2%	
Minimum Seat Width (in)	18.4	21.3
Percent Difference	15.8%	
Number of Ties	48	48
Percent Difference	0.0%	

4.8.3 Oseligee Creek Bridge

Oseligee Creek Bridge is the final bridge that was designed in both SDC A2 and SDC B. The SDC B design will be compared to the Standard Specification design to show the differences between the Standard Specification and Guide Specification in SDC B and it will be compared to the Guide Specification SDC A2 design to determine if it is more economical to design the bridge as SDC B instead of SDC A2. This bridge carries two lanes of County Road 1289 over Oseligee Creek in Chambers County. It has three spans of equal lengths of 80 feet. The 7 inch concrete deck is supported by 4 Type III girders. The two bridge piers are 30’ x 4’ x 5’ and

supported by two circular columns 3.5 feet in diameter with 3 inches of concrete cover. The columns are reinforced longitudinally with 12 #11 bars and transversely with #5 hoops uniformly spaced at 12 inches from the bottom of the pier cap to the rock line. The average clear height of Bent 2 is 17.93 feet and 25.83 feet for Bent 3. All columns are supported on drilled shafts 3.5 feet in diameter with concrete cover of 3 inches. Because no clear transition between the drilled shaft and the column existed, it was unknown where the plastic hinge would form. It was assumed that the soil would not provide enough lateral reinforcement alone to force the plastic hinge to form at the ground line, so the plastic hinge was designed to form at the rock line. For this reason, the height of the columns used for the plastic hinge calculation was assumed to be from the bottom of the bent cap to the rock line. Figure 4.21 shows the 3D model of the bridge used in the structural analysis. All the design calculations can be seen in Appendix L and the moment-axial force interaction diagrams can be seen in Appendix M.

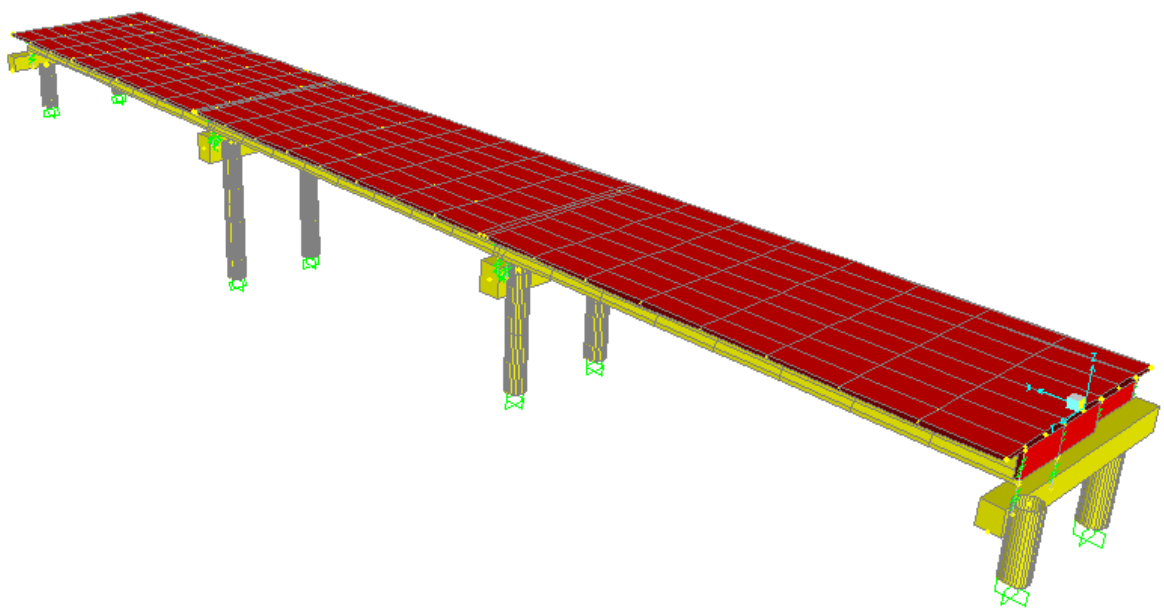

Figure 4.21: SAP2000 3D Model of Oseligee Creek Bridge

The first step was to determine the demand displacements and compare them to the bridge capacity. The SAP2000 bridge model and uniform load method were used to determine the displacement at each bent. Table 4.39 lists the results from the capacity analysis. The expected displacement was determined by multiplying the bent displacement from the model by the equivalent static earthquake load and short period magnification factor. The largest displacement from the square root sum of the squares of the two orthogonal displacements was compared to the smallest capacity. As the table shows, the capacity was greater than demand for both bents, so this bridge satisfied the capacity check.

Table 4.39: Displacement Results for Oseligee Creek Bridge

	Bent 2		Bent 3	
	Transverse	Longitudinal	Transverse	Longitudinal
Displacement at Bent from Model	2.081"	1.346"	2.90"	1.437"
Expected Displacement at Bent	0.446”	0.359”	0.621”	0.383”
Bent Capacity	1.833”	3.777”	4.149”	6.878”
SRSS Displacement	0.458”		0.632”"	

Once the capacity check was satisfied, a pushover analysis of the bridge was performed to determine the sequence of plastic hinging as well as determine the connection design forces. Figure 4.22 shows the static pushover curve for bent 3 of this bridge. The greatest displacement occurred at this bent. The connection design force was determined using the expected transverse displacement of the bent calculated in the structural analysis mentioned above. The base shear at the expected displacement of 0.50” was 173 kips, which works out to 43.3 kips per connection. This force was used to design the clip angles and anchor bolts, which will be discussed below.

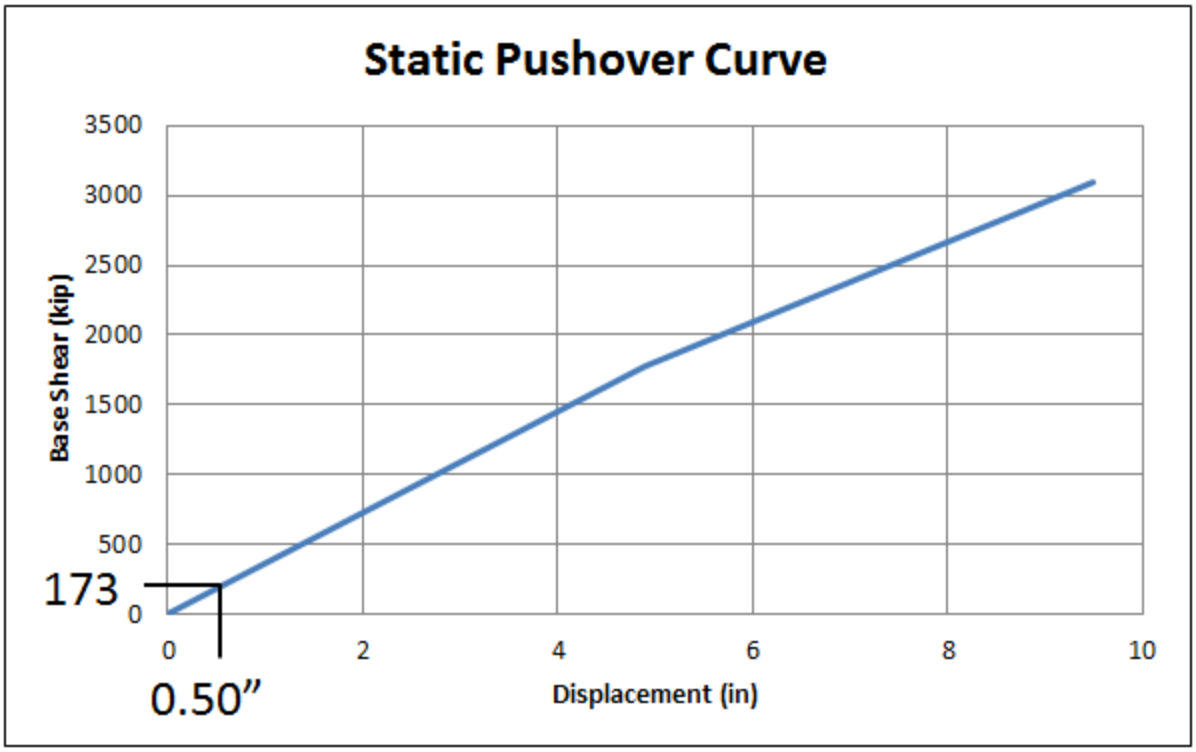

Figure 4.22: Static Pushover Curve for Oseligee Creek Bridge Bent 3

Using the design force from the pushover analysis, the transverse clip angles and anchor bolts were designed. The clip angle size was chosen from the original connection and block shear, tension and shear capacities of the angles were checked against the design force of 43.3 kips. Since this was larger than the previous connection design forces, the clip angles had to be checked. It was assumed that one of the angles would have to resist the entire design force because the other angle would not be able to transfer a tensile force. Table 4.40 shows the capacities of the clip angle as determined above using the design checks, and it can be seen that the clip angles can withstand the design force. The anchor bolt was designed for shear, bearing, tension, and combined tension and shear. Like the clip angle, only one anchor bolt was used to resist the loads. It was determined that an ASTM A307 Class C bolt with a diameter of 1.75

inches would be required for this connection. Since the bolt size is designed using the horizontal design force, the bolt should be specifically designed for each bridge.

Table 4.40: Capacity of the Steel Clip Angle

Limit State	Capacity (kips)
Block Shear	156
Tension	118
Shear	130

The minimum seat width was calculated for each bent using Equation 4.2 once the connection design was completed. The results, seen in Table 4.41 show that the minimum seat width using the new equation is 60-70% greater than the seat width calculated using the Standard Specifications. Bent 3 is a taller by almost 8 feet, and the effect of the height on the seat width can also be seen, since the minimum seat length is 2.5 inches greater for the taller column.

Table 4.41: Oseligee Creek Bridge Seat Width Specification Comparison (SDC B)

	Bent 2		Bent 3	
Specification	Standard	New Design	Standard	New Design
Minimum Seat Width (in)	11.0	17.6	11.7	20.1
Percent Difference	60%		71.8%	

The next step was to design the columns. The plastic hinge length was determined for each bent using both the Guide and LRFD Specifications to show the advantages of using the LRFD Specifications. These lengths can be seen in Table 4.42. As it shows, the plastic hinge lengths from the LRFD Specification is less than the Guide Specification length. This results in a larger length of column available for splicing to occur. For these columns, this length increased by 2 to 3.5 feet. The advantage of using the LRFD Specifications is that a shorter hinge length is required and having a shorter plastic hinge reduces the total number of ties and

increases the length over which splicing may occur. The LRFD Specifications also allow for an extension of the plastic hinge length into the connecting member in order to ensure the formation of a plastic hinge by increasing the shear resistance of the section. The extension length was 21 inches for both bents.

Table 4.42: Oseligee Creek Plastic Hinge Length Comparison (SDC B)

	Bent 2		Bent 3	
Specification	Guide	LRFD	Guide	LRFD
Plastic Hinge Length (in)	63	42	63	51.7
Available Splice Length (in)	89	131	183	206
Extension Length (in)	-	21	-	21
% Difference PHL	-33.3%		-17.9%	

The LRFD plastic hinge length was used throughout the remainder of this design. It is important to note that the diameter of the columns controlled the hinge length in Bent 2 but one-sixth of the column height controlled for Bent 3. This shows that the hinge lengths can vary for different columns supporting a bridge. And it can also vary for different columns at a bent if the columns differ significantly in height.

The longitudinal reinforcement was determined to be sufficient for the loads. The maximum and minimum longitudinal reinforcement checks were also satisfied, so the transverse reinforcement was designed next. Table 4.43 shows the final design of transverse reinforcement using both the Standard and Guide Specifications. #4 ties were used for the transverse reinforcement. Using the Guide Specifications, a maximum spacing of 6 inches was required inside the plastic hinge. The extension length, which is not required for SDC B but recommended, required the same maximum spacing as the PHL, which was 6 inches. The maximum spacing outside of the plastic hinge length was determined to be 12 inches using the Standard Specification and 9 inches using the Guide Specification. This spacing resulted in

approximately 60% more reinforcement in the Guide Specification design than the Standard Specification design. This is typical, because the addition of the plastic hinge length requires tighter hoop spacing. Figure 4.23 and Figure 4.24 show two details of a column at Bents 2 and 3, respectively, using each of the design specifications. The spacing of the reinforcement can be seen, as well as the plastic hinge zone and extension length.

Table 4.43: Oseligee Creek Final Design Comparison (SDC B)

	Bent 2		Bent 3	
Specification	Standard	Guide	Standard	Guide
Spacing within PHL (in)	-	6	-	6
Spacing outside PHL (in)	12	12	12	12
Total Number of Hoops	18	29	26	41
Area of Hoops (in^2)	5.6	5.8	8.1	8.2
% Difference	3.6%		1.2%	

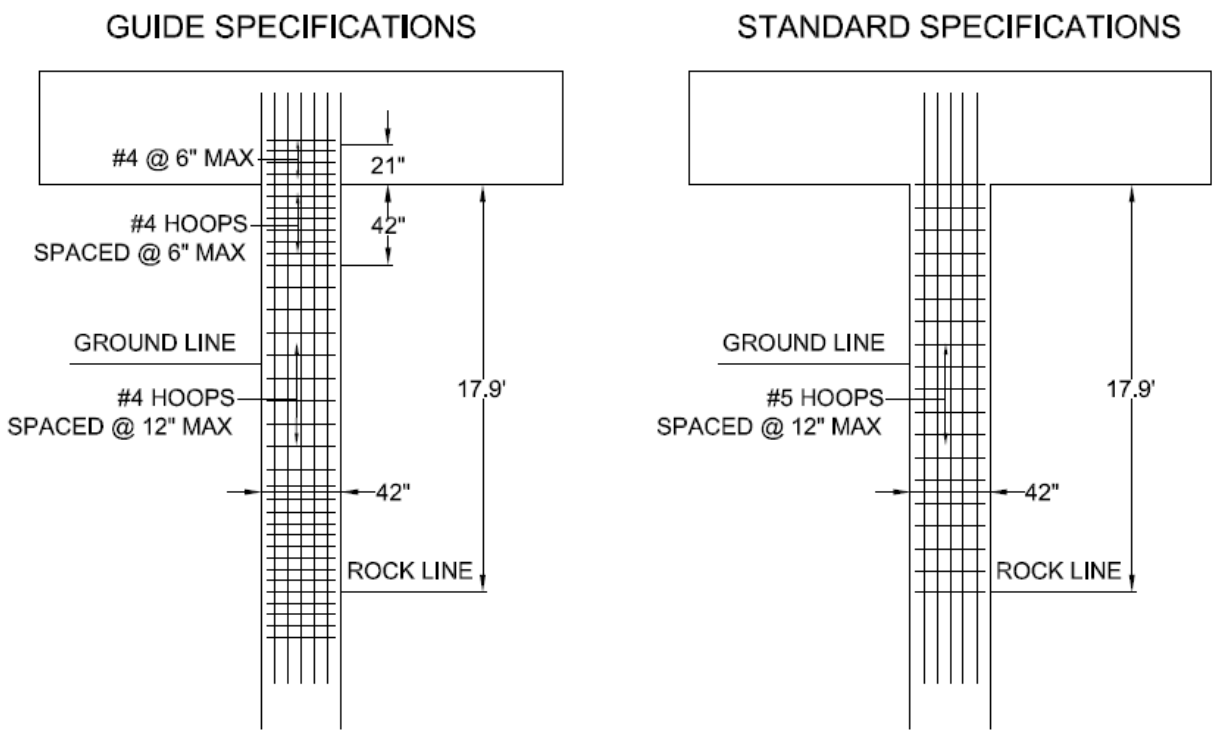

Figure 4.23: Oseligee Creek Bent 2 Final Design Details (SDC B)

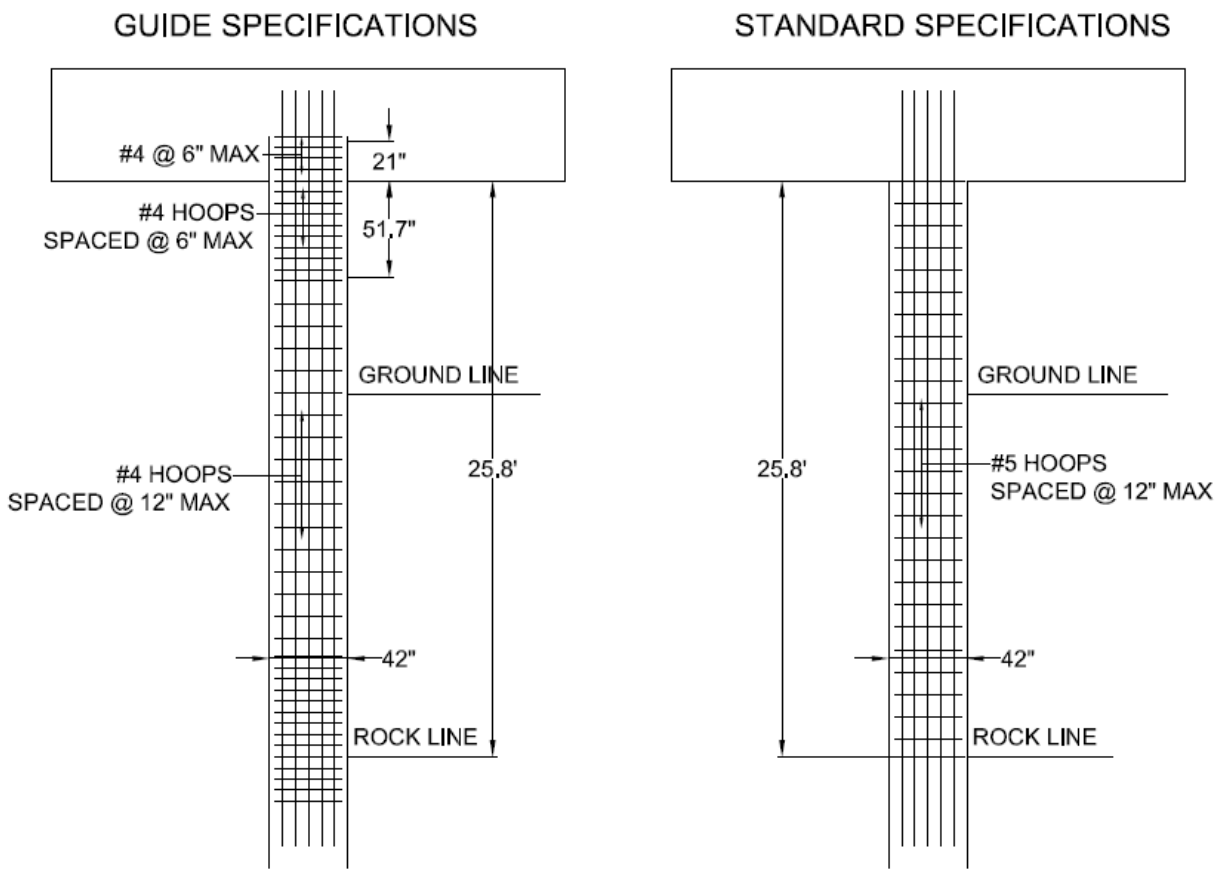

Figure 4.24: Oseligee Creek Bent 3 Final Design Details (SDC B)

The designs from SDC A2 and SDC B were compared in Table 4.44. The connection design forces in SDC B are 21.6% larger than the horizontal design force in SDC A2 that does not include the live load factor, meaning that performing a more rigorous analysis on the bridge does not guarantee smaller design forces. Therefore, it cannot be recommended to create a bridge model and perform a structural analysis for the sole purpose of getting lower design forces. The minimum seat width increased by about 20%, because SDC B bridges have higher spectral accelerations than SDC A2 bridge sites. The amount of transverse reinforcement did not change in the designs. This comparison shows that for this bridge, it would not be economical to design the bridge as SDC B because higher horizontal design forces would be required.

Table 4.44: Oseligee Creek Bridge SDC A2 and SDC B Comparison

	Bent 2		Bent 3	
	SDC A2	SDC B	SDC A2	SDC B
Design Force (kip)	35.6	43.3	35.6	43.3
% Difference	21.6%		21.6%	
Minimum Seat Width (in)	14.6	17.6	16.6	20.1
% Difference	20.5%		21.1%	
Number of Hoops	29	29	41	41
% Difference	0.0%		0.0%	

4.8.4 Little Bear Creek Bridge

Little Bear Creek Bridge was designed as SDC B to show the differences between designs from the Standard Specifications and Guide Specifications in SDC B. This bridge carries the two lanes of State Road 24 over Little Bear Creek in Franklin County. It is a three span bridge with spans of unequal lengths. The outer span lengths are 85 feet and the interior span is 130 feet. The outer spans support the 7 inch concrete deck with 6 Type III Girders and the interior span supports the deck with 6 BT-72 Girders. The two bridge piers are 40’ x 5’ x 7’ and supported by two circular columns 4.5 feet in diameter with 3 inches of concrete cover. The columns are reinforced longitudinally with 24 #11 bars and transversely with #5 hoops uniformly spaced at 12 inches from the bottom of the pier cap to the top of the foundation. The average clear height of Bent 2 is 12.06 feet and 16.88 feet for Bent 3. All columns are supported on drilled shafts 5 feet in diameter. The concrete cover of the drilled shafts is 6 inches but the longitudinal reinforcement in the drilled shaft still aligns with the longitudinal reinforcement of the column. Figure 4.25 shows the 3D model of the bridge used in the structural analysis. The design calculations for this bridge can be seen in Appendix N and the moment-axial force interaction diagrams can be seen in Appendix O.

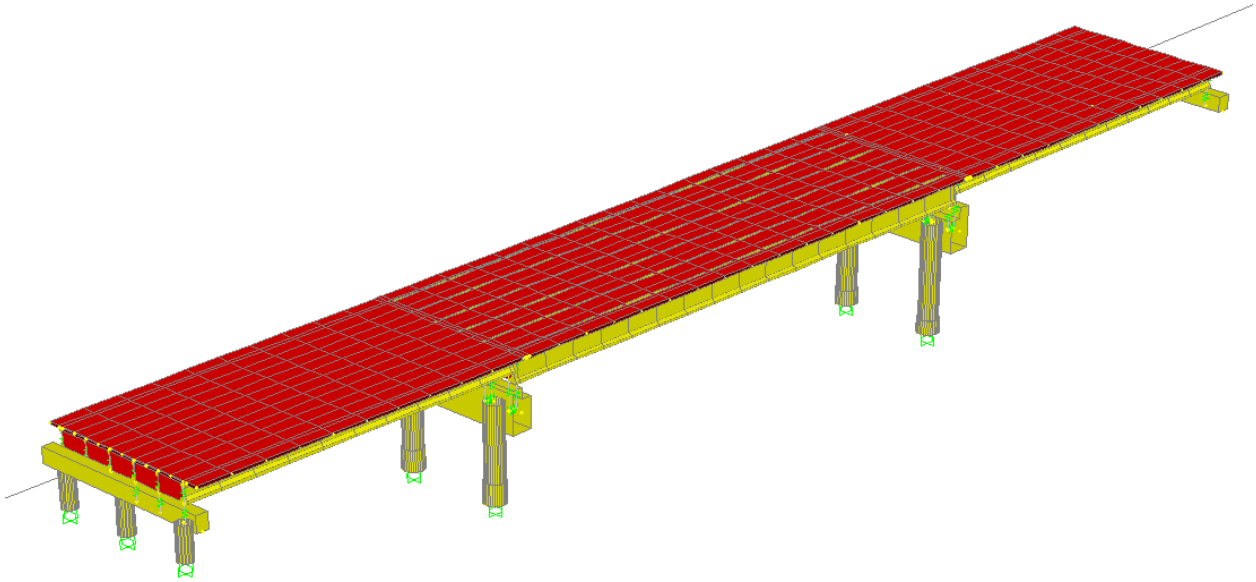

Figure 4.25: SAP2000 3D Model of Little Bear Creek Bridge

The first step was to perform the displacement capacity check. The SAP2000 bridge model and the uniform load method were used to determine the maximum displacements of the bridge. Table 4.45 lists the results from the capacity analysis. The expected displacement was determined by multiplying the bent displacement from the model by the equivalent static earthquake load and short period magnification factor. The largest displacement from the square root sum of the squares of the two orthogonal displacements was compared to the smallest capacity. For bent 2, the capacity in the longitudinal direction was smaller than the displacement demand. However, the Guide Specifications has a minimum value that can be taken as the bent capacity, which in this case was greater than the demand displacement. As the table shows, the capacity was greater than demand for both bents, so this bridge satisfied the capacity check.

Table 4.45: Displacement Results for Little Bear Creek Bridge

	Bent 2		Bent 3	
	Transverse	Longitudinal	Transverse	Longitudinal
Displacement at Bent from Model	0.795”	0.257”	2.241”	0.370”
Expected Displacement at Bent	0.183”	0.142”	0.516”	0.257”
Bent Capacity	1.35”	0.075”	0.97”	2.753”
Bent Capacity Lower Limit	1.448”		2.026”	
SRSS Displacement	0.188”		0.519”	

Once the capacity check was satisfied, a pushover analysis was performed to determine the connection design forces. Figure 4.26 shows the static pushover curve for Bent 3, which had the greatest expected displacement in the transverse direction. The displacement from the pushover analysis was less than the displacement from the elastic displacement of the bent in the structural analysis, so it was used as the displacement. As the figure shows, the design connection force was 400 kips, or 66.7 kips per connection.

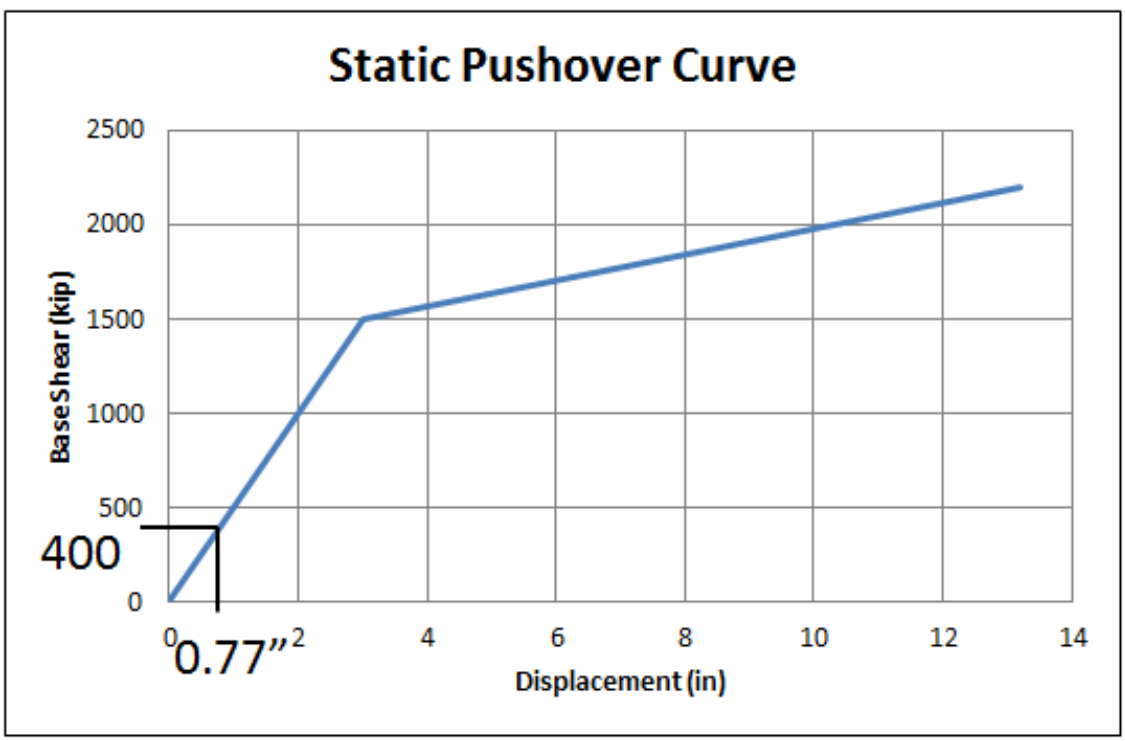

Figure 4.26: Static Pushover Curve for Little Bear Creek Bridge Bent 3

Using the design force of 66.7 kips from the pushover analysis, the transverse clip angles and anchor bolts were designed. The clip angle size was chosen from the original connection and block shear, tension and shear capacities of the angles were checked against the design force. Since this was larger than the previous connection design forces, the clip angles had to be checked. It was assumed that one of the angles would have to resist the entire design force because the other angle would not be able to transfer a tensile force because of the screw caps. Table 4.46 shows the capacities of the clip angle as determined above using the design checks, and it can be seen that the clip angles can withstand the design force. The anchor bolt was designed for shear, bearing, tension, and combined tension and shear. Like the clip angle, only one anchor bolt was used to resist the loads. It was determined that an ASTM A307 Class C bolt with a diameter of 2.25 inches would be required for this connection. This bolt size is different than the previous two connection designs. This shows that the bolt should be specifically designed for each bridge.

Table 4.46: Capacity of the Steel Clip Angle

Limit State	Capacity (kips)
Block Shear	156
Tension	118
Shear	130

Once the capacity check and connection design were completed, the bent was designed. First, the minimum seat width was calculated for each bent using Equation 4.2. The results, seen in Table 4.47, show that the results from Equation 4.2 are approximately 50% greater than Equation 4.1, which is used in the Standard Specifications.

Table 4.47: Little Bear Creek Bridge Seat Width Specification Comparison

	Bent 2		Bent 3	
Specification	Standard	Guide	Standard	Guide
Minimum Seat Width (in)	11.1	16.3	11.5	18.0
% Difference	46.8%		56.5%	

The next step was to design the columns. The minimum and maximum longitudinal reinforcement checks were satisfied and the longitudinal reinforcement was determined to be sufficient for the loads from the moment-axial force interaction diagram. The plastic hinge length was determined for each bent using both the Guide and LRFD Specifications and can be seen in Table 4.48. As it shows, the plastic hinge lengths from the LRFD Specification is less than the Guide Specification length. This results in a larger length of column available for splicing to occur. For Bent 2, there was no splice length because the plastic hinge extended the entire length of the column. Using the LRFD Specifications, however, allowed for a 36 inch section over which splicing could occur. For Bent 3, this available splice length increased by 4.5 feet. The advantage of using the LRFD Specifications for the plastic hinge length is includes having a shorter plastic hinge length, which results in a larger length over which splicing may occur. The LRFD Specifications also allow for an extension of the plastic hinge length into the connecting member in order to better ensure the formation of a plastic hinge by increasing the shear resistance of the section. This extension length was 27 inches.

Table 4.48: Little Bear Creek Plastic Hinge Length Comparison (SDC B)

	Bent 2		Bent 3	
Specification	Guide	LRFD	Guide	LRFD
Plastic Hinge Length (in)	81	54	81	54
Available Splice Length (in)	0	36	40	94
Extension Length (in)	-	27	-	27
% Difference PHL	-33.3%		-33.3%	

The LRFD plastic hinge length was used throughout the remainder of this design. It is important to note that the diameter of the columns controlled the plastic hinge lengths in both bents. This shows that for short columns, the hinge length will be controlled by the diameter of the columns.

The transverse reinforcement was designed next using both the Standard and Guide Specifications. Table 4.49 shows the results of the final designs. The spacing of reinforcement inside the hinge length was determined using #5 hoops. The Guide Specifications determined a maximum spacing of 6 inches inside the plastic hinge. The extension length, which is not required for SDC B but recommended, was 27 inches long with the same hoop spacing that was in the plastic hinge length. The maximum spacing outside of the plastic hinge length was determined to be 12 inches using the Standard Specification and 10 inches using the LRFD Specification. The Guide Specification design resulted in an increase of 65-80% of hoops compared to the original design. This shows that bridges requiring plastic hinges will need more transverse reinforcement. Figure 4.27 and Figure 4.28 show two details of a column at Bents 2 and 3 using both design specifications. The spacing of the reinforcement can be seen, as well as the plastic hinge zone and extension length.

Table 4.49: Little Bear Creek Final Design Comparison (SDC B)

	Bent 2		**Bent 3**	
Specification	Standard	Guide	Standard	Guide
Spacing within PHL (in)	-	6	-	6
Spacing outside PHL (in)	12	10	12	10
Total Number of Hoops	12	22	17	28
Area of Hoops (in^2)	3.72	6.82	5.27	8.68
% Difference	83.3%		64.7%	

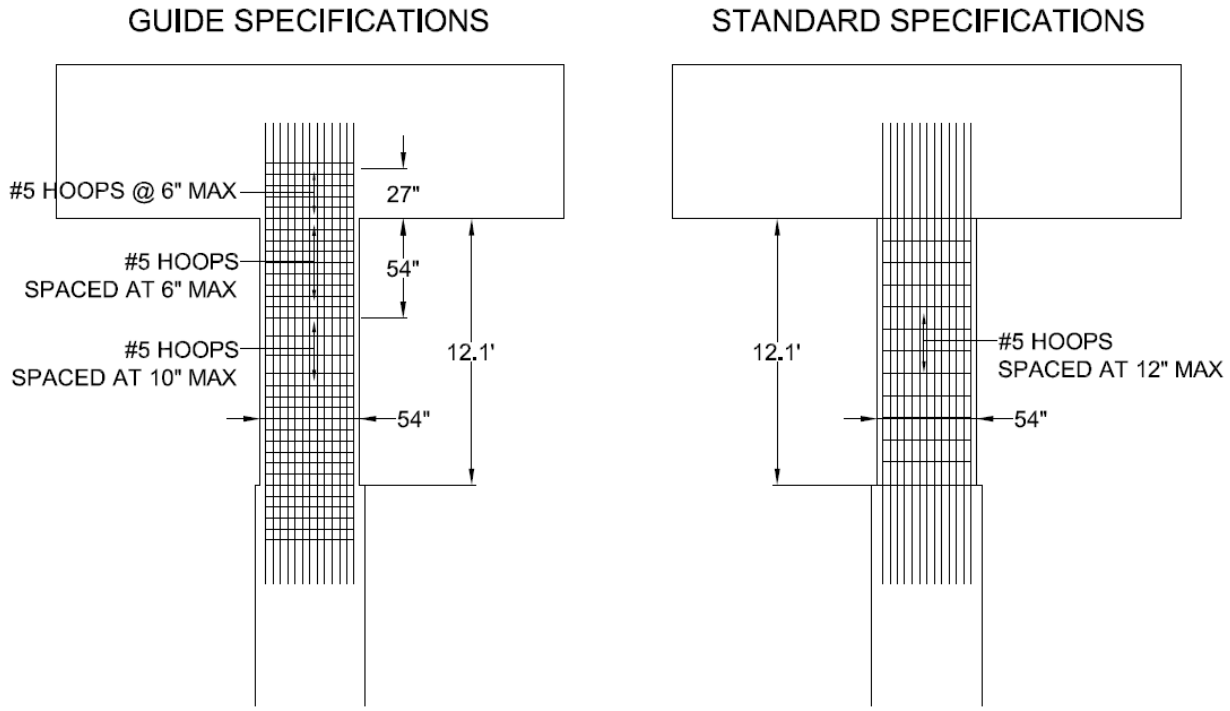

Figure 4.27: Little Bear Creek Bridge Bent 2 Final Design Details

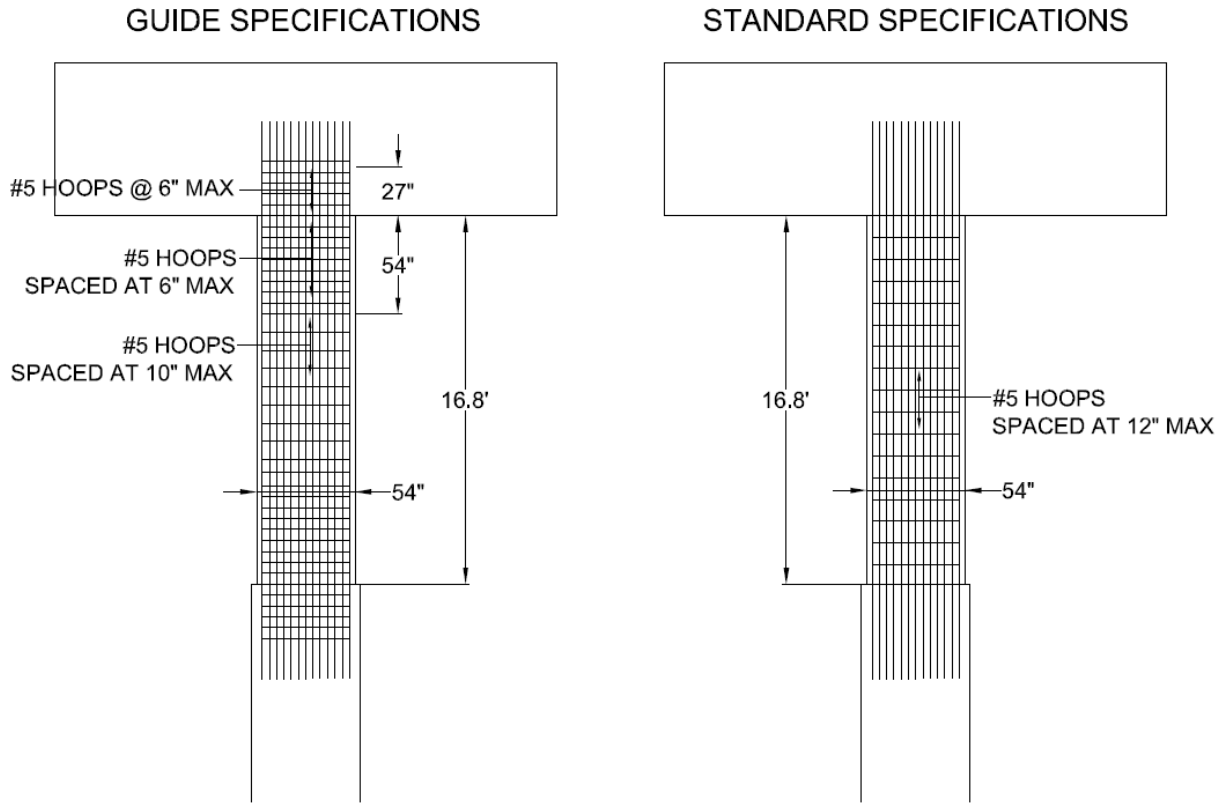

Figure 4.28: Little Bear Creek Bridge Bent 3 Final Design Details

4.8.5 Scarham Creek Bridge

Scarham Creek Bridge is the last bridge designed in SDC B. It differs from the other bridges because it is designed with struts at mid-height of the columns at each bent. These struts are required to provide stability and load transfer. These struts will also be redesigned since they play an important role in the behavior of the substructure. The bridge is two lanes and carries State Route 75 over Scarham Creek in Marshall County. It is a four span bridge with equal span lengths of 130 feet. The 7 inch concrete deck is supported by 6 BT-72 girders. The bridge pier at bents 2 and 4 are 40’ x 5.5’ x 7.5’ and the pier at bent 3 is 40’ x 6.5’ x 7.5.’ Bents 2 and 4 are supported by two circular columns 5 feet in diameter with 3 inches of concrete cover. Bent 3 is supported by two circular columns 6 feet in diameter with 3 inches of concrete cover. All columns are supported on drilled shafts, which are six inches larger in diameter than the columns. It is assumed that the plastic hinge will form at this transition, so the clear height of the columns is measured from the bottom of the bent cap to the transition between the column and drilled shaft. The average height of columns is 34.02 feet at Bent 2, 59.17 feet at Bent 3, and 32.16 feet at Bent 4. Because of the height of the columns, struts are provided at approximately mid-height of the columns and span the full length between columns with a thickness of 3.5 feet. The strut at bents 2 and 4 are 6 feet deep and 10 feet deep at bent 3. Figure 4.29 shows the 3D model of the bridge used in the structural analysis. The design calculations can be seen in Appendix P and the moment-axial force interaction diagrams can be seen in Appendix Q.

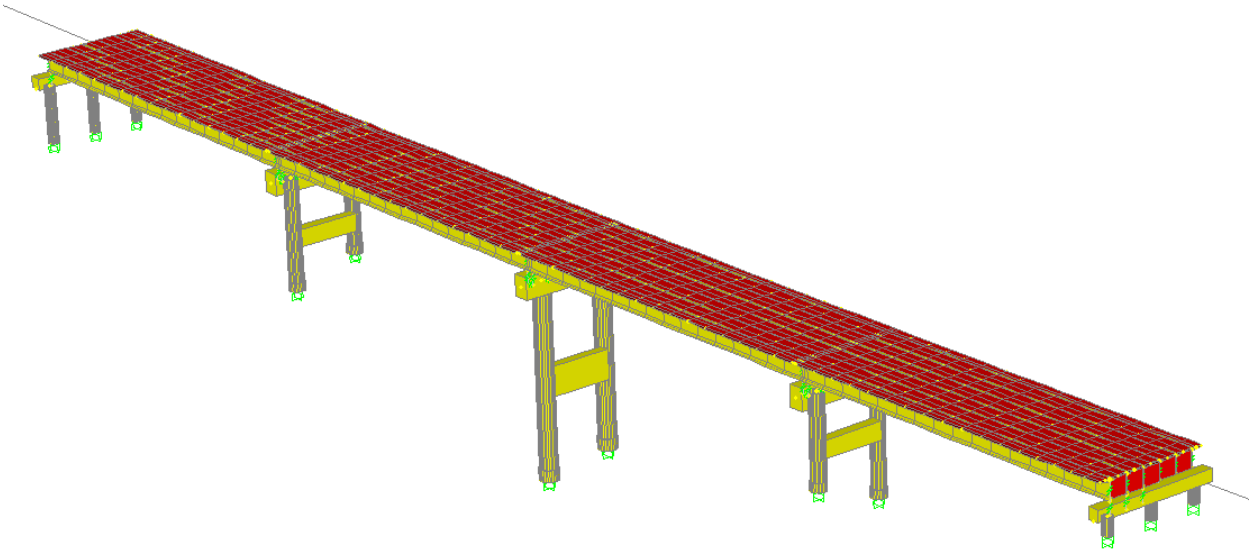

Figure 4.29: SAP2000 3D Model of Scarham Creek Bridge

The capacity check was completed first. However, the capacity equations for SDC B could not be used because of the struts. A pushover analysis was performed to verify the capacity of the columns for the expected displacements. The results from the pushover analysis performed using the computer software can be seen in Table 4.50. Since all three bents have greater capacities than demand in each orthogonal direction, the bridge satisfies the capacity check.

Table 4.50: Pushover Analysis Results for Scarham Creek Bridge

Location - Direction	Demand (in)	Capacity (in)	Check
Bent 2 - Transverse	2.44	9.77	**OK**
Bent 2 - Longitudinal	0.55	2.20	**OK**
Bent 3 - Transverse	6.90	25.64	**OK**
Bent 3 - Longitudinal	0.87	3.57	**OK**
Bent 4 - Transverse	2.87	11.47	**OK**
Bent 4 - Longitudinal	0.62	2.64	**OK**

A static pushover curve, seen in Figure 4.30, was developed for Bent 3, where the largest displacement demand occurs. This curve was used to determine the horizontal design force for

the connection as well as the sequence of plastic hinging. From the SAP2000 model, it could be seen that the plastic hinges in the bottom of the column and in the struts formed at the same time. At the time of the pushover analysis was completed, these were the only two hinges that had activated. This suggests that the struts were too large, because the struts should be the first to yield in order to protect the columns. If the struts were smaller, it would allow them to yield first and form plastic hinges, which would dissipate more energy from the system and protect the columns.

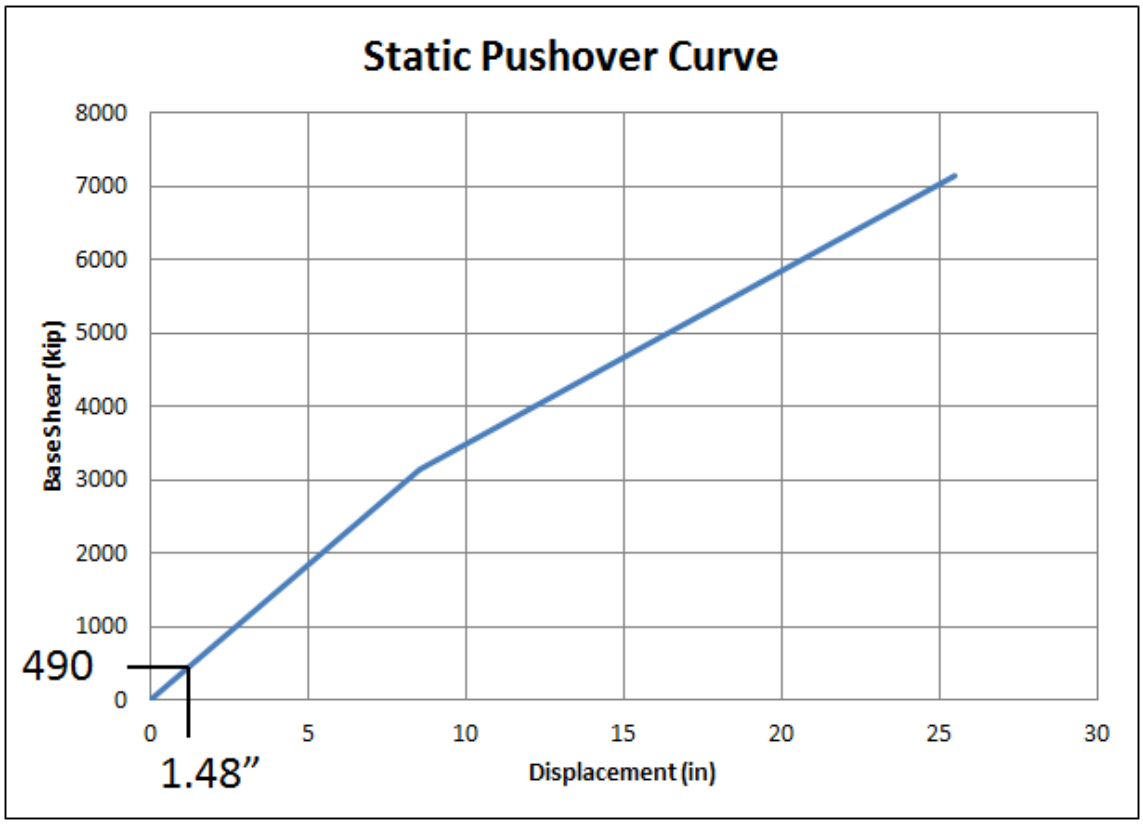

Figure 4.30: Static Pushover Curve for Scarham Creek Bridge Bent 3

The horizontal connection force was determined to be 81.67 kips. This comes from the 490 kips found in the graph above divided by 6 girders. The clip angles were designed to resist this force, and based on Table 4.51, were determined adequate. The anchor bolts were also

designed. Using ASTM A307 Class C grade bolts, it was determined that bolts with a diameter of 2.5 inches would be adequate to resist the loads. In all of the bridges in SDC B, the clip angles were adequate to resist the loads, but the anchor bolts were all different sizes, ranging from 1.25 inches to 2.5 inches.

Table 4.51: Capacity of the Steel Clip Angle

Limit State	Capacity (kips)
Block Shear	156
Tension	118
Shear	130

The next step was to calculate the minimum seat widths. Equation 4.2, the ATC-49 equation, was used to calculate the new design seat widths and was compared with the seat widths from the Standard Specifications, found using Equation 4.1. Table 4.52 shows the minimum seat widths. For bents 2 and 4, the seat widths increased by 78%. But for bent 3, the seat width was almost double what was required by the Standard Specifications. This is because the columns in bent 3 are very tall.

Table 4.52: Scarham Creek Minimum Seat Width Comparison

	Bent 2		Bent 3		Bent 4	
Specification	Standard	Guide	Standard	Guide	Standard	Guide
Minimum Seat Width (in)	13.3	23.7	15.3	30.0	13.2	23.2
% Difference	78.2%		96.1%		75.8%	

The next step was to design the columns and struts. The design of the columns will be discussed first. The plastic hinge lengths were calculated using the Guide and LRFD

Specifications in order to discuss their effect on the amount of splice length in the column. Table 4.53 displays the plastic hinge lengths, available splice lengths, and extension lengths for each bent. At Bents 2 and 4, the LRFD plastic hinge length was approximately 25% shorter than the hinge length from the Guide Specifications. The plastic hinge length was controlled by the column height instead of the column diameter. The available splice length was calculated a little differently than for the other bridges. Because of the presence of the struts, it was assumed splicing could not occur at a location where the strut connected to the column, which further shortened the splice length. However, because all of the columns were tall, there was still quite a bit of length over which splicing could occur. By using the LRFD plastic hinge length, the splicing length increased by about 2 feet for both Bents 2 and 4. Bent 3 was unique because it was very tall, and because of its height, the Guide Specifications hinge length was shorter than the LRFD hinge length. This is only bent in any of the bridges studied where the plastic hinge length from the Guide Specifications was shorter. Therefore, it should be noted that for extremely tall columns, it is recommended to check the plastic hinge lengths from both the LRFD Specifications and Guide Specifications. The length available for splicing was also larger using the Guide Specifications, allowing for ten more inches. The extension lengths were also calculated to be 30 inches for Bents 2 and 4, and 36 inches for Bent 3. These lengths were controlled by the column diameters.

Table 4.53: Scarham Creek Plastic Hinge Length Comparison

	Bent 2		**Bent 3**		**Bent 4**	
Specification	Guide	LRFD	Guide	LRFD	Guide	LRFD
Plastic Hinge Length (in)	90	68	108	118	90	64.3
Available Splice Length (in)	78	100	187	177	66.5	92.7
Extension Length (in)	-	30	-	36	-	30
% Difference PHL	-24.4%		9.3%		-28.6%	

Once the plastic hinge lengths were determined, the transverse reinforcement was designed and the results can be seen in Table 4.54. The design forces were determined from the structural analysis and uniform load method. #6 hoops were used in the columns so that an accurate comparison with the original design by the Standard Specifications could be made. Bents 2 and 4 required the same maximum hoop spacing of 6 inches in the plastic hinge zone and 12 inches outside of it. This resulted in an approximately 33% increase in the number of hoops in both bents. Bent 3 required a maximum spacing of 6 inches in the plastic hinge zone and 10 inches outside of it, increasing the number of hoops by 43% compared to the Standard Specifications. Once again, the redesign of this bridge shows that using the Guide Specifications will require more ties because of the tighter spacing requirements.

Table 4.54: Scarham Creek Final Column Design Summary

	Bent 2		**Bent 3**		**Bent 4**	
Specification	Standard	Guide	Standard	Guide	Standard	Guide
Spacing within PHL (in)	-	6	-	6	-	6
Spacing outside PHL (in)	12	12	12	10	12	12
Total Number of Hoops	34	46	60	86	33	44
Area of Hoops (in^2)	14.96	20.24	26.4	37.84	14.52	19.36
% Difference	35.3%		43.3%		33.3%	

The struts were designed next. Table 4.55 shows the final design results for the struts. Because the struts at Bents 2 and 4 were of equal geometry, their design will be the same. The plastic hinge lengths for the struts were determined using the Guide Specifications to be 72 inches for Struts 2 and 4, and 120 inches for Strut 3. The depth of the strut controlled the length of the plastic hinge. #5 ties were used as transverse reinforcement for Struts 2 and 4. The maximum spacing was 4 inches inside the plastic hinge zone and 14 inches outside. This resulted in a 120% increase in the amount of shear reinforcement in the strut. For Strut 3, #6 ties

were used. The maximum spacing requirements using #5 ties was determined to be 2 inches. It was determined that this spacing was too small to allow the concrete to be consolidated. If a self-consolidating concrete is used, #5 ties may be a possibility. Using #6 ties, the maximum spacing inside the plastic hinge length was 3.5 inches, and since the plastic hinge length covered the entire length of the strut, this spacing was used across its entire length. Because of the use of a larger tie size and the much tighter spacing, the amount of transverse reinforcement increased by 390%. Another option that could be used to increase the spacing of the ties would be to use cross-ties. Adding two additional vertical legs to the strut at Bent 3 would allow the spacing to be increased to the 6 inch maximum, which would make the reinforcement cage less congested and allow the concrete to be more easily consolidated. The depth of the struts contributes to the length of the plastic hinge zone. If the struts were smaller, the plastic hinge zone would be smaller and the amount of transverse reinforcement would be significantly smaller. Figure 4.31, Figure 4.32, and Figure 4.33 show the final design details for each bent using both the Standard Specification and Guide Specification for the columns and struts.

Table 4.55: Scarham Creek Final Strut Design Summary

	Strut 2		**Strut 3**		**Strut 4**	
Plastic Hinge Length (in)	72		120		72	
Specification	Standard	Guide	Standard	Guide	Standard	Guide
Spacing within PHL (in)	-	4	-	3.5	-	4
Spacing outside PHL (in)	12	14	12	18	12	14
Total Number of Ties	19	42	18	62	19	42
Area of Ties (in^2)	5.89	13.02	5.58	27.28	5.89	13.02
% Difference	121.1%		388.9%		121.1%	

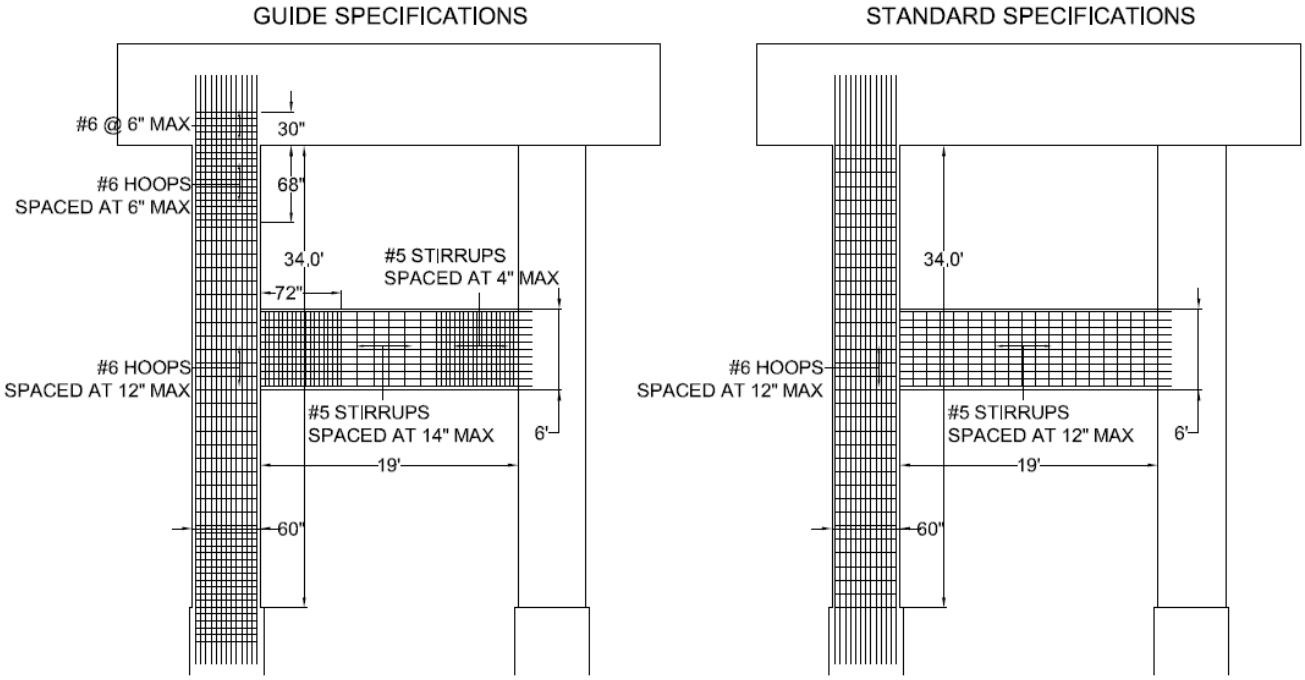

Figure 4.31: Scarham Creek Bridge Bent 2 Final Design Details

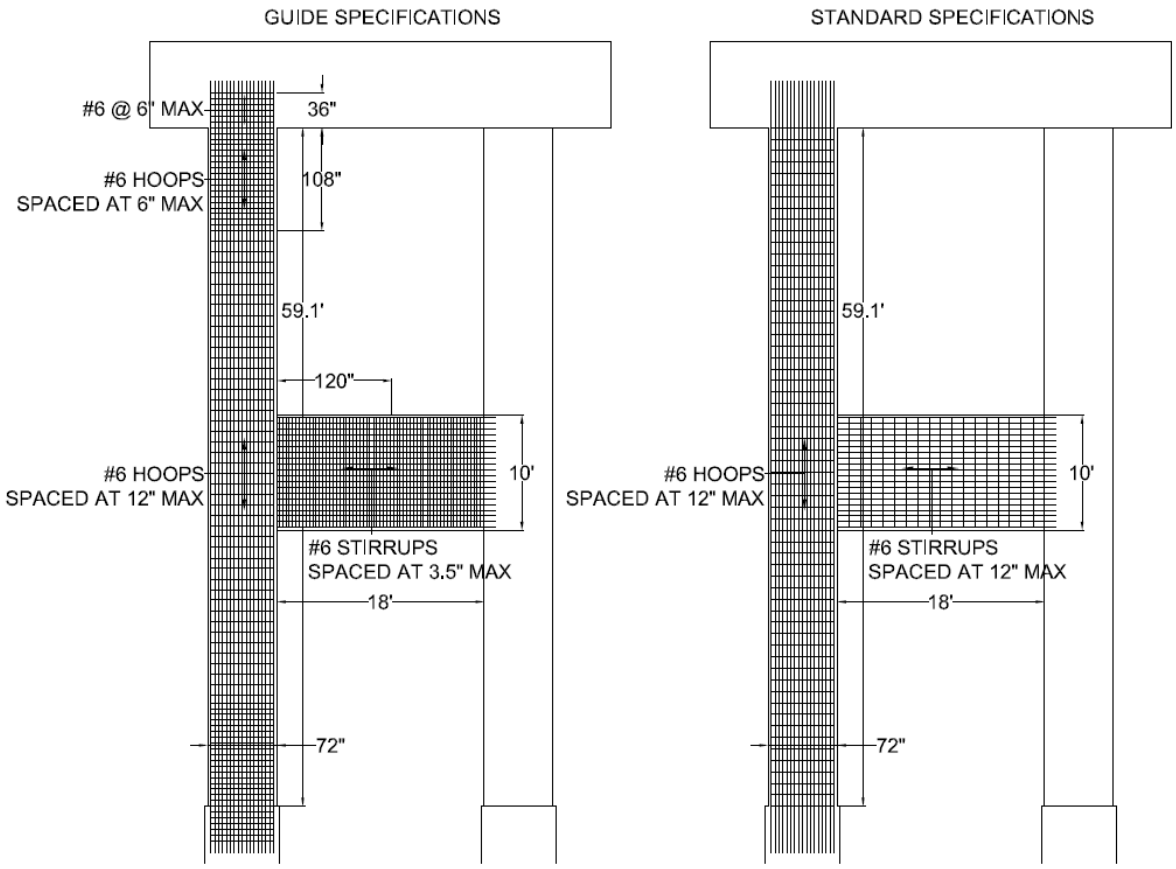

Figure 4.32: Scarham Creek Bridge Bent 3 Final Design Details

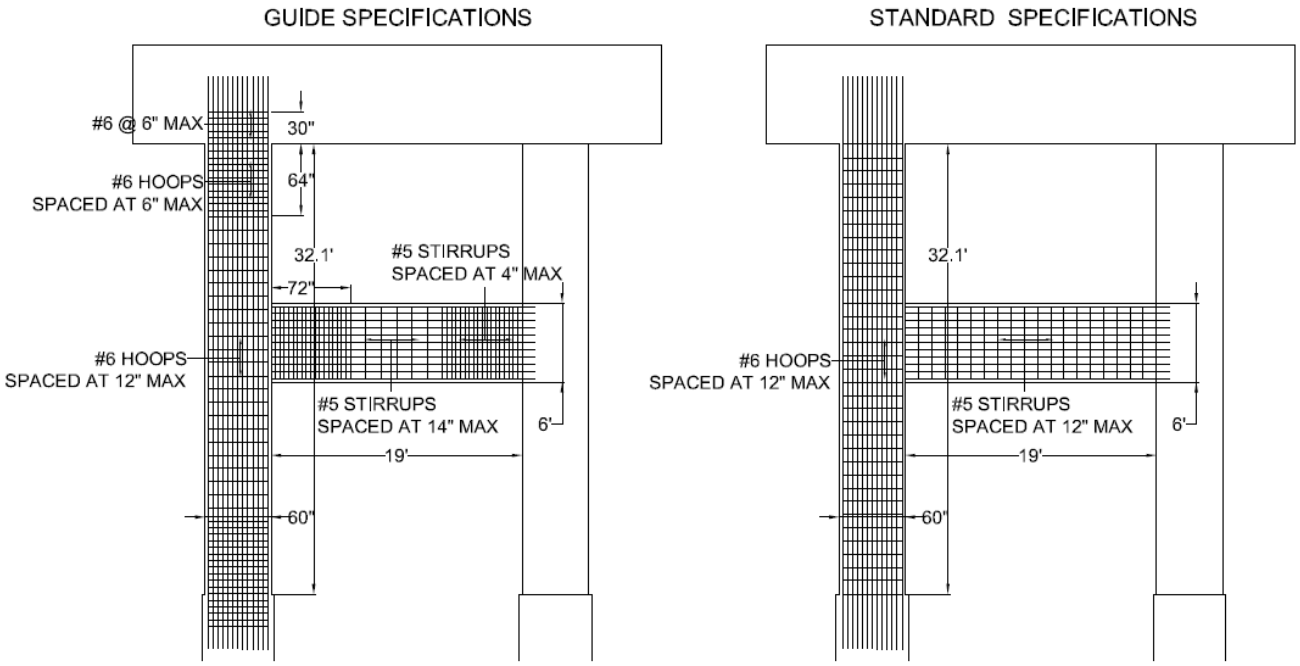

Figure 4.33: Scarham Creek Bridge Bent 4 Final Design Details

4.8.6 Summary of Differences in SDC B

In SDC B, designing by the Guide Specification resulted in many changes compared to the Standard Specification design. The most significant was the addition of the plastic hinge zone, which resulted in higher amounts of transverse reinforcement. The spacing inside of the plastic hinge zone could not be greater than 6 inches, and the spacing outside of the plastic hinge zone was either equal to or smaller than the spacing from the original designs. Another change was the larger minimum seat widths required by the recommended equation from the ATC-49 study, notated in Equation 4.2. All five bridges required a greater seat width than that required by the Standard Specifications. This is because the new equation is designed to give a better estimation of the displacement of the seat, which turns out to be larger. This change affected all bridges in SDC B.

The new designs also showed that using the LRFD Specifications to determine the plastic hinge length results in smaller hinge lengths, which decreased the amount of transverse reinforcement required and increased the length of the column over which splicing can occur. The one exception was for the very tall columns in Bent 3 of Scarham Creek Bridge. At this bent, the Guide Specifications actually resulted in a smaller hinge length. So while it is recommended to use the LRFD Specifications for the plastic hinge length, the Guide Specifications should be checked, especially for tall columns.

Three of the SDC A2 bridges were redesigned as SDC B bridges to determine if the horizontal design forces from a structural analysis method found in the Guide Specifications were smaller than those determined by the simple equations of SDC A2. This was the case in two of the bridges. The horizontal design forces for Bent Creek Road Bridge and the Bridge over Norfolk Southern Railroad were reduced when a structural analysis was completed. But the design forces for Oseligee Creek Bridge increased by 20%. Therefore, it cannot be assumed that a bridge in SDC B will have lower horizontal design forces than a bridge in SDC A. The other change from SDC A2 to SDC B was the increase in minimum seat width. The ATC-49 seat width equation uses the spectral acceleration to multiply the seat width. Since, by definition, SDC B sites have a higher spectral acceleration than SDC A sites, the minimum seat width will be greater in SDC B. The amount of transverse reinforcement did not change for the bridges studied with the exception of Oseligee Creek Bridge. Smaller transverse reinforcing bars were able to be used and even with the tighter spacing, the amount of reinforcement only increased by 1-3%.

4.9 Design Standards

Design standards were created by comparing the designs from bridges in each SDC. The procedures of the Guide Specifications were used to design these bridges. By designing multiple bridges, multiple designs could be checked against the standard details to ensure that a variety of bridges would satisfy the criteria, instead of the few that were designed. These new design standards and details will be discussed below.

4.9.1 Design Standards for SDC A1

SDC A1 is for bridges in low seismic hazard areas ($S_{D1} < 0.10$). There are three changes in the design to these bridges: an increase in the seat width, a change in the horizontal design forces and a possible decreased spacing of the transverse reinforcement. The seat length is calculated using Equation 4.2, which is the recommended ATC-49 equation. This equation results in a greater seat length than that calculated by the Standard Specifications as well as the Guide Specifications, as discussed in chapter 3. The design force is changed based on the expected ground acceleration at the site. For bridges in areas where the ground acceleration is less than 0.05g, the horizontal design force is 15% of the vertical reaction carried by the bent being designed. Otherwise, the horizontal design force is 25% of the vertical reaction carried by the bent. The vertical reaction includes the dead weight of the bridge tributary to the bent. It can also include the live load tributary to the bent at the discretion of the Owner. Choosing to include the live load will increase the design forces by approximately 10%. Since the live load is not required by the Specifications and choosing not to include it would decrease the horizontal design force, it is recommended that it not be included on every bridge. However, it should be considered for bridge that could experience a significant live load presence during an earthquake.

$$N = \left(4 + 0.02L + 0.08H + 1.09\sqrt{H}\sqrt{1 + (2\frac{B}{L})^2}\right) * \left(\frac{1+1.25S_{D1}}{\cos(\alpha)}\right) \qquad \text{Equation 4.2}$$

The final difference was a possible increase in the amount of transverse reinforcement. This change resulted from a new design equation in the LRFD Specifications for the required minimum amount of transverse reinforcement, which is used to design the reinforcement outside of the plastic hinge zone. Equation 4.5 can be seen below, and is applicable only if the design procedures used in this project are used, which are detailed in Article 5.8.3.4 of the LRFD Specifications. In the equation, the spacing is the variable that will be changed until the area of reinforcement supplied is greater than the minimum area required. This is only required when the design shear force in the column is greater than half of the factored shear resistance of the concrete. Only one of the bridges in this SDC required the minimum amount of reinforcement. If the minimum reinforcement equation is not required, a 12 inch ALDOT standard will control the spacing outside of the plastic hinge zone. If tight spacing outside of the hinge zone is a problem, cross-ties can be used to allow for the same amount of reinforcement at a larger spacing. For aid with determining the required spacing when the minimum requirements must be satisfied, Table 4.56 and Figure 4.34 were developed. For a given column width or diameter and known size of transverse reinforcement, the maximum spacing can be determined from the graph. The table can be used to find a specific value if it cannot be obtained from the graph. It should be noted that these aids do not include the effects of cross-ties, and are only applicable to columns with 4,000 psi concrete and 60 ksi reinforcing steel.

$$A_{v,min} = 0.0316 * \sqrt{f_c'} * \frac{b_v * s}{f_y} \qquad \text{Equation 4.5}$$

Table 4.56: Maximum Spacing Requirements outside of Plastic Hinge Zone

Column Width or Diameter (in)	Maximum Spacing (in)	
	#4 Bars	#5 Bars
24	16.0	24.5
30	13.0	20.0
36	11.0	16.5
42	9.5	14.0
48	8.0	12.5
54	7.0	11.0
60	6.5	10.0
66	6.0	9.0
72	5.5	8.5
78	5.0	8.0
84	4.5	7.0

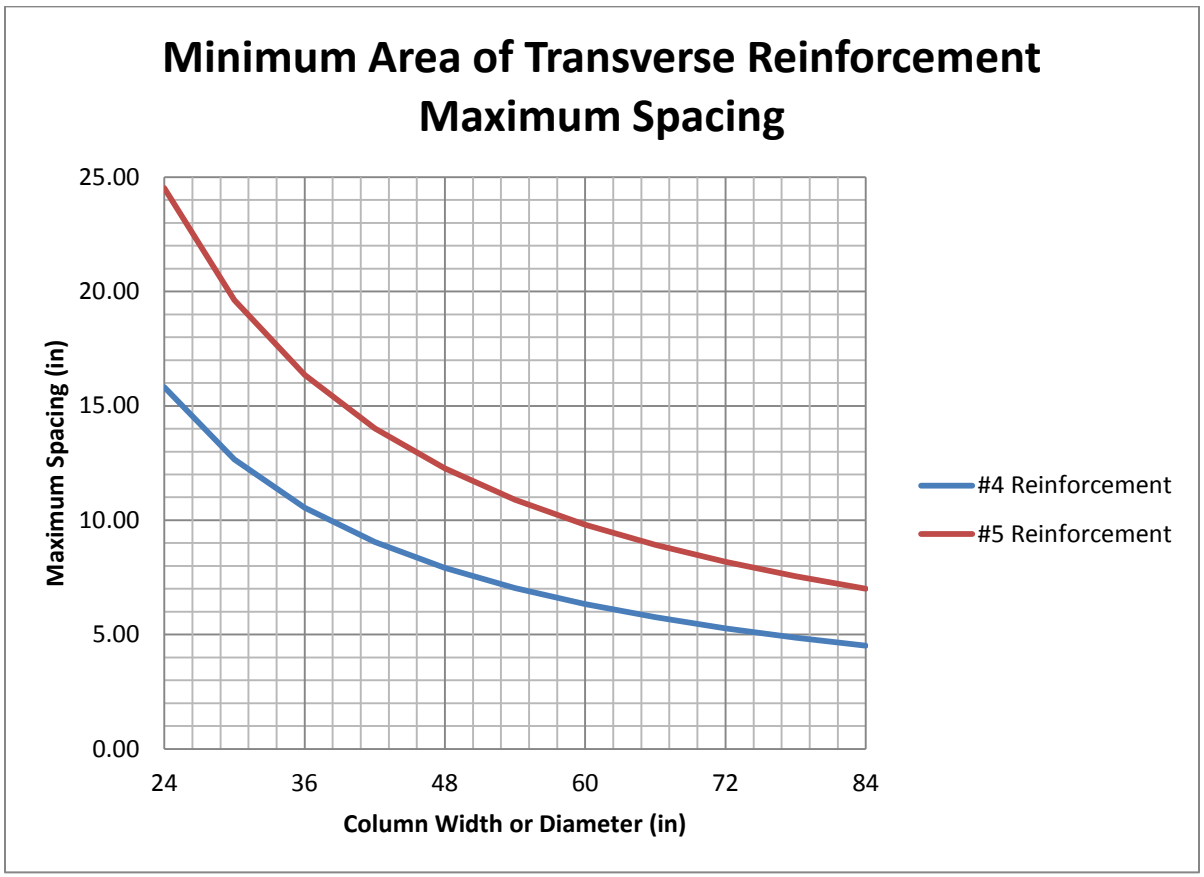

Figure 4.34: Maximum Spacing Requirements outside of Plastic Hinge Zone

4.9.2 Design Standards for SDC A2

SDC A2 bridges are still in areas of low seismicity ($0.10 \leq S_{D1} < 0.15$) but with a greater possibility of experiencing forces that could cause plastic behavior to occur in the column. The changes to this design category from the Standard Specification reflect this possibility. They include an increased minimum seat width, the addition of the plastic hinge zone, and smaller spacing of the reinforcement inside the hinge zone. The seat widths are increased because Equation 4.2 is used to determine them. By increasing the seat width, the girders are provided with more room to "ride out" a design earthquake, as discussed in chapter 3. The plastic hinge zone is calculated using the LRFD Specifications because it resulted in a smaller hinge length. However, for very tall columns, the length from the Guide Specifications may control and should be checked. The plastic hinge length is determined to be the maximum of the following:

- The largest cross-sectional dimension
- One-sixth the clear height of the column
- 18 inches

The spacing of the transverse reinforcement inside the plastic hinge zone is only required to satisfy minimum ratios and not shear capacity equations. The minimum ratio for circular columns is 0.002 and for rectangular columns is 0.003. Article 8.6.2 in the Guide Specifications shows how to calculate these ratios. Once a reinforcement size has been chosen, the spacing of the reinforcement will affect the ratio. Figure 4.35 and Figure 4.36 have been developed to provide standard design drawings for bridges in SDC A2. They are applicable to bridges with largest column widths or diameters less than or equal to 6 feet. The plastic hinge length is based on the LRFD Specifications, so it is recommended to check the Guide Specifications hinge length if the columns are very tall. Because none of the rectangular columns in this study were

large enough to require the use of cross-ties, the design drawings were developed using only one tie around the outside of the reinforcement. The transverse reinforcement spacing is based on the ratios, and the values given will satisfy them. The longitudinal reinforcement is not shown because it is determined on a project specific basis.

The reinforcement spacing outside of the plastic hinge zone is controlled either by the minimum area of transverse reinforcement requirement, discussed in the design standards for SDC A1, or by the 12 inch ALDOT standard. Therefore, those spacing requirements should also be checked. Figure 4.34 and Table 4.56 are recommended to be used when the minimum requirements are necessary.

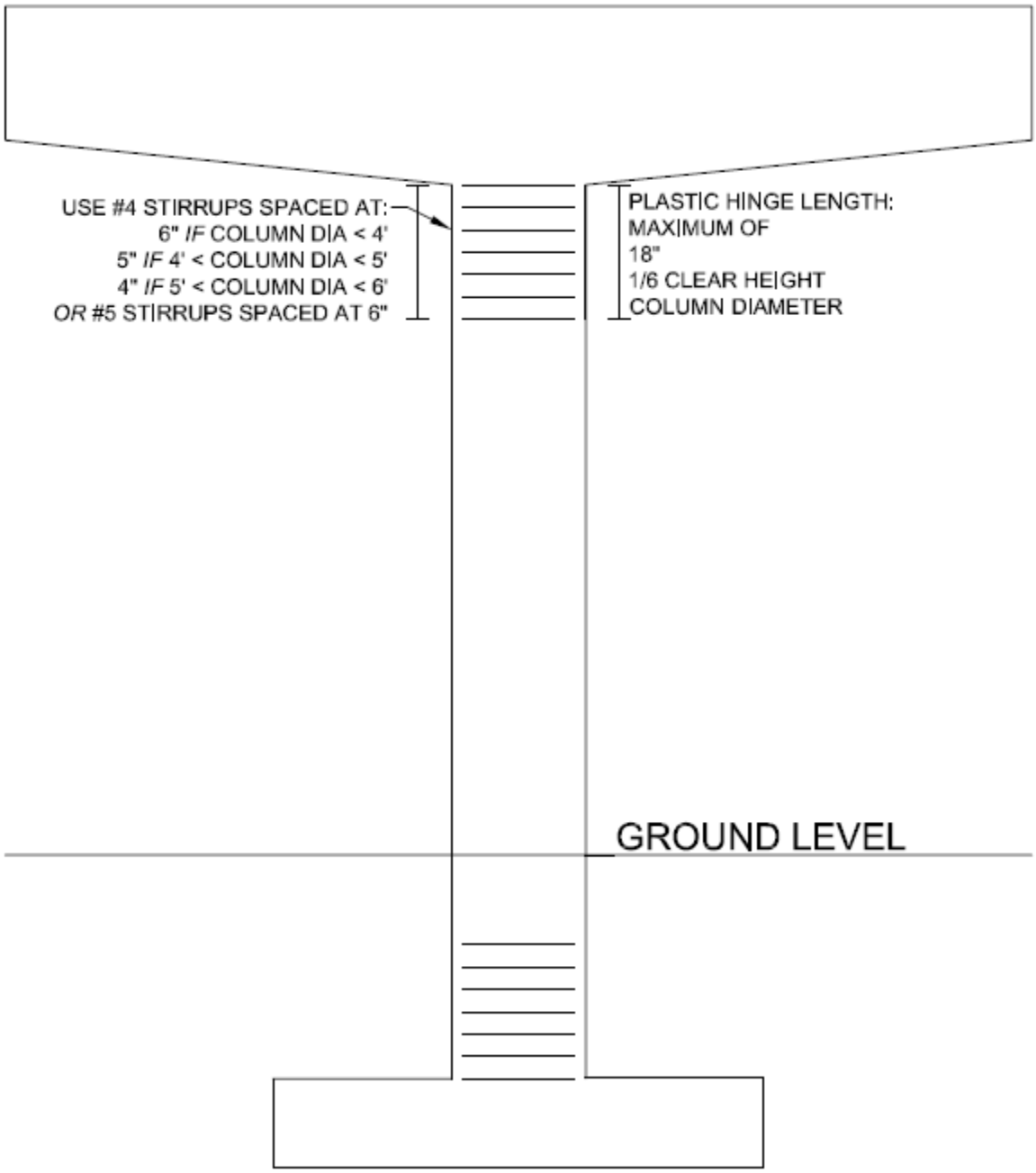

Figure 4.35: Standard Details for Circular Columns in SDC A2

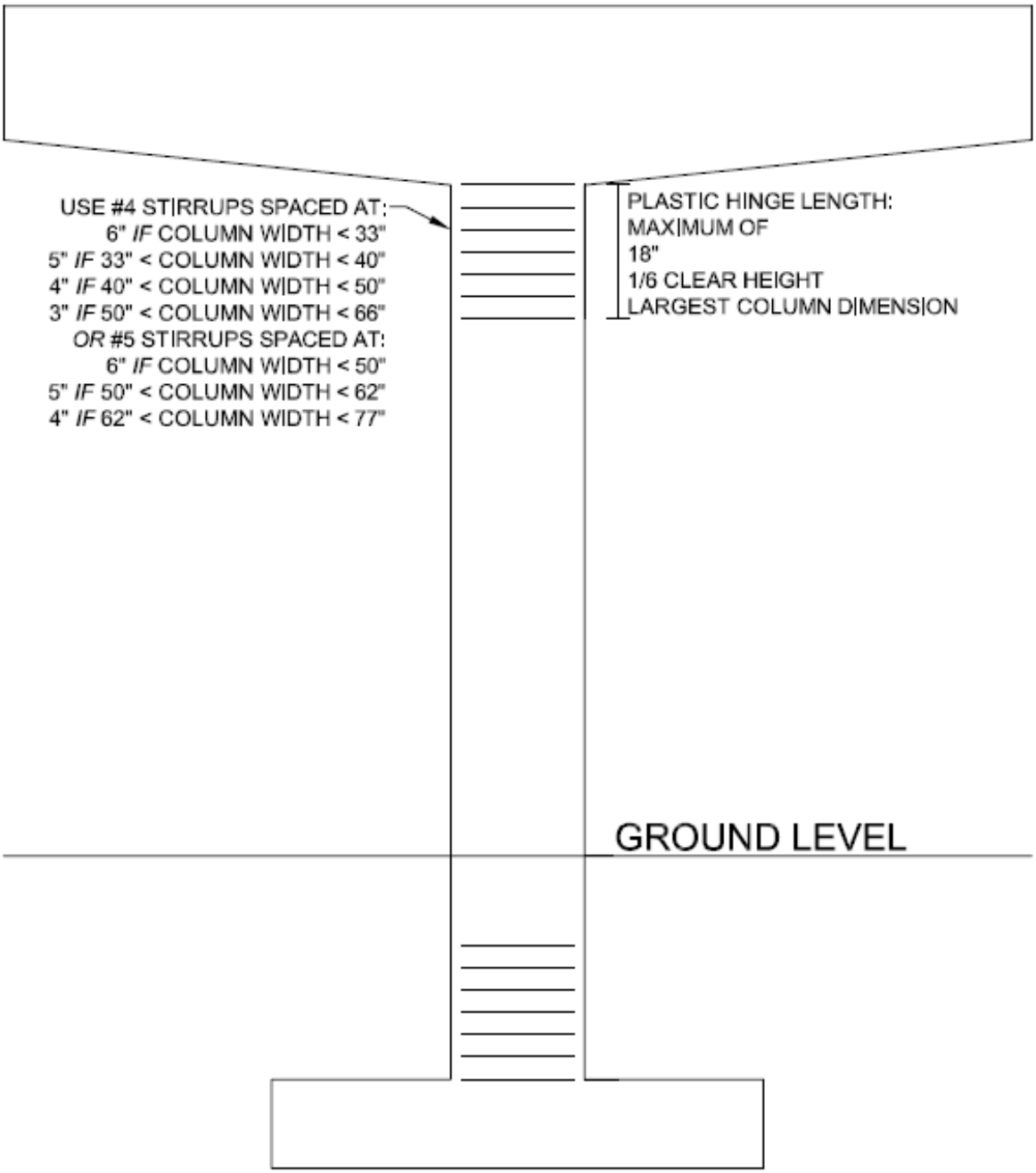

Figure 4.36: Standard Details for Rectangular Columns in SDC A2

4.9.3 Design Standards for SDC B

SDC B bridges are expected to experience moderate seismic forces ($0.15 \leq S_{D1} < 0.30$). These forces may be large enough that the columns must be designed with plastic hinges in order to dissipate the energy. Many changes were made to the design procedures for this category

including the need for a bridge model and structural analysis to determine the horizontal design forces, an increase in the minimum seat width, and the recommendation of an extension of the plastic hinge zone into the bent cap or footing.

When the horizontal design forces from the rigorous structural analysis in SDC B were compared with the horizontal forces from the simple relationships in SDC A2, it was discovered that the structural analysis resulted in lower forces in only two out of the three bridges. So it cannot be assumed that performing a structural analysis will result in lower design forces.

As discussed in chapter 3, the purpose of the superstructure-to-substructure connection was to transfer forces in the transverse direction and allow the girders to move in the longitudinal direction by providing greater seat width. For bridges in SDC B, the minimum seat width is increased by using Equation 4.2. This is by design since the superstructure-to-substructure connection does not provide a complete load path in the longitudinal direction and must have additional room to move during a design earthquake. The greater seat widths prevent them from becoming unseated. And since the original connection was to be used, the components of the connection that contribute to the resistance in the transverse direction were checked against the calculated capacity design forces. The clip angles were determined to be adequate for the largest forces encountered, and the diameter of the anchor bolts was increased until it was also adequate to resist the forces. However, the anchor bolt diameters were different for each bridge, and it is recommended they be designed on a per bridge basis, as indicated on the current connection details.

The plastic hinge length is determined in the same manner as in SDC A2, but the transverse reinforcement must resist the shear forces in the cross section as well as satisfy the minimum ratios. For all five bridges studied, however, the minimum ratios still controlled the

spacing of the transverse reinforcement in the plastic hinge length. The reinforcement outside of the hinge length was still controlled by either the minimum area of reinforcement check, if required, mentioned in the standards for SDC A1 or the 12 inch ALDOT standard. The extension of the plastic hinge zone is recommended by the Guide Specifications to increase the shear capacity of the cross section and allow the plastic hinge to form at the top of the column. This extension length should have the same transverse reinforcement spacing that is in the plastic hinge zone. This report recommends the use of the extension length in bridges in SDC B.

Figure 4.37 and Figure 4.38 were developed as standard details for SDC B. Like SDC A2, none of the rectangular columns in the bridges studied were large enough to require cross-ties, so the standard details were developed using only one tie to surround the longitudinal reinforcement in the plastic hinge zone. These details are similar to the details in SDC A2, except for the addition of the extension length. They are only applicable for columns with a width or diameter less than or equal to 72 inches.

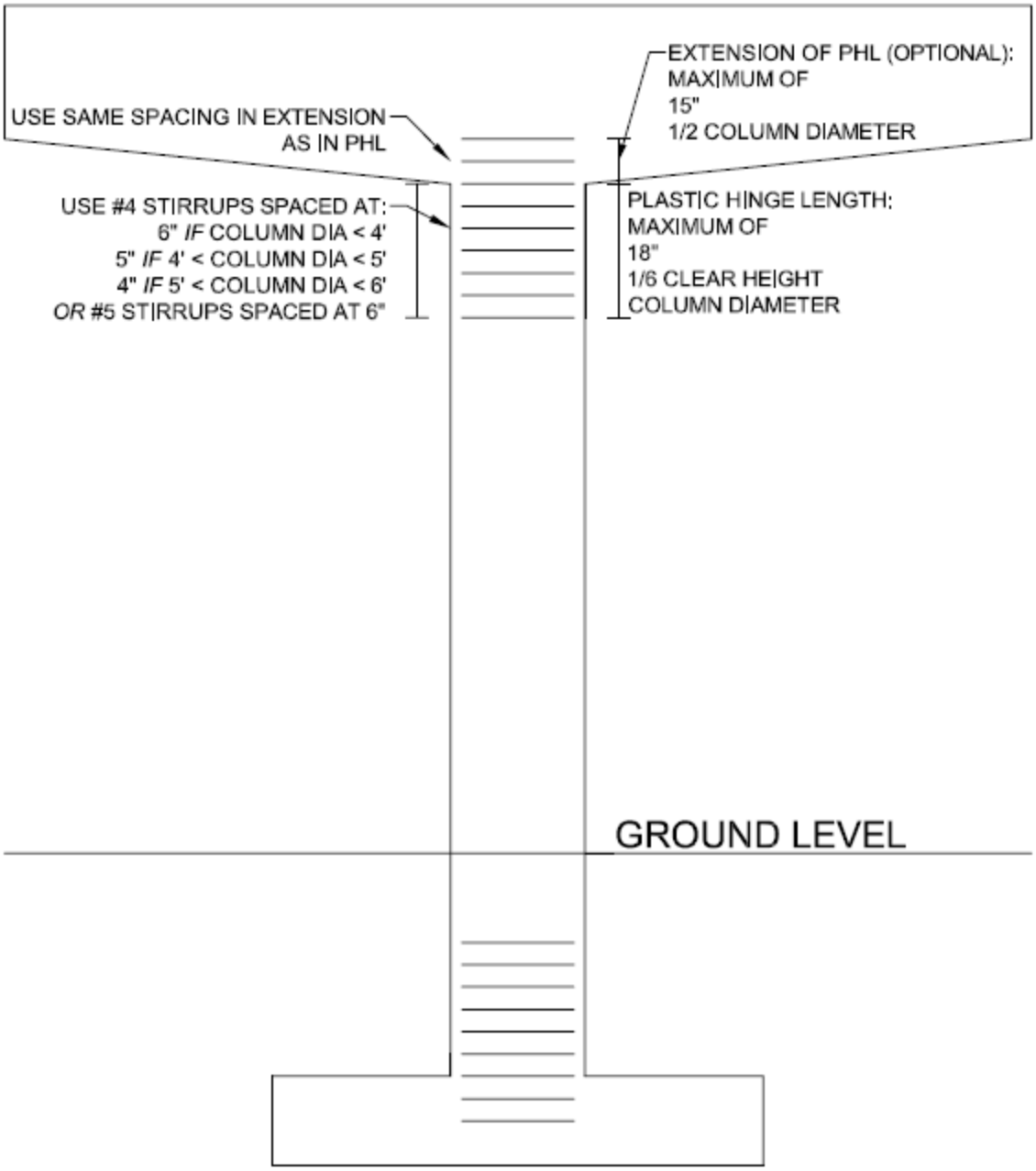

Figure 4.37: Standard Details for Circular Columns in SDC B

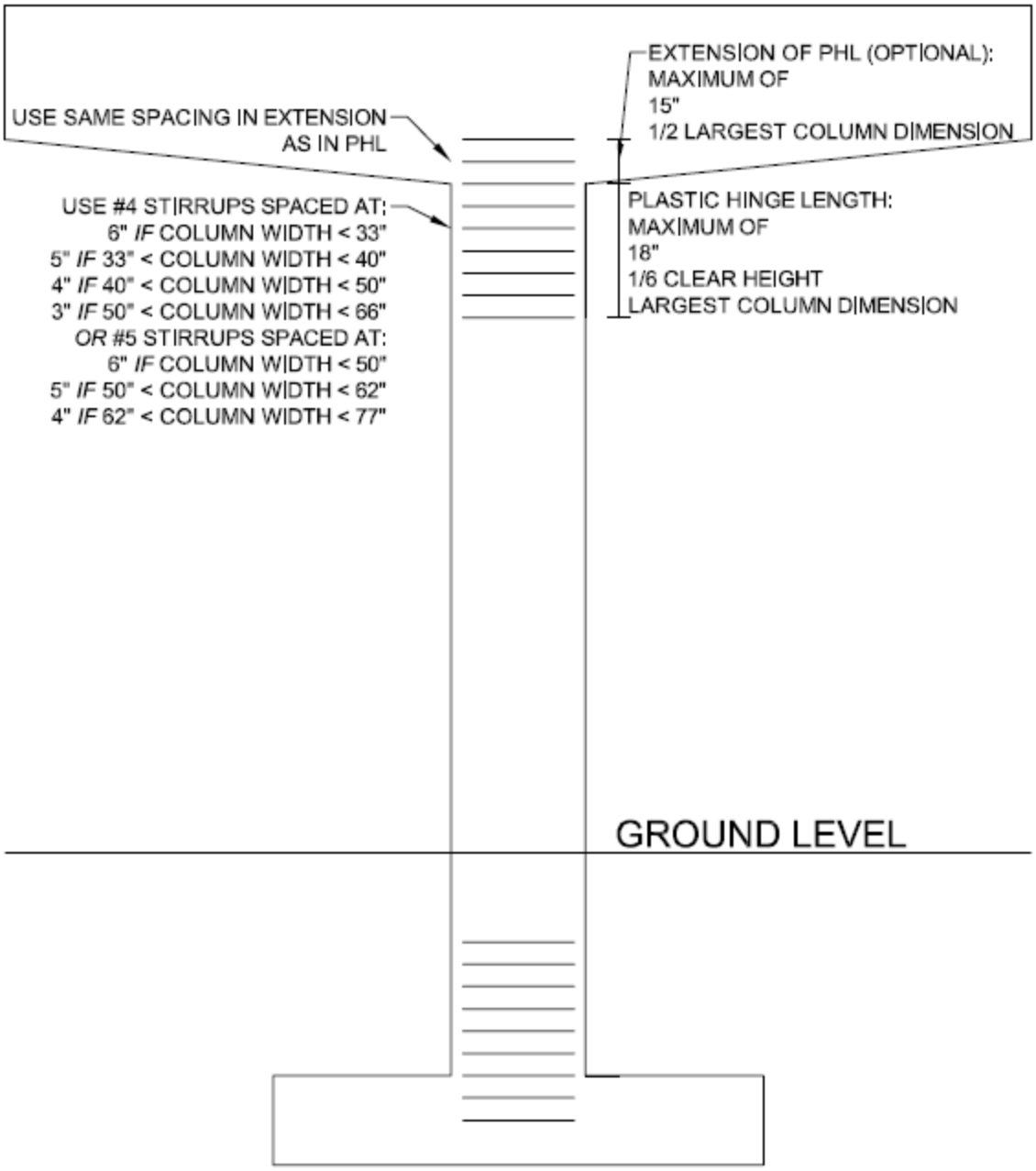

Figure 4.38: Standard Details for Rectangular Columns in SDC B

4.10 Conclusion

The purpose of this task was to develop new seismic design standards and details for bridges in the state of Alabama in Seismic Design Category A and B. These new standards are based on the Guide Specifications. This was accomplished by redesigned bridges in each SDC and comparing the new designs with the old designs under the Standard Specifications. 11

different bridges were re-designed by the Guide Specifications and compared with their designs using the Standard Specifications. The changes between the designs were used to develop design standards for each SDC.

For all of the bridges, the use of the ATC-49 equation (Equation 4.2) to determine the minimum seat length resulted in larger seat widths than those required by the Standard Specifications. The difference between the minimum lengths increased as the SDC increased, and specifically as the spectral accelerations within each SDC increased. The results from the research conducted in chapter 3 suggested that larger seat widths should be provided to allow the girders more room to displace in the longitudinal direction. The 11 bridges studied in this chapter proved that using the new equation did increase the minimum seat width.

The two bridges designed in SDC A1 showed that the horizontal design forces were different than they were in the Standard Specifications. The design force was either 15% or 25% of the vertical reaction resisted by the bent depending on the ground acceleration at the site, whereas in the Standard Specification, it was always 20%. The only other change in this SDC was a change in the LRFD Specifications that increased the amount of transverse steel in columns. This change affected all bridges that were designed, not just those in SDC A1.

One of the issues that was raised was the inclusion of the live load in the determination of the horizontal design force. The LRFD Specifications suggest including 50% of the live load at the Owner's discretion, but if the live load was included it would increase the horizontal design force, albeit only on the order of 10%. It was recommended not to include the live load in the design force calculation on every bridge, but to consider it on bridges that experience a significant live load presence throughout its service life. In summary for SDC A1, it was recommended to calculate the horizontal design force, minimum seat width, and maximum

spacing of transverse reinforcement for the column. These three design steps controlled the design for the two bridges studied.

The bridges designed in SDC A2 showed an increase in the amount of transverse reinforcement required for the columns because of the requirement that the plastic hinge zone be detailed. The transverse reinforcement in the plastic hinge zone also had to satisfy minimum ratios found in the Guide Specifications. Once these minimum ratios were satisfied the plastic hinge zone design was completed. The horizontal design forces were calculated to be 25% of the vertical reaction in all cases, which resulted in higher forces than in the Standard Specifications. In summary for SDC A2, it was recommended to calculate the horizontal design force, minimum seat width, plastic hinge length, maximum spacing within the plastic hinge length, and the maximum spacing of transverse reinforcement outside of the plastic hinge length. These design steps were easily calculated and did not require any computer analysis of the bridge.

The biggest changes occurred in SDC B. Unlike the Standard Specifications, which simply required that the columns be designed to resist the expected loads, the Guide Specifications required the bridge displacement capacity to be greater than the expected displacement. In order to accomplish this, a computer model was built and a structural analysis was run. Once the capacity was confirmed, minimum detailing requirements had to be met as well as checking that the column section in the plastic hinge zone was capable of resisting the expected shear forces. However, for the five bridges studied, the minimum ratios from the detailing controlled the transverse reinforcement design instead of the strength. An additional extension length was recommended by the LRFD Specifications to promote the forming of a

plastic hinge at the top and bottom of the column and protect the elements around the hinge. While not required for SDC B, it was recommended to use this extension length.

Another question that arose concerned the use of structural analysis to get smaller horizontal design forces for the connections and columns. Three bridges were designed in both SDC A2 and SDC B categories, and for only two of them were the design forces from SDC B lower than those for SDC A2. Therefore, it was not recommended to attempt a more complicated structural analysis to get smaller design forces.

Finally, the original superstructure-to-substructure connection used by ALDOT and discussed in chapter 3 was to be used. The longitudinal direction was allowed to displace and greater seat widths were provided to accommodate the movement, but the transverse direction needed to be analyzed to determine if it was adequate to resist the design forces. So for the five bridges studied in SDC B, the transverse connection was designed, and it was determined that the clip angles were adequate to resist the largest horizontal design force of 82 kips. The anchor bolts were also designed, but they varied in diameter from 1.25 inches to 2.5 inches. Therefore, as long as the anchor bolts were designed, it was recommended that the current connection be used as the superstructure-to-substructure connection since the minimum seat lengths provided were expected to provide enough room for the girders to move and the clip angles would provide enough resistance to transfer the forces into the substructure.

In summary for SDC B, it was recommended to first model the bridge in a structural analysis software package, such as SAP2000 or CSI Bridge, and determine the bridge displacement capacity and column and connection design forces. Next, the plastic hinge length, extension length, and spacing of the transverse reinforcement based on the minimum ratios were to be calculated, and then the section was checked to ensure it could resist the forces from the

structural analysis. The transverse reinforcement outside of the plastic hinge zone was designed next and, finally, the minimum seat width was calculated and anchor bolts for the connection were designed. While this SDC does require the use of computer software and analysis, the design sheets and design aids that were created provide guidance on how to accomplish certain design steps, as well as examples. The standard details and designs developed in this chapter are not intended to be used in lieu of designing the bridge, but do provide a starting point where designers can begin.

Chapter 5: Case Histories

5.1 Selection of Bridges

All bridges analyzed in this project were selected from a list of existing highway bridges in the state of Alabama. The seismic design details used in the analysis have been updated to the most recent edition of AASHTO's guide specification for seismic design in order to analyze designs according to current code, as well as anticipate future bridge design in the state. The bridge selection process revolved around three major factors: seismic hazard (based on location), soil condition and bridge geometry. Seven highway bridges were considered for this analysis, but only five were chosen based on the aforementioned factors. The locations of the selected bridges can be seen in Figure 5.1, along with their foundation type.

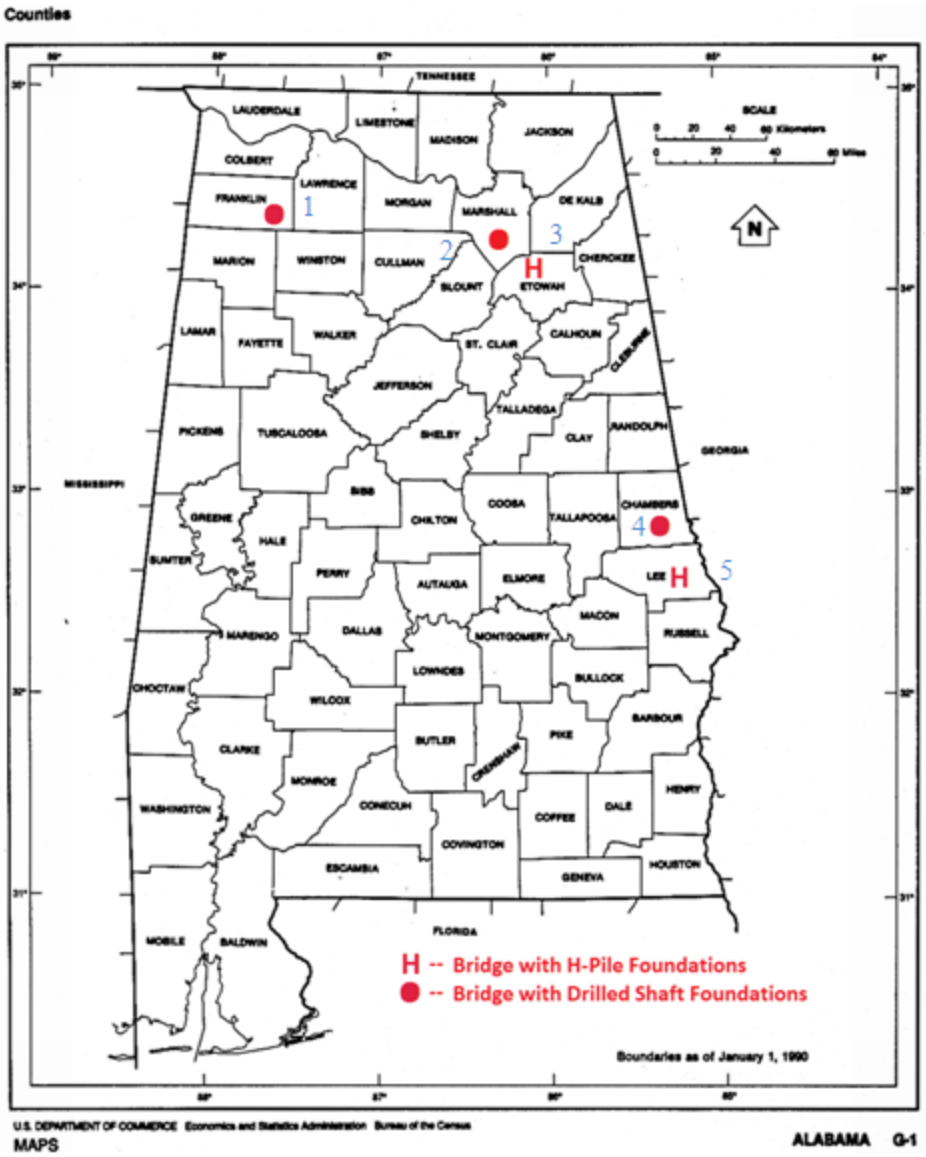

Figure 5.1. Map of Alabama Counties with bridge locations (modified after Yellow Maps 2010)

5.1.1 Seismic Hazard

The geography of Alabama is not constant throughout, although some generalizations can be made for the purpose of this project. The southern portion of the state tends to rest on deep layers of sandy soils. These regions also tend to have little exposure to seismic activity. The hazard originates in the Northwest region of Alabama (New Madrid Fault Zone), or in the mountainous region at the border of Alabama, Georgia and Tennessee (East Tennessee Seismic

Zone). Bridges in South Alabama tend to face a greater wind hazard than a seismic hazard. This information, in combination with soil conditions, led to the elimination of most of the southern bridge designs. Bridges that were selected for use in this project tended to be located in the northern section of the state where the foundation conditions were similar to what would be expected in the areas of highest seismicity. Selected bridges outside of this region still displayed characteristics consistent with bridges in the region.

5.1.2 Soil/Geologic Conditions

Geotechnical data became a defining factor in the selection of applicable bridges. Soil classifications at site locations can play a major role in overall earthquake hazard and structural performance. Soil information was included along with the bridge plans provided by ALDOT for this project. This soil information was used in the bridge selection process because it not only correlated to the bridges location in the state, but also correlated to the foundation types used in the bridges.

Geological properties helped create expected soil conditions throughout the state in regions without specific data. Basic generalizations were determined for different regions of the state, and helped classify bridges, as well as estimate which bridges could be designed in specific regions. The more mountainous regions of Alabama tended to have a soil layer between ten to thirty feet deep, resting on a hard rock layer. Foundations for these particular bridges consisted of drilled shafts that founded the bridge to the rock layer. Other locations in northern Alabama consisted of deeper soil layers, but still utilized similar foundation systems. Regions in central Alabama with similar soil conditions included bridges with pile group foundations, these bridges

were also considered to be constructible in areas of higher seismicity, and thus were not dismissed in the selection process. Overall, the bridges selected were bridges that could plausibly be constructed in higher hazard regions of Alabama, bridges that also rested on soil that could be found in these regions.

5.1.3 Bridge Geometry

A bridge's geometry contributes significantly to the seismic behavior. A bridge with tall columns and long spans will have a lower stiffness compared to a bridge with shorter spans and shorter columns. In addition to component lengths, component thickness is also a factor in bridge response. For the purpose of this project it was important to collect a range of bridge geometry in order to realistically account for a spectrum of possible bridge designs. Bridge configurations that included steel girders or concrete girders with changing thicknesses where not considered for this project. Bridges that did not include bearing pad supports were also excluded from this project due to significant analysis effort being placed on bearing pad behavior and the girder-to-cap connection.

5.2 Final Selection

A total of five bridge designs were selected for use in this project, all meeting the conditions required. A list of these bridges and their location can be seen in Table 5.1.

Table 5.57: Bridge Locations

Number	Bridge	Location
1	Little Bear Creek	Russellville
2	Scarham Creek	Albertville
3	Norfolk Southern RR	Gadsden
4	Oseligee Creek	Lanett
5	Bent Creek Road	Auburn

5.3 Little Bear Creek Bridge

5.3.1 Background Information (Structural)

The Little Bear Creek Bridge was selected due to its location in the North West corner of the state and spans over the Little Bear Creek on the east bound lane of S.R 24 (Corridor V). This bridge carries two lanes of State Road 24 over Little Bear Creek in Franklin County. It is a three span bridge with spans of unequal lengths. The outer span lengths are 85 feet and the interior span is 130 feet. The outer spans support the 7 inch concrete deck with 6 Type III Girders and the interior span supports the deck with 6 BT-72 Girders. Each of the 6 Type III girders rests upon 20.5” x 9” bearing pads and each of the 6 BT-72 girders rests upon 24.5” x 9” bearing pads. The two bridge piers are 40’ x 5’ x 7’ and supported by two circular columns 4.5 feet in diameter with 3 inches of concrete cover. The columns are reinforced longitudinally with 24 #11 bars and transversely with #5 hoops uniformly spaced at 10 inches from the bottom of the hinge zone to the top of the foundation, and spaced at 6 inches inside the hinge zone. The average clear height of Bent 2 is 12.06 feet and 16.88 feet for Bent 3. All columns are supported on drilled shafts 5 feet in diameter. The concrete cover of the drilled shafts is 6 inches but the longitudinal reinforcement in the drilled shaft still aligns with the longitudinal reinforcement of the column.

This bridge is unique in that it uses two different girder sizes and bearing pad sizes along its three spans. These discontinuities can provide unique dynamic behavior, like a tendency for a structure to deviate from its first mode shape. The soil conditions at this particular site consisted of a relatively shallow soil layer, as to be expected in this region of the state. The CSiBridge model for this bridge can be seen in Figure 5.2.

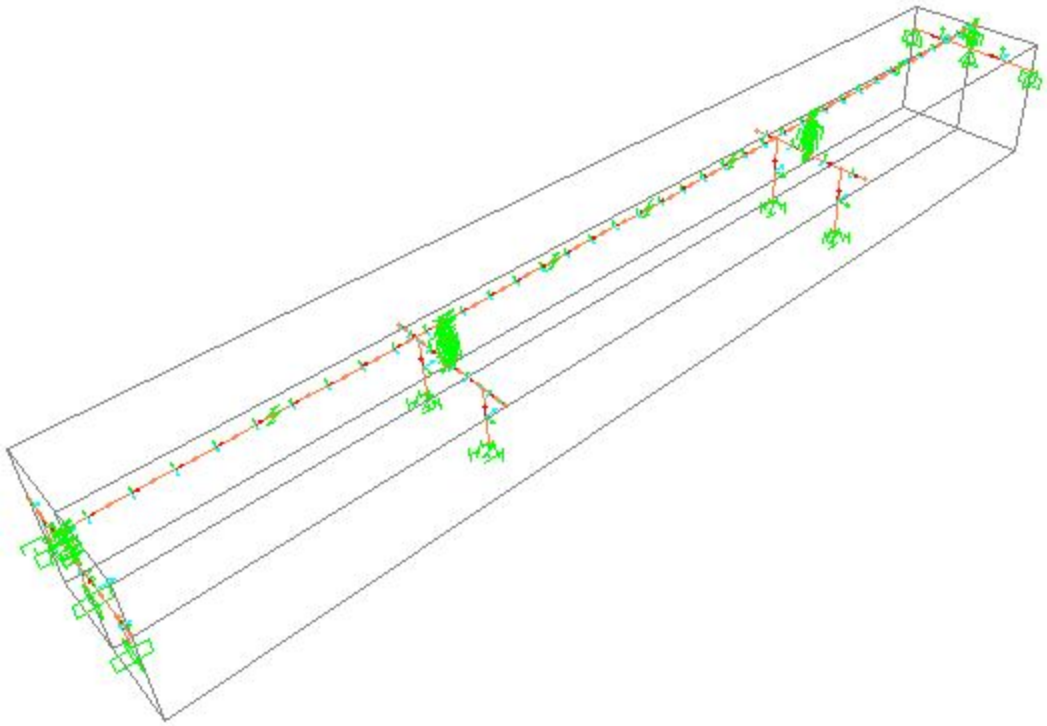

Figure 5.2: Little Bear Creek Bridge Model

5.3.2 Background Information (Foundation)

The foundations used for both the abutments and piers are drilled shafts. Because the abutments were not modeled, they are not discussed. Bent 3 was modeled in FB-MultiPier. Bent 2 and 3 are built the same but with slightly different tip elevations and soil conditions. Bent 3 consists of a pier cap and two shafts. The shafts are 4.5 ft in diameter with twelve No. 11 longitudinal reinforcing bars above the ground surface, and 5 ft in diameter with the same reinforcement alignment below the ground surface.

5.4 Scarham Creek Bridge

5.4.1 Background Information (Structural)

The Scarham Creek Bridge was the second bridge selected for this project. The Scarham Creek Bridge is two lanes and carries State Route 75 (southbound lane) over Scarham Creek in

Marshall County. It is a four span bridge with equal span lengths of 130 feet. The 7 inch concrete deck is supported by 6 BT-72 girders. Each of the 6 girders rests upon 24.5” x 9” bearing pads. The bridge pier at bents 2 and 4 are 40’ x 5.5’ x 7.5’ and the pier at bent 3 is 40’ x 6.5’ x 7.5.’ Bents 2 and 4 are supported by two circular columns 5 feet in diameter with 3 inches of concrete cover. Bent 3 is supported by two circular columns 6 feet in diameter with 3 inches of concrete cover. All columns are reinforced transversely with #6 hoops at a spacing of 6 inches at the top and bottom hinge zones, and spaced at 12 inches at all other regions. All columns are supported on drilled shafts, which are six inches larger in diameter than the columns. It is assumed that the plastic hinge will form at this transition, so the clear height of the columns is measured from the bottom of the bent cap to the transition between the column and drilled shaft. The average height of columns is 34.02 feet at Bent 2, 59.17 feet at Bent 3, and 32.16 feet at Bent 4. Because of the height of the columns, rectangular struts are provided at approximately mid-height of the columns and span the full length between columns with a thickness of 3.5 feet. The strut at bents 2 and 4 are 6 feet deep and 10 feet deep at bent 3.

The Scarham Bridge contained the tallest and largest bent columns, making it one of the more flexible bridges. Concrete struts were also developed for use in this bridge’s bent design in an effort to reduce the unbraced length of the columns. These struts presented a unique opportunity for dynamic element observation, since they appear to have been overdesigned for the purpose of stability and safety. Overdesigns like these can actually become harmful to earthquake response if members are not detailed accordingly, so this condition made this particular bridge an important one to analyze. The CSiBridge model for this bridge can be seen in Figure 5.3.

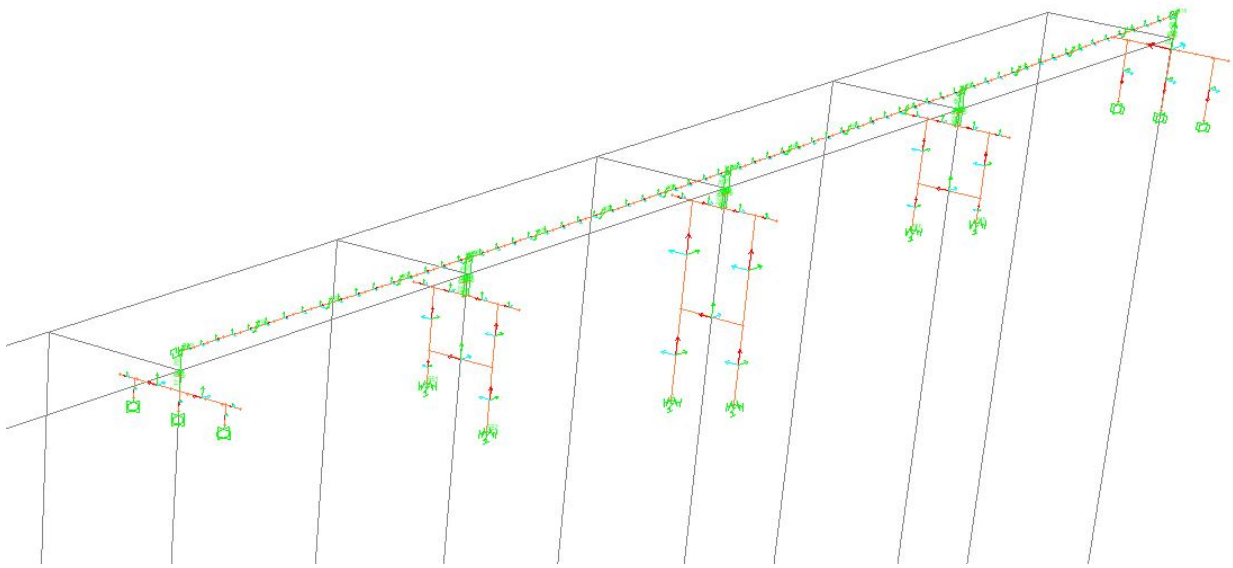

Figure 5.3: Scarham Creek Bridge Model

5.4.2 Background Information (Foundation)

The total bridge span is 520 ft and rests on two abutments and three central piers. It is not skewed and has a total roadway width of 40 ft. The foundations used for both the abutments and piers are drilled shafts. Because the abutments were not modeled, they are not discussed. The foundations for Bents 2, 3, and 4 were modeled in FB-MultiPier to develop static stiffness response curves for the SAP model. All of the bents were modeled using the same soil profile, which was the lower bound. Bent 2 and 4 have the same section properties; therefore, one model was developed to represent both bents. Bent 3 has a larger shaft diameter than that of Bents 2 and 3 was the bent modeled for direct analysis.

The shafts for Bent 2 and 4 are 5 ft in diameter with 24 No. 11 longitudinal reinforcing bars above the ground surface, and 5.5 ft in diameter with the same reinforcement alignment below the ground surface. The shafts for Bent 3 are 6 ft in diameter with 32 No. 11 longitudinal reinforcing bars above the ground surface, and 6.5 ft in diameter with the same reinforcement alignment below the ground surface.

5.5 Norfolk Southern Railroad Bridge

5.5.1 Background Information (Structural)

The third bridge that was selected was the Norfolk Southern Railroad Bridge. The bridge over Norfolk Southern Railroad is the southbound I-59 bridge in Etowah County, a two lane bridge that crosses over a Norfolk Southern railroad line and a state highway. It is a two span bridge with unequal span lengths of 125 feet and 140 feet. Nine modified BT-54 girders support a 6 inch concrete deck that is 46.75 feet wide. Each of the 9 girders rests upon 24.5” x 9” bearing pads. The only bridge pier is 53’ x 4.5’ x 4’ and supported by three square columns 3.5 feet in width. The columns are reinforced longitudinally with twelve #11 bars and transversely with #4 ties uniformly spaced at 9 inches from the bottom hinge zone to the top hinge zone, with a spacing of 4 inches inside each hinge zone. The average clear height of the columns is 25.25 feet. The bridge is supported on driven piles. The pile cap is 8.5’ x 8’ x 4.5’ and each pile cap is supported by 7 HP 12x53 steel piles.

The geometry of the Norfolk Bridge represents a typical highway bridge. It consists of two similarly spaced spans supported by a typical three column bridge bent. The soil conditions present at this location resulted in the bridge being supported on driven pile group footing foundations. This was the first bridge selected with these foundations, as well as being the first bridge selected that uses rectangular columns instead of circular columns. The CSiBridge model for this bridge can be seen in Figure 5.4.

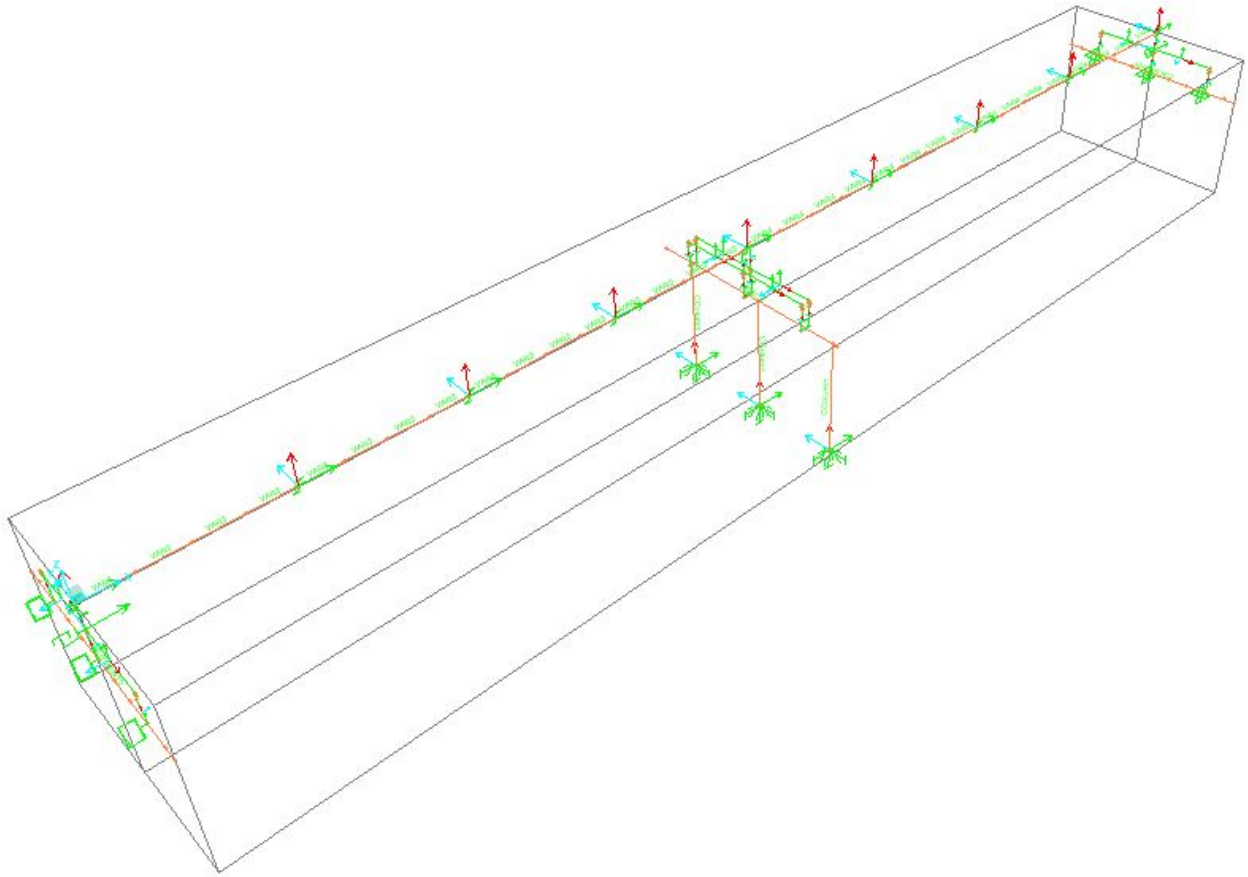

Figure 5.4: Norfolk Southern Bridge Model

5.5.2 Background Information (Foundation)

The Norfolk Southern Railroad Bridge is a bridge replacement on I-59 south bound lanes over US-11 and Norfolk Southern Railroad. The total bridge span is 265 feet and rests on two abutments and one central pier (bent 2). It is skewed approximately 30° and has a total roadway width of 46 feet and 9 in. The foundations used for both the abutments and piers are 12x53 H-piles. Because the abutments were not modeled, they are not discussed. Bent 2 was modeled in FB-MultiPier and consists of a pier cap and three columns that are each supported by pile footings.

5.6 Oseligee Creek Bridge

5.6.1 Background Information (Structural)

The first bridge selected outside of the northern area of Alabama was the Oseligee Creek Bridge. The Oseligee Creek Bridge is a two lane bridge that carries County Road 1289 over Oseligee Creek in Chambers County. It is a three span bridge with equal span lengths of 80 feet. The 7 inch concrete deck is supported by 4 Type III girders. Each of the 4 girders rests upon 20.5” x 9” bearing pads. The two bridge piers are 30’ x 4’ x 5’ and supported by two circular columns 3.5 feet in diameter with 3 inches of concrete cover. The columns are reinforced longitudinally with 12 #11 bars and transversely with #4 hoops uniformly spaced at 12 inches from the bottom of the hinge zone to the rock line, with the hinge zone being reinforced with #4 ties at 6 inch spacing. The average clear height of Bent 2 is 17.93 feet and 25.83 feet for Bent 3. All columns are supported on drilled shafts 3.5 feet in diameter with concrete cover of 3 inches.

The foundation of the bridge consists of driven pile foundations that extend all the way to bedrock. Soil at this location was determined to have poor strength, and showed susceptibility to scour. The geometry of this bridge was an important factor in the selection of this bridge, but its soil conditions may cause it to behave differently than expected. The CSiBridge model for this bridge can be seen in Figure 5.5.

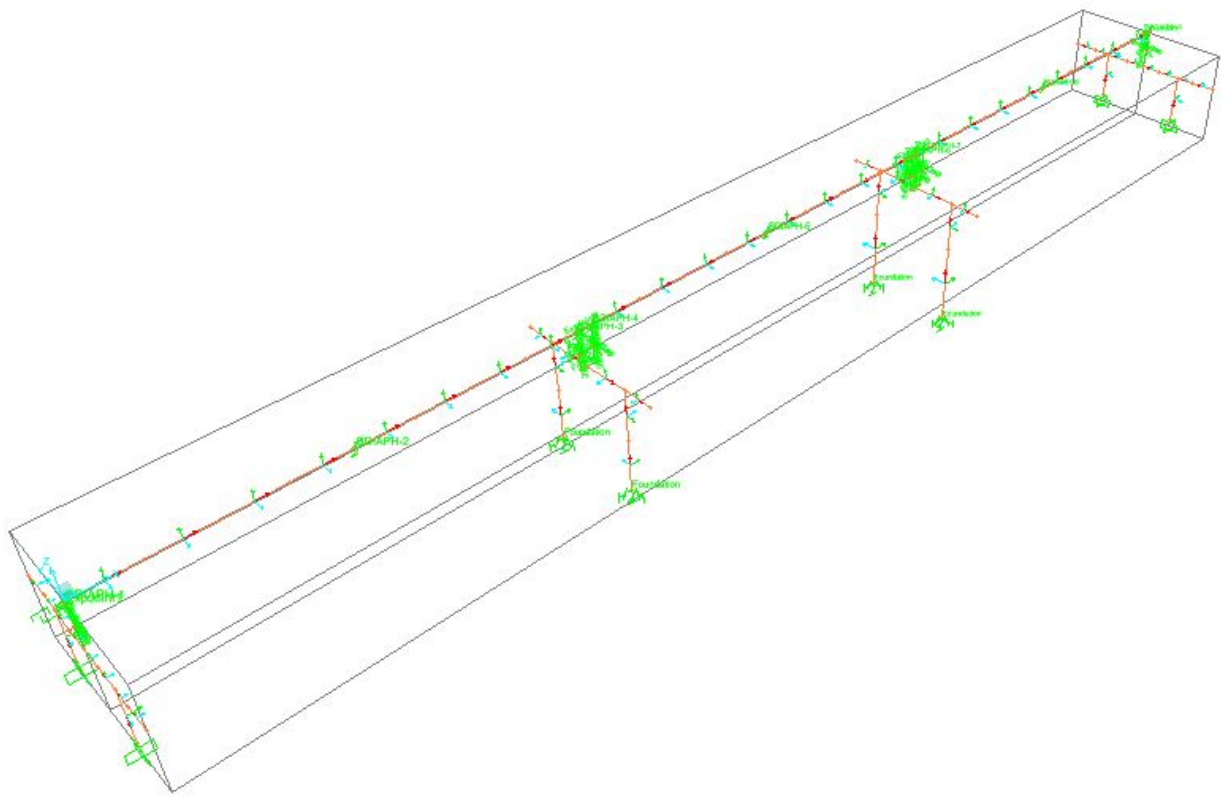

Figure 5.5: Oseligee Creek Bridge Model

5.6.2 Background Information (Foundation)

The Oseligee Creek Bridge is a bridge replacement project over Oseligee Creek. The total bridge span is 240 ft and rests on two abutments and two central piers. It is not skewed and has a total roadway width of 32 ft and 9 in. The foundations used for both the abutments and piers are drilled shafts. Because the abutments were not modeled, they are not discussed. Bent 3 was modeled in FB-MultiPier. Bent 2 and 3 are built the same but with slightly different tip elevations. Both have similar soil conditions. Bent 3 consists of a pier cap and two shafts. The shafts are 3.5 ft in diameter with twelve No. 11 longitudinal reinforcing bars.

5.7 Bent Creek Road Bridge

5.7.1 Background Information (Structural)

The last bridge, and largest bridge, selected for these analyses was the Bent Creek Bridge. The Bent Creek Road Bridge in Lee County is a five-lane bridge that crosses over Interstate 85 with two spans of 135 feet. Each span is comprised of 15 modified BT-54 girders spaced approximately 5.33 feet apart that support a 6 inch concrete deck that is 80.75 feet wide. Each of the 15 girders rests upon 24.5” x 9” bearing pads. The only bridge pier is 79’ x 4’ x 4.5’ and supported by five square columns 3.5 feet in width. The columns are reinforced longitudinally with 12 #11 bars and transversely with #4 ties uniformly spaced at 9 inches from the bottom of the bent to the top of the pile cap foundation, except for plastic hinge zone region which are reinforced with #4 ties at a spacing of 4 inches. The average clear height of the columns is 20.1 feet. The bridge is supported on driven piles. The pile cap is 8.5’ x 8’ x 4.5’ and each pile cap is supported by 9 HP 12x52 steel piles.

The mass and stiffness associated with this bridge made it an attractive option for analysis within this project. The bridge itself is not located in a region of seismicity, but it was deemed plausible that this design could be reused in a region of Alabama with higher seismicity. Some of the drawbacks regarding a bridge this size involve modeling concerns. This is the second bridge to be supported on pile footing foundations. The CSiBridge model for this bridge can be seen in Figure 5.6.

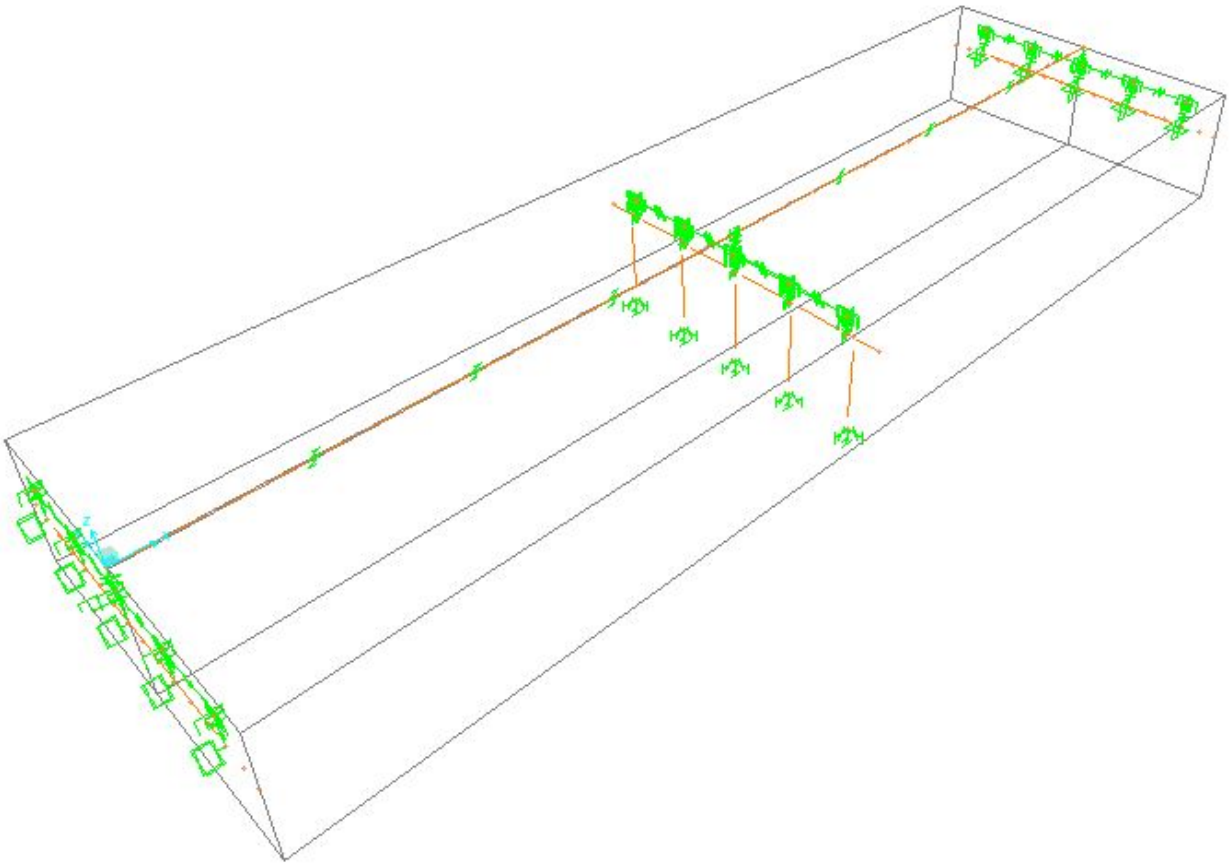

Figure 5.6: Bent Creek Bridge Model

5.7.2 Background Information (Foundation)

The Bent Creek Road Bridge is a bridge replacement for Bent Creek Road over I-85. The total bridge span is 270 feet and rests on two abutments and one central pier (bent 2). It is not skewed and has a total roadway width of 80 feet and 9 in. The foundations used for both the abutments and piers are 12x53 H-piles. Because the abutments were not modeled, they are not discussed. Bent 2 was modeled in FB-MultiPier and consists of a pier cap and three columns that are each supported by pile footings. The bridge was built in two stages to avoid closing the existing road. The bridge was modeled in FB-MultiPier as one bent, however, due to program limitations.

5.8 Summary

The previous sections outline the procedures related to the selection of bridges. The factors discussed include bridge geometry, bridge location hazard and bridge behaviors. The reasoning and justification for each of these selections is also provided. Bridge locations are provided and bridge details (structural and geotechnical) are included in this section. The bridges selected represent a diverse range of geometries consistent with highway bridges that could be built in the higher seismic hazard regions of Alabama.

Chapter 6 Modeling

6.1 Selection of Ground Motions

After the selection of bridges is performed, a determination of seismic hazard and the ground motions that represent them must be performed. A total of ten scaled ground motions (GMs) were selected for the worst design level hazard present in the state of Alabama. The analysis for selecting these ground motions involved the following tasks:

1. Perform a probabilistic seismic hazard analysis (PSHA) for each hazard location.
2. Collect GMs that contain values and properties similar to those highlighted by the PSHA.
3. Obtain a design spectra for the locations from the PSHA based on a Uniform Hazard Spectrum (UHS) with a probability of exceedance of 7% in 75 years.
4. Select 7-12 GMs that best match the UHS.
5. Apply scaling to the ground motions from (3) to fit the target spectra obtained from (2).

6.1.1 Probable Seismic Hazard Analysis (PSHA)

The PSH analyses for this project were performed using the tools provided by the USGS (https://geohazards.usgs.gov/deaggint/2008/). Details regarding the specifics of the procedures and calculations used by these tools can be found at the USGS website (USGS 2013). A PSHA requires some information to run, including site location, shear wave velocity of the top 30 meters of a soil (V_{s30}), and a seismic event return period for

the hazard. A V_{s30} of 760 m/s, corresponding to a site class of B, was selected for Alabama, and a return period of 1000 years was selected, being input as a 5% exceedance probability in the next 50 years (similar return period correlating to the 7% exceedance in the next 75 years as specified in AASHTO). The results of a PSHA analysis can be seen in the form of a deaggregation plot which allows the user to see the contributions from faults and other sources projected onto a 3–dimensional plot. The horizontal axis of the plot represents event magnitude; the vertical axis of the plot represents distance between event epicenter and location. The height of each bar represents the portion of contribution an event has towards the hazard of a location. Figure 6.1 displays the deaggregation plot for Muscle Shoals, Alabama.

From a PSHA performed for four different locations in Alabama, it was determined that the two locations that had the highest seismic hazards were the northeast and northwest corners of the state, with a probabilistic peak ground acceleration of 0.091g and 0.076g, respectively. It can be observed in Figure 6.2 that Bridgeport experiences a bimodal distribution meaning that the hazard is defined primarily by a magnitude 5-5.5 earthquake at a distance of 50 km (30 miles) or a magnitude 7.5-8 at a distance of 350 km (210 miles). Using this information, a bin of about 40 earthquakes was selected using the Pacific Earthquake Engineering Research (PEER) Center database, a collection of ground motions recorded around the world. These ground motions were then sorted by various parameters such as distance from fault, event magnitude, site class, response spectrum shape and PGA.

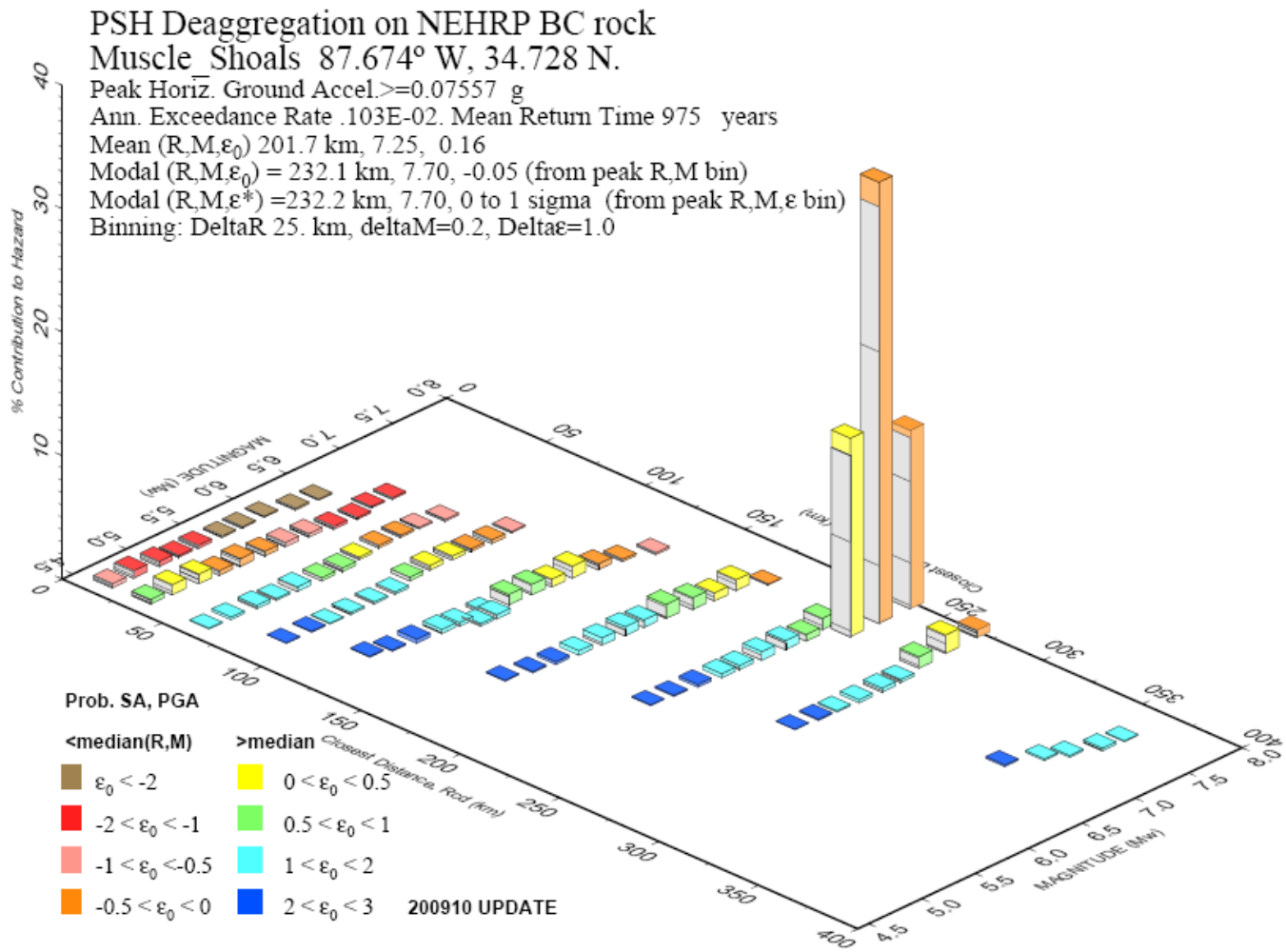

Figure 6.1: Deaggregation Plot for Muscle Shoals, AL

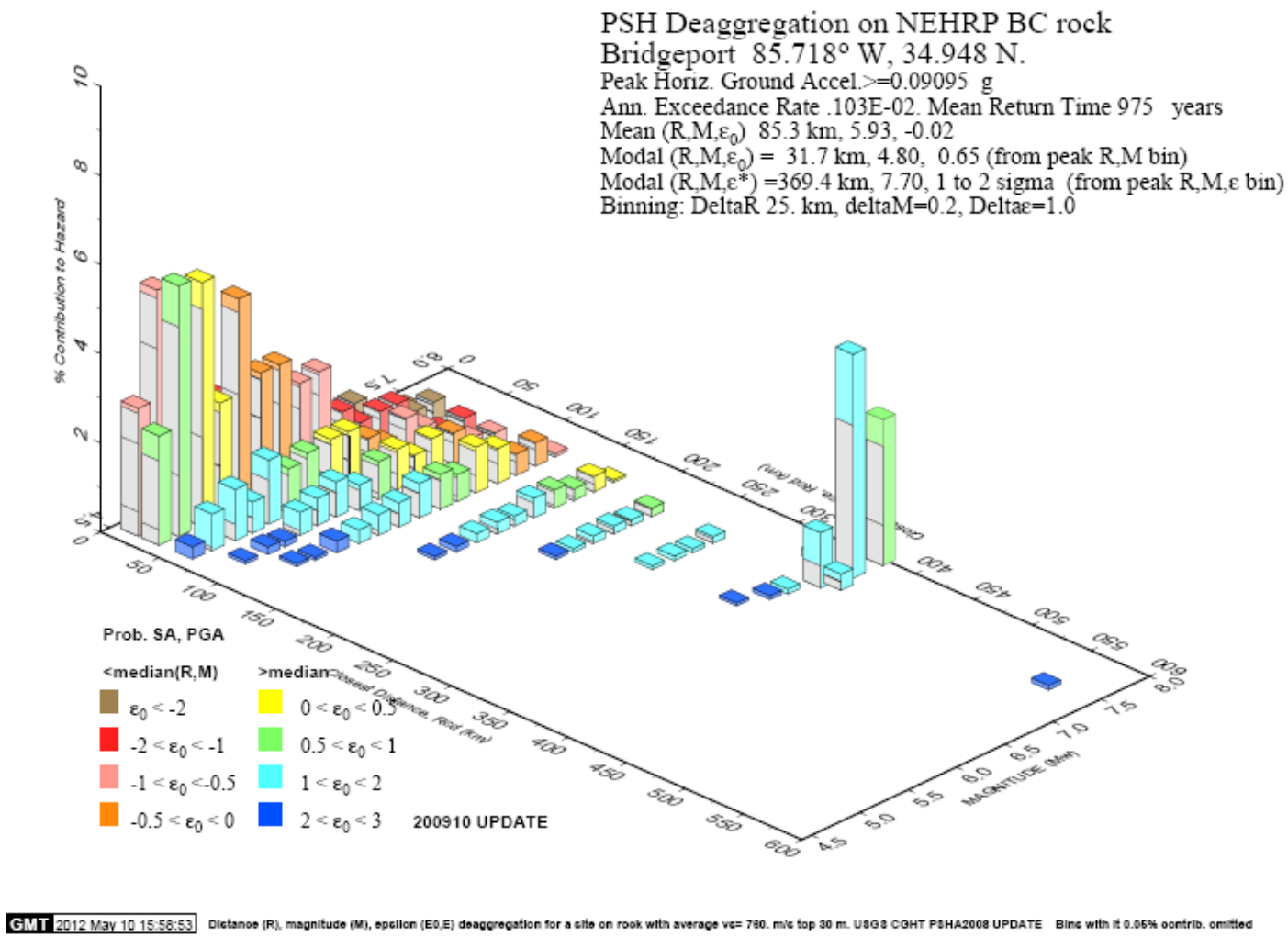

Figure 6.2: Deaggregation Plot for Bridgeport, AL

6.2 Uniform Hazard Spectrum (UHS)

A UHS was calculated for the two most critical locations in Alabama in the form of a DRS. These DRSs were calculated using maps and equations present in Section 3.4 of AASHTO's Guide Specification. The two locations selected for the creation of a UHS were Bridgeport, Alabama and Florence Alabama. Both locations were assumed to have soil corresponding to a site class C. Table 6.1 provides the site data obtained from AASHTO's ground motion maps. Natural bridge periods were assumed to be in the range of zero to three seconds, and the UHS was plotted accordingly. The target spectra for the bridges are displayed in Figure 6.3, which shows that the hazard spectra for the two sites and the resulting average response from the ground motions selected in the next section of this chapter. It can be observed that the DRS for each site remain similar to the other, despite the geographic distance between the two sites. The DRS for Florence shows a greater hazard for bridges of higher periods, while the Bridgeport site shows slightly larger hazard for stiffer bridges. This behavior can be explained by the expected event distance between event epicenter and site location, with close proximity events typically producing motions with higher frequencies. These higher frequencies motions tend to produce higher responses in stiff structures; however these high frequency motions dissipate energy as they travel. Longer frequency motions tend to travel longer distances and produce higher responses in flexible structures. Due to the different hazards present for the state, both DRS's were used in the ground motion scaling process.

Table 6.1: Hazard Map Data

Hazard Location	Values from map (g)			Site coefficients			Final Acceleration Values		
	PGA	S_s	S_1	F_{PGA}	F_a	F_v	A_s	S_{DS}	S_{D1}
Bridgeport, AL	0.111	0.221	0.068	1.2	1.2	1.7	0.1332	0.2652	0.1156
Florence, AL	0.089	0.213	0.078	1.2	1.2	1.7	0.1068	0.2556	0.1326

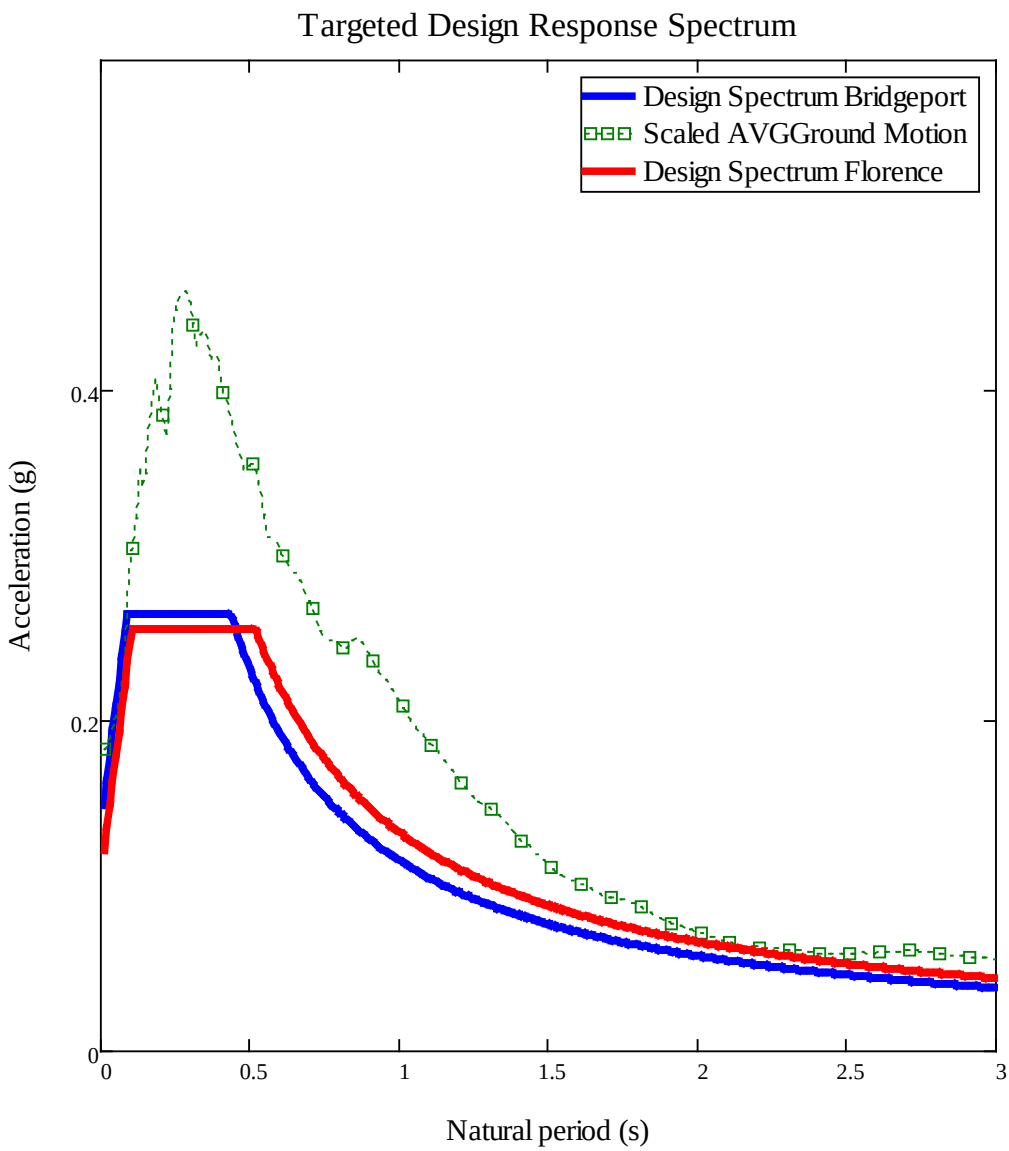

Figure 6.3: Targeted Design Spectrum

6.2.1 Ground Motion

Initially a set of 40 ground motions were selected for possible use in this project and needed to be reduced to a set size of 7-12. The initial constraints that led to the selection of these initial 40 included the following:

1. A PGA between .007 and .02g
2. A site V_{s30} that did not correlate to a site class of A, E or F.
3. An even magnitude between 5.5 and 7.5
4. Exclusion of any subduction zone events

After an initial 40 were selected, properties of the GMs were analyzed in order to create a diverse suite of motions. The first parameter used to eliminate motions was simply to limit the number of motions used from each event. Oversaturation of a ground motion data set with many GMs taken from a single event can bias expected behaviors, as well as harm the performance criteria of certain bridges that may have a unique response to the over selected event. It was decided to limit the ground motions a single event could contribute to two. This condition provided a decent reduction in the set of ground motions.

The next parameter included in GM elimination was the analysis of response spectrum produced by each GM. The behavior of each motion's RS was examined, especially between a natural period of 0.5 and 3 seconds. Values for these criteria were not specifically defined, and ground motions were eliminated based on engineering judgment. The main factor involved in this selection process was the compiling of a diverse response spectra. Similar responses resulted in ground motions being eliminated, as well as responses deemed too weak or two severe to be feasibly incorporated into this analysis. Any GM that needed to be scaled by a factor less than 0.5 or greater than 2 was also eliminated. Table 6.2 displays some of the

properties associated with the ten GMs selected for this analysis. The RS of each selected GM can be seen in Figure 6.4, as well as their average and the DRSs for the two hazard sites in Alabama.

Table 6.2: Ground Motion Data

NGA Event #	Event	Year	Station	Magnitude	Mechanism	Rupture distance (km)	V_{s30} (m/s)
68	San Fernando 1	1971	LA - Hollywood Stor FF	6.61	Reverse	22.8	316.5
70	San Fernando 2	1971	Lake Hughes #1	6.61	Reverse	27.4	425.3
186	Imperial Valley	1979	Niland Fire Station	6.53	Strike-Slip	36.9	207.5
333	Coalinga-01	1983	Parkfield - Cholame 8W	6.36	Reverse	51.8	256.8
512	N. Palm Springs	1986	Anza - Tule Canyon	6.06	Reverse-Oblique	52.1	684.9
832	Landers	1992	Amboy	7.28	Strike-Slip	69.2	271.4
1741	Little Skull Mnt.	1992	Station #2 NTS Control Point	5.65	Normal	24.7	659.6
1147	Kocaeli-Turkey 1	1999	Ambarli	7.51	Strike-Slip	69.6	175
1165	Kocaeli-Turkey 2	1999	Izmit	7.51	Strike-Slip	7.2	811
1107	Kobe	1999	Kakogawa	6.9	Strike-Slip	22.5	312

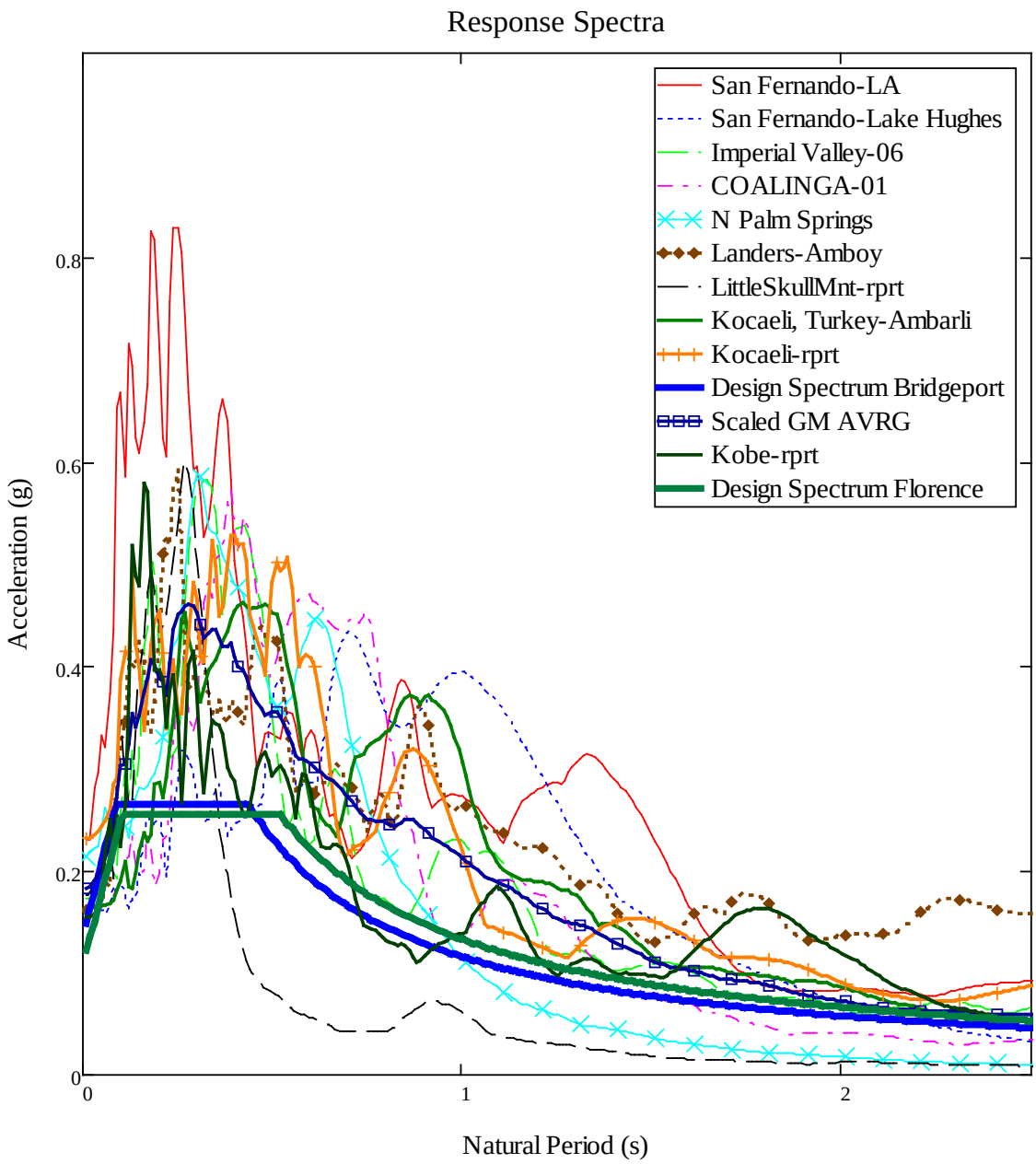

Figure 6.4: Design Level Response Spectra

An additional two ground motions were also initially included in the selected GMs, but have subsequently been eliminated. These ground motions were synthetic ground motions created as a prediction of future ground motions associated with a large scale New Madrid fault event. These GMs used soil conditions and behavior associated with Memphis, and the GMs

indicated behavior associated with large columns of sand, a geotechnical feature that is not associated with the regions being analyzed in this project.

6.3 Determination of Capacities

Overall dynamic bridge performance is measured by displacements and internals member forces as they relate to specified capacities. Some of these capacities are specified in design documents and codes, and others vary from project to project. This section will provide details regarding capacities selected for use in this project.

Foundation information provided for this project was analyzed using the geotechnical analysis software FB-Multipier. This information included a displacement limit on all foundation degrees of freedom. These limits could not be implemented in the modeling of the bridges, but they are used in the bridge evaluation procedure after analysis. The horizontal displacement and rotation capacities for each foundation are displayed in Table 6.3. Any recorded foundation rotation or displacement exceeding these limits will be classified as a foundation failure.

Table 6.3: Foundation Capacities

	Foundation Displacement and Rotation Limits			
	Transverse Direction		Longitudinal Direction	
	Displacement (in.)	Rotation (rad.)	Displacement (in.)	Rotation (rad.)
Little Bear Creek	0.54	0.005	0.52	0.0054
Norfolk RR	2	0.022	3	0.0072
Scarham (Bent 1 & 3)	0.58	0.002	0.55	0.002
Scarham (Bent 2)	0.71	0.003	0.7	0.003
Oseligee	0.22	0.0032	0.23	0.0033
Bent Creek	1.4	0.035	1.4	0.036

Bearing pad capacity is determined in terms of displacement. Although there exists a limit of shear force that each bearing pad is capable of resisting, this limit does not intrinsically

represent a failure criteria of the bearing pads, it simply represents the force in which slipping occurs within the system. The actual capacity that is of concern in this element is the displacement that occurs between the girder and the bearing pad. It was determined that the limit for differential movement between these two elements be set to half the dimension of the bearing pad in that direction. Any deflection beyond this limit would result in unseating of the girder.

Bolt strength capacity was conservatively estimated using Equation 6.1. Due to analysis concerns the limit specified for a bolt failure was selected as 95% of the calculated value. This 95% attempts to account for any values not recorded by the analysis software that may trigger failure of the bolt link, and is not meant to account for any loss of strength or safety factor correlated to a failure mode. Failure of the clip angle-anchor rod system does not result in overall structural failure, but its performance was monitored due to its importance in connection behavior. Table 6.4 contains all calculated bolt strengths for the bridge designs selected.

$$Vn = 0.6 * Fu * A \qquad \text{Equation 6.1}$$

Table 6.4: Calculated Bolt Strengths

	Bolt Shear Capacities
	Individual Bolts (kips)
Little Bear Creek	61
Norfolk RR	48
Scarham	61
Osel1gee	78
Bent Creek	87

A commonly recorded criterion of seismic behavior in structures and structural elements is ductility. Ductility in structures can refer to a variety of terms; however, in this analysis, it refers to the degree in which a structure can deform relative to its initial yield. The ductility of bridge bents was selected as an indicator of overall bridge performance. In order to determine

the overall ductility of a bridge bent, a state of initial yielding needed to be determined within each bridge bent. A backbone curve was created for each fiber hinge used in the bent columns, and a point of nominal strength was isolated. The rotation that correlated to this point was recorded and used in Equation 6.2 to determine the angle of rotation of the plastic hinges. This calculated angle of rotation was applied at midpoint of each hinge location in each bridge bent, and the overall displacement differential between the center of the bent cap and the foundation was calculated. This displacement was used as a measure of a ductility of 1. A maximum ductility capacity was also determined for each bridge based on pushover analysis performed in a previous section of this project (Law and Marshall 2013). The initial ductility displacements and the maximum ductility capacities can be seen in Table 6.5. AASHTO specifies a range of acceptable ductility demands for bents in section 4.9, with a ductility limit of six or less for bents consisting of multiple columns. The lesser of AASHTO and Law's ductility limit was selected as a maximum capacity for ductility in the bridge bents.

$$\theta_n = \frac{M_n}{E * I_e} * \left[L_p - \frac{1}{L} * \frac{{L_p}^2}{2} \right] \qquad \text{Equation 6.2}$$

Table 6.5: Bent Displacement Limits

	Bent Displacements					
	Transverse Direction			Longitudinal Direction		
	Ductility of 1 (in.)	Pushover Limit (in.)	Ductility Limit	Ductility of 1 (in.)	Pushover Limit (in.)	Ductility Limit
Little Bear Creek (Bent 1)	0.56	1.35	2.42	0.56	0.075	0.13
Little Bear Creek (Bent 2)	0.91	0.97	1.07	0.91	2.75	3.03
Norfolk RR	1.71	4.00	2.32	1.71	6.63	3.89
Scarham (Bent 1 & 3)	1.00	9.80	6.00	2.05	2.20	1.08
Scarham (Bent 2)	3.30	25.6	6.00	5.59	3.57	0.64
Oseligee	0.41	1.80	4.50	0.41	3.77	6.00
Bent Creek	1.79	2.45	1.37	1.79	4.57	2.56

Lastly a serviceability limit was established for the residual displacements of the models. Determining the state of functionality of a bridge after being subjected to a ground motion is a key factor in performance classification. Critical and essential bridges should be open to emergency vehicles and be open for security and defense purposes immediately after the design earthquake, with critical bridges also being open to all traffic (AASHTO 2009). The value for residual span displacements that was selected as an upper limit was one inch in either direction. This value was determined from engineering judgment. A residual displacement exceeding one inch could indicate substructure damage or a localized failure at a connection zone.

6.4 Selection of Modeling Elements

Computer models of existing structures, especially ones used for complicated analysis, require a balance of accuracy in geometry, behavior, and functionality. A model that includes every detail of a structure may be considered accurate, but not practical for the purpose of analysis. A structure simplified so much as to neglect important aspects of behavior may also be deemed impractical for analysis. It is with these ideas in mind that the models for this project were designed.

6.4.1 Superstructure Modeling

The bridge models are initially constructed using information taken from plans provided by ALDOT. This information helps to build the initial geometry of the entire bridge using the Bridge Designer toolbar found in CSI Bridge. This process includes the specification of bridge spans, bents, abutments, deck geometry, girder geometry; bent cap dimensions, bent column dimensions and span support conditions. Each parameter was imported into the bridge builder as the provided designs had indicated. Once this is done a modeling option is presented that will

determine the complexity of the model's superstructure. The first options present are a three dimensional meshed superstructure composed of smaller elements, representing each component of the deck, web walls and girders. A second option is that of a spine model, a model that calculates the stiffness of the overall superstructure, and simplifies it into a single beam element. The spine model also neglects inelastic behaviors that may be associated with large or deep elements. Typically elements of simply supported spans behave elastically in dynamic motions, elements like bridge decks and girders. Attempts at using the complex mesh model resulted in slow analysis with an eventual failure of analysis performance. This led to acceptance of the simplified spine model. The overall performance of the spine model may not contain the accuracy present in the meshed three dimensional model, but the meshed model also accounts for and records information that would not be used at the conclusion of the analysis. Superstructure behavior was also not a cause for concern in this analysis compared to the behavior of the substructure and connections. Thus it was acceptable to use a spine approximation for modeling of the bridges in this project.

Bridges that are designed as simply supported typically contain expansion joints at support locations. These joints consist of a small gap between spans that allows for the expansion and contractions due to thermal and long term displacements. For modeling considerations these elements needed to have their behavior represented due to their importance in longitudinal motions. This was accomplished by placing gap elements between span elements. These gap elements are specified as linear elements that only activate after they have compressed a certain distance. Once the springs are activated they function like a compression spring with a stiffness of 5000 kips/in. This stiffness is meant to transfer a large force for a small

amount of compressive displacement over the entire span element. A similar procedure was also performed for the expansion joint located at the abutments.

6.4.2 Substructure Model

A primary focus of this project is the observation and analysis of substructure behavior under the effects of a design level GMs. With this in mind special precautions were taken to ensure accurate modeling and behavioral considerations pertaining to the substructure of each bridge, beginning with the foundation. The analytical models incorporate geotechnical properties of each bridge in the form of multi-linear foundations. These foundation springs have been calculated using a static pushover analysis detailed in work done by Kane (2013). Stiffness associated with each of the six degrees of freedom are applied at each foundation location. These multi-linear springs do not contain a specific failure limit, due to the behavior of the spring elements in CSIBridge. The foundation displacements must be noted for final analysis in order to determine whether the displacements and rotations exceeded those generated in the soil-structure interaction model.

Columns represent the next aspect of the bridge models that needed to be carefully modeled. Column behavior in bridges is highly dependent on accurate detailing of the column and its connections to other elements. For this analysis it is assumed that detailing in the columns is consistent with that specified in AASHTO. Accurate detailing within columns will result in ductile plastic hinging at points determined in AASHTO. These hinges and their behavior are accounted for in the bridge models using the “define hinge function”. Hinges are placed within the columns at select points and with defined lengths. Hinges can be specified to account for multiple directions of behavior, as well as different controlling behavior limits. Shear hinges behave in the directions of shear and act as a sudden, non-ductile failure. Shear

hinges were considered later on in this project, but for a different element. The behavior needed for plastic hinges in columns results from a ductile interacting flexural-axial hinge. This hinge type accounts for rotational and axial behavior within the element. This hinge type was selected for the purpose of this analysis; however this particular hinge type is subdivided further by which directional movement it should include as well as which method is used for behavior determination. A biaxial direction was selected due to its more accurate application in a model that is subjected to dynamic GMs in two different global directions. The selection of behavioral analysis method for the column is a more complex issue that required supplementary study and testing.

The first option that was applicable for hinge analysis was the use of a Caltrans specified hinge. This particular hinge type uses a simplification to determine various capacities of a plastic hinge in an effort to alleviate design computations as well as provide a conservative estimation of hinge behavior. The backbone curve for a Caltrans Hinge can be seen in Figure 6.5 and can be observed to display a linear elastic behavior at low rotations, followed by a sequence of inelastic behaviors meant to represent yielding and eventual failure of a hinge. It is recommended that significant hysteresis should be avoided when using Caltrans Hinges in dynamic analysis (Computers & Structures inc. 2012). An analysis was performed on a simple reinforced concrete moment frame using Caltrans Hinges. The frame was loaded with a lateral force and results were measured to determine the applicability of the Caltrans Hinge compared to the second hinge analysis option, the Fiber Hinge.

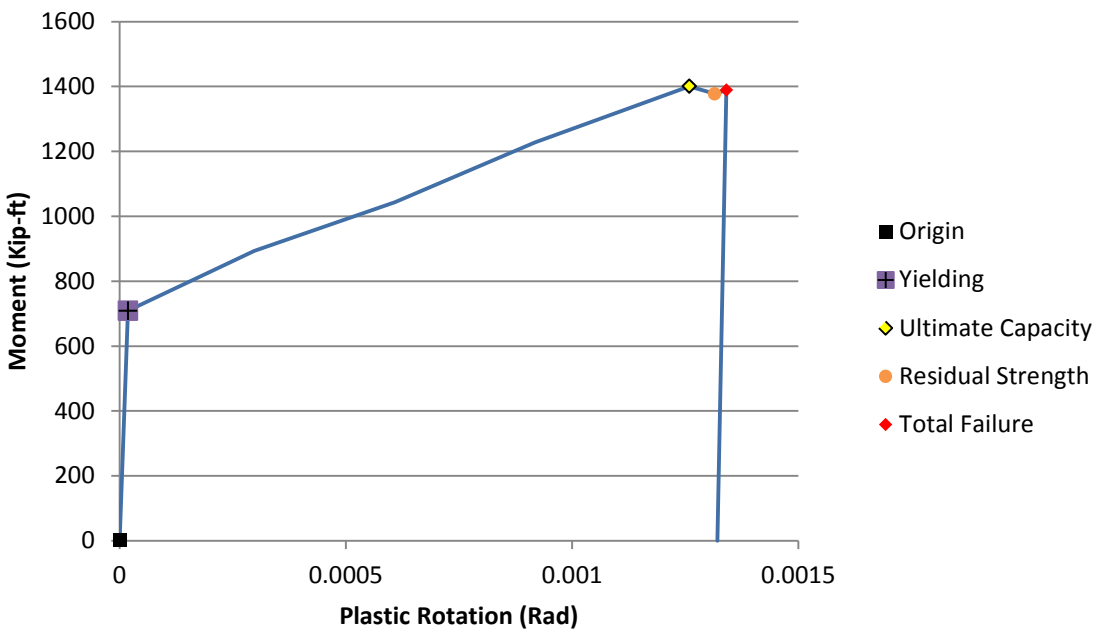

Figure 6.5: Idealized Caltrans Hinge

A Fiber Hinge analysis is a type of finite element analysis used in the determination of hinge behaviors and capacities. It operates under the theory that a real structural element can be modeled as a collection of smaller individual elements, and that the smaller the individual elements get, the more accurate the behavior of the collection of elements becomes. The fiber hinge model is the more complex option among the two hinge analyses. Sections of the cross section of a member are divided into sections of concrete and steel. Each section is analyzed based on the material properties and location of each fiber in order to determine cross-section behavior and capacities at given loading conditions. Figure 6.6 displays a backbone curve resulting from a fiber hinge analysis. "The fiber-hinge model is more accurate in that the nonlinear material relationship of each fiber automatically accounts for interaction, changes in moment-rotation curve, and plastic axial strain. A trade-off is that fiber application is more computationally intensive" (Computers & Structures inc. 2012).

An analysis was performed on a simple reinforced concrete moment frame using plastic hinges. The frame was loaded with a lateral force and results were compared to that of the Caltrans Hinge. The resulting capacities were similar, indicating that both hinges estimated similar strengths; however the displacements indicated that the fiber hinge was a much more flexible hinge. It was determined that both hinge types were viable and later testing would show that fiber hinges resulted in more favorable numerical analysis behavior.

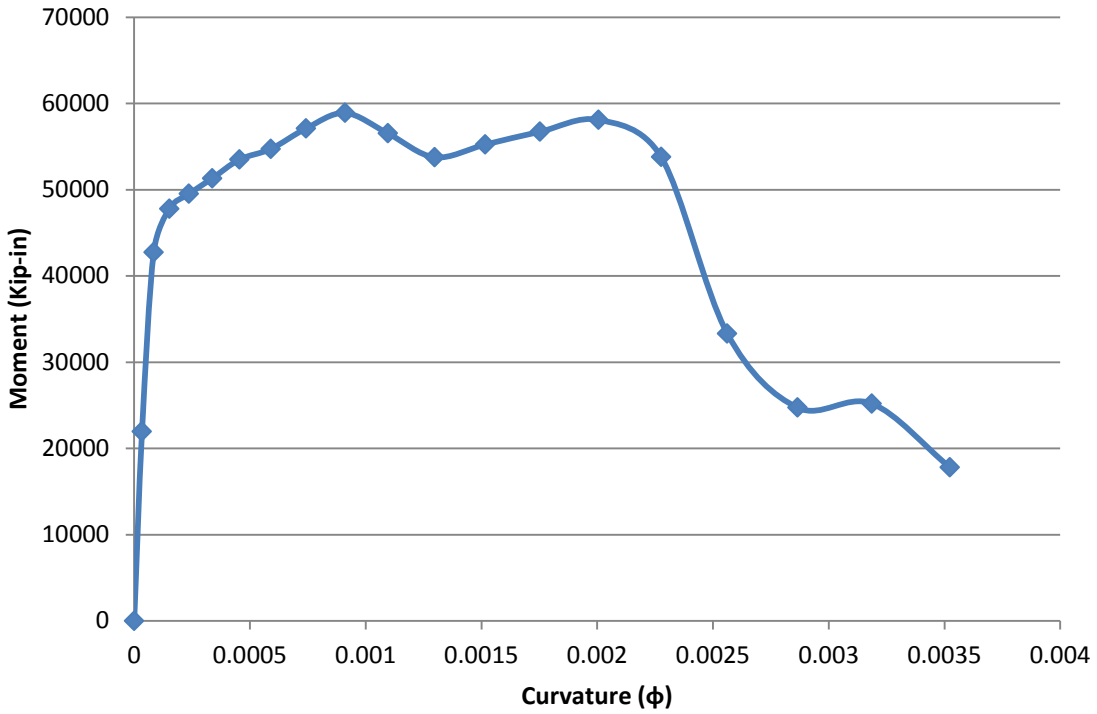

Figure 6.6: Fiber Analysis Backbone Curve

In order to use a plastic hinge in modeling, characteristics of the hinging element need to be specified in detail. A typical frame element in CSI Bridge and SAP 2000 can be specified with just cross-section geometry, concrete strength, reinforcement layout and steel properties. An accurate hinge will require a more in depth property specification. The Section Designer tool was used to create columns in the modeling for this project. Column designs included

specification of longitudinal and shear reinforcement as well as spacing and clear cover distances. Concrete was subdivided into confined and unconfined sections to be analyzed using the Mander-Confined and Mander-Unconfined concrete properties. An axial load was also specified on the columns in the creation of a backbone curve for each section. These properties help to establish nonlinear behavior where nonlinear behavior is expected.

Bent caps and Abutments, the last remaining substructure elements, were modeled as elastic frame elements. They are assumed to have adequate detailing and design strength to avoid any nonlinear hinging that may cause instabilities in the bridge structure. The size of these elements depth and stiffness should allow them to resist moments transferred from the bent columns, allowing the use of this assumption. Abutments were also assumed to be supported with fixed foundation connections for the purpose of this project. This property was determined when the geotechnical behavior of these elements was not considered a major concern for this project.

6.4.3 Connection Modeling

In addition to substructure behavior, connection behavior between the super and substructure was also a primary focus in this analysis. Special attention was paid to the behavior occurring in this region, and the impact each of these behaviors contributed to that of the overall bridge. The bridges in this project all contain a girder-to-elastomeric bearing pad connection at the end of each span. This connection detail can be seen in Figure 6.7. Each of these bearing pads is made from layers of elastomeric material interspersed with thin steel plates (steel shims). These shims act to reduce bulging of the elastomeric material when subjected to vertical loads by limiting the thickness of each individual layer of elastomeric material. It is with this in mind that

all bearing pads are initially designed, meaning that the overall thickness of a single bearing pad is determined from the amount of vertical load that it is designed to resist.

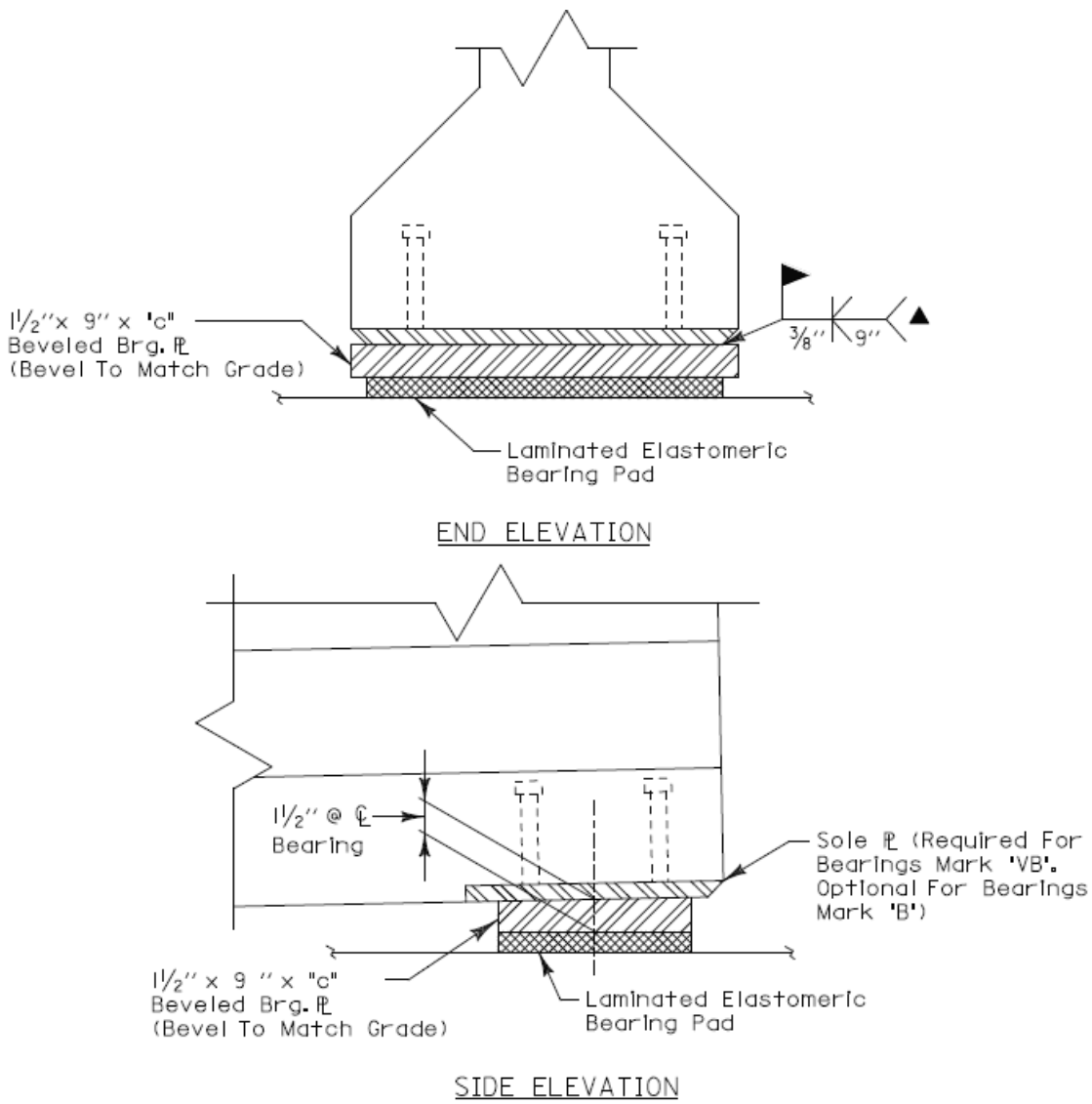

Figure 6.7: Example Bearing Pad Configuration (Alabama DOT 2012)

Elastomeric bearing pad thickness results in more flexible behavior during lateral shearing, regardless of the number of steel shims. An elastomeric bridge bearing's deformation in a lateral direction can be determined according to Equation 6.3. The dimensions of each bearing pad are extrapolated from bridge design drawings, and a Shear Modus (G) of 135 psi

was selected from values found in a Caltrans design memo (Caltrans 1994). The deflection equation will eventually change at larger forces, but can be used for the purpose of modeling because the shears experienced in these bearing pads are limited to a ceiling value determined by eventual slipping between the bearing pad and the girder. A Force-Displacement relationship for a bearing in shear can be seen in Figure 6.8, with a plateau being reached at the point of slipping.

$$\Delta s = \frac{(V*T)}{(G*A)} \qquad \text{Equation 6.3}$$

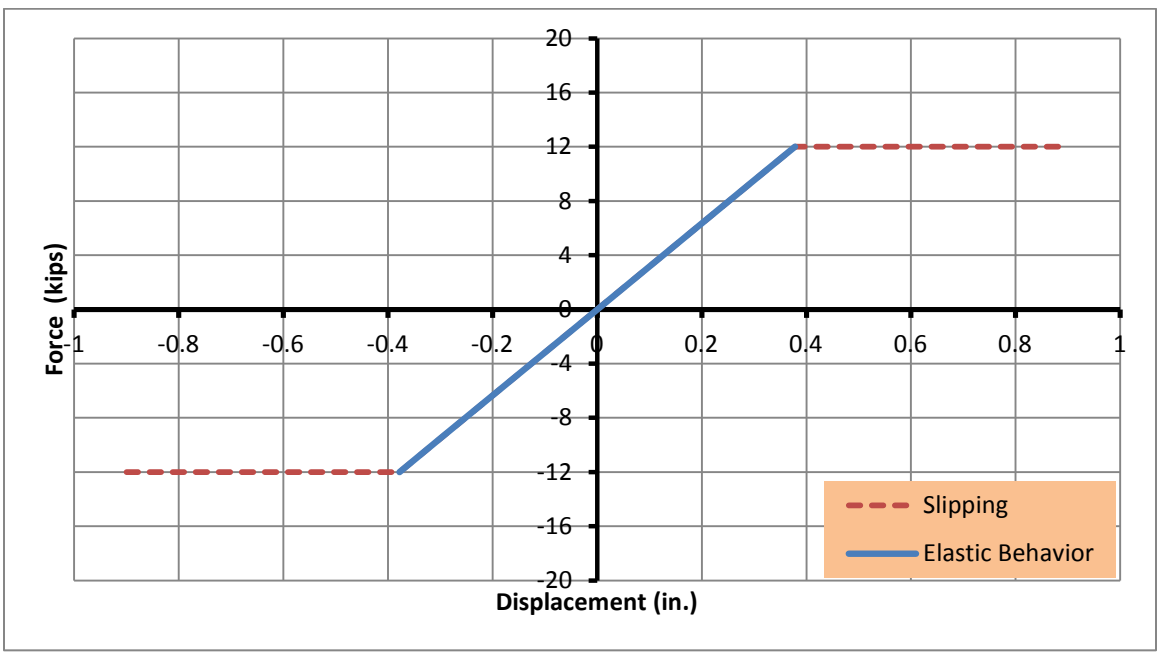

Figure 6.8: Example Bearing Pad Force-Displacement Relationship

Research performed on a connection detail in use by the Illinois DOT, similar the one used by ALDOT, observed a friction coefficient between 0.2 and 0.5 in its bearing pad-steel plate friction connection; however cyclical loading resulted in reduced values due to degradation of the rigidness of the bearing pad surface (Steelman, et al. 2012). A dynamic friction

coefficient of both 0.2 and 0.4 was selected for a lower and upper bound in this analysis, and the process of implementation can be found later in this chapter. All of these factors contributed to the creating of force-displacement plots for each bearing bad in use for this project, and these plots were implemented into the model using multi-elastic plastic kinetic link elements. The "kinetic" distinction of these link elements refers to the behavior these links exhibit during unloading. A plastic link element recognizes unloading of a link and follows a different stiffness than the one used in the loading process. The manner of which an unloading stiffness is determined varies depending on the type of plastic link, with "kinetic" most closely describing the behavior of a friction connection.

Each bridge model is meant to be loaded in a longitudinal direction (direction of travel) and a transverse direction (perpendicular to direction of travel). The connection that resists motion in the longitudinal direction consists solely of a bearing pad, but there is an additional connection detail in the lateral direction that is also considered in the model. Figure 6.9 displays a view of ALDOT's bridge connection, consisting of both a bearing pad system and a clip angle system meant to limit movement in the lateral direction. This clip angle system consists of steel clip angles fastened to the girder via small threaded inserts and fastened to either abutments or bent caps via anchor bolts. For the purpose of this analysis it is assumed that the small threaded inserts that transfer longitudinal or tensile forces from girder to clip angle are not sufficiently embedded within the girder to provide any real resistance. This configuration results in a single-level longitudinal connection system; however the anchor bolt provides the clip angles with sufficient stiffness to resist transverse forces when the movement is towards the angle. The overall failure of this clip angle system is determined to occur when the anchor bolts have experienced nominal shear strength capacity. This limit state was deemed conservative, and also

selected above a failure state of the clip angles themselves due to the girders eventual collision with the anchor bolt in the event of a clip angle failure. Equation 6.1 was used to determine the shear capacity of an anchor bolt, assuming adequate embedment was provided for the bolt.

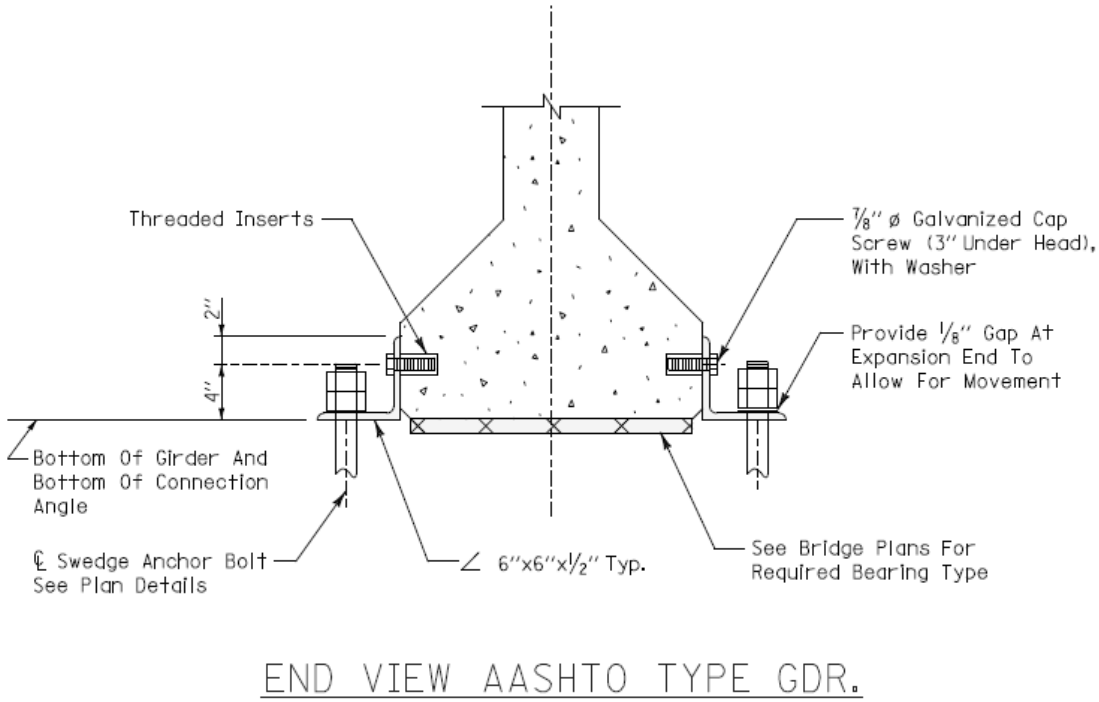

Figure 6.9: Clip Angle Connection Detail

Modeling the anchor bolt's contribution to the total bridge models connection proved to be a difficult challenge. Several options were attempted that appeared accurate in both behavior and geometry. The first option was the creation a frame element that acted as a fuse element, failing in shear. The frame element would act in parallel with the bearing pad link, and contain a shear hinge. This initial option was modified to incorporate two frame elements acting in parallel with one another, and connected to the bearing pad link via gap links. These gap links allow only one frame element to be loaded in shear for each direction of transverse movement. Theoretically this system would mimic the real life behavior of the bridge during transverse

movement in an accurate way. The implementation of this modeling option proved to behave differently than anticipated. Shear hinging resulted in the element being split into two different elements causing instabilities in the analysis, as well as the frame elements collecting additional forces and moments despite releases being implemented into the system as a measure of preventing that behavior from occurring.

The second option implemented for modeling the transverse restrainer connection was the use of multi-linear elastic links in place of frame elements. These elements require force displacement data in order to implement. Initial shear stiffness equations of anchor bolts resulted in an incredibly stiff system. Implementing the calculated shear stiffness values into elastic links created a system with large stiffness changes, resulting in numerical instability within models. These stiffness equations were then modified to account for displacements within the clip angle configuration, resulting in the selection of an overall displacement of 0.55 inches between loading and failure of all clip angle systems. This displacement was also meant to create a constant between all bridge models. The resulting model functioned, but still resulted in some numerical instability during some of the ground motions. It was also observed that this model did not accurately replicate shear failure behavior in the model, and a new link element was selected, the multi-linear plastic link element. This new link element has the capability to apply failure and strength degradation that is expected with the behavior of this connection; as well as continue to function after loss of strength, instead of causing a numerical instability. A "kinematic" plastic hinge was initially selected, but its behavior did not match up with the expected behavior of the system. A "Pivot" plastic link model was selected instead, based on its behavior matching that of the expected behavior of the system. The Pivot link requires additional inputs in order to shape the unloading and reloading properties of the link; all Pivot

factors for this link were set to zero in order to achieve desired behavior. The implementation of this link resulted in reduced numerical failures in many of the bridge analyses, and was selected as the best option for modeling the clip-angle connection.

The implementation of connection elements into the bridge models required an additional step. A simplification was made to combine connection elements together to form a single connection element in place of multiple connection models. This simplification was made in order to reduce overall complexity of the models. It was assumed that the bridge deck remains nearly rigid in its plane during ground motions, allowing the use of this simplification. Bridges that contain bents with more than two columns use an altered version of this simplification, multiple simplified connections at each column location.

The final step in the modeling process for each bridge is the creation of behavioral limits. The focus of the analysis in this project is centered on bridge behavior, but certain information cannot be accurately known. This fact resulted in the creation of two different versions of each bridge model, a lower limit model and an upper limit model. The principal difference between each of these models is the friction coefficient between bearing pad and girder surface. The lower bound model assumes slipping to occur at a friction coefficient of 0.2. The upper bound model assumed a coefficient of 0.4. The actual behavior of the bridge should fall somewhere between these two models. Another important range of uncertainty occurs in the prediction of system damping present within each bridge model. A method for determining and specifying a damping factor was established and implemented based on Rayleigh damping. The theory behind this damping method can be found in (Chopra 2007). A model analysis was performed for each bridge model, with certain elements altered to remain stiff or flexible, and natural periods were recorded at the first and third mode shape for movement in lateral and longitudinal

directions. These natural periods were correlated to a damping factor of 2% and entered into a CSI table that calculated Raleigh damping factors. These factors are applied to the model during the analysis procedure.

6.5 FB Multipier

As stated in Chapter 2, FB-MultiPier employs lateral (p-y), axial (t-z, Q-z), and torsional (T-θ) nonlinear spring functions (soil springs) to simulate the soil-foundation interaction. Structural elements are steel or concrete and represented by conventional non linear stress versus strain models. Far field or group interaction models are included as well.

6.5.1 Lateral Interaction

For the lateral soil-pile interaction, FB-MultiPier employs one of six p-y models as well as a user defined option. The models are not specific to foundation type (pile or drilled shaft). Typical p-y models are shown in Figure 6.10.

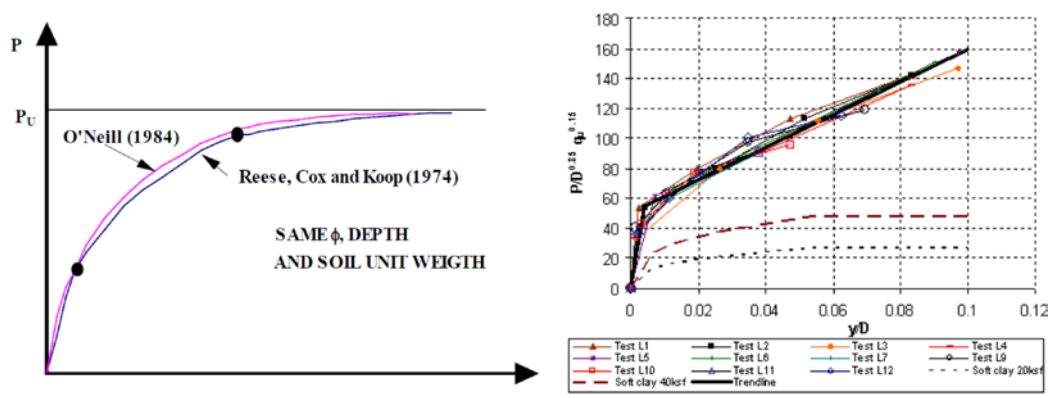

Figure 6.10. Example p-y curves for sand (O'Neil and Murchison 1983) and limestone (McVay and Niraula 2004)

6.5.2 Axial Interaction

Axial soil-pile interaction is simulated with vertical springs representing the load shedding in the vertical (t-z) and tip (Q-z) curves. These models are specific to foundation type. The standard models include driven piles, drilled shafts in soil, and drilled shafts in limestone.

There are tip models for driven piles and drilled shafts.AS before, in either case, a user defined option is available as well. Examples of the axial interaction curves are shown in Figures 6.11 and Figure 6.12.

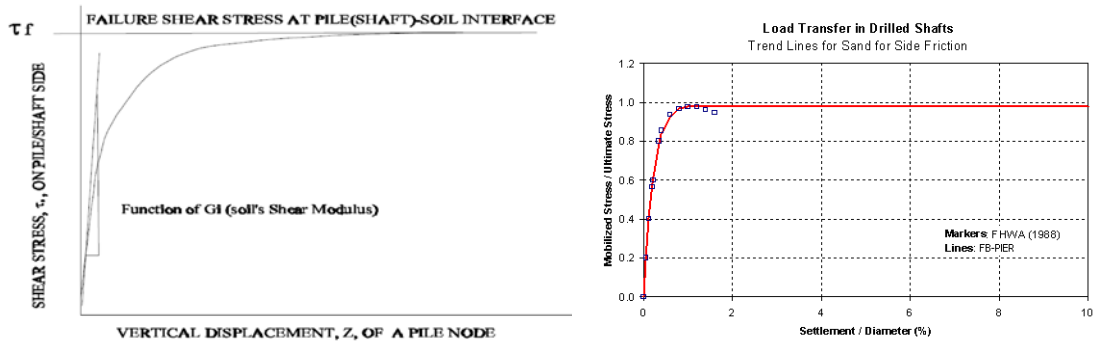

Figure 6.11. Axial t-z curves for driven piles (McVay et al. 1989) and drilled shafts in sand and Reese and O'Neill (1988).

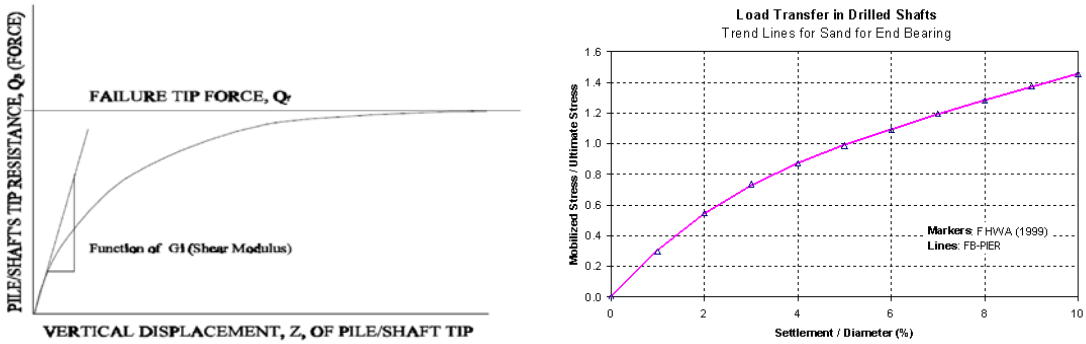

Figure 6.12. Axial Q-z curves for driven piles (BSI 2013(b)) and drilled shaft end bearing in sand O'Neill and Reese (1999)

6.5.3 Torsional Interaction

There is a single torsional model to account for the non-linear torsional (T-θ) behavior of the soil which is a simple a hyperbolic curve based on the axial side friction model. Figure 6.13 shows a hyperbolic representation of the T-θ curve.

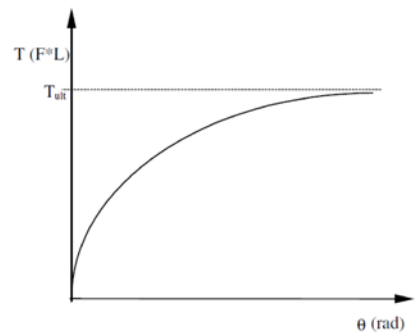

Figure 6.13 Hyperbolic representation of T-q curve (BSI 2013(b))

6.5.4 Structural Element Modeling

FB-MultiPier is capable of modeling complex structural components. The structural components are modeled by inputting the pier geometry (pier height, pier cap cantilever length, column spacing and offset, number of piers, and pier cap slope), cross-section parameters, and taper data (if applicable). The program has a database of typical structural component cross sections or the user can model a custom one. The cross section can be modeled as one of two types: gross properties and full cross section. The gross properties option is a linear structure and requires the input of the section dimensions (not specific to material type) and the elastic modulus. The full cross section option requires reinforcement details and material properties. The sectional properties are calculated by the program.

The program can conduct linear or non-linear analysis for both the pile and pier (column and cap). If linear behavior is selected, it is assumed the behavior is purely linear elastic and deflections do not cause secondary moments (BSI 2013(b)). If non-linear analysis is selected, the program accounts for second order effects (p-delta) as well as stiffness changes within the structure, such as cracking of concrete, and it uses either user defined or default stress-strain curves (BSI 2013(b)). P-delta effects occur when the axial force becomes eccentric within the element due to displacements of one end of the element relative to the other, causing an out-of-balance moment within the member (BSI 2013(b)). The standard non-linear stress strain curve

of concrete is a function of compressive strength and the Young's modulus of elasticity of the concrete and is adapated from Hognestad et al. (1955). The standard stress-strain curve for mild steel, such as an H-pile, is elastic-perfectly plastic and a function of Young's modulus of elasticity and the yield strength. These standard stress-strain curves are shown in Figure 6.14 and Figure 6.15.

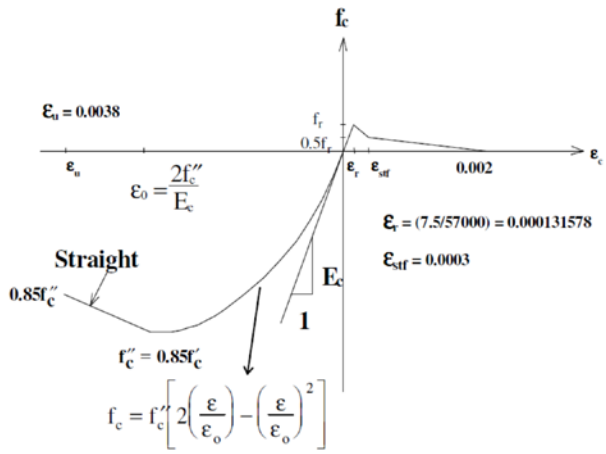

Figure 6.14 Hognestad model for concrete (Hognestad et al. 1955)

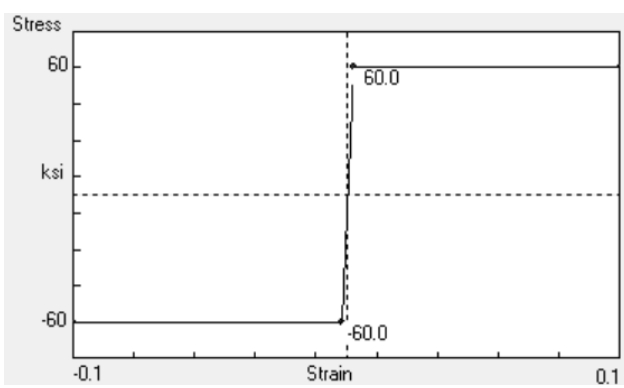

Figure 6.15 Default stress-strain curve for 60 ksi steel (BSI 2013(b))

6.5.5 Pile Cap Modeling

The pile cap is modeled based on the concrete's Young's modulus of elasticity, Poisson's ratio, thickness, and unit weight of the pile cap material (usually concrete). To avoid stress concentrations at the base column node where it connects to the pile, FB-MultiPier spreads the

load to the four adjacent nodes on the pile cap using rigid connectors built in to the program (BSI 2013(b)). The user has the option to choose whether to treat the pile-to-cap connection as pinned or rigid.

6.5.6 Group Effects

Lateral and axial resistance of soil for a group of piles is typically not equal to the sum of the individual resistances relative to each pile (BSI 2013(b)). Generally, the soil resistance to a pile within a group is less than the same individual pile (not in a group). This difference in resistance of soil to a pile within a group is a function of the pile center-to-center (c-c) spacing and location within the group (Brown et al. 1988). Lateral group effects are typically handled by use of p-y multipliers. P-y multipliers are used to degrade the p-y curve to account for the "shadowing" effect (i.e., loss of soil resistance of piles in the trailing rows) (Brown et al. 1988). When a pile group is loaded, the front row (or lead row) carries a larger proportion of the load, whereas the trailing rows carry less of a proportion.

FB-MultiPier also considers group efficiency for axial loads. Group efficiency for axial loads is the ratio of the amount of axial load the group can resist relative to the sum of the single pile resistances that make up the group. Typically, driven pile group efficiencies are greater than 1.0 because the soil consolidates during driving, which increases the soil axial resistance. The user has the option to input an efficiency factor. See Hannigan et al. (2006) for recommendations for axial group efficiency factors.

6.6 Overview of Bridge Models

The following section will include the details used to create each bridge model and the soil associated with each bridge's foundations, and an overview of the modifications and features

of each bridge. Simplifications will be explained and justified. Expected behavior is also included in the description of each bridge as well as the bridge's natural periods taken from modal analysis.

6.6.1 Little Bear Creek Bridge

6.6.1.1 Bridge Modeling

This three span bridge carries the two lanes of State Road 24 over Little Bear Creek in Franklin County. The outer span lengths are 85 feet and the interior span is 130 feet. The outer spans support the 7 inch concrete deck with 6 Type III Girders and the interior span supports the deck with 6 BT-72 Girders. Each of the 6 Type III girders rests upon 20.5" x 9" bearing pads. These bearing pads were calculated to slip after an average (0.3 friction coefficient) displacement of 0.57" correlating to a shear of 18.15 kips per bearing pad. The clip-angle/anchor bolt configuration for the transverse connection contained anchor bolts with a diameter of 1.25". These bolts were modeled with a shear capacity of 45 kips. Each of the 6 BT-72 girders rests upon 24.5" x 9" bearing pads. These bearing pads were calculated to slip after an average (0.3 friction coefficient) displacement of 1.19" correlating to a shear of 33 kips per bearing pad. The clip-angle/anchor bolt configuration for the transverse connection contained anchor bolts with a diameter of 1.5". These bolts were modeled with a shear capacity of 61 kips. A simplification was also modeled for this bridge using a redesigned clip-angle/anchor bolt configuration for the transverse connection at each span which contained anchor bolts with a diameter of 1.7". These bolts were modeled with a shear capacity of 78 kips. This bridge model contains a single girder connection to represent 6 girder connections. The selection of a single connection representing

6 total connections miscalculates the gravity moments imparted into the bent columns in a conservative fashion. A non-rectangular member was selected to model the bent caps, and a gap link was established to model possible impact stiffness between the deeper girder and this abutment. Plastic hinges were modeled at the top and bottom column locations.

The overall model of this bridge was found to be moderately stiff in the context of the other bridges modeled due to shorter columns and stiff foundations. Differences in mass between spans could result in secondary mode shapes dictating dynamic behavior in the transverse direction. Modal analysis of the model revealed a first mode natural period of 0.47 seconds in the transverse direction and 0.818 seconds in the longitudinal direction. The third mode natural periods of the fixed version of this bridge resulted in a natural period of 0.14 seconds in the transverse direction and 0.164 seconds in the longitudinal direction. Foundation behavior for this could result in hinging forming in the foundations, but that cannot be predicted in this particular model which specifies hinges in the column only.

6.6.1.2 Substructure Modeling

The foundations used for both the abutments and piers are drilled shafts. Bent 3 was modeled in FB-MultiPier. Bent 2 and 3 are built the same but with slightly different tip elevations and soil conditions. Bent 3, shown in Figure 6.16, consists of a pier cap and two shafts. The shafts are 4.5 ft in diameter with twelve No. 11 longitudinal reinforcing bars above the ground surface, and 5 ft in diameter with the same reinforcement alignment below the ground surface.

A formal site investigation, using the SPT and rock coring, was conducted by the Bureau of Materials and Tests within ALDOT. According to the geotechnical report, the site is located in the Moulton Valley district of the Highland Rim physiographic section and underlain by

Bangor Limestone of Mississippian age (ALDOT 2005). The GWT elevation at Bent 3 was recorded as 528 ft at a 24 hour reading after the initial site investigation (ALDOT 2005). There is roughly 3 ft of top soil that was assumed to scour to bedrock at an elevation of 525.6 ft. Static analysis of the lateral capacity of the drilled shafts was done using LPile and the input parameters were included in the geotechnical report. The same input parameters were used in FB-MultiPier. However, some parameters that were needed for FB-MultiPier were not provided and had to be determined based on the boring logs. Figure 6.17 shows the idealized soil profile that was developed and used in FB-MultiPier. The soft clay layer was not included in the analysis, but shown here for reference. Due to the bedrock being very close to the surface, the soil is a site class C.

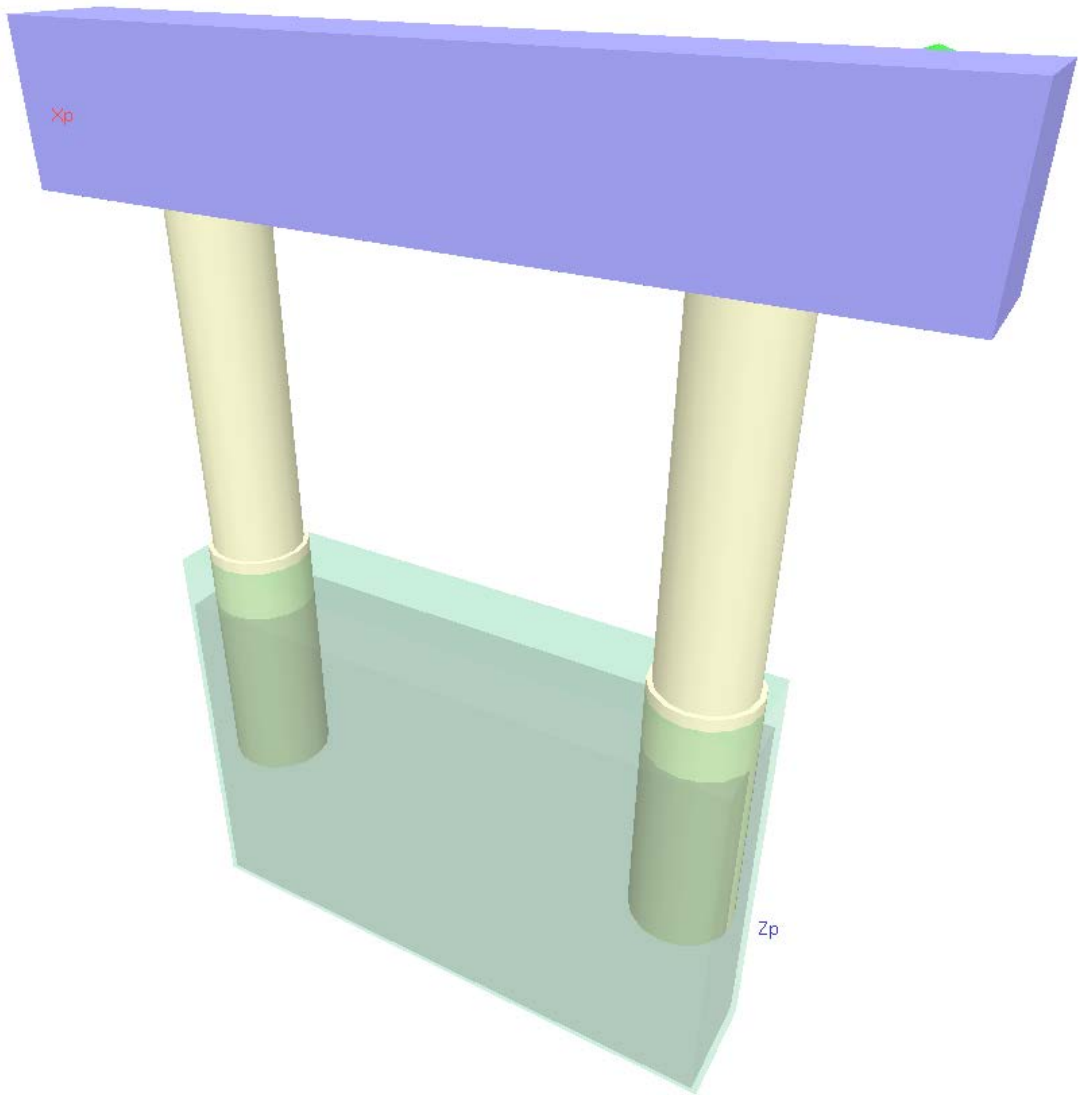

Figure 6.16. Little Bear Creek Bridge model

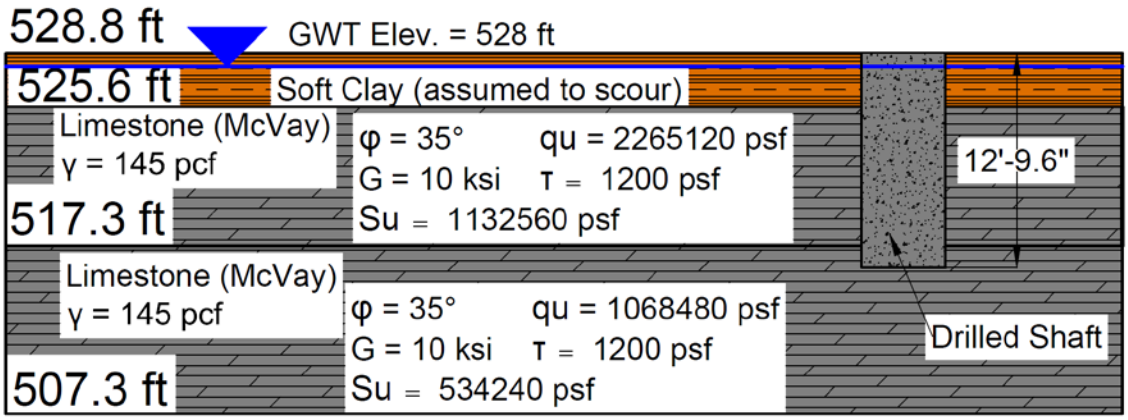

Figure 6.17. Little Bear Creek Bridge idealized soil profile

6.6.2 Oseligee Creek Bridge

6.6.2.1 Bridge Modeling

The Oseligee Creek Bridge is a two lane bridge that carries County Road 1289 over Oseligee Creek in Chambers County. It is a three span bridge with equal span lengths of 80 feet. The 7 inch concrete deck is supported by 4 Type III girders. Each of the 4 girders rests upon 20.5” x 9” bearing pads. These bearing pads were calculated to slip after an average (0.3 friction coefficient) displacement of 0.66” correlating to a shear of 21 kips per bearing pad. The clip-angle/anchor bolt configuration for the transverse connection contained anchor bolts with a diameter of 1.75”. These bolts were modeled with a shear capacity of 60.9 kips. This bridge model contains a single girder connection to represent 4 girder connections. The selection of a single connection representing 4 total connections miscalculates the gravity moments imparted into the bent columns in a conservative fashion. Plastic hinges were modeled at the top and bottom column locations.

The overall model of this bridge was found to be moderately flexible in the context of the other bridges modeled due to a 100% scour condition that was selected by geotechnical analysis of the bridge. Initial modal analysis of this bridge show stiff bridge behavior, however bridge geometry of the model results in more flexible behavior after hinge formation. This behavior combined with second order effects could result in column buckling, however a bridge with these conditions helps to diversify the overall bridge suit. Modal analysis of the model revealed a first mode natural period of 0.689 seconds in the transverse direction and 1.066 seconds in the longitudinal direction. The third mode natural periods of the fixed version of this bridge resulted in a natural period of 0.154 seconds in the transverse direction and 0.262 seconds in the longitudinal direction. The combination of a tall, flexible substructure and short span lengths

could result in dissimilar behaviors in super and substructure, resulting in possible higher forces at the connection location. Foundation behavior for this could result in hinging forming in the foundations, but that cannot be predicted in this particular model which specifies hinges in the column only. Large foundation rotations could result due to second order effects as well as large moments occurring in the substructure.

6.6.2.2 Substructure Modeling

The foundations used for both the abutments and piers are drilled shafts. Bent 3 was modeled in FB-MultiPier, as shown in Figure 6.18 Bent 2 and 3 are built the same but with slightly different tip elevations. Both have similar soil conditions. Bent 3 consists of a pier cap and two shafts. The shafts are 3.5 ft in diameter with twelve No. 11 longitudinal reinforcing bars.

A formal site investigation, using the standard penetration test (SPT) and rock coring, was conducted by the Bureau of Materials and Tests within ALDOT. According to the geotechnical report, the site is located in the Southern Piedmont Upland district and underlain by Ropes Creek Amphibolite and the Agricola Schist of Precambrian to Paleozoic age (ALDOT 2008). The ground water table (GWT) elevation at Bent 3 was found to be that of the water elevation of Oseligee Creek at 72 ft (ALDOT 2008). There is roughly 16 feet of top soil that was assumed to scour to bedrock at an elevation of 63 ft. Static analysis of the lateral capacity of the drilled shafts was done using LPile and the input parameters were included in the geotechnical report. The same input parameters were used in FB-MultiPier. However, some parameters that were needed for FB-MultiPier were not provided and had to be determined based on the boring logs. Figure 6.19 shows the idealized soil profile that was developed and used in FB-MultiPier.

For the 25% scour case, the top 25% of the soil (above the bedrock) was simply removed from the existing conditions. The insitu soils were determined to be a site class E. However, if 100% scour is assumed, the site class would be C.

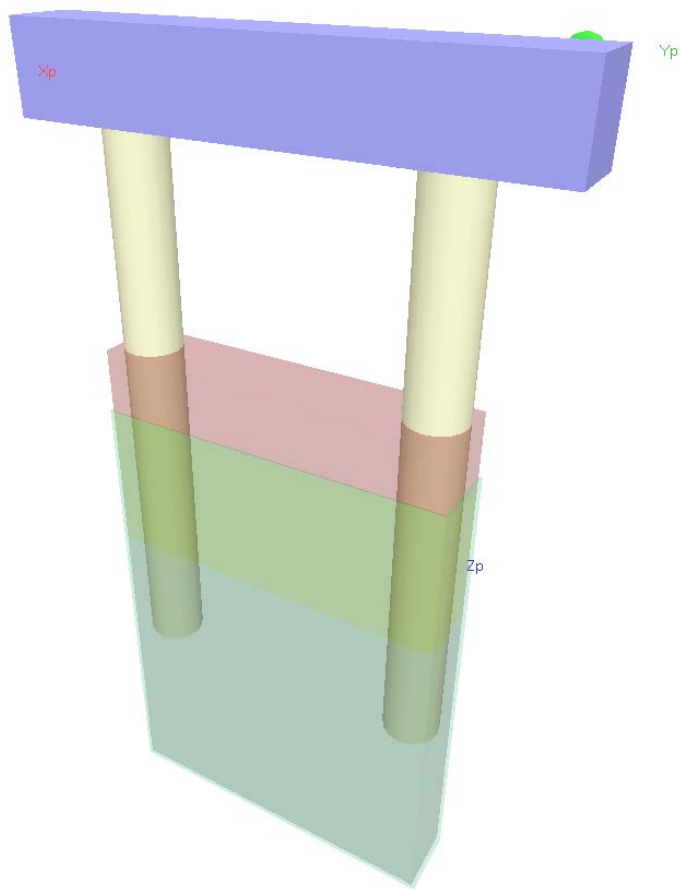

Figure 6.18. Oseligee Creek Bridge model

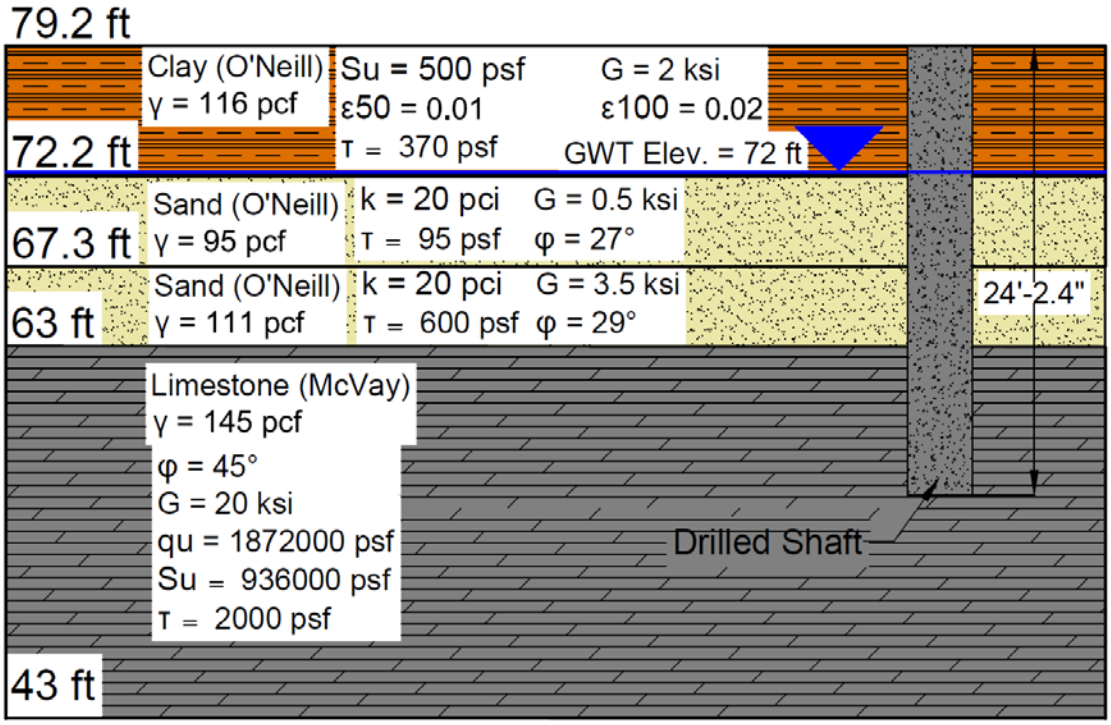

Figure 6.19. Oseligee Creek Bridge idealized soil profile for Bent 3

6.6.3 Norfolk Southern Railroad Bridge

6.6.3.1 Bridge Modeling

The bridge over Norfolk Southern Railroad is the southbound I-59 bridge in Etowah County, a two lane bridge that crosses over a Norfolk Southern railroad line and a state highway. It is a two span bridge with unequal span lengths of 125 feet and 140 feet. Nine modified BT-54 girders support a 6 inch concrete deck that is 46.75 feet wide. Each of the 9 girders rests upon 24.5” x 9” bearing pads. These bearing pads were calculated to slip after an average (0.3 friction coefficient) displacement of 1.132” correlating to a shear of 31.5 kips per bearing pad. The clip-angle/anchor bolt configuration for the transverse connection contained anchor bolts with a diameter of 1.375”. These bolts were modeled with a shear capacity of 47.9 kips. This bridge model contains three girder connections to represent 9 girder connections. The selection of

multi connection representing 6 total connections miscalculates the gravity moments imparted into the bent columns in a conservative fashion. Plastic hinges were modeled at the top and bottom column locations.

The overall model of this bridge was found to be initially stiff due to the large column diameters and the strut members; however bridge geometry of the model results in more flexible behavior after hinge formation. Modal analysis of the model revealed a first mode natural period of 0.415 seconds in the transverse direction and 0.705 seconds in the longitudinal direction. The third mode natural periods of the fixed version of this bridge resulted in a natural period of 0.133 seconds in the transverse direction and 0.086 seconds in the longitudinal direction. The combination of short, stiff substructure and large span lengths could result in dissimilar behaviors in super and substructure, resulting in possible higher forces at the connection location. Foundation behavior for this bridge is difficult to predict, but a triple column bent should limit foundations rotations in the lateral direction.

6.6.3.2 Substructure Modeling

The foundations used for both the abutments and piers are 12x53 H-piles. Because the abutments were not modeled, they are not discussed. Bent 2, shown in Figure 6.20, was modeled in FB-MultiPier and consists of a pier cap and three columns that are each supported by pile footings.

A formal site investigation, using the SPT and rock coring, was conducted by Terracon (formerly Gallet and Associates). According to the geotechnical report, the site is at or very near the contact between Bangor Limestone and Monteagle Limestone deposits. Bangor Limestone consists of medium-gray bioclastic and oolitic limestone containing interbeds of dusky red and olive green mudstone (Gallet 2008). The Monteagle Limestone deposit consists of light-gray

oolitic limestone containing interbedded argillaceous, bioclastic, or dolomitic limestone, dolomite, and medium gray shale (Gallet 2008).

The GWT elevation at Bent 2 was recorded as 620 feet during the initial site investigation (Gallet 2008). The boring logs taken near bent 2 indicated that insitu soils consist of approximately 50 feet of soft clay from the ground surface. A void was then encountered for roughly 15 feet until limestone bedrock was reached at an approximate depth of 65 feet (578.5 feet elevation). All input parameters needed for FB-MultiPier were determined based on the boring logs and rock core testing. The mobilized end bearing resistance (referred to as axial bearing failure in FB-MultiPier) was determined using FB-Deep. Figure 6.21 shows the idealized soil profile that was developed and used in FB-MultiPier. The insitu soils were determined to be a site class E.

Default p-y multipliers were used for lateral analysis in Etowah models. A pile group efficiency of 1.0 was used for the axial analysis based on recommendations made by Hannigan et al. (2006). The pile cap, in this case, was buried several feet below the ground surface.

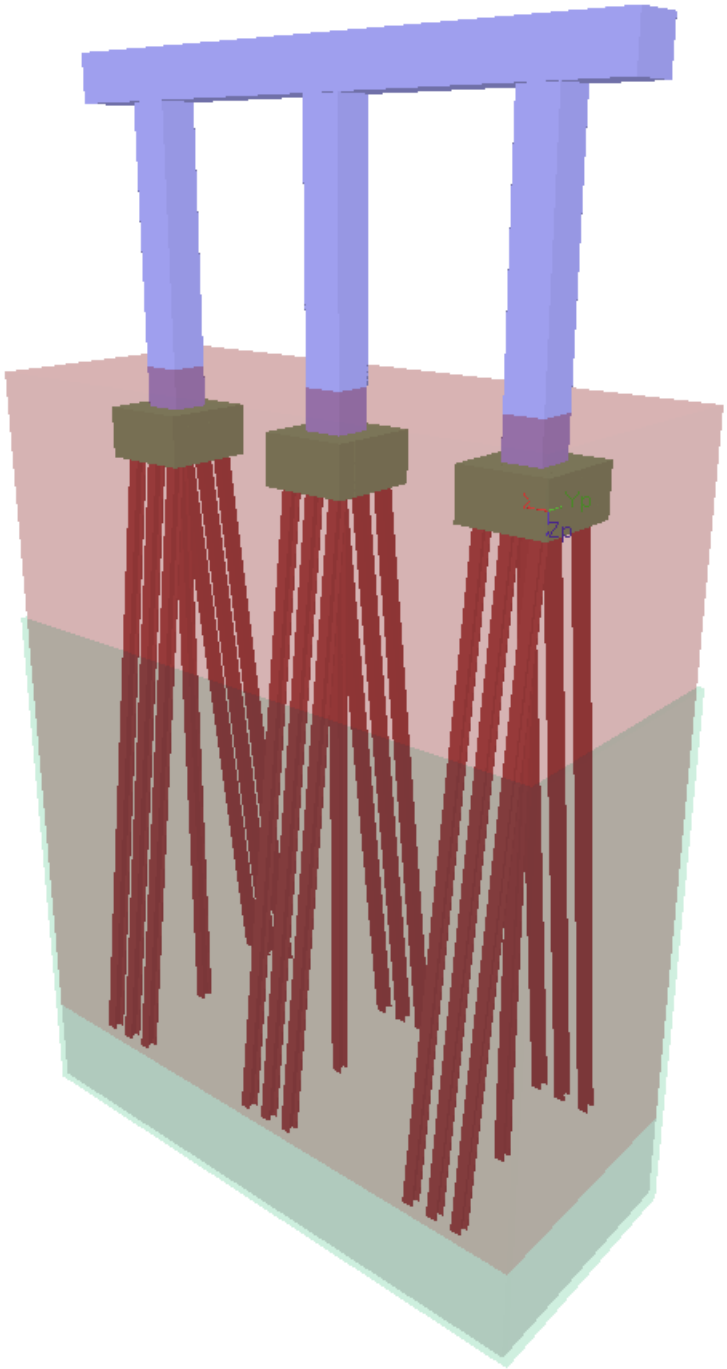

Figure 6.20. Norfolk Southern Railroad Bridge model

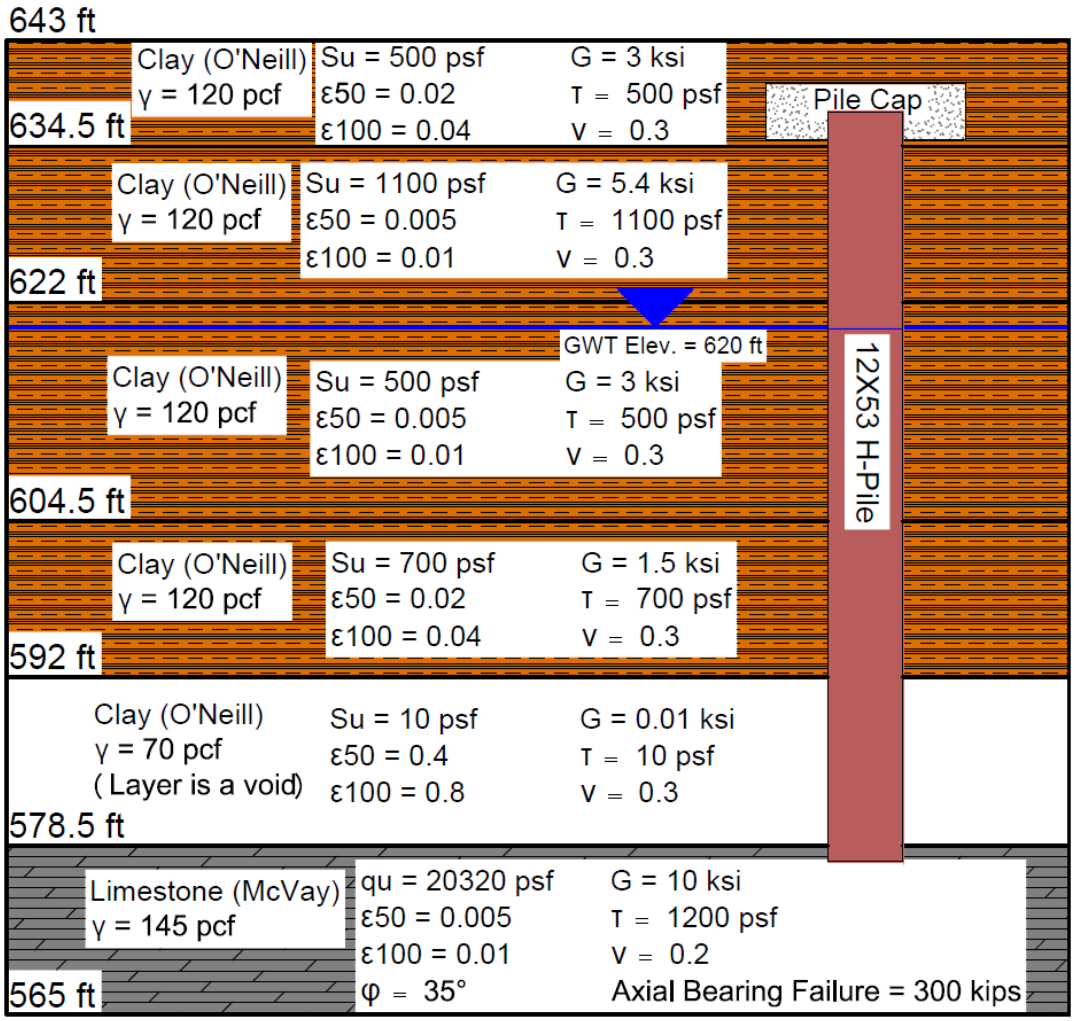

Figure 6.21. Norfolk Southern Railroad Bridge idealized soil profile

6.6.4 Scarham Creek

6.6.4.1 Bridge Modeling

The Scarham Creek Bridge is a four span bridge with equal span lengths of 130 feet. The 7 inch concrete deck is supported by 6 BT-72 girders resting upon 24.5” x 9” bearing pads. These bearing pads were calculated to slip after an average (0.3 friction coefficient) displacement of 1.336” correlating to a shear of 37.5 kips per bearing pad. The clip-angle/anchor bolt configuration for the transverse connection contained anchor bolts with a diameter of 2.5”. These bolts were modeled with a shear capacity of 87 kips. The bridge pier at bents 2 and 4 are 40’ x 5.5’ x 7.5’ and the pier at bent 3 is 40’ x 6.5’ x 7.5.’ This bridge model contained a single girder connection to represent 6 girder connections. The selection of a single connection representing 6 total connections miscalculates the gravity moments imparted into the bent columns in a conservative fashion. Plastic hinges were modeled at the column locations above and below strut locations due to the large depth and stiffness of the struts. Behaviors at these locations are of particular concern during ground motions.

The overall model of this bridge was found to be initially stiff due to the large column diameters and the strut members; however bridge geometry of the model results in more flexible behavior after hinge formation. Modal analysis of the model revealed a first mode natural period of 0.76 seconds in the transverse direction and 1.08 seconds in the longitudinal direction. The third mode natural periods of the fixed version of this bridge resulted in a natural period of 0.30 seconds in the transverse direction and 0.34 seconds in the longitudinal direction. The combination of tall substructure and large span lengths could result in similar behaviors in super and substructure, resulting in possible lower forces at the connection location. Foundation

behavior for this bridge is difficult to predict, given the unpredictability of this bridges behavior as it enters the inelastic range.

6.6.4.2 Substructure Modeling

The foundations used for both the abutments and piers are drilled shafts. All of the bents were modeled using the same soil profile, which was the lower bound. Bent 2 and 4 have the same section properties; therefore, one model was developed to represent both bents. Bent 3 has a larger shaft diameter than that of Bents 2 and 3 was the bent modeled for direct analysis.

The shafts for Bent 2 and 4 are 5 ft in diameter with 24 No. 11 longitudinal reinforcing bars above the ground surface, and 5.5 ft in diameter with the same reinforcement alignment below the ground surface. The shafts for Bent 3 are 6 ft in diameter with 32 No. 11 longitudinal reinforcing bars above the ground surface, and 6.5 ft in diameter with the same reinforcement alignment below the ground surface. The FB-Multupier model for Bent 3 is included as Figure 6.22.

A formal site investigation, using the SPT and rock coring, was conducted by the Bureau of Materials and Tests within ALDOT. According to the geotechnical report, the site is located in the Sand Mountain district of the Cumberland Plateau physiographic section and underlain by Pottsville Formation of Pennsylvanian age (ALDOT 2003). The Pottsville Formation consists of over 400 feet of brown gray thin- to thick-bedded sandstone, gray shale, siltstone, conglomerate, and coal beds (ALDOT 2003). The GWT elevation at Bent 3 was recorded as 860 feet at a 24 hour reading after the initial site investigation (ALDOT 2003). There was not a GWT elevation recorded for Bents 2 and 4. There is roughly 3-4 ft of top soil that was assumed to scour to bedrock at all of the bents. Uniaxial compression testing was done at different stations and depths. The lowest value was used as a representative unconfined compressive strength. All

other input parameters needed for FB-MultiPier were determined based on the boring logs. Figure 6.23 shows the idealized soil profile that was developed and used in FB-MultiPier (elevations shown are for Bent 3). The same soil parameters were used for all the bents. The soft clay layer was not included in the analysis, but shown here for reference. Due to the bedrock being very close to the surface, the soil is a site class C. Note that the multiple elevations in Figure 6.23 refer to the elevations of the soil profile at each drilled shaft for Bent 3.

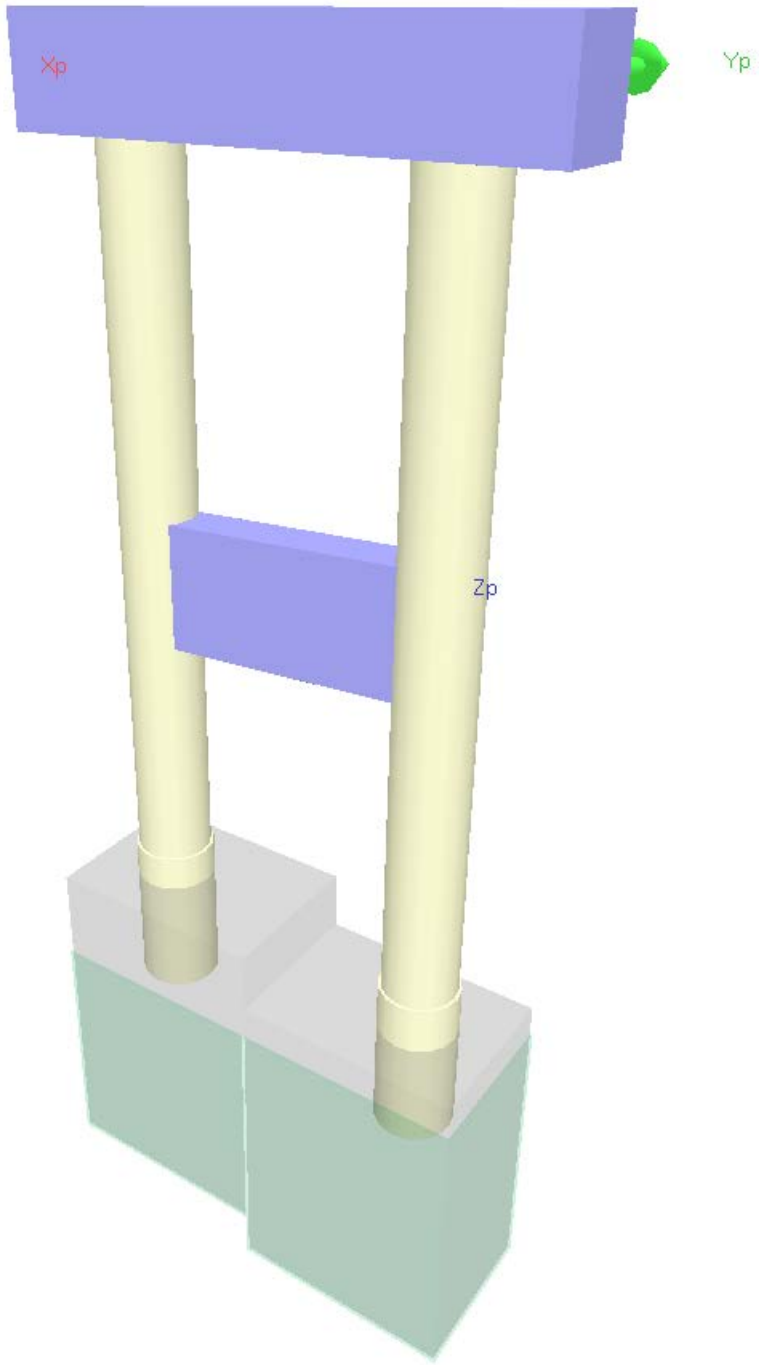

Figure 6.22. Scarham Creek Bridge model

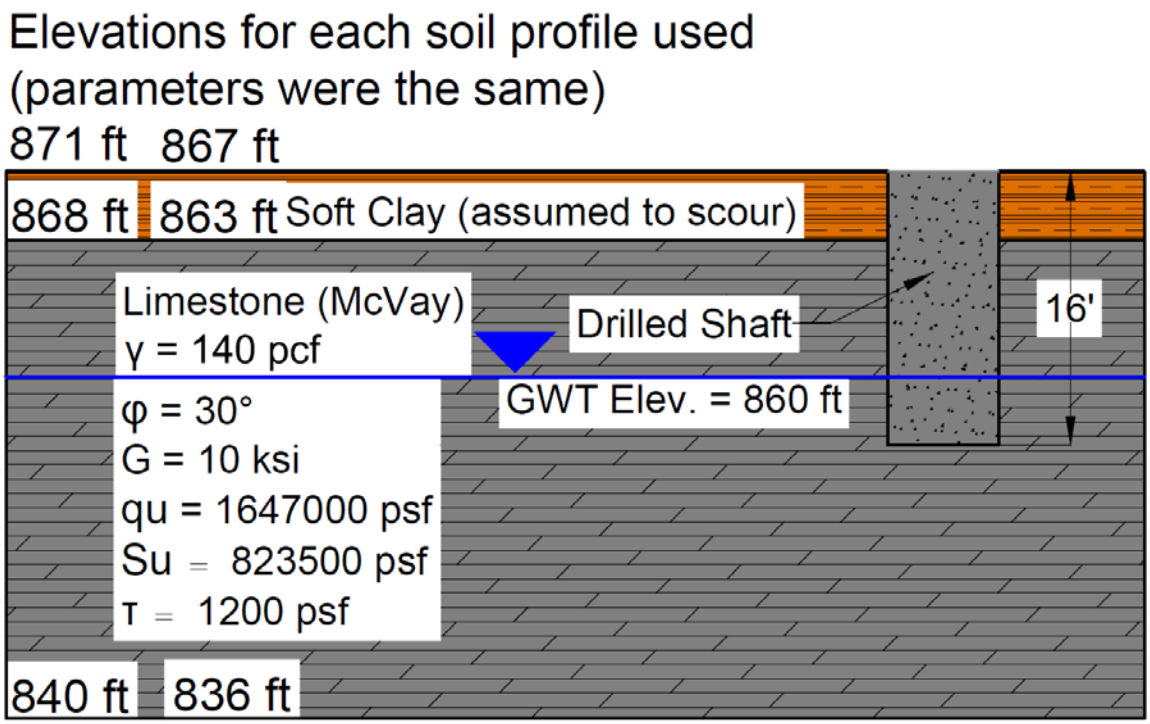

Figure 6.23. Scarham Creek Bridge idealized soil profile

6.6.5 Bent Creek Road

6.6.5.1 Bridge Modeling

The Bent Creek Road Bridge crosses over Interstate 85 with two spans of 135 feet. Each span is comprised of 15 modified BT-54 girders that rest upon 24.5” x 9” bearing pads. These bearing pads were calculated to slip after an average (0.3 friction coefficient) displacement of 1.19” correlating to a shear of 33 kips per bearing pad. The clip-angle/anchor bolt configuration for the transverse connection contained anchor bolts with a diameter of 1.75”. These bolts were modeled with a shear capacity of 60.9 kips. This bridge model contained 5 girder connections to represent 15 girder connections. This simplification was chosen due to the bridge bent

containing 5 columns, instead of a configuration of 2 columns found in other bridges. A selection of a single connection representing 15 total connections would dramatically miscalculate the gravity loads and moments imparted into the bent columns. The selection of 5 connections resulted in a more complex model then the other bridges, and it was predicted that analyses problems could arise.

The overall model of this bridge was found to be rather stiff, despite its large mass. Modal analysis of the model revealed a first mode natural period of 0.717 seconds in the transverse direction and 0.933 seconds in the longitudinal direction. The third mode natural periods of the fixed version of this bridge resulted in a natural period of 0.108 seconds in the transverse direction and 0.133 seconds in the longitudinal direction. The combination of stiff substructure and large superstructure mass could result in large forces at the connection location. Foundation behavior for this bridge may also be inconsistent to the other bridges given a pile cap foundation group located under such a large and stout bridge bent.

6.6.5.2 Substructure Modeling

The foundations used for both the abutments and piers are 12x53 H-piles. Bent 2, depicted in Figure 6.24, was modeled in FB-MultiPier and consists of a pier cap and three columns that are each supported by pile footings. The bridge was built in two stages to avoid closing the existing road. The bridge was modeled in FB-MultiPier as one bent, however, due to program limitations.

A formal site investigation, using the SPT and rock coring, was conducted by the Bureau of Materials and Tests within ALDOT. According to the geotechnical report, the site is in the Southern Piedmont Upland district of the Piedmont Upland physiographic section. The project is

located in the Towaliga fault zone and is underlain by blastomylonite which is schist and gneiss that has been pulverized by the lateral movement of the fault (ALDOT 2006).

The GWT elevation at Bent 2 at 24 hours after drilling was estimated to be 655 feet elevation during the initial site investigation (ALDOT 2006). The boring logs taken near bent 2 indicated that insitu soils consist of approximately 30 feet of stiff sandy silt from the ground surface underlain by hard weathered gneiss. All input parameters needed for FB-MultiPier were determined based on the boring logs and rock core testing. The axial bearing failure (or mobilized end bearing) was determined using FB-Deep. Figure 6.25 shows the idealized soil profile that was developed and used in FB-MultiPier. The insitu soils were determined to be a site class D.

Default p-y multipliers were used for lateral analysis in the Bent Creek Road Bridge models. It was determined that these were adequate for use. A pile group efficiency of 1 was used for the axial analysis. For driven piles, axial group efficiency can be greater than 1 in some cases, due to densification of the surrounding soil during pile driving.

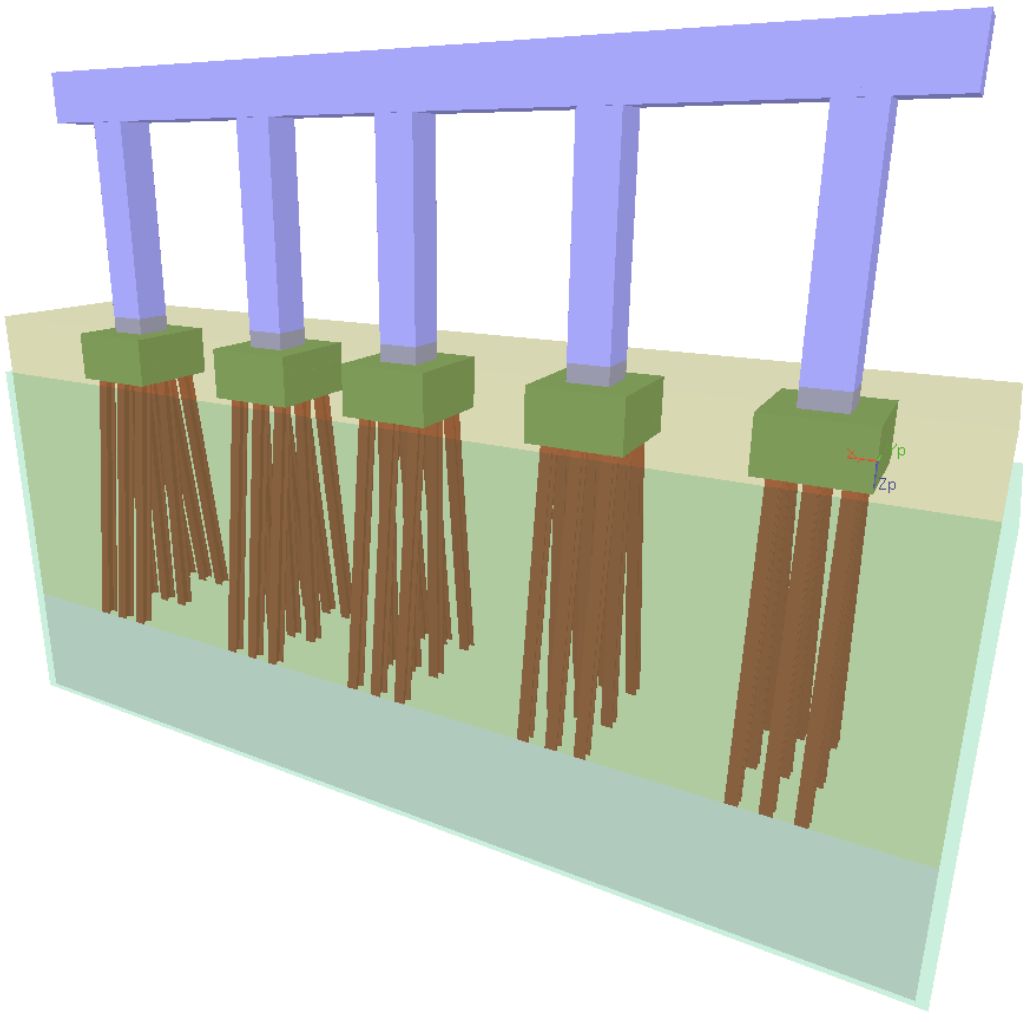

Figure 6.24. Bent Creek Road Bridge model

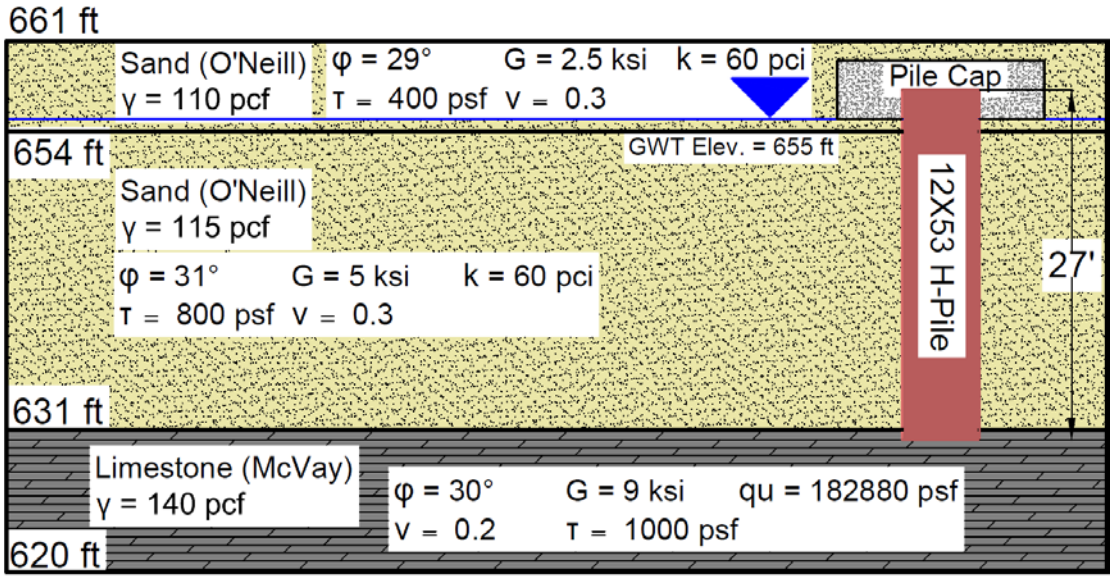

Figure 6.25. Bent Creek Road Bridge idealized soil profile

6.7 Summary

The previous sections outline the procedures and rationale behind bridge modeling in CSiBridge and FB-Multipier, as well as the selection of the hazards and ground motions used to analyze them. The hazard selected for this analysis consists of the two largest seismic hazards found in Alabama, and the ground motions selected to represent these hazards are diverse. These ground motions contain a wide range of response behaviors. The information related to each bridge that was modeled is included in this section, followed by expected behaviors of those bridges. Simplifications were selected for the modeling of abutments and connection locations in order to simplify analysis and improve model performance. Soil and foundation modeling methods and information are also included for each bridge. Predicted behaviors of each bridge were also included in these sections based on the bridge elements modeled. This concludes information regarding the hazard analysis and structural modeling processes used in this project.

Chapter 7: Task 3 Results and Discussion

7.1 Introduction

This section will present the results from the time history analyses performed on each bridge model. Some sections will compare the results taken from specific bridges, while other sections will simply provide an overview of observed behaviors and trends. Unique behavior or abnormalities will also be examined. Explanations for observed phenomena will also be provided when necessary. This section will provide insight into both the bridges analyzed as well as the ground motions used in the analysis.

7.1.1 Description of Results Presented

Each of the five bridges were analyzed in four ways. Each bridge was modeled as an upper limit bearing pad configuration (coefficient of friction of 0.4), and a lower limit bearing pad configuration (coefficient of friction of 0.2). Each bridge was modeling incorporating soil interaction springs that provide foundation flexibility. Both of these bridge models were then analyzed using ten design level ground motions, applied in both the longitudinal and transverse direction. The results of each analysis have been recorded and graphed using MathCAD (PTC, 2007). Maximum span and bent displacements are recorded for each bridge analysis, as well as maximum foundation displacements and rotations. Bolt shears and bearing displacements are also recorded at each connection location, with the largest value being used to calculate demand capacity ratios. Each response history analysis performed is categorized based on the results recorded. Analyses that did not complete are rerun using altered analysis constraints in an effort

to eliminate numerical instabilities that occur during analysis. After numerous iterations of attempted analysis, motions that did not complete are recorded in their state of farthest completion. The analysis is classified as one of the following: 1) Complete: indicating that the entire analysis was completed, 2) Numerical: indicating that no elements appeared to have failed but the analysis could not be completed due to numerical convergence issues and 3) Failure: indicating a numerical failure that either results from a structural failure within the model, or a set of recorded results that indicated possible future structural failure of the model during continued analysis. Data taken from analyses deemed "Numerical" is excluded from statistical analysis of each bridge due to the unknown behaviors of the model during analysis. Data taken from analyses deemed "Failure" is included in statistical analysis of each bridge given predictable behaviors or data related to failures that have already occurred. All major structural component failures are recorded and highlighted for each analysis. Foundation information is displayed as a demand/capacity value in reference to displacements and rotations. The demand/capacity value is taken from each analysis as the maximum demand/capacity value out of each of the bents for the entirety of each ground motion. The value associated with "Bearing Capacity" represents a demand/capacity value that contains the highest bearing pad lateral or longitudinal displacement recorded from the displacements of every bearing pad in the bridge during the entirety of the ground motion. "Bent Ductility" is a value of the largest differential displacement between bent displacement and its respective foundation displacement. The value representing "Bent Ductility" is the quotient of the aforementioned displacement divided by the displacement determined as the bent displacement relating to nominal moment capacity occurring at a hinge in that bent. "Bolt Status" indicates the highest shear demand present in all

anchor bolts within the model compared to the shear capacity of the anchor bolts in the model. All values indicated in **Bold** font represent values that exceed their acceptable limits.

7.1.2 Limits of Bridge Behaviors

Each bridge is analyzed for the purpose of determining performance acceptability. Acceptable bridge behavior is based on many different criteria stemming from the limits specified in Section 6.3. The average response of each model will be used to determine that models estimated behavior. In the event that a model contains numerous numerical failures, a prediction of overall behavior will be made, but recommendations for that bridge will not be made unless further complete analysis is performed.

Each bridge result will be checked for failures or exceedance of capacity limits. A classification of each of these results will be made in the event of a capacity limit being exceeded. The following behaviors will be classified as resulting in structural failure: 1) excessive span and/or bent deflections (values are dependent on bridges), 2) bearing pad capacities exceeding a value of “1”, 3) Bent ductility exceeding the limits specified in Section 6.3. A residual displacement of span or bents that exceeds 1 inch will be classified as a failure on the grounds of a serviceability limit being exceeded. Bolt failure will also be addressed, but will not be considered as a structural failure due to the anchor bolts only providing a non-essential barrier to transverse displacement. Bridges that contain multiple instances of structural failures will be deemed to have inadequate behavior. Bridges that contain only one or two structural failure analysis cases will be classified as having acceptable behavior. This is deemed allowable due to overall analysis results being evaluated as an average of bridge response, and a small amount of failure cases are allowable in a large number of analyses.

7.2 Bent Creek Road Bridge

Results show that the average behavior of the Bent Creek Road Bridge was favorable for most aspects of the bridge components. No design level (1,000 year hazard) or MCE level (2,500 year hazard) events resulted in specific structural failures; however one event may lead to possible structural failures. Foundation failures occurred in six of the design level longitudinal events; however the occurrence of these failures is not consistent with other structural behavior during the events. Substructure behavior appears to be adequate at column and bent locations with the exception of foundation displacement capacities in the longitudinal direction of the bridge. Bolt failure was the most frequent behavioral occurrence in the connection during transverse motion. An additional observation regarding the analysis of this bridge is the large number of numerical failures present in the data. This result is thought to have occurred due to the complexity of the bridge model. Judgments needed to be made regarding the inclusion or exclusion of these results. A more in-depth analysis of each set of analysis results is provided in the next sections.

7.2.1 Transverse Motion

The transverse analysis for this bridge resulted in stiff structural behavior. See Table 7.1 and Table 7.2 for an overview of the design level transverse results. Bolt failure and low bent displacements indicate a stiff substructure able to transfer large loads to the connection. Both frictions models responded similarly to the design level transverse ground motions, showing low foundation rotations and low residual displacements. Overall design level bent ductility did not

exceed a value of 1, likely due to the stiff bridge bent. Thirteen of the twenty design level ground motions ran successfully with this bridge model, with a larger number of incomplete analyses occurring in the upper limit friction model. Six of the seven design level ground motions that did not run successfully were classified as numerical failures. No data examined from these six ground motions indicated a large structural failure before the analysis ceased. The one design level analysis failure that was classified as such displayed bolt failure prior to the onset of larger ground motions during the Coalinga record. It was estimated that larger shaking, given the existing bolt failure, may result in larger displacements of deck sections. These displacements could result in failure of the structure, or at least a suspension of serviceability. Another numerical failure (Imperial Valley) displayed similar bolt status to the Coalinga event, but had already withstood the majority of its associated ground motion, and was not classified as a "failure" analysis. Successful design level analysis results and the single "failure" event were used to classify the design level behavior of this model.

Table 7.1: Results Overview for Lower Limit Friction Bent Creek Transverse Model

Bent Creek	Friction ".2"											
Transverse Motion	Ground Motion	Run Status	Run Time	Foundation Capacity (D/R)		Bearing Capacity	Bent Ductility	Bolt Status	Max Span Disp. (in.)	Max Bent Disp. (in.)	Residual Span Disp. (in.)	Residual Bent Disp. (in.)
San Fernando 1	Design	Comp.	48.00	0.086	0.0006	0.090	0.623	**0.994**	1.170	1.009	0.048	0.105
San Fernando 2	Design	Comp.	50.00	0.034	0.0000	0.022	0.191	0.535	0.367	0.294	0.002	0.000
Imperial Valley	Design	Num.	38.32	0.067	0.0001	0.065	0.470	**0.966**	0.877	0.750		
Coalinga	Design	Fail.	16.25	0.058	0.0016	0.091	0.471	**0.987**	1.183	0.759		
North Palm Springs	Design	Comp.	40.00	0.069	0.0000	0.065	0.464	**0.996**	0.872	0.732	0.001	0.001
Landers	Design	Comp.	70.00	0.040	0.0000	0.027	0.235	0.659	0.452	0.364	0.001	0.001
Little Skull Mountain	Design	Comp.	132.00	0.032	0.0000	0.022	0.191	0.542	0.374	0.296	0.000	0.001
Kocaeli 1	Design	Num.	36.06	0.006	0.0000	0.004	0.033	0.093	0.064	0.051		
Kocaeli 2	Design	Comp.	48.00	0.106	0.0001	0.138	0.984	**0.999**	1.815	1.608	0.401	0.392
Kobe	Design	Comp.	60.00	0.051	0.0000	0.036	0.316	0.885	0.607	0.493	0.042	0.026
Mean				0.0595	0.0003	0.0614	0.4345	0.8246	0.8549	0.6943	0.0706	0.0752
Standard Deviation				0.0261	0.0006	0.0424	0.2705	0.2103	0.5100	0.4485	0.1472	0.1448
Relative Stand Deviation				43.87%	**191.63%**	69.07%	62.25%	25.51%	59.66%	64.60%	**208.29%**	**192.41%**

Table 7.2: Results Overview for Upper Limit Friction Bent Creek Transverse Model

Bent Creek	Friction ".4"											
Transverse Motion	Ground Motion	Run Status	Run Time	Foundation Capacity (D/R)		Bearing Capacity	Bent Ductility	Bolt Status	Max Span Disp. (in.)	Max Bent Disp. (in.)	Residual Span Disp. (in.)	Residual Bent Disp. (in.)
San Fernando 1	Design	Comp.	48.00	0.083	0.0001	0.094	0.677	**0.931**	1.247	1.097	0.121	0.059
San Fernando 2	Design	Comp.	50.00	0.034	0.0000	0.022	0.191	0.535	0.367	0.294	0.001	0.001
Imperial Valley	Design	Num.	26.18	0.067	0.0001	0.065	0.470	**0.966**	0.877	0.750		
Coalinga	Design	Comp.	52.00	0.070	0.0001	0.096	0.654	**0.999**	1.332	1.137	0.071	0.005
North Palm Springs	Design	Num.	6.50	0.005	0.0000	0.003	0.029	0.082	0.057	0.045		
Landers	Design	Comp.	70.00	0.040	0.0000	0.027	0.235	0.659	0.452	0.364	0.001	0.001
Little Skull Mountain	Design	Comp.	132.00	0.032	0.0000	0.022	0.191	0.542	0.374	0.296	0.001	0.001
Kocaeli 1	Design	Num.	36.06	0.006	0.0000	0.004	0.033	0.093	0.064	0.051		
Kocaeli 2	Design	Comp.	48.00	0.086	0.0001	0.095	0.679	**0.999**	1.266	1.092	0.108	0.024
Kobe	Design	Num.	18.28	0.049	0.0001	0.036	0.316	0.885	0.612	0.495		
Mean				0.0576	0.0000	0.0593	0.4379	0.7774	0.8397	0.7132	0.0504	0.0152
Standard Deviation				0.0292	0.0000	0.0377	0.2560	0.3546	0.4879	0.4279	0.0567	0.0233
Relative Stand Deviation				50.62%	**100.57%**	63.56%	58.47%	45.61%	58.10%	59.99%	**112.47%**	**153.50%**

A total of fourteen MCE level events were applied to this bridge model. See Table 7.3 and Table 7.4 for an overview of the MCE level transverse results. Overall bent ductility did not exceed a value of 1.2, likely due to the stiff bridge bent. Ten of the Fourteen MCE level ground motions ran successfully with this bridge model, with an equal number of incomplete analyses occurring in both friction models. Three of the four ground motions that did not run successfully were classified as numerical failures. No data examined from these three ground motions indicated a large structural failure before the analysis ceased. The one analysis failure that was classified as such displayed bolt failure prior to the onset of larger ground motions during the first Kocaeli record. It was estimated that larger shaking, given the existing bolt failure, may result in larger displacements of deck sections. These displacements could result in failure of the structure, or at least a suspension of serviceability. Successful analysis results and the single "failure" event design level ground motions were used to classify the MCE level behavior of this model. All successful analyses resulted in acceptable bridge behavior in the transverse direction of loading, however the complexity of the model makes it difficult to analyze and thus state any

solid conclusions regarding overall bridge behavior. A solution to this would be to continue simplifying the model by reducing the number of modeled connections.

Table 7.3: MCE Level Results Overview for Lower Limit Friction Bent Creek Transverse Model

Bent Creek	Friction ".2"											
Transverse Motion	Ground Motion	Run Status	Run Time	Foundation Capacity (D/R)		Bearing Capacity	Bent Ductility	Bolt Status	Max Span Disp.	Max Bent Disp.	Residual Span Disp.	Residual Bent Disp.
San Fernando 1	MCE	Comp.	48.00	0.072	0.0000	0.071	0.512	**0.964**	0.958	0.814	0.044	0.036
San Fernando 2	MCE	Comp.	50.00	0.043	0.0000	0.029	0.257	0.722	0.494	0.399	0.000	0.000
Imperial Valley	MCE	Num.	30.00	0.082	0.0001	0.089	0.627	**0.968**	1.162	1.004		
Landers	MCE	Comp.	70.00	0.104	0.0002	0.155	1.104	**0.962**	2.091	1.924	0.672	0.600
Kocaeli 1	MCE	Fail.	99.14	0.129	0.0001	0.153	1.111	**0.988**	2.017	1.801		
Kocaeli 2	MCE	Comp.	48.00	0.149	0.0001	0.163	1.193	**0.965**	2.156	1.920	0.162	0.203
Kobe	MCE	Comp.	60.00	0.139	0.0000	0.158	1.154	**0.989**	2.079	1.864	0.525	0.449
Mean				0.1026	0.0001	0.1170	0.8513	0.9367	1.5651	1.3894	0.2806	0.2576
Standard Deviation				0.0389	0.0001	0.0533	0.3782	0.0955	0.6796	0.6356	0.3007	0.2609
Relative Stand Deviation				37.89%	90.03%	45.57%	44.43%	10.20%	43.42%	45.74%	**107.14%**	**101.29%**

Table 7.4: MCE Level Results Overview for Upper Limit Friction Bent Creek Transverse Model

Bent Creek	Friction ".4"											
Transverse Motion	Ground Motion	Run Status	Run Time	Foundation Capacity (D/R)		Bearing Capacity	Bent Ductility	Bolt Status	Max Span Disp.	Max Bent Disp.	Residual Span Disp.	Residual Bent Disp.
San Fernando 1	MCE	Comp.	48.00	0.072	0.0000	0.071	0.511	**0.964**	0.955	0.812	0.002	0.001
San Fernando 2	MCE	Comp.	50.00	0.043	0.0000	0.029	0.257	0.722	0.494	0.399	0.001	0.001
Imperial Valley	MCE	Num.	17.23	0.107	0.0001	0.122	0.894	**0.968**	1.642	1.446		
Landers	MCE	Comp.	70.00	0.096	0.0001	0.143	1.102	**0.991**	2.064	1.850	0.002	0.068
Kocaeli 1	MCE	Num.	30.64	0.008	0.0000	0.005	0.047	0.131	0.089	0.071		
Kocaeli 2	MCE	Comp.	48.00	0.141	0.0001	0.159	1.168	**0.965**	2.141	1.887	0.585	0.456
Kobe	MCE	Comp.	60.00	0.112	0.0002	0.129	0.940	**0.984**	1.743	1.522	0.133	0.013
Mean				0.0828	0.0001	0.0942	0.7028	0.8179	1.3041	1.1410	0.1445	0.1077
Standard Deviation				0.0450	0.0001	0.0595	0.4349	0.3175	0.7997	0.7188	0.2528	0.1967
Relative Stand Deviation				54.39%	**117.48%**	63.18%	61.88%	38.82%	61.32%	62.99%	**174.94%**	**182.68%**

7.2.2 Longitudinal Motion

Analysis of the Bent Creek Bridge under longitudinal ground motions provided mixed behavioral results. Table 7.5 and Table 7.6 provide an overview of Bent Creek's design level longitudinal analysis. Both friction models exhibited numerical failures (nine in total) as well as conflicting completed results. Six of the eleven completed design level analyses exhibited large foundation displacements. This foundation behavior does not seem to be supported by forces

within the recorded model data however, and its existence may be the result of errors propagated within the analysis. The remaining successful design level analyses indicate very little displacements; however the overall behavior of the structure may not be adequately described with the results obtained.

Table 7.5: Results Overview for Lower Limit Friction Bent Creek Longitudinal Model

Bent Creek	Friction ".2"										
Longitudinal Motion	Ground Motion	Run Status	Run Time	Foundation Capacity (D/R)		Bearing Capacity	Bent Ductility	Max Span Disp. (in.)	Max Bent Disp. (in.)	Residual Span Disp. (in.)	Residual Bent Disp. (in.)
San Fernando 1	Design	Comp.	48.00	**6.702**	0.0436	0.297	5.213	1.363	0.995	0.492	0.164
San Fernando 2	Design	Comp.	50.00	**2.846**	0.0416	0.216	2.246	0.982	0.664	0.719	0.072
Imperial Valley	Design	Num.	5.82	0.048	0.0081	0.053	0.038	0.240	0.121		
Coalinga	Design	Comp.	52.00	**6.590**	0.0603	0.341	5.526	1.565	1.020	0.694	0.139
North Palm Springs	Design	Num.	7.29	0.048	0.0176	0.100	0.110	0.453	0.263		
Landers	Design	Num.	11.15	0.048	0.0045	0.025	0.075	0.114	0.067		
Little Skull Mountain	Design	Comp.	132.00	0.048	0.0000	0.000	0.038	0.001	0.000	0.001	0.000
Kocaeli 1	Design	Num.	21.70	0.048	0.0276	0.150	0.204	0.681	0.431		
Kocaeli 2	Design	Comp.	48.00	0.803	0.0740	0.376	0.708	1.736	1.179	0.767	0.107
Kobe	Design	Comp.	60.00	0.219	0.0299	0.175	0.365	0.799	0.602	0.613	0.017
Mean				**2.8681**	0.0416	0.2341	2.3492	1.0742	0.7432	0.5477	0.0832
Standard Deviation				**3.0916**	0.0256	0.1371	2.4607	0.6321	0.4263	0.2847	0.0658
Relative Stand Deviation				**107.79%**	61.55%	58.55%	**104.75%**	58.84%	57.36%	51.98%	79.07%

Table 7.6: Results Overview for Upper Limit Friction Bent Creek Longitudinal Model

Bent Creek	Friction ".4"										
Longitudinal Motion	Ground Motion	Run Status	Run Time	Foundation Capacity (D/R)		Bearing Capacity	Bent Ductility	Max Span Disp. (in.)	Max Bent Disp. (in.)	Residual Span Disp. (in.)	Residual Bent Disp. (in.)
San Fernando 1	Design	Comp.	48.00	**5.781**	0.0651	0.372	4.666	1.719	1.302	0.819	0.181
San Fernando 2	Design	Num.	34.28	0.186	0.0416	0.229	0.447	1.044	0.728		
Imperial Valley	Design	Num.	5.82	0.048	0.0081	0.053	0.038	0.240	0.121		
Coalinga	Design	Comp.	52.00	**5.937**	0.0760	0.419	4.773	1.949	1.524	0.985	0.184
North Palm Springs	Design	Num.	7.29	0.048	0.0176	0.100	0.110	0.453	0.263		
Landers	Design	Num.	11.15	0.048	0.0045	0.025	0.075	0.114	0.067		
Little Skull Mountain	Design	Comp.	132.00	0.048	0.0001	0.000	0.038	0.002	0.001	0.001	0.000
Kocaeli 1	Design	Num.	21.70	0.048	0.0276	0.150	0.204	0.681	0.431		
Kocaeli 2	Design	Comp.	48.00	**3.431**	0.0743	0.382	2.807	1.773	1.313	0.787	0.185
Kobe	Design	Comp.	60.00	0.132	0.0282	0.176	0.357	0.800	0.605	0.055	0.109
Mean				**3.0658**	0.0487	0.2698	2.5284	1.2489	0.9490	0.5294	0.1318
Standard Deviation				**2.8923**	0.0334	0.1780	2.2695	0.8280	0.6335	0.4643	0.0804
Relative Stand Deviation				94.34%	68.47%	65.97%	89.76%	66.30%	66.75%	87.70%	60.98%

A total of fourteen MCE level events were applied to this bridge model. See Table 7.7 and Table 7.8 for an overview of the MCE level longitudinal results. Bent ductility was inconsistent throughout the analysis, with large and small values being recorded at the MCE level. Eight of the fourteen MCE level ground motions ran successfully with this bridge model, with an equal number of incomplete analyses occurring in both friction models. All of the ground motions that did not run successfully were classified as numerical failures. No data examined from these ground motions indicated a large structural failure before the analysis ceased. One case of residual deformation exceedance was recorded, and seven cases of foundation displacement exceedance were recorded. These large foundation displacements were recorded as a result of unexpected and sudden foundation movement. These displacements could result in failure of the structure, or at least a suspension of serviceability.

Table 7.7: MCE Level Results Overview for Lower Limit Friction Bent Creek Longitudinal Model

Bent Creek	Friction ".2"										
Longitudinal Motion	Ground Motion	Run Status	Run Time	Foundation Capacity (D/R)		Bearing Capacity	Bent Ductility	Max Span Disp.	Max Bent Disp.	Residual Span Disp.	Residual Bent Disp.
San Fernando 1	MCE	Comp.	48.00	0.730	0.0430	0.263	0.570	1.204	0.911	0.409	0.198
San Fernando 2	MCE	Num.	1.58	0.048	0.0025	0.013	0.053	0.060	0.028		
Imperial Valley	MCE	Num.	6.60	0.048	0.0207	0.116	0.188	0.527	0.284		
Landers	MCE	Comp.	70.00	**7.468**	0.0534	0.595	6.080	2.589	1.893	0.802	0.323
Kocaeli 1	MCE	Num.	20.52	0.048	0.0132	0.073	0.150	0.329	0.200		
Kocaeli 2	MCE	Comp.	48.00	**3.009**	0.1098	0.545	2.423	2.591	1.837	0.741	0.014
Kobe	MCE	Comp.	60.00	**3.551**	0.0436	0.375	2.941	1.733	1.223	**1.033**	0.175
Mean				2.1289	0.0409	0.2829	1.7722	1.2905	0.9108	0.7463	0.1775
Standard Deviation				2.7764	0.0355	0.2307	2.2320	1.0488	0.7744	0.2576	0.1269
Relative Stand Deviation				**130.41%**	86.89%	81.54%	**125.95%**	81.27%	85.03%	34.52%	71.51%

Table 7.8: MCE Level Results Overview for Upper Limit Friction Bent Creek Longitudinal Model

Bent Creek	Friction ".4"										
Longitudinal Motion	Ground Motion	Run Status	Run Time	Foundation Capacity (D/R)		Bearing Capacity	Bent Ductility	Max Span Disp.	Max Bent Disp.	Residual Span Disp.	Residual Bent Disp.
San Fernando 1	MCE	Comp.	48.00	**3.309**	0.0564	0.372	2.634	1.725	1.273	0.737	0.036
San Fernando 2	MCE	Num.	1.58	0.048	0.0025	0.013	0.053	0.060	0.028		
Imperial Valley	MCE	Num.	6.60	0.048	0.0207	0.116	0.188	0.527	0.284		
Landers	MCE	Comp.	70.00	**13.604**	0.0726	0.769	11.112	2.586	1.702	0.509	0.068
Kocaeli 1	MCE	Num.	20.52	0.048	0.0132	0.073	0.150	0.329	0.200		
Kocaeli 2	MCE	Comp.	48.00	**8.072**	0.0944	0.484	6.492	2.278	1.600	0.888	0.205
Kobe	MCE	Comp.	60.00	**7.092**	0.0525	0.429	5.688	2.001	1.530	0.826	0.074
Mean				4.6031	0.0446	0.3223	3.7596	1.3580	0.9451	0.7400	0.0958
Standard Deviation				5.2149	0.0337	0.2707	4.2040	1.0275	0.7398	0.1660	0.0747
Relative Stand Deviation				**113.29%**	75.47%	83.97%	**111.82%**	75.67%	78.28%	22.43%	78.04%

7.3 Scarham Creek Bridge

Results show that the average behavior of the Scarham Creek Bridge was favorable for design level events. This behavior does not carry over to the MCE level behaviors. Design level events resulted in behaviors typical with flexible bridges, including larger span displacements and bent deflections. Foundation performance for this bridge was mixed, and dependent on event direction. All design analysis performed for this bridge succeeded in completing except for the second San Fernando ground motion applied to the upper limit friction model in the longitudinal direction. Substructure behavior appears to be adequate at column, strut and bent

cap locations with the exception of foundation displacement capacities in the longitudinal direction of the bridge. Connection behavior also appears to be adequate from the results of each design level analysis. Bearing pad slippage was minimal in both directions of loading, and did not approach levels indicative of unseating. A more in-depth analysis of each bridge model's results is proved in the next sections.

7.3.1 Transverse Motion

The transverse analysis for this bridge resulted in flexible structural behavior. See Table 7.9 and Table 7.10 for an overview of the design level transverse results. High bent displacements are indicative of a flexible substructure able to accommodate large deflections. This behavior is in keeping with tall column bridge bents, like the ones present in the Scarham Bridge. Excessive deflections were a concern for the transverse motion of this bridge, in both span and bent locations. A hallmark of long period structures is large deflections, especially during certain ground motions. Results from both friction models indicated design level deflections that were within acceptable limits for this bridge, however the magnitude of these deflections may not be acceptable for other bridges in this project. All transverse design level analyses of the Scarham Creek Bridge ran successfully. One very important observation of the recorded data from both friction models of this bridge is the fact that every single data point is the same for the transverse direction motions. The only difference between both bridge models is the change in bearing pad friction factor. Both models behave in exactly the same manner during events that do not allow friction slips to occur. This information points to a variety of possible conclusions. The first conclusion assumes a very flexible bearing pad in use at each connection, one that is able to accommodate all connection motion without reaching a slipping

point. A second conclusion could be made indicating that the stiffness of both the substructure and superstructure were so similar that the resulting differential movement between the two at the connection zones was minimal and did not cause slipping. This second conclusion is not supported by shear bolt behavior however; which did carry a significant load at the connection location. Results seem to favor the first conclusion, but the lack of slipping is still noted.

Table 7.9: Results Overview for Lower Limit Friction Scarham Creek Transverse Model

Scarham	Friction ".2"												
Transverse Motion	Ground Motion	Run Status	Run Time	Foundation Capacity (D/R)		Bearing Capacity	Bent Ductility	Bolt Status	Max Column Shear	Max Span Disp. (in.)	Max Bent Disp. (in.)	Residual Span Disp. (in.)	Residual Bent Disp. (in.)
San Fernando 1	Design	Comp.	48.00	0.286	0.4461	0.023	2.322	0.848	1761.905	4.341	**3.742**	0.015	0.008
San Fernando 2	Design	Comp.	50.00	0.255	0.3800	0.023	1.877	0.746	1735.696	3.652	**3.104**	0.031	0.039
Imperial Valley	Design	Comp.	60.00	0.134	0.1747	0.020	0.905	0.565	1379.593	1.676	**1.367**	0.010	0.007
Coalinga	Design	Comp.	52.00	0.190	0.2618	0.020	1.408	0.696	1626.783	2.798	**2.381**	0.034	0.027
North Palm Springs	Design	Comp.	40.00	0.144	0.2140	0.020	1.071	0.567	1430.486	2.049	**1.669**	0.012	0.009
Landers	Design	Comp.	70.00	0.317	0.5033	0.024	2.643	**0.943**	1853.291	4.846	**4.235**	0.041	0.017
Little Skull Mountain	Design	Comp.	132.00	0.055	0.0750	0.018	0.376	0.184	1174.141	0.736	0.597	0.011	0.008
Kocaeli 1	Design	Comp.	170.00	0.335	0.5500	0.026	2.823	**0.991**	2010.688	5.219	**4.549**	0.104	0.041
Kocaeli 2	Design	Comp.	48.00	0.256	0.3700	0.022	1.864	0.768	1759.118	3.541	**3.018**	0.017	0.014
Kobe	Design	Comp.	60.00	0.111	0.1638	0.020	0.733	0.308	1327.181	1.413	**1.185**	0.013	0.010
Mean				0.2084	0.3139	0.0215	1.6023	0.6615	1605.8882	3.0270	**2.5846**	0.0288	0.0181
Standard Deviation				0.0950	0.1593	0.0025	0.8366	0.2610	265.8816	1.5342	**1.3605**	0.0286	0.0130
Relative Stand Deviation				45.57%	50.74%	11.48%	52.21%	39.46%	16.56%	50.68%	52.64%	99.35%	71.50%

Table 7.10: Results Overview for Upper Limit Friction Scarham Creek Transverse Model

Scarham	Friction ".4"												
Transverse Motion	Ground Motion	Run Status	Run Time	Foundation Capacity (D/R)		Bearing Capacity	Bent Ductility	Bolt Status	Max Column Shear	Max Span Disp. (in.)	Max Bent Disp. (in.)	Residual Span Disp. (in.)	Residual Bent Disp. (in.)
San Fernando 1	Design	Comp.	48.00	0.286	0.4461	0.023	2.322	0.848	1761.905	4.341	**3.742**	0.015	0.008
San Fernando 2	Design	Comp.	50.00	0.255	0.3800	0.023	1.877	0.746	1735.696	3.652	**3.104**	0.031	0.039
Imperial Valley	Design	Comp.	60.00	0.134	0.1747	0.020	0.905	0.565	1379.593	1.676	**1.367**	0.010	0.007
Coalinga	Design	Comp.	52.00	0.190	0.2618	0.020	1.408	0.696	1626.783	2.798	**2.381**	0.034	0.027
North Palm Springs	Design	Comp.	40.00	0.144	0.2140	0.020	1.071	0.567	1430.486	2.049	**1.669**	0.012	0.009
Landers	Design	Comp.	70.00	0.317	0.5033	0.024	2.643	**0.943**	1853.291	4.846	**4.235**	0.041	0.017
Little Skull Mountain	Design	Comp.	132.00	0.055	0.0750	0.018	0.376	0.184	1174.141	0.736	0.597	0.011	0.008
Kocaeli 1	Design	Comp.	170.00	0.335	0.5500	0.026	2.823	**0.991**	2010.688	5.219	**4.549**	0.430	0.315
Kocaeli 2	Design	Comp.	48.00	0.256	0.3700	0.022	1.864	0.768	1759.118	3.541	**3.018**	0.017	0.014
Kobe	Design	Comp.	60.00	0.111	0.1638	0.020	0.733	0.308	1327.181	1.413	**1.185**	0.013	0.010
Mean				0.2084	0.3139	0.0214	1.6023	0.6615	1605.8882	3.0270	**2.5846**	0.0614	0.0455
Standard Deviation				0.0950	0.1593	0.0023	0.8366	0.2610	265.8816	1.5342	**1.3604**	0.1300	0.0952
Relative Stand Deviation				45.57%	50.74%	10.91%	52.21%	39.46%	16.56%	50.68%	52.64%	**211.69%**	**209.21%**

A total of fourteen MCE level events were applied to this bridge model. All transverse MCE level analyses of the Scarham Creek Bridge ran successfully. Only one case of limit exceedance was reported and the results can be found in Table 7.11 and Table 7.12. Results between the two friction models are the same with the exception of the Landers MCE event. This event in the upper friction limit model results in a high foundation rotation case similar to the cases recorded for longitudinal motion. All residual displacements are below the 1" limit, indicating acceptable serviceability of the structure post event.

Table 7.11: MCE Level Results Overview for Lower Limit Friction Scarham Creek Transverse Model

Scarham	Friction ".2"												
Transverse Motion	Ground Motion	Run Status	Run Time	Foundation Capacity (D/R)		Bearing Capacity	Bent Ductility	Bolt Status	Max Column Shear	Max Span Disp.	Max Bent Disp.	Residual Span Disp.	Residual Bent Disp.
San Fernando 1	MCE	Comp.	48.00	0.306	0.4732	0.024	2.536	**0.926**	1785.350	4.746	4.068	0.017	0.010
San Fernando 2	MCE	Comp.	50.00	0.318	0.5100	0.024	2.553	**0.967**	1921.752	4.897	4.183	0.023	0.027
Imperial Valley	MCE	Comp.	60.00	0.190	0.2381	0.021	1.305	0.793	1520.694	2.387	1.956	0.008	0.006
Landers	MCE	Comp.	70.00	0.305	0.4258	0.025	2.565	**0.983**	1953.014	5.384	4.390	0.615	0.727
Kocaeli 1	MCE	Comp.	170.00	0.308	0.4700	0.027	2.585	**0.994**	1714.110	5.025	4.215	0.438	0.351
Kocaeli 2	MCE	Comp.	48.00	0.335	0.4067	0.027	3.095	**0.979**	2172.828	5.808	5.009	0.200	0.103
Kobe	MCE	Comp.	60.00	0.172	0.2382	0.021	1.152	0.496	1462.366	2.090	1.775	0.016	0.012
Mean				0.2762	0.3946	0.0241	2.2558	0.8769	1790.0164	4.3338	3.6565	0.1881	0.1766
Standard Deviation				0.0661	0.1120	0.0025	0.7300	0.1816	250.3800	1.4756	1.2623	0.2462	0.2724
Relative Stand Deviation				23.93%	28.38%	10.43%	32.36%	20.71%	13.99%	34.05%	34.52%	**130.89%**	**154.25%**

Table 7.12: MCE Level Results Overview for Upper Limit Friction Scarham Creek Transverse Model

Scarham	Friction ".4"												
Transverse Motion	Ground Motion	Run Status	Run Time	Foundation Capacity (D/R)		Bearing Capacity	Bent Ductility	Bolt Status	Max Column Shear	Max Span Disp.	Max Bent Disp.	Residual Span Disp.	Residual Bent Disp.
San Fernando 1	MCE	Comp.	48.00	0.306	0.4732	0.024	2.536	**0.926**	1785.350	4.746	4.068	0.017	0.010
San Fernando 2	MCE	Comp.	50.00	0.318	0.5100	0.024	2.553	**0.967**	1921.752	4.897	4.183	0.023	0.027
Imperial Valley	MCE	Comp.	60.00	0.190	0.2381	0.021	1.305	0.793	1520.694	2.387	1.956	0.008	0.006
Landers	MCE	Comp.	70.00	0.363	**1.5600**	0.058	4.863	**0.997**	1848.441	7.307	5.368	0.293	0.640
Kocaeli 1	MCE	Comp.	170.00	0.308	0.6367	0.028	2.585	**0.957**	1928.681	7.244	5.558	0.754	0.428
Kocaeli 2	MCE	Comp.	48.00	0.335	0.4233	0.025	3.095	**0.979**	2172.574	5.809	5.007	0.557	0.349
Kobe	MCE	Comp.	60.00	0.172	0.2382	0.021	1.152	0.496	1462.366	2.090	1.775	0.016	0.012
Mean				0.2845	0.5828	0.0287	2.5841	0.8738	1805.6941	4.9257	3.9878	0.2382	0.2103
Standard Deviation				0.0735	0.4543	0.0132	1.2346	0.1798	246.4877	2.0954	1.5536	0.3078	0.2601
Relative Stand Deviation				25.83%	77.95%	46.08%	47.78%	20.58%	13.65%	42.54%	38.96%	**129.22%**	**123.71%**

7.3.2 Longitudinal Motion

The longitudinal analysis for this bridge resulted in fairly consistent design level results. See Table 7.13 and Table 7.14 for an overview of the design level transverse results. Maximum span displacements of about 2.5 inches occurred for most ground motions in each bridge model, and bent displacements hovered around 2 inches. These results are to be expected in bridges with such tall columns. Bent ductility appears to remain below the established maximum for the second and fourth bent (1.076 inches), with only one design level ground motion, (San Fernando 2) causing a ductility in excess of this limit. Foundation capacity for this bridge exceeds the displacement limit set by geotechnical data. This foundation displacement is present in all design level events, and is thus a conclusive failure in the longitudinal direction of this bridge. These deformations at foundation level are a result of shear forces carried by the substructure, and not a product of excessive moments or structural failures.

Table 7.13: Results Overview for Lower Limit Friction Scarham Creek Longitudinal Model

Scarham	Friction ".2"											
Longitudinal Motion	Ground Motion	Run Status	Run Time	Foundation Capacity (D/R)		Bearing Capacity	Bent Ductility	Max Column Shear	Max Span Disp. (in.)	Max Bent Disp. (in.)	Residual Span Disp. (in.)	Residual Bent Disp. (in.)
San Fernando 1	Design	Comp.	48.00	**1.685**	0.2917	0.278	0.787	968.259	2.927	2.459	0.413	0.355
San Fernando 2	Design	Comp.	50.00	**1.868**	0.3976	0.239	1.081	1046.208	3.682	3.174	0.453	0.267
Imperial Valley	Design	Comp.	60.00	**1.698**	0.2767	0.195	0.714	973.824	2.729	2.453	0.372	0.250
Coalinga	Design	Comp.	52.00	**1.692**	0.2185	0.182	0.695	971.426	2.341	1.900	0.405	0.275
North Palm Springs	Design	Comp.	40.00	**1.648**	0.1456	0.125	0.520	952.760	1.535	1.249	0.062	0.060
Landers	Design	Comp.	70.00	**1.703**	0.2891	0.234	0.765	975.806	3.013	2.445	0.211	0.131
Little Skull Mountain	Design	Comp.	132.00	**1.600**	0.0814	0.042	0.385	932.183	0.689	0.592	0.172	0.050
Kocaeli 1	Design	Comp.	170.00	**1.744**	0.3006	0.223	0.782	993.502	3.023	2.638	0.240	0.123
Kocaeli 2	Design	Comp.	48.00	**1.718**	0.2314	0.206	0.657	982.143	2.620	2.002	0.050	0.002
Kobe	Design	Comp.	60.00	**1.663**	0.2282	0.180	0.672	958.920	2.380	1.971	0.296	0.178
Mean				**1.7019**	0.2461	0.1905	0.7058	975.5031	2.4938	2.0882	0.2674	0.1691
Standard Deviation				0.0706	0.0878	0.0663	0.1819	30.0148	0.8453	0.7362	0.1448	0.1152
Relative Stand Deviation				4.15%	35.66%	34.80%	25.77%	3.08%	33.90%	35.25%	54.17%	68.11%

Table 7.14: Results Overview for Upper Limit Friction Scarham Creek Longitudinal Model

Scarham	Friction ".4"											
Longitudinal Motion	Ground Motion	Run Status	Run Time	Foundation Capacity (D/R)		Bearing Capacity	Bent Ductility	Max Column Shear	Max Span Disp. (in.)	Max Bent Disp. (in.)	Residual Span Disp. (in.)	Residual Bent Disp. (in.)
San Fernando 1	Design	Comp.	48.00	**1.722**	0.3486	0.207	0.889	984.097	3.294	2.961	0.010	0.002
San Fernando 2	Design	Fail	4.45	**1.640**	0.4037	0.235	1.108	949.414	3.950	3.342		
Imperial Valley	Design	Comp.	60.00	**1.744**	0.2974	0.215	0.959	993.480	3.203	2.680	0.131	0.094
Coalinga	Design	Comp.	52.00	**1.690**	0.2340	0.135	0.764	970.624	2.328	2.038	0.217	0.129
North Palm Springs	Design	Comp.	40.00	**1.653**	0.1456	0.119	0.520	954.562	1.535	1.247	0.174	0.051
Landers	Design	Comp.	70.00	**1.757**	0.3303	0.211	0.962	998.828	3.277	2.847	0.112	0.061
Little Skull Mountain	Design	Comp.	132.00	**1.600**	0.0814	0.042	0.385	932.183	0.689	0.592	0.172	0.050
Kocaeli 1	Design	Comp.	170.00	**1.787**	0.3242	0.210	0.976	1011.495	3.447	2.837	0.022	0.063
Kocaeli 2	Design	Comp.	48.00	**1.707**	0.2398	0.174	0.701	977.714	2.592	2.165	0.103	0.022
Kobe	Design	Comp.	60.00	**1.726**	0.2342	0.167	0.904	985.809	2.727	2.054	0.165	0.081
Mean				**1.7026**	0.2639	0.1714	0.8168	975.8206	2.7042	2.2762	0.1229	0.0614
Standard Deviation				0.0575	0.0975	0.0587	0.2248	24.4181	0.9780	0.8447	0.0700	0.0376
Relative Stand Deviation				3.38%	36.94%	34.26%	27.53%	2.50%	36.17%	37.11%	56.94%	61.27%

A total of fourteen MCE level events were applied to this bridge model. See Table 7.15 and Table 7.16 for an overview of the MCE level longitudinal results. Only six of the fourteen analyses were completed with all incomplete analyses showing signs of possible structural failure. It is difficult to classify the MCE level of behavior for this bridge as acceptable given the large amount of unknowns found in the results. Conservative estimates would suggest that this bridge's behavior is unsuitable for an MCE level event.

Table 7.15: MCE Level Results Overview for Lower Limit Friction Scarham Creek Longitudinal Model

Scarham	Friction ".2"											
Longitudinal Motion	Ground Motion	Run Status	Run Time	Foundation Capacity (D/R)		Bearing Capacity	Bent Ductility	Max Column Shear	Max Span Disp.	Max Bent Disp.	Residual Span Disp.	Residual Bent Disp.
San Fernando 1	MCE	Comp.	48.00	**1.697**	0.3033	0.280	0.840	**973.314**	3.198	2.698	0.431	0.348
San Fernando 2	MCE	Fail	4.39	**1.647**	0.3700	0.315	0.844	**952.314**	3.820	3.299		
Imperial Valley	MCE	Comp.	60.00	**1.721**	0.3089	0.233	0.829	**983.621**	3.118	2.701	0.170	0.150
Landers	MCE	Comp.	70.00	**1.770**	0.3303	0.291	0.835	**1004.557**	3.215	2.864	0.437	0.278
Kocaeli 1	MCE	Fail	24.36	**1.802**	0.5199	0.809	2.462	**1018.009**	3.559	5.110		
Kocaeli 2	MCE	Fail	7.62	**1.819**	0.3119	0.323	0.757	**1025.210**	3.409	2.812		
Kobe	MCE	Comp.	60.00	**1.668**	0.2864	0.247	0.792	**960.924**	3.037	2.475	0.049	0.075
Mean				1.7320	0.3472	0.3568	1.0514	988.2784	3.3366	3.1369	0.2718	0.2128
Standard Deviation				0.0666	0.0806	0.2021	0.6230	28.2847	0.2768	0.9056	0.1938	0.1231
Relative Stand Deviation				3.84%	23.21%	56.62%	59.25%	2.86%	8.30%	28.87%	71.30%	57.86%

Table 7.16: MCE Level Results Overview for Upper Limit Friction Scarham Creek Longitudinal Model

Scarham	Friction ".4"										
Longitudinal Motion	Ground Motion	Run Status	Run Time	Foundation Capacity (D/R)	Bearing Capacity	Bent Ductility	Max Column Shear	Max Span Disp.	Max Bent Disp.	Residual Span Disp.	Residual Bent Disp.
San Fernando 1	MCE	Comp.	48.00	**1.761**	0.8685	0.451	1.797	**1000.505**	3.425	3.805	**1.139**	0.622
San Fernando 2	MCE	Fail	3.87	**1.641**	0.2634	0.161	0.829	**949.502**	2.515	2.217		
Imperial Valley	MCE	Fail	10.55	**1.760**	0.3517	0.231	1.026	**1000.349**	3.719	2.879		
Landers	MCE	Fail	22.89	**1.740**	0.3578	0.208	1.222	**991.567**	3.595	3.160		
Kocaeli 1	MCE	Fail	22.52	**1.779**	0.5199	0.706	1.061	**1008.230**	3.529	2.960		
Kocaeli 2	MCE	Fail	7.11	**1.666**	0.3272	0.223	1.062	**960.427**	3.806	3.219		
Kobe	MCE	Comp.	60.00	**1.740**	0.3058	0.205	0.957	**991.848**	3.224	2.652	0.076	0.042
Mean				1.7268	0.4278	0.3121	1.1363	986.0612	3.4017	2.9846	0.6075	0.3320
Standard Deviation				0.0523	0.2103	0.1976	0.3146	22.2177	0.4350	0.4951	0.7517	0.4101
Relative Stand Deviation				3.03%	49.17%	63.30%	27.68%	2.25%	12.79%	16.59%	**123.73%**	**123.53%**

7.4 Norfolk Southern Railroad Bridge

Results show that the average behavior of the Norfolk Southern Bridge was favorable for design and MCE level events. Design level events resulted in behaviors typical with stiff elastic bridges, including smaller span displacements and bent deflections. Foundation performance for this bridge was acceptable in both directions of motion. All design level analysis performed for this bridge succeeded in completing in the lateral direction. Three design level analyses performed in the longitudinal direction failed to complete. Substructure behavior appears to be adequate at column and bent cap locations. Connection behavior also appears to be adequate from the results of each analysis with anchor bolts failing, but no cases of unseating. Bearing pad slippage was minimal in both directions of loading, and did not approach levels indicative of unseating. A more in-depth analysis of each bridge model's results is proved in the next sections.

7.4.1 Transverse Motion

The transverse analysis for this bridge resulted in stiff structural behavior. See Table 7.17 and Table 7.18 for an overview of the design level transverse results. Lower bent

displacements are indicative of a stiff substructure. This behavior is in keeping with triple column bridge bents, like the ones present in the Norfolk Southern Railroad Bridge. Design level results from both friction models indicated residual deflections that were within acceptable limits for this bridge. All transverse design level analyses of the Norfolk Southern Railroad Bridge ran successfully. Many anchor bolt failures can be observed in the transverse analyses. These failures are a result of high levels of forces being transferred between the super and substructure of the bridge. This is more common in bridges with stiffer substructures, since the superstructure of each bridge is simply supported with long span lengths and generally behaves in a more flexible manner. Overall these results are in keeping with the predicted behaviors of this bridge.

Table 7.17: Results Overview for Lower Limit Friction Norfolk Southern Railroad Transverse Model

Norfolk	Friction ".2"												
Transverse Motion	Ground Motion	Run Status	Run Time	Foundation Capacity (D/R)		Bearing Capacity	Bent Ductility	Bolt Status	Max Column Shear	Max Span Disp. (in.)	Max Bent Disp. (in.)	Residual Span Disp. (in.)	Residual Bent Disp. (in.)
San Fernando 1	Design	Comp.	48.00	0.124	0.0095	0.115	0.768	**0.981**	28.022	0.973	0.941	0.049	0.162
San Fernando 2	Design	Comp.	50.00	0.083	0.0004	0.040	0.554	0.798	17.716	0.810	0.717	0.020	0.018
Imperial Valley	Design	Comp.	60.00	0.125	0.0143	0.146	0.816	**0.982**	19.424	1.221	**1.019**	0.066	0.181
Coalinga	Design	Comp.	52.00	0.124	0.0005	0.049	0.768	**0.986**	20.088	1.000	0.942	0.017	0.052
North Palm Springs	Design	Comp.	40.00	0.115	0.0007	0.050	0.715	**0.997**	18.315	0.985	0.877	0.019	0.000
Landers	Design	Comp.	70.00	0.141	0.0101	0.160	0.869	**0.990**	23.942	1.305	**1.070**	0.060	0.183
Little Skull Mountain	Design	Comp.	132.00	0.014	0.0005	0.011	0.133	0.221	17.246	0.223	0.185	0.019	0.014
Kocaeli 1	Design	Comp.	170.00	0.147	0.0148	0.194	0.950	**0.991**	32.714	1.769	**1.193**	0.326	0.153
Kocaeli 2	Design	Comp.	48.00	0.138	0.0173	0.216	0.861	**0.990**	20.060	1.748	**1.059**	0.070	0.198
Kobe	Design	Comp.	60.00	0.092	0.0007	0.042	0.612	0.846	18.093	0.849	0.768	0.030	0.027
Mean				0.1104	0.0069	0.1024	0.7046	0.8782	21.5621	1.0882	0.8771	0.0676	0.0988
Standard Deviation				0.0394	0.0070	0.0732	0.2332	0.2412	5.1289	0.4567	0.2817	0.0932	0.0826
Relative Stand Deviation				35.65%	**101.77%**	71.47%	33.10%	27.47%	23.79%	41.97%	32.12%	**137.84%**	83.53%

Table 7.18: Results Overview for Upper Limit Friction Norfolk Southern Railroad Transverse Model

Norfolk	Friction ".4"												
Transverse Motion	Ground Motion	Run Status	Run Time	Foundation Capacity (D/R)		Bearing Capacity	Bent Ductility	Bolt Status	Max Column Shear	Max Span Disp. (in.)	Max Bent Disp. (in.)	Residual Span Disp. (in.)	Residual Bent Disp. (in.)
San Fernando 1	Design	Comp.	48.00	0.124	0.0088	0.107	0.768	**0.983**	27.118	0.973	0.941	0.010	0.049
San Fernando 2	Design	Comp.	50.00	0.083	0.0004	0.040	0.554	0.798	17.716	0.810	0.717	0.020	0.018
Imperial Valley	Design	Comp.	60.00	0.125	0.0119	0.121	0.816	**0.982**	22.432	1.120	**1.019**	0.013	0.031
Coalinga	Design	Comp.	52.00	0.124	0.0005	0.049	0.768	**0.986**	20.088	1.000	0.942	0.017	0.052
North Palm Springs	Design	Comp.	40.00	0.115	0.0007	0.050	0.715	**0.997**	18.315	0.985	0.877	0.018	0.001
Landers	Design	Comp.	70.00	0.539	0.0054	0.136	3.173	**0.993**	37.700	1.481	**3.837**	**1.014**	3.602
Little Skull Mountain	Design	Comp.	132.00	0.014	0.0005	0.011	0.133	0.221	17.246	0.223	0.185	0.019	0.014
Kocaeli 1	Design	Comp.	170.00	0.112	0.0160	0.176	0.747	**0.991**	28.415	1.496	0.949	0.021	0.103
Kocaeli 2	Design	Comp.	48.00	0.118	0.0114	0.150	0.754	**0.990**	29.420	1.407	0.952	0.032	0.023
Kobe	Design	Comp.	60.00	0.092	0.0007	0.042	0.612	0.846	18.093	0.849	0.768	0.030	0.027
Mean				0.1446	0.0056	0.0881	0.9039	0.8787	23.6542	1.0343	**1.1187**	0.1194	0.3920
Standard Deviation				0.1425	0.0060	0.0563	0.8216	0.2415	6.7916	0.3814	0.9850	0.3144	1.1282
Relative Stand Deviation				98.51%	**105.47%**	63.86%	90.90%	27.48%	28.71%	36.87%	88.05%	**263.32%**	**287.78%**

A total of fourteen MCE level events were analyzed with this bridge model. See Table 7.19 and Table 7.20 for an overview of the MCE level transverse results. A majority of these MCE results indicated lower bent displacements and span displacements with a single exception. This behavior is in keeping with triple column bridge bents, like the ones present in the Norfolk Southern Railroad Bridge. The Landers event for the lower friction limit model resulted in behavior that is indicative of span unseating. A high bearing pad displacement was recorded as well as a high residual displacement. High residual displacement was also recorded in the upper bound friction model during the same ground motion. All transverse design level analyses of the Norfolk Southern Railroad Bridge ran successfully. Many anchor bolt failures were observed in the MCE level transverse analyses. This is more common in bridges with stiffer substructures, since the superstructure of each bridge is simply supported with long span lengths and generally behaves in a more flexible manner. Overall these results are in keeping with the predicted behaviors of this bridge, and the average behavior of these models indicates acceptable behavior at the MCE level.

Table 7.19: MCE Level Results Overview for Lower Limit Friction Norfolk Southern Railroad Transverse Model

Norfolk	Friction ".2"												
Transverse Motion	Ground Motion	Run Status	Run Time	Foundation Capacity (D/R)		Bearing Capacity	Bent Ductility	Bolt Status	Max Column Shear	Max Span Disp.	Max Bent Disp.	Residual Span Disp.	Residual Bent Disp.
San Fernando 1	MCE	Comp.	48.00	0.128	0.0092	0.109	0.783	**0.979**	26.267	0.974	0.954	0.043	0.148
San Fernando 2	MCE	Comp.	50.00	0.124	0.0138	0.173	0.771	**0.978**	30.382	1.441	0.947	0.051	0.017
Imperial Valley	MCE	Comp.	60.00	0.222	0.0088	0.195	1.383	**0.996**	22.689	2.006	1.699	0.411	0.420
Landers	MCE	Comp.	70.00	0.434	0.0542	**1.492**	2.977	**0.986**	34.799	14.166	6.326	**13.606**	**5.907**
Kocaeli 1	MCE	Comp.	170.00	0.240	0.0263	0.274	1.506	**0.910**	30.369	2.176	1.882	0.883	0.050
Kocaeli 2	MCE	Comp.	48.00	0.271	0.0053	0.219	1.624	**0.993**	20.615	2.161	1.986	0.516	0.525
Kobe	MCE	Comp.	60.00	0.189	0.0054	0.164	1.165	**0.947**	21.888	1.610	1.439	0.337	0.370
Mean				0.2295	0.0176	0.3750	1.4584	0.9698	26.7156	3.5048	2.1762	2.2639	1.0624
Standard Deviation				0.1055	0.0177	0.4950	0.7481	0.0310	5.3084	4.7212	1.8762	5.0097	2.1450
Relative Stand Deviation				45.97%	**100.84%**	**132.00%**	51.30%	3.20%	19.87%	**134.70%**	86.21%	**221.29%**	**201.89%**

Table 7.20: MCE Level Results Overview for Upper Limit Friction Norfolk Southern Railroad Transverse Model

Norfolk	Friction ".4"												
Transverse Motion	Ground Motion	Run Status	Run Time	Foundation Capacity (D/R)		Bearing Capacity	Bent Ductility	Bolt Status	Max Column Shear	Max Span Disp.	Max Bent Disp.	Residual Span Disp.	Residual Bent Disp.
San Fernando 1	MCE	Comp.	48.00	0.128	0.0084	0.102	0.783	**0.979**	25.533	0.974	0.954	0.003	0.069
San Fernando 2	MCE	Comp.	50.00	0.124	0.0147	0.198	0.833	**0.978**	31.423	1.828	1.080	0.281	0.115
Imperial Valley	MCE	Comp.	60.00	0.178	0.0059	0.163	1.129	**0.996**	24.991	1.721	1.402	0.018	0.081
Landers	MCE	Comp.	70.00	0.353	0.0053	0.402	1.267	**0.971**	34.230	4.577	1.618	**3.399**	0.348
Kocaeli 1	MCE	Comp.	170.00	0.293	0.0064	0.243	1.847	**0.995**	40.217	2.582	2.276	0.096	0.283
Kocaeli 2	MCE	Comp.	48.00	0.234	0.0125	0.208	1.452	**0.993**	28.246	2.028	1.812	0.097	0.123
Kobe	MCE	Comp.	60.00	0.173	0.0126	0.175	1.085	**0.963**	27.853	1.627	1.342	0.148	0.048
Mean				0.2117	0.0094	0.2130	1.1994	0.9821	30.3562	2.1911	1.4978	0.5775	0.1524
Standard Deviation				0.0862	0.0038	0.0942	0.3683	0.0129	5.4184	1.1564	0.4513	1.2476	0.1159
Relative Stand Deviation				40.72%	40.62%	44.22%	30.71%	1.31%	17.85%	52.77%	30.13%	**216.05%**	76.00%

7.4.2 Longitudinal Motion

The longitudinal analysis for this bridge resulted in fairly consistent results. See Table 7.21 and Table 7.22 for an overview of the design level longitudinal results. Maximum span displacements of about 1 inch occurred for most design level ground motions in each bridge model, and bent displacements hovered around 1.1 inches. These results are to be expected in bridges with such stiff substructure. Bent ductility appears to remain well below the established maximum (3.88 inches). Foundation capacity for this bridge does not exceed the displacement limit set by geotechnical data. Recorded column shears for this model appear to be incorrectly

recorded due to very small recorded values when compared to every other analysis performed in the chapter. Three of the design level analyses performed on the models resulted in analysis failure, with the Kocaeli 1 event resulting in possible structural failure. The results from this event only last for 22.52 seconds of the applied ground motion, but they already exhibit reasonable bridge response before the largest accelerations are even applied. A judgment was made to classify these results as a possible structural failure. Despite this, overall behavior of this bridge appears to be sufficient in the design level longitudinal direction.

Table 7.21: Results Overview for Lower Limit Friction Norfolk Southern Longitudinal Model

Norfolk	Friction ".2"											
Longitudinal Motion	Ground Motion	Run Status	Run Time	Foundation Capacity (D/R)		Bearing Capacity	Bent Ductility	Max Column Shear	Max Span Disp. (in.)	Max Bent Disp. (in.)	Residual Span Disp. (in.)	Residual Bent Disp. (in.)
San Fernando 1	Design	Num.	17.44	0.061	0.2009	0.180	0.593	3.332	1.564	0.891		
San Fernando 2	Design	Comp.	50.00	0.066	0.3339	0.500	0.670	7.527	2.272	1.263	0.245	0.110
Imperial Valley	Design	Comp.	60.00	0.066	0.1801	0.233	0.382	6.051	1.078	0.595	0.214	0.094
Coalinga	Design	Comp.	52.00	0.065	0.2494	0.405	0.741	6.556	1.749	1.146	0.333	0.191
North Palm Springs	Design	Comp.	40.00	0.063	0.1871	0.276	0.462	3.271	1.155	0.668	0.327	0.194
Landers	Design	Comp.	70.00	0.352	0.2065	0.376	0.762	306.738	1.622	1.073	0.707	0.229
Little Skull Mountain	Design	Comp.	132.00	0.063	0.0379	0.074	0.178	3.079	0.284	0.185	0.044	0.046
Kocaeli 1	Design	Comp.	170.00	0.064	0.2286	0.340	0.560	7.162	1.486	0.835	0.262	0.127
Kocaeli 2	Design	Comp.	48.00	0.064	0.1968	0.318	0.549	8.072	1.367	0.817	0.343	0.176
Kobe	Design	Comp.	60.00	0.063	0.1427	0.278	0.454	4.119	1.169	0.656	0.283	0.157
Mean				0.0963	0.1959	0.3109	0.5288	39.1749	1.3536	0.8043	0.3064	0.1471
Standard Deviation				0.0961	0.0800	0.1196	0.1855	100.3530	0.5458	0.3295	0.1756	0.0577
Relative Stand Deviation				99.79%	40.85%	38.46%	35.08%	**256.17%**	40.32%	40.97%	57.30%	39.19%

Table 7.22: Results Overview for Upper Limit Friction Norfolk Southern Longitudinal Model

Norfolk	Friction ".4"											
Longitudinal Motion	Ground Motion	Run Status	Run Time	Foundation Capacity (D/R)		Bearing Capacity	Bent Ductility	Max Column Shear	Max Span Disp. (in.)	Max Bent Disp. (in.)	Residual Span Disp. (in.)	Residual Bent Disp. (in.)
San Fernando 1	Design	Comp.	48.00	0.063	0.2356	0.295	0.493	3.870	1.259	0.730	0.036	0.028
San Fernando 2	Design	Comp.	50.00	0.275	0.3686	0.536	0.779	285.206	2.425	1.450	0.225	0.276
Imperial Valley	Design	Comp.	60.00	0.065	0.1871	0.250	0.427	6.588	1.099	0.627	0.040	0.037
Coalinga	Design	Comp.	52.00	0.086	0.2910	0.507	0.924	13.648	2.216	1.459	0.214	0.131
North Palm Springs	Design	Num.	8.10	0.061	0.2425	0.346	0.624	2.613	1.515	0.946		
Landers	Design	Comp.	70.00	0.320	0.2647	0.371	1.181	288.173	2.041	1.437	0.486	0.027
Little Skull Mountain	Design	Comp.	132.00	0.063	0.0379	0.074	0.178	3.096	0.284	0.185	0.044	0.046
Kocaeli 1	Design	Fail.	22.52	0.062	0.3298	0.401	0.651	2.690	1.857	1.232		
Kocaeli 2	Design	Comp.	48.00	0.064	0.2217	0.298	0.501	10.761	1.359	0.793	0.025	0.001
Kobe	Design	Comp.	60.00	0.063	0.1690	0.249	0.421	4.074	1.043	0.599	0.041	0.035
Mean				0.0983	0.2171	0.3054	0.5970	41.6123	1.3949	0.8828	0.1389	0.0726
Standard Deviation				0.0900	0.0895	0.1278	0.3175	99.7030	0.6290	0.4512	0.1628	0.0905
Relative Stand Deviation				91.52%	41.24%	41.85%	53.18%	**239.60%**	45.09%	51.11%	**117.21%**	**124.68%**

A total of fourteen MCE level events were applied to this bridge model. See Table 7.23 and Table 7.24 for an overview of the MCE level longitudinal results. Ten of the fourteen analyses ran completely. Three of the four that did not complete were determined to cause possible failure in the form of eventual span unseating. The displacements of the bearing pads in these analyses were relatively high at the time of analysis failure. This combined with the fact that these analysis ceased before sections of the largest ground motion accelerations were applied to the models lead to the prediction of possible unseating. This was determined due to high recorded bearing displacements during sections of the ground motion that proceeded larger ground motion accelerations that were never applied in the analysis. The overall behavior of this bridge appears to be acceptable for critical and essential bridges.

Table 7.23: MCE Level Results Overview for Lower Limit Friction Norfolk Southern Longitudinal Model

Norfolk	Friction ".2"											
Longitudinal Motion	Ground Motion	Run Status	Run Time	Foundation Capacity (D/R)		Bearing Capacity	Bent Ductility	Max Column Shear	Max Span Disp.	Max Bent Disp.	Residual Span Disp.	Residual Bent Disp.
San Fernando 1	MCE	Comp.	48.00	0.063	0.2425	0.363	0.596	**5.178**	1.578	0.895	0.051	0.004
San Fernando 2	MCE	Comp.	50.00	0.064	0.3810	0.563	0.811	**8.467**	2.542	1.505	0.099	0.119
Imperial Valley	MCE	Comp.	60.00	0.065	0.2660	0.361	0.488	**6.479**	1.639	0.953	0.218	0.109
Landers	MCE	Comp.	70.00	0.350	0.2314	0.439	0.842	**316.381**	1.924	1.286	0.171	0.360
Kocaeli 1	MCE	Fail.	23.40	0.067	0.3131	0.493	0.861	**3.548**	2.173	1.352		
Kocaeli 2	MCE	Fail.	6.95	0.061	0.3048	0.370	0.568	**2.696**	1.721	1.091		
Kobe	MCE	Comp.	60.00	0.063	0.2120	0.364	0.658	**4.725**	1.565	1.001	0.379	0.230
Mean				0.1046	0.2787	0.4219	0.6890	49.6392	1.8775	1.1548	0.1836	0.1645
Standard Deviation				0.1084	0.0585	0.0801	0.1488	117.6375	0.3651	0.2287	0.1268	0.1354
Relative Stand Deviation				**103.58%**	20.97%	18.99%	21.60%	**236.98%**	19.45%	19.81%	69.04%	82.34%

Table 7.24: MCE Level Results Overview for Upper Limit Friction Norfolk Southern Longitudinal Model

Norfolk	Friction ".4"											
Longitudinal Motion	Ground Motion	Run Status	Run Time	Foundation Capacity (D/R)		Bearing Capacity	Bent Ductility	Max Column Shear	Max Span Disp.	Max Bent Disp.	Residual Span Disp.	Residual Bent Disp.
San Fernando 1	MCE	Comp.	48.00	0.064	0.2536	0.325	0.538	**6.219**	1.395	0.820	0.031	0.016
San Fernando 2	MCE	Num.	15.26	0.325	0.3907	0.577	0.848	**121.211**	2.593	1.569		
Imperial Valley	MCE	Comp.	60.00	0.064	0.2633	0.336	0.550	**9.397**	1.543	0.943	0.026	0.001
Landers	MCE	Comp.	70.00	**23.185**	0.3575	0.509	27.825	**438.334**	3.154	1.645	0.556	0.138
Kocaeli 1	MCE	Fail.	21.58	0.063	0.2882	0.372	0.694	**2.932**	1.638	1.115		
Kocaeli 2	MCE	Comp.	48.00	0.072	0.2536	0.381	0.762	**14.259**	1.711	1.180	0.108	0.070
Kobe	MCE	Comp.	60.00	0.063	0.2217	0.355	0.613	**5.940**	1.523	0.925	0.093	0.051
Mean				3.4052	0.2898	0.4078	4.5473	85.4702	1.9366	1.1709	0.1628	0.0552
Standard Deviation				8.7226	0.0616	0.0964	10.2653	161.2800	0.6675	0.3221	0.2228	0.0538
Relative Stand Deviation				**256.15%**	21.24%	23.64%	**225.74%**	**188.70%**	34.47%	27.51%	**136.86%**	97.50%

7.5 Oseligee Creek Bridge

Results show that the average behavior of the Oseligee Creek Bridge was mixed for design and MCE level events. Design level events resulted in behaviors typical with flexible bridges, including larger span displacements and bent deflections. These large span deflections and bent deflections also lead to some cases of collapse of the bridge model. Foundation performance for this bridge was also mixed, and varied from event to event. All design and MCE level analysis performed for this bridge succeeded in completing except for one transverse analysis at each level. Substructure behavior appears to be inadequate at column and foundation

locations due to the large scour situation recommended by geotechnical information. Connection behavior appears to be adequate from the results of each analysis, with design level unseating only occurring in cases of bridge collapse. A more in-depth analysis of each bridge model's results is proved in the next sections.

7.5.1 Transverse Motion

The transverse analysis for this bridge resulted in flexible structural behavior. See Table 7.25 and Table 7.26 for an overview of the design level transverse results. High bent displacements are indicative of a flexible substructure able to accommodate large deflections. This behavior is in keeping with tall column bridge bents, like the ones present in the 100% scour condition of the Oseligee Creek Bridge. Excessive deflections were a concern for the transverse motion of this bridge, in both span and bent locations. These deflections led to the collapse of the lower limit friction bridge model during the design level Landers event. A hallmark of long period structures is large deflections, especially during certain ground motions. Results from both friction models indicated a majority of design level deflections that were within acceptable limits for this bridge. The ductility for both models exceeds the limit stated in Table 6.5 of Section 6.3 during the second San Fernando event, however the limit established for ductility of this bridge did not incorporate a 100% scour case. This 100% scour case could alter the limits established by the static pushover analysis. All transverse design level analyses of the Oseligee Creek Bridge ran successfully with the exception of the Landers ground motion applied to the upper limit friction model. This design level event was assumed to cause a collapse failure

due to the results observed from the previous model, as well as the results recorded before the analysis ceased. Excessive foundation rotations were also observed in 14 of the 20 design level transverse analyses, with a few other recorded rotations approaching the rotational limits. Ground motion analyses that exhibit these large foundation rotations also tended to exhibit bolt failures at the connection locations.

Table 7.25: Results Overview for Lower Limit Friction Oseligee Creek Transverse Model

Oseligee	Friction ".2"												
Transverse Motion	Ground Motion	Run Status	Run Time	Foundation Capacity (D/R)		Bearing Capacity	Bent Ductility	Bolt Status	Max Column Shear	Max Span Disp. (in.)	Max Bent Disp. (in.)	Residual Span Disp. (in.)	Residual Bent Disp. (in.)
San Fernando 1	Design	Comp.	48.00	0.098	**1.0917**	0.245	3.566	**0.985**	492.010	2.087	**1.473**	0.188	0.073
San Fernando 2	Design	Comp.	50.00	0.120	**1.4006**	0.389	5.342	**0.985**	558.379	3.095	**2.205**	0.082	0.028
Imperial Valley	Design	Comp.	60.00	0.106	**1.1223**	0.182	3.389	**0.991**	515.962	1.832	**1.405**	0.068	0.054
Coalinga	Design	Comp.	52.00	0.102	**1.1040**	0.253	3.991	**0.995**	514.999	2.159	**1.645**	0.071	0.022
North Palm Springs	Design	Comp.	40.00	0.101	**1.0336**	0.196	3.213	**1.000**	509.962	1.858	**1.333**	0.051	0.009
Landers	Design	Comp.	70.00	0.199	**3.0673**	**79.975**	27.572	**0.999**	1909.399	786.149	**11.267**	**587.008**	6.838
Little Skull Mountain	Design	Comp.	132.00	0.022	0.1084	0.017	0.455	0.347	361.541	0.320	0.188	0.000	0.000
Kocaeli 1	Design	Comp.	170.00	0.101	**1.0428**	0.050	3.054	**0.996**	498.337	1.710	**1.267**	0.003	0.002
Kocaeli 2	Design	Comp.	48.00	0.116	**1.2355**	0.220	3.693	**0.997**	521.881	2.198	**1.532**	0.099	0.042
Kobe	Design	Comp.	60.00	0.085	0.7951	0.034	2.147	0.686	1525.157	1.276	0.891	0.248	0.047
Mean				0.1050	**1.2001**	**8.1561**	5.6422	0.8981	740.7628	80.2684	**2.3207**	**58.7818**	0.7115
Standard Deviation				0.0430	0.7426	**25.2349**	7.8078	0.2166	525.0808	248.0220	**3.1863**	**185.5998**	2.1527
Relative Stand Deviation				40.93%	61.88%	**309.40%**	**138.38%**	24.11%	70.88%	**308.99%**	**137.30%**	**315.74%**	**302.55%**

Table 7.26: Results Overview for Upper Limit Friction Oseligee Creek Transverse Model

Oseligee	Friction ".4"												
Transverse Motion	Ground Motion	Run Status	Run Time	Foundation Capacity (D/R)		Bearing Capacity	Bent Ductility	Bolt Status	Max Column Shear	Max Span Disp. (in.)	Max Bent Disp. (in.)	Residual Span Disp. (in.)	Residual Bent Disp. (in.)
San Fernando 1	Design	Comp.	48.00	0.099	**1.1070**	0.148	3.554	**0.986**	495.895	1.819	**1.468**	0.304	0.188
San Fernando 2	Design	Comp.	50.00	0.088	0.9694	0.359	5.141	**0.979**	517.882	3.138	**2.116**	0.010	0.002
Imperial Valley	Design	Comp.	60.00	0.107	**1.1193**	0.187	3.389	**0.994**	512.425	1.855	**1.406**	0.108	0.057
Coalinga	Design	Comp.	52.00	0.104	**1.1162**	0.251	3.719	**0.969**	522.410	2.155	**1.539**	0.034	0.009
North Palm Springs	Design	Comp.	40.00	0.103	**1.1193**	0.179	3.827	**0.985**	517.922	1.863	**1.584**	0.038	0.009
Landers	Design	Fail	35.03	0.009	**1.3089**	0.335	2.914	**0.994**	1749.252	3.469	**1.188**		
Little Skull Mountain	Design	Comp.	132.00	0.022	0.1076	0.017	0.464	0.345	362.162	0.327	0.192	0.000	0.000
Kocaeli 1	Design	Comp.	170.00	0.097	0.9572	0.046	2.909	**0.914**	494.917	1.645	**1.204**	0.003	0.003
Kocaeli 2	Design	Comp.	48.00	0.115	**1.2538**	0.172	3.691	**0.988**	521.406	2.260	**1.531**	0.067	0.105
Kobe	Design	Comp.	60.00	0.070	0.5872	0.033	2.050	0.658	452.858	1.194	0.852	0.000	0.004
Mean				0.0813	0.9646	0.1726	3.1658	0.8810	614.7129	1.9726	**1.3079**	0.0627	0.0419
Standard Deviation				0.0370	0.3606	0.1193	1.2380	0.2145	401.6717	0.8934	0.5105	0.0974	0.0652
Relative Stand Deviation				45.49%	37.38%	69.09%	39.11%	24.35%	65.34%	45.29%	39.03%	**155.43%**	**155.58%**

A total of fourteen MCE level events were analyzed with this bridge model. See Table 7.27 and Table 7.28 for an overview of the MCE level transverse results. High bent ductilities

can be observed in these results, as well as high foundation rotations. Four of the fourteen analyses resulted in residual displacements in excess of the 1” limit. All of these undesired behaviors result in questions with this bridge’s adequacy but it is important to consider the 100% scour condition present in this bridge. A reduction in this scour amount would result in lower deflections and a more rigid bridge.

Table 7.27: MCE Level Results Overview for Lower Limit Friction Oseligee Creek Transverse Model

Oseligee	Friction ".2"												
Transverse Motion	Ground Motion	Run Status	Run Time	Foundation Capacity (D/R)		Bearing Capacity	Bent Ductility	Bolt Status	Max Column Shear	Max Span Disp.	Max Bent Disp.	Residual Span Disp.	Residual Bent Disp.
San Fernando 1	MCE	Comp.	48.00	0.088	0.8532	0.370	4.408	**0.984**	488.994	3.041	1.811	0.001	0.004
San Fernando 2	MCE	Comp.	50.00	0.116	**1.3211**	0.623	7.554	**0.986**	589.055	5.049	3.099	0.100	0.033
Imperial Valley	MCE	Comp.	60.00	0.115	**1.2599**	0.257	3.670	**0.995**	525.915	2.209	1.522	0.041	0.013
Landers	MCE	Comp.	70.00	0.114	**1.4343**	0.717	7.496	**0.992**	1674.884	6.938	3.073	**2.127**	**1.554**
Kocaeli 1	MCE	Comp.	170.00	0.194	**2.7278**	0.429	7.303	**0.986**	673.276	3.961	3.019	0.354	0.000
Kocaeli 2	MCE	Comp.	48.00	0.164	**2.1896**	0.342	6.378	**0.986**	636.391	3.338	2.638	0.006	0.023
Kobe	MCE	Comp.	60.00	0.097	**1.1162**	0.260	3.864	**0.980**	492.120	2.100	1.593	0.040	0.016
Mean				0.1269	1.5574	0.4284	5.8103	0.9869	725.8052	3.8051	2.3936	0.3813	0.2348
Standard Deviation				0.0383	0.6608	0.1778	1.7684	0.0050	424.4309	1.7148	0.7246	0.7794	0.5818
Relative Stand Deviation				30.18%	42.43%	41.51%	30.43%	0.51%	58.48%	45.07%	30.27%	**204.44%**	**247.84%**

Table 7.28: MCE Level Results Overview for Upper Limit Friction Oseligee Creek Transverse Model

Oseligee	Friction ".4"												
Transverse Motion	Ground Motion	Run Status	Run Time	Foundation Capacity (D/R)		Bearing Capacity	Bent Ductility	Bolt Status	Max Column Shear	Max Span Disp.	Max Bent Disp.	Residual Span Disp.	Residual Bent Disp.
San Fernando 1	MCE	Comp.	48.00	0.139	**1.7339**	**1.593**	8.055	**0.997**	1678.787	14.866	3.288	**1.726**	**1.940**
San Fernando 2	MCE	Comp.	50.00	0.173	**2.3180**	0.421	7.154	**0.995**	1901.130	3.984	2.954	**1.679**	0.689
Imperial Valley	MCE	Comp.	60.00	0.112	**1.2263**	0.208	3.942	**0.987**	527.159	2.184	1.631	0.135	0.053
Landers	MCE	Comp.	70.00	0.011	**1.6391**	0.042	0.469	**0.979**	1508.386	0.431	0.192	0.132	0.066
Kocaeli 1	MCE	Comp.	170.00	0.153	**2.0000**	0.422	5.439	**0.980**	1375.549	3.498	2.250	**2.146**	0.265
Kocaeli 2	MCE	Comp.	48.00	0.121	**1.4709**	0.320	5.812	**0.999**	586.393	3.003	2.397	0.054	0.058
Kobe	MCE	Comp.	60.00	0.094	**1.1162**	0.183	3.659	**0.987**	483.933	2.024	1.513	0.009	0.013
Mean				0.1147	1.6435	0.4554	4.9330	0.9893	1151.6196	4.2842	2.0322	0.8401	0.4406
Standard Deviation				0.0527	0.4227	0.5196	2.5246	0.0079	601.7111	4.8077	1.0346	0.9576	0.7024
Relative Stand Deviation				45.96%	25.72%	**114.10%**	51.18%	0.80%	52.25%	**112.22%**	50.91%	**113.98%**	**159.44%**

7.5.2 Longitudinal Motion

The longitudinal analysis for this bridge resulted in fairly consistent results. See Table 7.29 and Table 7.30 for an overview of the design level transverse results. Maximum span displacements of about 2 inches occurred for most ground motions in each bridge model, and bent displacements hovered around 1 inch. These results are to be expected in bridges with such tall columns. Bent ductility remains below the established maximum (6 inches), with larger ductility occurring in the upper limit friction model. Foundation capacity for some design level analyses of this bridge exceeds the rotational limit set by geotechnical data. This foundation rotation is present in three design level events, two of which also cause collapse of the bridge. These collapse events also show span unseating and high residual displacements, both behaviors support the conclusion of bridge collapse.

Table 7.29: Results Overview for Lower Limit Friction Oseligee Creek Longitudinal Model

Oseligee	Friction ".2"											
Longitudinal Motion	Ground Motion	Run Status	Run Time	Foundation Capacity (D/R)		Bearing Capacity	Bent Ductility	Max Column Shear	Max Span Disp. (in.)	Max Bent Disp. (in.)	Residual Span Disp. (in.)	Residual Bent Disp. (in.)
San Fernando 1	Design	Comp.	48.00	0.071	0.5780	0.447	2.122	10.342	2.305	1.170	0.044	0.052
San Fernando 2	Design	Comp.	50.00	0.080	0.6728	0.504	2.512	11.138	2.475	1.549	0.352	0.018
Imperial Valley	Design	Comp.	60.00	0.061	0.4373	0.391	1.588	10.781	1.607	0.887	0.063	0.003
Coalinga	Design	Comp.	52.00	0.063	0.4281	0.320	1.439	10.407	1.453	0.835	0.370	0.028
North Palm Springs	Design	Comp.	40.00	0.055	0.3731	0.272	1.307	10.540	1.417	0.721	0.024	0.039
Landers	Design	Comp.	70.00	0.073	0.5872	0.618	2.242	10.594	3.215	1.281	**1.371**	0.018
Little Skull Mountain	Design	Comp.	132.00	0.037	0.2006	0.147	0.728	10.260	0.724	0.443	0.083	0.015
Kocaeli 1	Design	Comp.	170.00	0.065	0.4587	0.353	2.125	10.701	1.683	1.050	0.056	0.027
Kocaeli 2	Design	Comp.	48.00	0.078	0.6697	0.658	2.673	11.807	3.280	1.584	0.504	0.004
Kobe	Design	Comp.	60.00	0.053	0.3211	0.253	1.138	10.215	1.326	0.694	0.199	0.075
Mean				0.0635	0.4727	0.3964	1.7876	10.6785	1.9487	1.0213	0.3066	0.0279
Standard Deviation				0.0129	0.1540	0.1625	0.6391	0.4830	0.8422	0.3757	0.4097	0.0223
Relative Stand Deviation				20.38%	32.58%	40.98%	35.75%	4.52%	43.22%	36.78%	**133.62%**	79.90%

Table 7.30: Results Overview for Upper Limit Friction Oseligee Creek Longitudinal Model

Oseligee	Friction ".4"											
Longitudinal Motion	Ground Motion	Run Status	Run Time	Foundation Capacity (D/R)		Bearing Capacity	Bent Ductility	Max Column Shear	Max Span Disp. (in.)	Max Bent Disp. (in.)	Residual Span Disp. (in.)	Residual Bent Disp. (in.)
San Fernando 1	Design	Comp.	48.00	0.096	0.8899	0.438	3.299	10.324	2.359	1.779	0.422	0.217
San Fernando 2	Design	Comp.	50.00	0.108	**1.1223**	0.523	3.477	10.903	2.983	2.133	0.224	0.090
Imperial Valley	Design	Comp.	60.00	0.066	0.4954	0.277	1.613	10.402	1.630	1.039	0.063	0.033
Coalinga	Design	Comp.	52.00	0.124	**1.8685**	**3.781**	24.891	117.009	2.912	7.636	**2.912**	**2.512**
North Palm Springs	Design	Comp.	40.00	0.075	0.6391	0.321	1.963	11.240	1.817	1.164	0.030	0.033
Landers	Design	Comp.	70.00	0.112	**1.5291**	**4.392**	37.605	128.021	3.104	8.918	**3.086**	**6.413**
Little Skull Mountain	Design	Comp.	132.00	0.038	0.2100	0.124	0.728	10.255	0.756	0.449	0.080	0.010
Kocaeli 1	Design	Comp.	170.00	0.105	**1.0917**	0.422	3.137	12.322	2.579	1.583	0.029	0.006
Kocaeli 2	Design	Comp.	48.00	0.093	0.9602	0.657	3.747	11.664	3.211	2.347	0.033	0.013
Kobe	Design	Comp.	60.00	0.066	0.5015	0.292	1.453	10.214	1.488	0.863	0.155	0.048

Mean	0.0883	0.9308	**1.1227**	8.1913	33.2353	2.2839	2.7911	0.7034	0.9375
Standard Deviation	0.0263	0.5034	**1.5754**	12.5551	47.1309	0.8248	2.9636	**1.2166**	**2.0739**
Relative Stand Deviation	29.79%	54.08%	**140.33%**	**153.27%**	**141.81%**	36.11%	**106.18%**	**172.96%**	**221.22%**

A total of fourteen MCE level events were applied to this bridge model. See Table 7.31 and Table 7.32 for an overview of the MCE level longitudinal results. All MCE level analyses of this bridge were completed, and most resulted in acceptable bridge behavior. Four cases of residual displacements exceeding the limit of 1" were recorded, including 3 cases of bridge collapse. An additional case of span unseating was also recorded. The recorded foundation rotations of the upper limit friction model were also very high in some cases.

Table 7.31: MCE Level Results Overview for Lower Limit Friction Oseligee Creek Longitudinal Model

Oseligee	Friction ".2"											
Longitudinal Motion	Ground Motion	Run Status	Run Time	Foundation Capacity (D/R)		Bearing Capacity	Bent Ductility	Max Column Shear	Max Span Disp.	Max Bent Disp.	Residual Span Disp.	Residual Bent Disp.
San Fernando 1	MCE	Comp.	48.00	0.071	0.5810	0.449	3.155	**10.215**	2.295	1.243	0.189	0.037
San Fernando 2	MCE	Comp.	50.00	0.089	0.8043	0.831	3.112	**11.794**	3.922	1.783	0.382	0.010
Imperial Valley	MCE	Comp.	60.00	0.073	0.6116	0.444	2.321	**10.783**	2.217	1.278	0.473	0.070
Landers	MCE	Comp.	70.00	0.082	0.6728	**4.054**	29.851	**272.679**	3.436	8.247	**2.855**	**3.916**
Kocaeli 1	MCE	Comp.	170.00	0.083	0.7523	0.666	3.435	**10.853**	3.242	1.491	0.147	0.055
Kocaeli 2	MCE	Comp.	48.00	0.080	0.6575	0.945	4.628	**11.131**	4.439	2.114	0.262	0.050
Kobe	MCE	Comp.	60.00	0.061	0.4281	0.401	1.911	**10.212**	2.154	1.146	**1.030**	0.064

Mean	0.0772	0.6439	1.1129	6.9161	48.2381	3.1005	2.4716	0.7626	0.6002
Standard Deviation	0.0093	0.1225	1.3137	10.1500	98.9707	0.9058	2.5694	0.9693	1.4623
Relative Stand Deviation	12.07%	19.02%	**118.05%**	**146.76%**	**205.17%**	29.21%	**103.96%**	**127.11%**	**243.61%**

Table 7.32: MCE Level Results Overview for Upper Limit Friction Oseligee Creek Longitudinal Model

Oseligee	Friction ".4"											
Longitudinal Motion	Ground Motion	Run Status	Run Time	Foundation Capacity (D/R)		Bearing Capacity	Bent Ductility	Max Column Shear	Max Span Disp.	Max Bent Disp.	Residual Span Disp.	Residual Bent Disp.
San Fernando 1	MCE	Comp.	48.00	0.100	**1.0183**	0.511	3.539	**10.655**	2.555	1.915	0.718	0.191
San Fernando 2	MCE	Comp.	50.00	0.129	**1.4740**	0.563	3.733	**14.612**	3.284	1.831	0.266	0.140
Imperial Valley	MCE	Comp.	60.00	0.102	**1.0550**	0.408	3.091	**11.482**	2.314	1.480	0.159	0.081
Landers	MCE	Comp.	70.00	**1.473**	**1.8135**	**4.667**	41.169	**125.317**	3.367	9.459	**3.177**	**7.235**
Kocaeli 1	MCE	Comp.	170.00	0.277	**4.8746**	**5.097**	39.118	**379.941**	3.423	8.910	**3.261**	**8.900**
Kocaeli 2	MCE	Comp.	48.00	0.121	**1.4037**	**1.005**	4.924	**14.827**	4.769	3.130	0.020	0.021
Kobe	MCE	Comp.	60.00	0.085	0.7951	0.362	2.122	**10.212**	2.004	1.177	0.169	0.088
Mean				0.3267	1.7763	1.8017	13.9564	81.0067	3.1022	3.9859	1.1100	2.3794
Standard Deviation				0.5097	1.4076	2.1181	17.9181	138.3884	0.9228	3.6063	1.4574	3.9157
Relative Stand Deviation				**156.01%**	79.24%	**117.56%**	**128.39%**	**170.84%**	29.75%	90.48%	**131.29%**	**164.56%**

7.6 Little Bear Creek Bridge

Results show that the average behavior of the Little Bear Creek Bridge was favorable for design and MCE level events. Super and substructure behaviors of this bridge were found to have acceptable behavior. Foundation performance for this bridge was mixed, and dependent on event direction. Most design level analysis performed for this bridge succeeded in completing except for four ground motions applied in the transverse direction. Substructure behavior appears to be adequate at column, strut and bent cap locations with the exception of foundation displacement capacities in the transverse direction of the bridge. Connection behavior also appears to be adequate from the results of each analysis with one design level case of unseating being recorded. This bridge had three separate models analyzed in the transverse direction, two of which contain a newly designed anchor bolt configuration, while the third contains a previously designed anchor bolt configuration. A more in-depth analysis of each bridge model's results is proved in the next sections.

7.6.1 Transverse Motion

The transverse analysis for this bridge resulted in stiff structural behavior. See Table 7.33, Table 7.34 and Table 7.35 for an overview of the design level transverse results. Each of the three connection details used in this model behaved in an acceptable manner during all design level ground motions. No bolt failure was recorded, and the old bolt configuration consists of smaller anchor bolts than the new configuration. This old configuration results in a connection that is less stiff, and some behavioral effects of this stiffness change can be observed. The model containing the old configuration experienced higher bent displacements, higher span displacement and higher bolt demands then that of the newer bolt configuration. Higher residual displacements were also observed in the older bolt configuration. These results make sense given that structures with less strength and/or stiffness have a tendency for higher displacements. Results from all transverse models indicated design level deflections that were within acceptable limits for this bridge. Small residual displacements occurred in each ground motion as a result of the survival of the anchor bolts as well as the lower levels of ductility that occurred during each ground motion. Transverse design level analyses of the Little Bear Creek Bridge ran successfully with the exception of the Landers event. There was also an analysis failure in the upper limit friction model containing the new bolt configuration. This failure occurred during the first San Fernando event. Large foundation deformations were recorded in the transverse direction for every design event except the Little Skull Mountain event. This Little Skull Mountain event has generally resulted in lower bridge response throughout this project. The exact cause of these large foundation displacements can be assumed to have been caused by weaker foundation capacity and a bridge with a relatively large mass. The inertia of the bridge's components may have caused large forces to develop at the foundation level during motion.

Table 7.33: Results Overview for Lower Limit Friction Little Bear Creek Transverse Model

Little Bear Creek	Friction ".2"												
Transverse Motion	Ground Motion	Run Status	Run Time	Foundation Capacity (D/R)		Bearing Capacity	Bent Ductility	Bolt Status	Max Column Shear	Max Span Disp. (in.)	Max Bent Disp. (in.)	Residual Span Disp. (in.)	Residual Bent Disp. (in.)
San Fernando 1	Design	Comp.	48.00	**2.354**	0.3953	0.024	1.396	0.581	259.906	3.550	**2.148**	0.003	0.005
San Fernando 2	Design	Comp.	50.00	**2.334**	0.4396	0.022	1.573	0.529	255.101	3.773	**2.178**	0.001	0.004
Imperial Valley	Design	Comp.	60.00	**1.206**	0.1793	0.012	0.641	0.299	134.007	1.776	**1.007**	0.005	0.003
Coalinga	Design	Comp.	52.00	**1.651**	0.2475	0.016	0.875	0.380	183.425	2.439	**1.418**	0.000	0.001
North Palm Springs	Design	Comp.	40.00	**1.251**	0.1812	0.013	0.668	0.322	139.298	1.838	**1.046**	0.001	0.001
Landers	Design	Num.	27.36	**2.667**	0.5412	0.028	1.805	0.684	295.194	4.332	**2.580**		
Little Skull Mountain	Design	Comp.	132.00	0.631	0.0977	0.008	0.361	0.201	69.433	0.864	0.508	0.000	0.000
Kocaeli 1	Design	Comp.	170.00	**2.729**	0.4673	0.025	1.593	0.603	300.714	3.969	**2.347**	0.005	0.012
Kocaeli 2	Design	Comp.	48.00	**2.257**	0.3934	0.024	1.276	0.598	249.961	3.555	**1.998**	0.003	0.003
Kobe	Design	Comp.	60.00	0.976	0.1433	0.011	0.552	0.257	107.446	1.442	0.827	0.001	0.000

Mean	**1.7100**	0.2827	0.0171	0.9930	0.4189	188.8102	2.5786	**1.4974**	0.0021	0.0032
Standard Deviation	0.7340	0.1412	0.0065	0.4711	0.1593	80.6738	1.1564	0.6834	0.0019	0.0037
Relative Stand Deviation	42.93%	49.95%	38.03%	47.44%	38.02%	42.73%	44.85%	45.64%	92.69%	**115.54%**

Table 7.34: Results Overview for Upper Limit Friction Little Bear Creek Transverse Model

Little Bear Creek	Friction ".4"												
Transverse Motion	Ground Motion	Run Status	Run Time	Foundation Capacity (D/R)		Bearing Capacity	Bent Ductility	Bolt Status	Max Column Shear	Max Span Disp. (in.)	Max Bent Disp. (in.)	Residual Span Disp. (in.)	Residual Bent Disp. (in.)
San Fernando 1	Design	Num.	22.01	**2.354**	0.3953	0.024	1.395	0.581	259.828	3.544	**2.146**		
San Fernando 2	Design	Comp.	50.00	**2.333**	0.4396	0.022	1.573	0.528	255.064	3.773	**2.178**	0.001	0.000
Imperial Valley	Design	Comp.	60.00	**1.208**	0.1790	0.012	0.641	0.299	134.221	1.776	**1.008**	0.005	0.003
Coalinga	Design	Comp.	52.00	**1.649**	0.2457	0.015	0.877	0.378	183.276	2.437	**1.416**	0.001	0.003
North Palm Springs	Design	Comp.	40.00	**1.251**	0.1812	0.013	0.669	0.322	139.301	1.838	**1.046**	0.001	0.001
Landers	Design	Num.	26.81	**2.676**	0.5283	0.028	1.799	0.683	296.308	4.335	**2.604**	0.534	0.329
Little Skull Mountain	Design	Comp.	132.00	0.631	0.0977	0.008	0.361	0.201	69.433	0.864	0.508	0.000	0.000
Kocaeli 1	Design	Comp.	170.00	**2.898**	0.4784	0.026	1.621	0.639	319.989	4.248	**2.512**	0.044	0.031
Kocaeli 2	Design	Comp.	48.00	**2.258**	0.3934	0.024	1.277	0.598	250.024	3.556	**1.998**	0.005	0.005
Kobe	Design	Comp.	60.00	0.976	0.1431	0.011	0.552	0.257	107.448	1.442	0.827	0.000	0.000

Mean	**1.4725**	0.2399	0.0151	0.8500	0.3692	162.6811	2.2410	**1.2830**	0.0019	0.0017
Standard Deviation	0.6405	0.1293	0.0059	0.4300	0.1447	70.3444	1.0823	0.6151	0.0022	0.0018
Relative Stand Deviation	43.50%	53.87%	39.20%	50.59%	39.20%	43.24%	48.29%	47.94%	**116.82%**	**107.99%**

Table 7.35: Results Overview for Upper Limit Friction Little Bear Creek Transverse Model with Old Bolts

Little Bear Creek	Friction ".4"												
Transverse Motion	Ground Motion	Run Status	Run Time	Foundation Capacity (D/R)		Bearing Capacity	Bent Ductility	Bolt Status	Max Column Shear	Max Span Disp. (in.)	Max Bent Disp. (in.)	Residual Span Disp. (in.)	Residual Bent Disp. (in.)
San Fernando 1	Design	Comp.	48.00	**2.221**	0.3639	0.031	1.309	0.639	244.733	3.448	**2.027**	0.005	0.002
San Fernando 2	Design	Comp.	50.00	**2.356**	0.4581	0.026	1.618	0.633	256.994	3.858	**2.228**	0.005	0.004
Imperial Valley	Design	Comp.	60.00	**1.283**	0.1884	0.017	0.677	0.428	142.614	1.924	**1.086**	0.007	0.005
Coalinga	Design	Comp.	52.00	**1.499**	0.2235	0.018	0.835	0.451	166.765	2.286	**1.289**	0.007	0.004
North Palm Springs	Design	Comp.	40.00	**1.159**	0.1688	0.021	0.621	0.519	129.902	1.927	0.988	0.002	0.002
Landers	Design	Num.	27.01	**2.667**	0.5098	0.033	1.755	0.813	295.667	4.415	**2.580**		
Little Skull Mountain	Design	Comp.	132.00	0.644	0.0992	0.015	0.368	0.319	70.952	0.904	0.521	0.000	0.000
Kocaeli 1	Design	Comp.	170.00	**2.720**	0.4655	0.035	1.625	0.859	300.356	4.053	**2.367**	0.002	0.001
Kocaeli 2	Design	Comp.	48.00	**2.207**	0.3879	0.028	1.259	0.683	245.046	3.585	**1.974**	0.000	0.001
Kobe	Design	Comp.	60.00	0.974	0.1398	0.017	0.526	0.372	107.606	1.449	0.789	0.001	-0.002
Mean				**1.6735**	0.2772	0.0232	0.9821	0.5448	184.9964	2.6037	**1.4743**	0.0034	0.0020
Standard Deviation				0.7196	0.1418	0.0070	0.4786	0.1727	78.9187	1.1506	0.6819	0.0028	0.0020
Relative Stand Deviation				43.00%	51.17%	30.23%	48.73%	31.70%	42.66%	44.19%	46.26%	80.97%	98.22%

A total of twenty-one MCE level events were analyzed with this bridge model. See Table 7.36, Table 7.37 and Table 7.38 for an overview of the MCE level transverse results. Each of the three connection details used in this model behaved in an acceptable manner during most MCE level events. Two cases of collapse and span unseating were recorded for MCE level events; however these results are taken from analyses that did not complete. A total of seven events did not result in a complete analysis, with three resulting in data that suggests structural failure. Foundation displacement capacity is exceeded in all transverse MCE events, just like the design level results.

Table 7.36: MCE Level Results Overview for Lower Limit Friction Little Bear Creek Transverse Model

Little Bear Creek	Friction ".2"												
Transverse Motion	Ground Motion	Run Status	Run Time	Foundation Capacity (D/R)		Bearing Capacity	Bent Ductility	Bolt Status	Max Column Shear	Max Span Disp.	Max Bent Disp.	Residual Span Disp.	Residual Bent Disp.
San Fernando 1	MCE	Num.	14.51	**2.497**	0.4267	0.026	1.490	0.627	275.069	3.766	2.283		
San Fernando 2	MCE	Comp.	50.00	**2.884**	0.6317	0.027	2.186	0.650	316.127	4.799	2.783	0.004	0.005
Imperial Valley	MCE	Comp.	60.00	**1.677**	0.2678	0.017	0.918	0.428	185.918	2.639	1.458	0.033	0.020
Landers	MCE	Num.	22.16	**2.503**	0.4211	0.027	1.487	0.650	277.383	3.773	2.265		
Kocaeli 1	MCE	Comp.	170.00	**3.578**	0.7628	0.036	2.401	0.887	397.417	5.662	3.293	0.091	0.093
Kocaeli 2	MCE	Fail	23.51	**4.331**	**1.2634**	**12.654**	59.610	**0.991**	416.514	12.764	32.495		
Kobe	MCE	Comp.	60.00	**1.298**	0.1939	0.017	0.759	0.415	142.944	2.019	1.140	0.007	0.004
Mean				2.6810	0.5668	1.8291	9.8360	0.6642	287.3388	5.0605	6.5309	0.0336	0.0305
Standard Deviation				1.0452	0.3645	4.7734	21.9565	0.2145	100.8447	3.6108	11.4725	0.0405	0.0423
Relative Stand Deviation				38.98%	64.31%	**260.97%**	**223.23%**	32.30%	35.10%	71.35%	**175.67%**	**120.51%**	**139.01%**

Table 7.37: MCE Level Results Overview for Upper Limit Friction Little Bear Creek Transverse Model

Little Bear Creek	Friction ".4"												
Transverse Motion	Ground Motion	Run Status	Run Time	Foundation Capacity (D/R)		Bearing Capacity	Bent Ductility	Bolt Status	Max Column Shear	Max Span Disp.	Max Bent Disp.	Residual Span Disp.	Residual Bent Disp.
San Fernando 1	MCE	Num.	12.01	**2.491**	0.4341	0.026	1.497	0.627	274.381	3.767	2.281		
San Fernando 2	MCE	Comp.	50.00	**2.885**	0.6317	0.027	2.186	0.650	316.135	4.799	2.783	0.000	0.012
Imperial Valley	MCE	Comp.	60.00	**1.674**	0.2678	0.017	0.918	0.428	185.575	2.639	1.458	0.022	0.017
Landers	MCE	Fail	39.51	**6.282**	**1.5312**	**10.437**	31.778	**0.947**	680.943	24.092	16.503		
Kocaeli 1	MCE	Comp.	170.00	**3.575**	0.7204	0.036	2.311	0.888	397.610	5.555	3.278	0.055	0.056
Kocaeli 2	MCE	Comp.	48.00	**3.189**	0.7185	0.035	2.243	0.853	349.186	5.305	2.967	0.041	0.004
Kobe	MCE	Comp.	60.00	**1.298**	0.1939	0.017	0.757	0.416	142.918	2.017	1.138	0.007	0.005
Mean				3.0564	0.6425	1.5136	5.9557	0.6870	335.2496	6.8821	4.3440	0.0251	0.0187
Standard Deviation				1.6354	0.4447	3.9350	11.4043	0.2166	176.5650	7.7043	5.4189	0.0229	0.0216
Relative Stand Deviation				53.51%	69.22%	**259.98%**	**191.49%**	31.53%	52.67%	**111.95%**	**124.74%**	91.26%	**115.48%**

Table 7.38: MCE Level Results Overview for Upper Limit Friction Little Bear Creek Transverse Model with Old Bolts

Little Bear Creek-Old	Friction ".4"												
Transverse Motion	Ground Motion	Run Status	Run Time	Foundation Capacity (D/R)		Bearing Capacity	Bent Ductility	Bolt Status	Max Column Shear	Max Span Disp.	Max Bent Disp.	Residual Span Disp.	Residual Bent Disp.
San Fernando 1	MCE	Num.	24.51	**2.343**	0.3916	0.033	1.396	0.683	258.183	3.663	2.149		
San Fernando 2	MCE	Comp.	50.00	**2.910**	0.6594	0.032	2.222	0.786	319.602	4.874	2.842	0.005	0.001
Imperial Valley	MCE	Comp.	60.00	**1.793**	0.3048	0.027	1.033	0.636	199.631	2.828	1.601	0.005	0.006
Landers	MCE	Fail	22.51	**3.195**	0.9328	0.381	4.242	**1.033**	311.538	6.168	3.567		
Kocaeli 1	MCE	Comp.	170.00	**2.865**	0.5116	0.292	1.958	**0.972**	321.904	5.839	3.055	0.192	0.083
Kocaeli 2	MCE	Comp.	48.00	**3.114**	0.7074	0.037	2.202	**0.914**	344.173	5.323	2.928	0.019	0.006
Kobe	MCE	Comp.	60.00	**1.301**	0.1921	0.025	0.746	0.533	142.812	2.027	1.083	0.004	0.001
Mean				2.5029	0.5285	0.1182	1.9714	0.7936	271.1205	4.3890	2.4610	0.0451	0.0194
Standard Deviation				0.7217	0.2565	0.1514	1.1536	0.1866	74.8786	1.5768	0.8827	0.0824	0.0356
Relative Stand Deviation				28.83%	48.54%	**128.17%**	58.52%	23.51%	27.62%	35.93%	35.87%	**182.64%**	**183.48%**

7.6.2 Longitudinal Motion

The longitudinal analysis for this bridge resulted in fairly consistent results. See Table 7.39 and Table 7.40 for an overview of the design level transverse results. Maximum span displacements of about 2.5 inches occurred for most ground motions in each bridge model, and bent displacements hovered around 1.5 inches. These results are larger than expected, and may point to possible amplified bridge response. Bent ductility appears to remain below the established maximum for the second bent (3.032 inches), with only one ground motion, (Landers) causing a ductility in excess of this limit. This excess in the upper limit friction model's ductility appears to have been caused due to a collapse of a bridge bent. Results show that this design level event also contains large foundation displacements and a large case of span end displacements, resulting in unseating. Despite the results of the aforementioned event, all other events appear to behave in an acceptable manner. Foundation behavior in the longitudinal direction appears to suggest low shears and moments within bent columns. Bearing pad displacements also indicate constant movement and slipping, given maximum demand capacity ratios of about 0.4 for each model. Lastly the residual displacements in this direction are below the acceptable limit in all but two cases, the case of collapse and the Coalinga analysis of the lower limit bearing pad model.

Table 7.39: Results Overview for Lower Limit Friction Little Bear Creek Longitudinal Model

Little Bear Creek	Friction ".2"											
Longitudinal Motion	Ground Motion	Run Status	Run Time	Foundation Capacity (D/R)		Bearing Capacity	Bent Ductility	Max Column Shear	Max Span Disp. (in.)	Max Bent Disp. (in.)	Residual Span Disp. (in.)	Residual Bent Disp. (in.)
San Fernando 1	Design	Comp.	48.00	0.008	0.1676	0.345	0.857	149.824	1.313	0.668	0.579	0.218
San Fernando 2	Design	Comp.	50.00	0.008	0.1786	0.559	0.780	144.559	2.345	0.730	0.296	0.204
Imperial Valley	Design	Comp.	60.00	0.005	0.1399	0.415	0.674	130.554	1.638	0.563	0.176	0.197
Coalinga	Design	Comp.	52.00	0.008	0.1995	0.474	0.873	159.838	2.095	0.592	**1.357**	0.179
North Palm Springs	Design	Comp.	40.00	0.006	0.1710	0.357	0.737	115.856	1.308	0.524	0.611	0.194
Landers	Design	Comp.	70.00	0.006	0.1342	0.513	0.754	124.155	2.323	0.720	0.955	0.181
Little Skull Mountain	Design	Comp.	132.00	0.003	0.0531	0.118	0.314	77.611	0.366	0.190	0.153	0.109
Kocaeli 1	Design	Comp.	170.00	0.007	0.1713	0.524	0.729	129.000	2.197	0.706	0.143	0.186
Kocaeli 2	Design	Comp.	48.00	0.006	0.1357	0.477	0.675	116.030	1.844	0.516	0.101	0.215
Kobe	Design	Comp.	60.00	0.005	0.1041	0.287	0.646	105.904	1.002	0.480	0.303	0.190
Mean				0.0062	0.1455	0.4068	0.7039	125.3332	1.6431	0.5688	0.4674	0.1873
Standard Deviation				0.0015	0.0426	0.1338	0.1560	23.6488	0.6472	0.1612	0.4139	0.0305
Relative Stand Deviation				24.86%	29.27%	32.90%	22.16%	18.87%	39.39%	28.34%	88.56%	16.29%

Table 7.40: Results Overview for Upper Limit Friction Little Bear Creek Longitudinal Model

Little Bear Creek	Friction ".4"											
Longitudinal Motion	Ground Motion	Run Status	Run Time	Foundation Capacity (D/R)		Bearing Capacity	Bent Ductility	Max Column Shear	Max Span Disp. (in.)	Max Bent Disp. (in.)	Residual Span Disp. (in.)	Residual Bent Disp. (in.)
San Fernando 1	Design	Comp.	48.00	0.008	0.1212	0.311	0.675	164.178	1.412	0.517	0.162	0.108
San Fernando 2	Design	Comp.	50.00	0.012	0.2992	0.523	1.184	238.002	2.430	0.919	0.374	0.222
Imperial Valley	Design	Comp.	60.00	0.009	0.1736	0.437	0.832	170.966	1.919	0.817	0.065	0.138
Coalinga	Design	Comp.	52.00	0.013	0.2789	0.589	1.191	241.389	2.754	0.989	0.255	0.174
North Palm Springs	Design	Comp.	40.00	0.011	0.2734	0.494	1.118	218.942	2.265	0.851	0.461	0.201
Landers	Design	Comp.	70.00	**1.107**	0.1748	**5.097**	10.408	146.902	28.140	14.851	**4.316**	**1.146**
Little Skull Mountain	Design	Comp.	132.00	0.003	0.0554	0.118	0.314	77.611	0.366	0.190	0.153	0.110
Kocaeli 1	Design	Comp.	170.00	0.011	0.1958	0.441	0.843	201.198	1.966	0.736	0.093	0.156
Kocaeli 2	Design	Comp.	48.00	0.008	0.1368	0.364	0.657	153.498	1.629	0.479	0.331	0.128
Kobe	Design	Comp.	60.00	0.007	0.1185	0.327	0.598	140.905	1.452	0.425	0.153	0.107
Mean				0.1189	0.1828	0.8700	1.7820	175.3592	4.4333	2.0774	0.6363	0.2490
Standard Deviation				0.3473	0.0800	**1.4909**	3.0438	50.5801	8.3557	4.4952	**1.2992**	0.3177
Relative Stand Deviation				**292.04%**	43.77%	**171.37%**	**170.81%**	28.84%	**188.48%**	**216.39%**	**204.19%**	**127.58%**

A total of fourteen MCE level events were applied to this bridge model. See Table 7.41 and Table 7.42 for an overview of the MCE level longitudinal results. All of the MCE level analyses completed, resulting in acceptable bridge behavior. A single case of residual displacement exceedance was observed in the lower bound friction model during the Landers event.

Table 7.41: MCE Level Results Overview for Lower Limit Friction Little Bear Creek Longitudinal Model

Little Bear Creek	Friction ".2"											
Longitudinal Motion	Ground Motion	Run Status	Run Time	Foundation Capacity (D/R)		Bearing Capacity	Bent Ductility	Max Column Shear	Max Span Disp.	Max Bent Disp.	Residual Span Disp.	Residual Bent Disp.
San Fernando 1	MCE	Comp.	48.00	0.008	0.1676	0.345	0.857	**149.824**	1.313	0.668	0.579	0.218
San Fernando 2	MCE	Comp.	50.00	0.009	0.1736	0.704	0.922	**178.721**	3.010	0.889	0.819	0.200
Imperial Valley	MCE	Comp.	60.00	0.006	0.1470	0.657	0.753	**151.814**	2.802	0.671	0.469	0.177
Landers	MCE	Comp.	70.00	0.007	0.1550	0.686	0.910	**145.619**	3.050	0.863	**1.776**	0.118
Kocaeli 1	MCE	Comp.	170.00	0.009	0.2198	0.471	0.896	**168.571**	1.978	0.799	0.477	0.188
Kocaeli 2	MCE	Comp.	48.00	0.008	0.1457	0.666	0.781	**157.187**	2.641	0.708	0.239	0.235
Kobe	MCE	Comp.	60.00	0.006	0.1258	0.388	0.745	**115.832**	1.506	0.577	0.408	0.171
Mean				0.0076	0.1621	0.5595	0.8377	152.5095	2.3286	0.7394	0.6810	0.1867
Standard Deviation				0.0011	0.0299	0.1534	0.0765	19.8633	0.7229	0.1143	0.5140	0.0378
Relative Stand Deviation				14.69%	18.44%	27.42%	9.13%	13.02%	31.05%	15.46%	75.47%	20.22%

Table 7.42: MCE Level Results Overview for Upper Limit Friction Little Bear Creek Longitudinal Model

Little Bear Creek	Friction ".4"											
Longitudinal Motion	Ground Motion	Run Status	Run Time	Foundation Capacity (D/R)		Bearing Capacity	Bent Ductility	Max Column Shear	Max Span Disp.	Max Bent Disp.	Residual Span Disp.	Residual Bent Disp.
San Fernando 1	MCE	Comp.	48.00	0.008	0.1212	0.311	0.675	**164.178**	1.412	0.517	0.162	0.108
San Fernando 2	MCE	Comp.	50.00	0.013	0.3085	0.585	1.258	**253.462**	2.791	1.232	0.330	0.236
Imperial Valley	MCE	Comp.	60.00	0.013	0.2124	0.612	1.143	**247.484**	2.851	1.119	0.440	0.157
Landers	MCE	Comp.	70.00	0.014	0.2992	0.491	1.209	**260.593**	2.354	0.910	0.104	0.075
Kocaeli 1	MCE	Comp.	170.00	0.013	0.2881	0.623	1.165	**240.275**	2.820	1.133	0.053	0.201
Kocaeli 2	MCE	Comp.	48.00	0.011	0.2530	0.535	1.062	**206.596**	2.541	0.930	0.496	0.205
Kobe	MCE	Comp.	60.00	0.009	0.1623	0.481	0.830	**181.152**	2.425	0.774	0.138	0.155
Mean				0.0115	0.2350	0.5197	1.0489	221.9626	2.4564	0.9450	0.2461	0.1624
Standard Deviation				0.0021	0.0724	0.1075	0.2159	38.1048	0.5016	0.2456	0.1748	0.0569
Relative Stand Deviation				18.15%	30.80%	20.68%	20.58%	17.17%	20.42%	25.99%	71.01%	35.01%

7.7 Summary of Results

Overall each bridge in these analysis contained some flaw or behavior that will need to be improved upon, but the majority of analyses provided results deemed. The Bent Creek Road Bridge consistently produced partially complete analyses, but the few that did complete suggested adequate performance. The Scarham Creek Bridge demonstrated expected behaviors in regards to overall design level performance, utilizing large displacements as a method of surviving the earthquake. The Scarham model did however present large foundation displacements. The MCE level behavior for the Scarham Bridge proved to be less than acceptable. Incomplete analyses were present in most MCE level longitudinal events along with

high displacements. These results indicate the need for additional design of tall substructure long span bridges like The Scarham Creek Bridge. The Norfolk Southern Railroad Bridge behaved as a stiff bridge would, results of these analyses include lower displacements and anchor bolt connection failure. Despite this, bridge behavior still remained within the range of acceptable behavior at the design level and MCE level. The Oseligee Creek Bridge presented the challenge of a 100% scour condition during an earthquake event. Total bent collapse occurred in both directions of motion, at both design and MCE level events. Special design actions may need to be implemented in order to prevent occurrences like this. The Little Bear Creek Bridge performed acceptably under most ground motions. This bridge was also used to compare old bolt configurations with code specified configurations. The new bolt configurations caused a slight increase in overall bridge performance in that it reduced overall deflections of the structure. This reduction of overall deflection does not necessarily result in better seismic bridge behavior for all bridges, and greater connection stiffness can actually lead to damage in other components of the bridge. The main reason for selection of the new connection anchor bolt is the redundancy that it provides for the connection, as well as an increase in the connection shear capacity. An isolated occurrence of bent collapse was observed in the design level analysis of the Little Bear Creek Bridge. A summary of critical events taken from all design level analyses can be found in Table 7.43. A summary of critical events taken from all MCE level analyses can be found in Table 7.44. Conclusions and design recommendations will be provided in the next chapter of this thesis.

Table 7.43: Summary of Critical Design Level Analysis Behaviors

Bridge Case	Number of Analyses	Critical Analysis Behaviors
Bent Creek Bridge	40	16 cases of unfinished analysis
		6 cases of foundation displacement exceedance
Scarham Creek Bridge	40	foundation displacement exceedance in all longitudinal events
Norfolk Southern Bridge	40	3 cases of unfinished analysis
		1 case of residual displacement exceedance
Oseligee Creek Bridge	40	17 cases of foundation rotation exceedance
		3 cases of residual displacement exceedance
		3 cases of bent collapse
Little Bear Creek	50	4 cases of unfinished analysis
		25 cases of foundation displacement exceedance
		1 case of bent collapse
		2 cases of residual displacement exceedance

Table 7.44: Summary of Critical MCE Level Analysis Behaviors

Bridge Case	Number of Analyses	Critical Analysis Behaviors
Bent Creek Bridge	28	10 cases of unfinished analysis
		1 case of residual displacement exceedance
		7 cases of foundation displacement exceedance
Scarham Creek Bridge	28	Foundation displacement exceedance in all longitudinal events
		8 cases of unfinished analysis
		1 case of residual displacement exceedance
Norfolk Southern Bridge	28	4 cases of unfinished analysis
		1 case of bent collapse
		1 case of span unseating
		2 cases of residual displacement exceedance
Oseligee Creek Bridge	28	17 cases of foundation rotation exceedance
		7 cases of residual displacement exceedance
		4 cases of bent collapse
Little Bear Creek	35	7 cases of unfinished analysis
		21 cases of foundation displacement exceedance
		2 cases of bent collapse
		1 case of residual displacement exceedance

Chapter 8: Task 4 Results and Discussion

8.1 FB Multipier Direct Analysis

As discussed previously FB-Multiplier, the hybrid finite element program, was used to perform a direct analysis of piers/bents of the same bridges as conducted using CSI Bridge. The FB-Multipier models were somewhat simpler. Due to program limitations, it was not feasible to model the entire bridge. Thus, selected bents were modeled with some adjustments or additions to account for the impact of the deck and overall bridge stiffness. Before the direct seismic analyses were conducted, the damping of the system was evaluated for each bridge and implemented.

8.1.1 Dynamic Analysis Method Used

Time-history analysis was used to evaluate the dynamic structural response of the bridge piers modeled. There are three time stepping options available: average acceleration (Newmark), linear acceleration (Newmark), and Wilson-θ. The average acceleration option was used because it is typically more stable from a computational standpoint, and is one of the most effective and popular implicit techniques used for structural dynamic problems (Hughes and Belytschko 1983).

8.1.2 Damping Analysis

For each model, Eigenvector analysis was conducted using FB-MultiPier's modal analysis option to determine the natural period and the circular frequency of the pier. Then, a classic sine wave time-history curve was developed for each model and run using the Rayleigh damping factor values for the pier. Mass and stiffness damping factors for the piles and soil were ignored in this analysis for simplicity (and consistency) and due to

lack of information regarding cyclic response of the soil for each case history. This approach was accepted as reasonable because it is conservative to ignore the damping effects of the soil and piles. However, it was noticed that if zero is entered into any one of the six input boxes of the mass and stiffness damping factors, Rayleigh damping would not be considered at all within the program analysis. Therefore, a low mass and stiffness factor of 0.000001 was applied to both the piles and soil.

The displacement at the top of the pier versus time was plotted and the damping was calculated using the peak displacements that occurred once the forcing function was no longer active. The sine wave curves were plotted so that the bridge would go through three cycles (time [in seconds] of three times the structural period) of the sine wave, then would experience free vibration for roughly 10 seconds.

The calculated damping ratios for four of the six bridge piers were all within 1-4%; therefore, for simplicity, the initial damping factors were used for the dynamic analysis. The Scarham Creek Bridge was not included because the damping ratios were extremely high. This is believed to be because of the large strut that is used to connect the columns of the bent. . Table 8.1 shows the average calculated damping factors for both the longitudinal and transverse directions respectively for each bridge.

Table 8.1 – Frequency, structural period, and calculated average damping ratios for each bridge

Bridge	Longitudinal			Transverse		
	Frequency (rad/sec)	**Period (sec)**	**Percent Damping**	**Frequency (rad/sec)**	**Period (sec)**	**Percent Damping**
Oseligee Creek 25%	6.454	0.974	0.25%	11.455	0.549	0.2%
Oseligee Creek 100%	5.935	1.059	3.96%	10.724	0.586	3.18%
Norfolk Southern Railroad	4.307	1.459	2.14%	7.551	0.832	1.70%
Little Bear Creek	7.566	0.83	2.1%	12.725	0.494	1.2%
Bent Creek Road	5.492	1.144	1.92%	8.958	0.701	2.82%
Scarham Creek	2.483	2.531	N/A	0.707	0.889	N/A

8.2 Dead Load and Discrete Mass

Dead loads and discrete masses were applied to each direct analysis model. This was done to account for the weight of the bridge deck and girders. Factored live load was not taken into account for this analysis. Dead loads were calculated based on typical cross sections given and the standard unit weight of normal weight, reinforced concrete (150 pcf). The discrete masses were calculated using the dead weight divided by the acceleration of gravity (386.2 in/sec^2). The dead load was applied in the z (vertical) direction and the discrete masses were applied in the x and y (horizontal) direction because vertical acceleration was not used for the case studies. The dead weight was applied to each bearing pad location, whereas the discrete masses were applied in between the bearing pad locations. The bearing pad locations were taken from the center line of each girder in the typical cross section provided in the subsequent sections for each case study. Therefore, the dead load used to calculate each discrete mass was the combination of the loads on each bearing pad. The reason for applying dead loads at each bearing pad is because in some cases, the spans supported by the bent were different

lengths and therefore the dead load applied to the pads would be different on each side of the bent. Table 8.2 presents the dead loads and discrete masses used for each case study.

Table 8.2 – Dead loads and discrete masses used for each case study

Bearing Pad Location	Left Bearing Pad (kips)	Discrete Mass (kip-sec^2/in)	Right Bearing Pad (kips)
Oseligee Creek Bridge			
Exterior	65	0.34	65
Interior (for all)	60	0.31	60
Exterior	65	0.34	65
Norfolk Southern Railroad Bridge			
Exterior	130	0.67	116
Interior (for all)	105	0.54	82
Exterior	130	0.67	116
Little Bear Creek Bridge			
Exterior	125	0.65	125
Interior (for all)	100	0.52	100
Exterior	125	0.65	125
Bent Creek Road Bridge			
Exterior	120	0.62	120
Interior (for all)	100	0.52	100
Exterior	120	0.62	120
Scarham Creek Bridge			
Exterior	120	0.62	120
Interior (for all)	110	0.57	110
Exterior	120	0.62	120

8.3 Direct Analysis Results

The results from the direct analysis of the five bridge case studies are presented. For each bridge, the earthquake time-history used and the displacement at the top of the pier and the head of the shaft or pile footing was recorded. The largest shear force, bending moment, and D/C ratio distribution for a shaft or pile is also presented for one time step. This time step is indicated by a black vertical line on the time-history plots. Note that the D/C ratio is based on the axial-force D/C (which is a function of bending moment). For the failed models, the time step in which these distributions are taken at

are not necessarily the last time step before the program terminated. Typically, the last time step before failure is numerically flawed and inconclusive; therefore, the time-step with the next largest shear force and bending moment are shown. This is to give an indication of where the shear forces and bending moments are developing relative to the ground surface or rock line.

There were 17 scaled time-history events used for each bridge case in each direction (longitudinal and transverse): Coalinga North, Imperial Valley NMCE and North, Kobe NMCE and North, Kocaeli NMCE and North, Kocaeli2 NMCE and North, Landers NMCE and North, LSM North, NPS North, San Fernando NMCE and North, and San Fernando2 NMCE and North. The following presents a discussion of each case history and its overall performance, as well as a selection of detailed results and tabular summary for each case history. The case histories provided did not have liquefaction potential; therefore, a liquefaction case was not explicitly done. However, parallels from the Norfolk Southern Railroad Bridge case history can be drawn due to the weak insitu soil that the foundations are embedded.

The results overview table indicates how the structure performed based on whether the program converged or not. If the model did not converge, the performance was described as “failed,” and a probable cause of failure (structural, soil, or numerical instability) was provided (refer back to section 2.4.1). The time of occurrence that the maximum forces were generated is provided for each model, as well as the location of the maximum values along the shaft, pile, or column to compare to the elevation of the ground surface or pier cap.

8.4 Oseligee Creek Bridge 25% Scour Discussion

The Oseligee Creek Bridge 25% scour Bridge performed poorly, overall. Most of the failed models were suspected to have failed because of either structural failure or soil failure. Soil failure is likely due to large displacements that the soil spring undergoes. These displacements can become so large that the soil can no longer resist the lateral forces and the out-of-balance forces become extremely large. Referring back to the soil profile for Oseligee Creek Bridge (Figure 6.18), the soil layers over rock are relatively weak, which suggests that large displacements at the ground surface are not unlikely to occur. Also, there is an interface of soft and hard soils. The maximum bending moments appeared to develop above the rock line, but below the ground surface line. This is important because typically, bridges are detailed to develop a plastic hinge at the ground surface and at the pier cap/column connection because that is inherently the most likely place it will occur. This is to allow enough ductility so the structure does not collapse (see Section 2.3). If damage occurs at those hinge zones, it also allows the damage to be identified and repaired without excavating to the damaged areas. The models that were loaded in the transverse direction generally showed that the largest moment and D/C ratio were at the top of the bent where the column connects to the pier cap. This is a desired plastic hinge zone location. However, large moments and D/C ratios were still developing well below the ground surface, which could possibly develop into plastic hinge zones as well.

It is difficult to discern whether scour, the soft/hard soil interface, or a combination of the two had the most impact of the bridge bent performance.

Liquefaction was not taken into account for this model. However, there are two cohesionless layers that could have the potential to liquefy; however, the scouring effect is a similar loss in soil resistance and is compared for the Oseligee Creek Bridge 100% scour case. Tables 8.3 and Table 8.4 show an overview of the results; this includes the location of the maximum shear force, bending moment and D/C ratio along the drilled shaft.

Table 8.3 – Results overview for Chambers 25% scour longitudinal models

Chambers 25% Scour Longitudinal Earthquake Event	Performance	Plastic Hinge Developed	Location of Plastic Hinge (ft)	Probable Cause of Failure	Time of Occurrence (sec)	Maximum Shear (kip)	Elevation of Shear Occurrence (ft)	Maximum Moment (kip-ft)	Elevation of Moment Occurrence (ft)	Maximum D/C Ratio	Elevation of D/C Occurrence (ft)
Coalinga North	Failed	Yes*	77	Structural	24.03	233	61	1409	68	0.83**	68
Imperial Valley NMCE	Failed	Yes	75	Structural	28.85	1344	76	956	77	1.20	73
Imperial Valley North	Failed	Yes*	77	Structural	16.79	241	61	1416	68	0.83**	68
Kobe NMCE	Failed	No	--	Soil	21.05	270	61	1563	68	0.93	68
Kobe North	Failed	No	--	Numerical Instability	10.57	57	77	1213	68	0.70	68
Kocaeli NMCE	Failed	No	--	Soil	26.33	282	61	1635	68	0.97	68
Kocaeli North	Survived	No	--	--	24.4	172	61	991	68	0.56	68
Kocaeli2 NMCE	Survived	No	--	--	8.64	193	61	1123	68	0.64	68
Kocaeli2 North	Survived	No	--	--	6.5	156	61	873	68	0.47	66
Landers NMCE	Failed	No	--	Soil	25.52	280	61	1630	68	0.98	69
Landers North	Failed	No	--	Soil	38.24	234	65	1651	66	0.90	69
LSM North	Failed	Yes*	65	Structural	10.34	141	61	779	66	0.41**	65
NPS North	Survived	No	--	--	7.95	135	61	737	66	0.39	65
SanFernando NMCE	Survived	No	--	--	5.57	282	61	1601	68	0.94	68
SanFernando North	Failed	No	--	Structural	5.43	276	61	1594	68	0.93	68
SanFernando2 NMCE	Failed	Yes*	66	Structural	4.27	263	61	1533	68	0.91**	68
SanFernando2 North	Failed	Yes	73	Structural	4.2	221	61	1284	68	0.75**	68
Percent Survived	29%										

* Plastic Hinge developed at last time step

** D/C ratio not at last time step

Table 8.4 – Results overview for Oseligee Creek Bridge 25% scour transverse models

Chambers 25% Scour Transverse Earthquake Event	Performance	Plastic Hinge Developed	Location of Plastic Hinge (ft)	Probable Cause of Failure	Time of Occurrence (sec)	Maximum Shear (kip)	Elevation of Shear Occurrence (ft)	Maximum Moment (kip-ft)	Elevation of Moment Occurrence (ft)	Maximum D/C Ratio	Elevation of D/C Occurrence (ft)
Coalinga North	Failed	No	--	Structural	10.8	254	61	1757	91	0.98	91
Imperial Valley NMCE	Failed	No	--	Structural	13.97	232	61	1639	91	0.97	91
Imperial Valley North	Failed	No	--	Structural	15.37	197	59	1380	91	0.71	91
Kobe NMCE	Failed	Yes	90*	Structural	8.46	240	61	1747	91	0.95**	91
Kobe North	Survived	No	--	--	6.19	176	59	1195	91	0.61	91
Kocaeli NMCE	Failed	No	--	Structural	29.08	290	61	1811	91	1.03	91
Kocaeli North	Failed	No	--	Structural	29.02	274	61	1826	91	1.04	91
Kocaeli2 NMCE	Survived	No	--	--	9.09	293	61	1851	91	1.04	91
Kocaeli2 North	Failed	No	--	Structural	8.95	261	61	1831	91	1.00	91
Landers N-MCE	Failed	Yes	91	Structural	18.64	265	59	1892	91	1.00	91
Landers North	Failed	No	--	Structural	24.38	222	59	1879	91	0.99	91
LSM North	Survived	No	--	--	15.65	52	59	359	91	0.15	91
NPS North	Failed	No	--	Structural	8.89	242	61	1755	91	0.97	91
SanFernando NMCE	Survived	No	--	--	5	241	61	1674	91	0.92	91
SanFernando North	Failed	No	--	Structural	5.06	250	61	1739	91	0.95	91
SanFernando2 NMCE	Failed	No	--	Structural	4.42	301	61	1878	91	1.04	91
SanFernando2 North	Survived	No	--	--	4.88	286	61	1888	91	1.04	91
Percent Survived	29%										

* Plastic hinge developed at last time step

** D/C ratio not at last time step

8.5 Oseligee Creek Bridge 100% Scour Discussion

The Chambers 100% scour model performed well, overall. The three models that failed all used NMCE scaled time-history events, which are of larger magnitude and, typically, more harmful than the North scaled time-histories. The North scaled events are more representative of what the state of Alabama would generally experience.

The 100% scour model performed much better than the 25% scour model (based on structural performance of the bent). This shows the importance of checking both scenarios because it is difficult to determine which case could be worse. Results of the models demonstrated the possibility of plastic hinges developing beneath the ground surface in the 25% scour case; whereas, the plastic hinges would most likely develop at the rock line or slightly above for the 100% scour case.

Table 8.5 presents the results overview of all the longitudinal models. The transverse models showed that the hinge zones would most likely develop at the column/pier cap interface or at the rock line. This is important because it shows that the plastic hinge zones are developing at the desired locations. See Table 8.6 for the results overview.

Table 8.5 – Results overview for Oseligee Creek Bridge 100% scour longitudinal models

Chambers 100% Scour Longitudinal Earthquake Event	Performance	Plastic Hinge Developed	Location of Plastic Hinge (ft)	Probable Cause of Failure	Time of Occurrence (sec)	Maximum Shear (kip)	Elevation of Shear Occurrence (ft)	Maximum Moment (kip-ft)	Elevation of Moment Occurrence (ft)	Maximum D/C Ratio	Elevation of D/C Occurrence (ft)
Coalinga North	Survived	No	--	--	12.87	222	60	1165	63	0.67	62
Imperial Valley NMCE	Survived	No	--	--	9.36	226	60	1190	63	0.67	62
Imperial Valley North	Survived	No	--	--	9.29	199	70	1045	63	0.59	62
Kobe NMCE	Survived	No	--	--	10.59	241	60	1265	63	0.74	63
Kobe North	Survived	No	--	--	7.22	185	60	971	63	0.52	62
Kocaeli NMCE	Failed	Yes	65.83	Structural	92.82	2848	66	1908	66	1.31	66
Kocaeli North	Survived	No	--	--	24.44	211	60	1111	63	0.62	62
Kocaeli2 NMCE	Survived	No	--	--	11.91	248	60	1308	63	0.76	63
Kocaeli2 North	Survived	No	--	--	5.47	179	60	941	63	0.51	62
Landers NMCE	Survived	No	--	--	25.38	292	60	1534	63	0.91	63
Landers North	Survived	No	--	--	24.42	259	60	1364	63	0.80	63
LSM North	Survived	No	--	--	10.9	81	59	419	63	0.17	62
NPS North	Survived	No	--	--	7.96	145	60	755	63	0.40	62
SanFernando NMCE	Survived	No	--	--	7.68	293	60	1555	63	0.92	63
SanFernando North	Survived	No	--	--	7.66	286	60	1500	63	0.91	63
SanFernando2 NMCE	Survived	No	--	--	4.26	296	60	1556	63	0.93	63
SanFernando2 North	Survived	No	--	--	4.23	261	60	1376	63	0.80	63
Percent Survived	94.12%										

Table 8.6 – Results overview for Oseligee Creek Bridge 100% Scour transverse models

Chambers 100% Scour Transverse Earthquake Event	Performance	Plastic Hinge Developed	Location of Plastic Hinge (ft)	Probable Cause of Failure	Time of Occurrence (sec)	Maximum Shear (kip)	Elevation of Shear Occurrence (ft)	Maximum Moment (kip-ft)	Elevation of Moment Occurrence (ft)	Maximum D/C Ratio	Elevation of D/C Occurrence (ft)
Coalinga North	Survived	No	--	--	13.64	308	60	1824	91	1.02	91
Imperial Valley NMCE	Survived	No	--	--	10.52	272	60	1618	91	0.89	91
Imperial Valley North	Survived	No	--	--	10.42	229	59	1295	91	0.67	91
Kobe NMCE	Survived	No	--	--	11.04	238	60	1381	91	0.75	91
Kobe North	Survived	No	--	--	6.26	192	59	1076	91	0.57	91
Kocaeli NMCE	Failed	No	--	Structural	22.65	329	60	1822	91	1.06	91
Kocaeli North	Survived	No	--	--	29.87	263	60	1565	91	0.87	91
Kocaeli2 NMCE	Survived	No	--	--	8.99	287	60	1642	91	0.91	91
Kocaeli2 North	Survived	No	--	--	8.99	249	60	1422	91	0.76	91
Landers NMCE	Failed	No	--	Structural	26.66	307	60	1802	91	0.99	91
Landers North	Survived	No	--	--	20.32	248	59	1419	91	0.77	91
LSM North	Survived	No	--	--	5.05	51	59	292	91	0.11	91
NPS North	Survived	No	--	--	8.54	239	60	1418	91	0.78	91
SanFernando NMCE	Survived	No	--	--	2.81	209	59	1203	91	0.61	91
SanFernando North	Survived	No	--	--	4.98	214	59	1221	91	0.65	91
SanFernando2 NMCE	Survived	No	--	--	4.51	346	60	1899	91	1.05	91
SanFernando2 North	Survived	No	--	--	4.89	319	60	1816	91	1.01	91
Percent Survived	88%										

8.6 Norfolk Southern Railroad Bridge Discussion

The Norfolk Southern Railroad Bridge models performed poorly. Moreover, the piles were the main cause of failure. The models suggested that the piles were failing in bending. This is thought to be a buckling problem due to several factors. The length of the piles was approximately 60 feet (including embedment into the pile cap) and the width of the pile is only 12.045 inches. Referring back to Figure 6.20 in Chapter 6, the soil profile of Norfolk Southern Railroad Bridge, it is apparent that the insitu soils are relatively weak (shear strength is 700 psf or less in lower layers). There is also a void layer that is almost 15 feet in depth, which does not provide any lateral resistance.

To determine if the problem is, in fact, most likely buckling, equation 3.1, presented in Chapter 3, was used to check Bhattacharya's (2003) recommendation that a P_{des}/P_{cr} ratio of greater than 0.5 indicated that buckling may be an issue. Table 8.7 shows the assumptions made to calculate the ratios.

Table 8.7 – Assumptions used in buckling analysis for Norfolk Southern Railroad Bridge

L_{eff}	100	ft
E	29000	ksi
I	393	in^4
Section Area of H-pile	15.5	in^2
P_{cr}	78	kips
r_{min}	5.04	in
P_{column}	680	kips/column
No. of piles/column	7	
$FS_{(assumed)}$	2	
P_{des}/pile	194	kips

L_{eff} was determined based on the assumption that the pile is pinned at the rock line and fixed at the pile cap. Therefore, the depth of the soft soil region, which was estimated as roughly 50 feet, was multiplied by a factor of 2 to estimate the effective

length. The largest moment of inertia was used because the bending was about the axis it was calculated. This also was a conservative assumption. The load per column was based on the dead loads from the bridge deck. The load of the pier cap, column, and pile cap were not included as it only increased the P_{des}/P_{cr} ratio. A pile efficiency of one was assumed for each pile. Table 8.8 summarizes the calculations made.

Table 8.8 – Norfolk Southern Railroad Bridge P_{des}/P_{cr} and L_{eff}/r_{min} results

P_{des}/P_{cr}	2.49
L_{eff}/r_{min}	238

Based from these calculations, buckling is most likely the main cause for pile failure for the Norfolk Southern Railroad Bridge models. It is also important to note that the transverse models were failing about the same axis as the longitudinal models. This suggests that it was failing regardless of which direction the load function was applied. See Table 8.9 and Table 8.10 for an overview of the longitudinal and transverse results, respectively.

Table 8.9 – Results overview for Norfolk Southern Railroad Bridge longitudinal models

Etowah Longitudinal Earthquake Event	Performance	Plastic Hinge Developed	Location of Plastic Hinge (ft)	Pile No.	Probable Cause of Failure	Time of Occurrence (sec)	Maximum Shear (kip)	Elevation of Shear Occurrence (ft)	Maximum Moment (kip-ft)	Elevation of Moment Occurrence (ft)	Maximum D/C Ratio	Elevation of D/C Occurrence (ft)
Coalinga North	Failed	Yes	615	14	Structural	7.58	240	615	447	615	1.26	615
Imperial Valley NMCE	Failed	Yes	600	9	Structural	9.17	329	600	608	596	1.74	600
Imperial Valley North	Failed	Yes	596	6	Structural	9.26	339	596	649	596	1.80	596
Kobe N-MCE	Failed	Yes	615	14	Structural	7.69	347	615	650	615	1.80	615
Kobe North	Failed	No	--	--	Structural	6.51	54	581	361	585	1.00	585
Kocaeli NMCE	Failed	Yes	600	7	Structural	9.45	353	600	658	600	1.85	600
Kocaeli North	Failed	Yes	615	1	Structural	9.34	328	615	619	615	1.72	615
Kocaeli2 N-MCE	Failed	Yes	615	14	Structural	7.86	-359	615	-672	615	1.86	615
Kocaeli2 North	Failed	Yes	615	18	Structural	7.74	323	615	602	615	1.70	615
Landers N-MCE	Failed	No	--	--	Structural	28.26	30	581	346	589	0.97	589
Landers North	Failed	No	--	--	Structural	22.8	36	581	332	589	0.93	589
LSM North	Failed	Yes	615	14	Structural	7.77	330	615	622	615	1.72	615
NPS North	Failed	Yes	600	7	Structural	9.34	350	600	647	600	1.84	600
SanFernando NMCE	Failed	Yes	596	9	Structural	9.1	352	596	663	596	1.84	596
SanFernando North	Failed	Yes	611	14	Structural	7.61	308	611	596	611	1.66	611
SanFernando2 N-MCE	Failed	Yes	615	14	Structural	7.84	359	615	676	615	1.87	615
SanFernando2 North	Failed	Yes	615	14	Structural	7.89	360	615	673	615	1.87	615
Percent Survived	0%											

Table 8.10 – Results overview for Norfolk Southern Railroad Bridge transverse models

Etowah Transverse Earthquake Event	Performance	Plastic Hinge Developed	Location of Plastic Hinge (ft)	Pile/Column No.	Probable Cause of Failure	Time of Occurrence (sec)	Maximum Shear (kip)	Elevation of Shear Occurrence (ft)	Maximum Moment (kip-ft)	Elevation of Moment Occurrence (ft)	Maximum Demand Capacity Ratio	Elevation of D/C Occurrence (ft)
Coalinga North	Failed	Yes	615	16	Structural	7.8	331	615	607	615	1.76	615
Imperial Valley NMCE	Failed	Yes	600	7	Structural	9.24	333	596	622	596	1.75	600
Imperial Valley North	Failed	Yes	600	6	Structural	9.24	335	600	618	600	1.77	600
Kobe NMCE	Failed	Yes	585	4	Structural	6.54	62	581	366	585	1.01	585
Kobe North	Failed	No	--	--	Structural	6.7	39	581	357	589	0.99	589
Kocaeli NMCE	Failed	Yes	596	7	Structural	9.4	348	596	656	596	1.82	596
Kocaeli North	Failed	Yes	615	1	Structural	9.38	349	615	656	615	1.82	614
Kocaeli2 NMCE	Failed	Yes	585	3	Structural	6.95	64	681	377	585	1.04	585
Kocaeli2 North	Failed	Yes	615	17	Structural	7.76	311	615	573	615	1.64	615
Landers NMCE	Failed	No	--	--	Structural	25.8	43	581	343	589	0.96	589
Landers North	Column Failed	Yes	667	3	Structural (column)	25.28	149	637	2088	662	1.05	662
LSM North	Failed	Yes	615	14	Structural	7.68	325	615	607	615	1.70	615
NPS North	Failed	Yes	600	7	Structural	9.35	345	600	646	600	1.79	600
SanFernando NMCE	Failed	Yes	596	1	Structural	9.16	331	596	631	596	1.75	596
SanFernando North	Failed	Yes	615	17	Structural	7.63	335	615	627	615	1.75	615
SanFernando2 NMCE	Failed	Yes	615	18	Structural	7.69	292	615	540	619	1.66	615
SanFernando2 North	Failed	Yes	615	21	Structural	7.55	219	615	336	622	1.50	615
Percent Survived	0%											

8.7 Little Bear Creek Bridge Discussion

The Little Bear Creek Bridge models performed fair, overall. Most of the models that failed were NMCE earthquake events, which are the higher magnitude events. See Table 8.11 and Table 8.12 for the longitudinal and transverse results, respectively. Only one model (San Fernando2 NMCE Longitudinal) showed a plastic hinge developing due to structural failure. Note that the change in D/C ratio distribution at elevation 530 feet is due to the change in shaft size, which is consistent with what is to be expected (lower capacity for a smaller shaft size). When the model does not show a plastic hinge zone developing in the last time step before it fails, it is difficult to discern whether the failure was structural, or numerical. Soil failure is unlikely because the drilled shafts are embedded into bedrock. If the last time step shows large bending moments and shear forces, and D/C ratios are approaching one, then structural failure may be a likely cause that the model failed. Otherwise, it could be due to numerical instability within the model. However, the bending moment and D/C ratio distributions for Little Bear Creek Bridge show that if the structure does fail, it is likely the failure will occur in the desired plastic hinge zones and not in the foundations. Liquefaction was not taken into account for this model because of the thin layer of soil over bedrock.

Table 8.11 – Results overview for Little Bear Creek Bridge longitudinal models

Franklin Longitudinal Earthquake Event	Performance	Plastic Hinge Developed	Location of Plastic Hinge (ft)	Probable Cause of Failure	Time of Occurrence (sec)	Maximum Shear (kip)	Elevation of Shear Occurrence (ft)	Maximum Moment (kip-ft)	Elevation of Moment Occurrence (ft)	Maximum D/C Ratio	Elevation of D/C Occurrence (ft)
Coalinga North	Survived	No	--	--	24.79	518	522	3138	525	0.54	526
Imperial Valley NMCE	Failed	No	--	Structural	15.77	865	522	5300	525	1.00	525
Imperial Valley North	Survived	No	--	--	21.14	423	521	2563	525	0.41	525
Kobe NMCE	Failed	No	--	Structural	13.08	823	522	5069	525	0.92	525
Kobe North	Survived	No	--	--	11.76	565	521	3450	525	0.58	525
Kocaeli NMCE	Failed	No	--	Structural	23.89	845	522	5238	525	0.99	525
Kocaeli North	Failed	No	--	Structural	23.88	826	522	5107	525	0.96	525
Kocaeli2 NMCE	Survived	No	--	--	7.28	729	522	4505	525	0.91	525
Kocaeli2 North	Survived	No	--	--	7.24	767	521	4729	525	0.90	525
Landers NMCE	Failed	No	--	Structural	22.98	868	521	5394	525	0.99	525
Landers North	Failed	No	--	Structural	23.44	845	522	5142	525	0.94	525
LSM North	Survived	No	--	--	7.99	219	521	1326	525	0.17	530
NPS North	Survived	No	--	--	8.34	486	521	2960	525	0.50	525
SanFernando NMCE	Survived	No	--	--	9.19	845	521	5215	525	0.99	525
SanFernando North	Survived	No	--	--	9.04	724	521	4473	525	0.90	525
SanFernando2 NMCE	Failed	Yes	525	Structural	4.52	864	521	5341	525	1.01	525
SanFernando2 North	Survived	No	--	--	6.25	756	522	4692	525	0.97	525
Percent Survived	59%										

Table 8.12 – Results overview for Little Bear Creek Bridge transverse models

Franklin Transverse Earthquake Event	Performance	Plastic Hinge Developed	Location of Plastic Hinge (ft)	Probable Cause of Failure	Time of Occurrence (sec)	Maximum Shear (kip)	Elevation of Shear Occurrence (ft)	Maximum Moment (kip-ft)	Elevation of Moment Occurrence (ft)	Maximum Demand Capacity Ratio	Elevation of D/C Occurrence (ft)
Coalinga North	Failed	No	--	Structural	13.03	818	521	5279	549	1.04	549
Imperial Valley NMCE	Failed	No	--	Numerical Instability	20.09	609	521	3804	549	0.69	549
Imperial Valley North	Survived	No	--	--	8.73	433	521	2793	549	0.50	549
Kobe N-MCE	Survived	No	--	--	9.69	917	521	5350	549	1.06	549
Kobe North	Survived	No	--	--	12.8	593	521	3906	549	0.77	549
Kocaeli NMCE	Failed	No	--	Structural	22.61	855	521	5490	549	1.07	549
Kocaeli North	Survived	No	--	--	22.89	705	521	4634	549	0.90	549
Kocaeli2 NMCE	Failed	No	--	Structural	8.03	894	521	5402	549	1.07	549
Kocaeli2 North	Survived	No	--	--	11.69	671	521	4536	549	0.91	549
Landers NMCE	Failed	No	--	Structural	28.58	806	521	5011	549	1.07	549
Landers North	Survived	No	--	--	24.24	554	521	3454	549	0.81	549
LSM North	Survived	No	--	--	5.99	153	520	1467	549	0.25	549
NPS North	Failed	No	--	Structural	11.68	787	521	5183	549	1.02	549
SanFernando NMCE	Failed	No	--	Structural	7.3	807	521	5184	549	1.03	549
SanFernando North	Survived	No	--	--	3.41	629	521	4382	549	0.89	549
SanFernando2 NMCE	Survived	No	--	--	3.85	742	521	4612	549	0.89	549
SanFernando2 North	Survived	No	--	--	4.83	588	521	3945	549	0.75	549
Percent Survived	59%										

8.8 Bent Creek Road Bridge Discussion

The Bent Creek Road Bridge models performed well. None of the models failed in the longitudinal or transverse direction. Like the Norfolk Southern Railroad Bridge, the Bent Creek Road Bridge foundations are H-piles. The soil profile for Bent Creek Road Bridge was saturated cohesionless soil over bedrock. The potential for liquefaction is low in this part of the state, and therefore, was not considered for this analysis. The depth to rock was about half of that of Norfolk Southern Railroad Bridge, and the soil had moderate strength. For comparison, buckling analysis was done for the Bent Creek Road Bridge model as well. Table 8.13 shows the assumptions made.

Table 8.13 – Assumptions used in buckling analysis for Bent Creek Road Bridge

L_{eff}	50	ft
E	29000	ksi
I	393	in^4
Section Area of H-pile	15.5	in^2
P_{cr}	312	kips
r_{min}	5.04	in
P_{column}	725	kips/pile footing
No. of piles/column	9	
$FS_{(assumed)}$	2	
P_{des}/pile	161	kips

The free length of the pile was estimated as 25 feet. L_{eff} was determined by multiplying the free length by 2. This is because the pile is assumed to be pinned at the rock layer and fixed at the pile cap. Instead of using just the bridge deck dead load, the column and pile footing load was also taken into account. The section properties remained the same as Etowah. Pile efficiency of 1 was assumed and the number of piles for each footing is nine. Table 8.14 summarizes the calculations made.

Table 8.14 – Bent Creek Road Bridge P_{des}/P_{cr} and L_{eff}/r_{min} results

P_{des}/P_{cr}	0.52
L_{eff}/r_{min}	119

Based from these calculations, buckling could be an issue for the Bent Creek Road Bridge model. It is important to note that when evaluating the buckling stability of a pile embedded in cohesionless soils, it is assumed that the soil liquefied and lateral resistance is basically zero. However, it should be noted that even in a liquefied state, soil still possesses residual strength (which is typically low) that can be relied on. However, it is more conservative to assume the lateral resistance is zero. It should also be noted that for the Bent Creek Road Bridge models, the time steps were larger than the other models. This was due to FB-MultiPier's restriction of memory that could be used for analysis at the time these models were run. The file sizes were simply too big for the program to access during analysis and the program would crash. Therefore, the time steps were increased to decrease the size of the output files being created. The increase in time steps is not thought to have a significant impact on the analysis, as the time steps were still relatively small (greatest one being 0.05 seconds). See Table 8.15 and 8.16 for an overview of the longitudinal and transverse results, respectively.

Table 8.15 – Results overview for Bent Creek Road Bridge longitudinal models

Lee Longitudinal Earthquake Event	Performance	Plastic Hinge Developed	Time of Occurrence (sec)	Maximum Shear (kip)	Elevation of Shear Occurrence (ft)	Maximum Moment (kip-ft)	Elevation of Moment Occurrence (ft)	Maximum D/C Ratio	Elevation of D/C Occurrence (ft)
Coalinga North	Survived	No	13.98	21	657	124	657	0.43	657
Imperial Valley NMCE	Survived	No	34.68	17	652	117	656	0.44	657
Imperial Valley North	Survived	No	16.77	8	654	73	657	0.31	657
Kobe NMCE	Survived	No	8.76	27	652	176	656	0.60	657
Kobe North	Survived	No	9.42	14	652	125	657	0.46	657
Kocaeli NMCE	Survived	No	33.72	15	652	130	657	0.48	657
Kocaeli North	Survived	No	41.2	12	652	105	657	0.41	657
Kocaeli2 NMCE	Survived	No	8.5	26	652	174	656	0.59	657
Kocaeli2 North	Survived	No	7.24	12	652	105	657	0.41	657
Landers NMCE	Survived	No	30.72	19	652	173	657	0.58	657
Landers North	Survived	No	47.56	22	652	148	656	0.52	657
LSM North	Survived	No	8.96	3	656	22	657	0.15	657
NPS North	Survived	No	16.3	5	654	43	657	0.22	657
SanFernando NMCE	Survived	No	4.86	13	652	117	657	0.44	657
SanFernando North	Survived	No	4.86	12	652	111	657	0.42	657
SanFernando2 NMCE	Survived	No	4.32	18	652	124	656	0.46	657
SanFernando2 North	Survived	No	4.29	15	652	101	656	0.40	657
Percent Survived	100%								

Table 8.16 – Results overview for Bent Creek Road Bridge transverse models

Lee Transverse Earthquake Event	Performance	Plastic Hinge Developed	Time of Occurrence (sec)	Maximum Shear (kip)	Elevation of Shear Occurrence (ft)	Maximum Moment (kip-ft)	Elevation of Moment Occurrence (ft)	Maximum D/C Ratio	Elevation of D/C Occurrence (ft)
Coalinga North	Survived	No	7.32	29	657	65	657	0.41	657
Imperial Valley NMCE	Survived	No	10.47	12	657	30	657	0.22	657
Imperial Valley North	Survived	No	10.47	11	657	28	657	0.21	657
Kobe NMCE	Survived	No	6.06	34	657	74	657	0.46	657
Kobe North	Survived	No	8.25	32	657	71	657	0.45	657
Kocaeli NMCE	Survived	No	23.92	32	657	65	654	0.41	657
Kocaeli North	Survived	No	24.36	27	657	54	654	0.37	657
Kocaeli2 NMCE	Survived	No	7.24	31	657	61	654	0.38	656
Kocaeli2 North	Survived	No	7.06	18	657	47	657	0.32	657
Landers NMCE	Survived	No	22.92	30	657	62	654	0.41	656
Landers North	Survived	No	22.88	24	657	46	654	0.32	656
LSM North	Survived	No	5.76	3	657	7	657	0.11	657
NPS North	Survived	No	8.3	16	657	33	657	0.21	657
SanFernando NMCE	Survived	No	8.97	22	657	44	657	0.28	657
SanFernando North	Survived	No	9	17	657	42	657	0.30	657
SanFernando2 NMCE	Survived	No	5.13	26	657	62	654	0.40	656
SanFernando2 North	Survived	No	4.29	18	657	46	657	0.31	657
Percent Survived	100%								

8.9 Scarham Creek Bridge Discussion

The Scarham Creek Bridge model performed well, overall. The longitudinal model seemed to have instability problems for some time-history events. This is most likely due to the large displacements that were generated. These displacements can cause secondary moments which can cause large out-of-balance forces to occur. See Table 8.17 and Table 8.18 for an overview of the longitudinal and transverse results, respectively. The displacement when the acceleration is zero is nearly zero as well. However, the failed models showed that the bending moment and shear force were very high at the last time step, which then caused the model to fail. The Kobe NMCE and the Kocaeli2 NMCE models are thought to have failed due to numerical instability because the displacements were nearly zero for the last 35 seconds. The transverse models performed well. The strut provided extra stiffness in the transverse direction. For the longitudinal models, there is an indication that the strut's mass created some inertial effects within the model. The bending moment and D/C distributions show slight changes at the strut elevation, which indicates that the strut affected the response of the pier slightly in the longitudinal direction. This can be seen on the shear force distribution figures (more drastically in the transverse direction). The models also showed that the largest moment was developing at the rock line, which is a desired plastic hinge zone location. It should also be noted that the bent is very tall. The free length of the columns is approximately 60 feet, which can lead to large displacements at the top of the pier, especially in the longitudinal direction. Liquefaction was not considered because the rock layer is very shallow on site and the thin soil layer is assumed to scour. Buckling was not checked for this model even though the pier was very tall (approximately 60 feet

from the ground surface). This is because of the extra transverse resistance the strut provided and its overall performance when seismically loaded.

Table 8.17 – Results overview for Scarham Creek Bridge longitudinal models

Marshall Longitudinal Earthquake Event	Performance	Plastic Hinge Developed	Location of Plastic Hinge (ft)	Probable Cause of Failure	Time of Occurrence (sec)	Maximum Shear (kip)	Elevation of Shear Occurrence (ft)	Maximum Moment (kip-ft)	Elevation of Moment Occurrence (ft)	Maximum D/C Ratio	Elevation of D/C Occurrence (ft)
Coalinga North	Survived	No	--	--	19.99	248	863	1631	868	0.11	872
Imperial Valley NMCE	Survived	No	--	--	14.99	588	863	3855	868	0.33	872
Imperial Valley North	Survived	No	--	--	15	435	863	2858	868	0.22	872
Kobe NMCE	As if Survived	--	--	--	7.06	568	863	3782	868	0.38	872
Kobe NMCE	Failed	Yes	876	Numerical Instability	75.31	11240	876	13141	874	1.69	876
Kobe North	Survived	No	--	--	6.13	473	863	3103	868	0.29	872
Kocaeli NMCE	Failed	Yes	876	Structural	90.09	11637	876	12638	876	1.68	876
Kocaeli North	Survived	No	--	--	25.18	490	863	3227	868	0.26	872
Kocaeli2 NMCE	As if Survived	--	--	--	9.29	1091	863	7176	868	0.80	872
Kocaeli2 NMCE	Failed	Yes	867	Numerical Instability	64.9	10806	867	12507	867	1.46	867
Kocaeli2 North	Failed	Yes	876	Structural	69.7	12538	880	13868	880	1.79	880
Landers NMCE	Survived	No	--	--	46.8	953	863	6269	868	0.66	872
Landers North	Survived	No	--	--	46.74	791	863	5195	868	0.51	872
LSM North	Failed	Yes	881	Structural	92.94	12946	914	12997	879	1.88	814
NPS North	Survived	No	--	--	7.61	136	859	798	863	0.62	870
SanFernando NMCE	Survived	No	--	--	9.52	678	863	4444	868	0.41	872
SanFernando North	Survived	No	--	--	7.69	628	863	4111	868	0.41	872
SanFernando2 NMCE	Survived	No	--	--	4.27	537	863	3524	868	0.34	872
SanFernando2 North	Survived	No	--	--	4.27	420	863	2752	868	0.24	872
Percent Survived	71%										

Table 8.18 – Results overview for Scarham Creek Bridge transverse models

Marshall Transverse Earthquake Event	Performance	Plastic Hinge Developed	Time of Occurrence (sec)	Maximum Shear (kip)	Elevation of Shear Occurrence (ft)	Maximum Moment (kip-ft)	Elevation of Moment Occurrence (ft)	Maximum D/C Ratio	Elevation of D/C Occurrence (ft)
Coalinga North	Survived	No	11.28	426	863	2656	867	0.31	867
Imperial Valley NMCE	Survived	No	10.73	625	863	3899	867	0.55	868
Imperial Valley North	Survived	No	10.68	513	863	3206	867	0.39	867
Kobe NMCE	Survived	No	10.35	589	863	3673	867	0.51	868
Kobe North	Survived	No	10.35	406	863	2525	867	0.28	867
Kocaeli NMCE	Survived	No	23.81	774	863	4861	867	0.71	868
Kocaeli North	Survived	No	23.8	574	863	3582	867	0.46	867
Kocaeli2 NMCE	Survived	No	7.22	663	863	4163	867	0.61	867
Kocaeli2 North	Survived	No	7.22	517	863	3220	867	0.43	867
Landers NMCE	Survived	No	23.48	770	863	4830	867	0.71	868
Landers North	Survived	No	23.4	638	862	3997	867	0.56	868
LSM North	Survived	No	10.83	131	863	811	867	0.05	895
NPS North	Survived	No	7.96	308	863	1921	867	0.19	867
SanFernando NMCE	Survived	No	3.23	641	863	4000	867	0.51	867
SanFernando North	Survived	No	3.23	612	863	3836	867	0.45	867
SanFernando2 NMCE	Survived	No	4.58	877	863	5562	867	0.82	868
SanFernando2 North	Survived	No	4.6	791	863	4991	867	0.74	868
Percent Survived	100%								

8.10 Direct Analysis Results Summary

Five bridge pier case histories were modeled in FB-MultiPier: Oseligee Creek Bridge 25% and 100% scour, Norfolk Southern Railroad Bridge, Little Bear Creek Bridge, Bent Creek Road Bridge, and Scarham Creek Bridge. Dynamic analysis was run for each model using a suite of scaled earthquake time-history events.

The Oseligee Creek Bridge case history was modeled for two cases: 25% scour and 100% scour. The Oseligee Creek Bridge bent for the 25% scour case performed poorly, overall. Most of the failed models were suspected to have failed because of either structural failure or soil failure. Soil failure is likely due to large displacements that the soil spring undergoes. The insitu soil above the rock line for the Oseligee Creek Bridge case history was very weak and provided little lateral resistance. Bending moment and D/C ratio was typically largest below the ground surface and above the rock line in the longitudinal direction. In the transverse direction, it was largest at the column/pier cap connection. However, large bending moments were still developing below the ground surface. This suggests that plastic hinges may develop in these locations. If a plastic hinge developed under the ground surface, it would be difficult to identify and repair.

In comparison, the Oseligee Creek Bridge bent for the 100% scour case performed well, overall. The three models that failed all used NMCE scaled earthquake time-history events, which are of larger magnitude and, typically, more harmful than the North scaled time-histories. The North scale factor events are more representative of what the state of Alabama would generally experience. Bending moment and D/C ratio was typically largest at the rock line and column/pier cap connection when seismically loaded in the longitudinal and transverse

directions, respectively. This suggests that plastic hinges may develop in these locations, which would be ideal.

The Norfolk Southern Railroad Bridge pier models performed poorly due to pile failure. Every model failed due to structural failure within the H-pile foundations (specifically the battered piles). It appeared that the soft clay provided very little lateral resistance, causing the piles to buckle.

The Little Bear Creek Bridge bent models performed fair, overall. Most of the models that failed were subjected NMCE earthquake events, which are the higher magnitude events. Bending moment and D/C ratio was typically largest at the rock line and column/pier cap connection when seismically loaded in the longitudinal and transverse directions, respectively. This suggests that plastic hinges may develop in these locations, which would be ideal.

The Bent Creek Road Bridge pier models performed well, overall. All of the models survived the earthquake event they were subjected to. The moderate strength cohesionless soil seemed to provide adequate lateral resistance. The highest D/C ratio for any pile was 0.6. The bending moment and D/C ratio in the columns were largest at the column base and the column/pier cap connection in the longitudinal and transverse directions, respectively. This suggests that plastic hinges are most likely to form at these locations.

The Scarham Creek Bridge bent models performed well, overall. Bending moment and D/C ratio was typically largest at the rock line and column/pier cap connection when seismically loaded in the longitudinal and transverse directions, respectively. This suggests that plastic hinges may develop in these locations, which would be ideal. Some displacements at the top of the pier were very large. This is expected because of the free length of the bent. Typically, structures with longer period tend to displace more that structures with shorter periods.

The major limitation to these models is that only one bridge pier was modeled. In the complete system for a bridge, interaction between the bridge deck, abutments, and other bridge piers (if applicable) is very important. The interaction between these components can possibly provide additional stiffness, which could reduce the inertial forces generated within the bridge piers. Without the interaction of the bridge deck, the displacements at the top of the pier are not completely accurate. However, these models provided an indication of where maximum shear forces and bending moments would develop within the bridge pier, specifically in the foundations. This subsequently suggests probable locations of plastic hinge zones that would develop, which is a key component of seismic design of bridges.

Chapter 9: State DOT Survey

9.1 State DOT Survey

As part of the research scope, several southeastern state DOTs were surveyed to compare their seismic design process, specifically to deep foundations, to ALDOT's current practice. The survey was sent to eleven states: Arkansas, Florida, Georgia, Kentucky, Louisiana, Mississippi, North Carolina (NC), South Carolina (SC), Tennessee, Virginia, and West Virginia. At the time of writing this document, three had replied: Arkansas, Kentucky, and South Carolina. Below is the survey submitted to the state DOTs:

1. Do you use/prefer driven piles, drilled shafts, spread footings, or a combination of the three for foundation design in a seismic area?
2. If driven piles are used for foundation design in a seismic area, what type(s) and configuration(s) is/are most often used? If it is a group configuration, please provide typical spacing, batter (if applicable), and driving criteria.
3. Is there a specific standard you use to determine if insitu soils on site are potentially susceptible to liquefaction (i.e. geologic age and origin, water table levels, fines content, etc.)?
4. Have you ever taken remedial measures to meet seismic standards (current foundations not adequate or weak soil layer is a concern), specifically in regards to the foundations? If so, what was done and why?
5. Have your foundation designs been validated through computer program modeling or some other method? If so, what program(s) did you use and how (combination of programs, run dynamic analysis or push-over analysis, etc.)?

9.2 Arkansas Survey Response

1. Since our bridge foundations in seismic zones are predominantly in soils with very deep overburden, we typically use driven trestle pile bents or pile footings. Drilled shafts may also be used, however, we have experienced difficulties in the past with construction procedures used in the placement of slurry-displaced drilled shafts; so. the majority of our seismic bridges are designed using piling.

2. Pile Types: Steel H-piles where significant depth of sand or clay exists over rock, Concrete piles in Seismic Zone 2 (assumed to also mean SDC B) or less, and Concrete-filled steel shell piles in all seismic zones.

Pile Spacing: As required by design, but not less than LRFD Specification minimum requirements.

Pile Batter: Typically use vertical piles unless other present or more frequently occurring design concerns such as earth pressure (end bents), bridge curvature, water velocity, etc. out weigh concerns from the extreme seismic event. When battered piling is used in seismic zones, the batter is minimized from our standard 4H:12V to 1.5H:12V.

Driving Criteria: Ultimate bearing capacity is typically determined using a Wave Equation Analysis (WEAP) where hammer approval and bearing graph relationships are determined and provided for the Contractor's use.

3. Liquefaction susceptibility is determined by using the water table, soil type, and SPT blow counts from field sampling to calculate a factor of safety using a procedure developed by Youd and Idriss (2001).

4. No remedial measures have been taken on in-situ soil to date. Geosynthetic internal reinforcement is used in bridge embankments when required by design and

minimum pile tip elevations may be specified to ensure pile tips are not established in a liquefiable layer. Pile buckling due to a longer unsupported length in liquefiable layers is not typically considered. Our liquefactions calculations often result in a combination of liquefiable and non-liquefiable layers. Some soil resistance is considered to be available during liquefaction and steel shell piles are concrete-filled to help resist buckling.

5. We model our bridges using the SEISAB program in conjunction with a response spectrum analysis and this provides us with the seismic forces to use in our foundation design for the extreme event case.

9.3 Kentucky Survey Response

1. We typically use driven piles in areas where seismic design is a consideration. However, the selection of foundation type is typically not governed by seismic design considerations. Due to considerations other than seismic design driven piles are typically the appropriate foundation type in the New Madrid Seismic Zone (NMSZ) where there are significant seismic design considerations. However, we would potentially use another foundation type such as drilled shafts or spread footings on bedrock if warranted by the site conditions.

2. We typically use steel piles (H or pipe) with a group configuration when we use driven piles. The spacings are typically 3 ft to 10 ft depending on loads, and whether pile is point bearing or friction. We typically avoid battered piles in seismic zones. Driving criteria would typically be determined using dynamic testing and in some cases only dynamic formulas. We are currently working on a bridge over Kentucky Lake (in the NMSZ) where we will be performing static and pseudo-static (i.e. Statnamic) testing in conjunction with dynamic testing to determine pile driving criteria.

3. Preliminary liquefaction assessments may be based on SPT blow counts, CPT testing, water table, and fines content. On our Lake Bridges Project (the previously-mentioned bridge over Kentucky Lake and a nearby bridge over Lake Barkley) rigorous liquefaction analyses were performed using site-specific ground motions, equivalent linear site response analyses using shear modulus values determined from in-situ and laboratory resonant column testing, and both CPT and SPT data. These analyses are generally based on the NCEER workshop recommendations as published in the American Society of Civil Engineers (ASCE) Journal (2001) (Youd and Idriss 2001).

4. On our Lake Bridges project we specified deep soil mixing (DSM) to mitigate against liquefaction due to the liquefaction predicted for a 2500 year seismic event. We had a single bidder that was significantly higher than the Engineer's estimate and the bid was rejected. Subsequently, the seismic design criteria were changed to design for the 1000 year event and DSM was no longer required. We re-let the project and construction is currently ongoing.

5. Foundations are sometimes modeled with GT STRUDL to estimate seismic response. On our Lake Bridge Projects, dynamic modeling using time histories are being performed using SAP and MIDAS. Push over analyses was also performed.

9.4 South Carolina Survey Response

1. South Carolina Department of Transportation (SCDOT) exclusively uses either driven piles or drilled shafts to support our bridges. Spread footings are not allowed at any location that will undergo soil Shear Strength Loss (SSL) (i.e. liquefaction). Deep foundations are designed to incorporate downdrag should settlement caused by SSL be present at the location.

2. SCDOT uses precast, prestressed concrete piles, H-piles and combination piles to support our bridges depending on the load (axial and lateral) and the soil that the foundations will be driven into. Our typical pile sizes are indicated in Table 7.1.

Table 9.1 – South Carolina's Typical Pile Types and Sizes

Pile Type	Size
Steel H-piles	HP 12x53
	HP 14x73
	HP 14x89
	HP 14x117[1]
Steel Pipe Piles	16-inch[2]
	18-inch[2]
	20-inch[2]
	24-inch[2]
Prestressed Concrete Piles[3]	18-inch
	20-inch
	24-inch
	30-inch[4]
	36-inch[4]
Combination Piles	18-inch[3] with W 8x58 stinger
	20-inch[3] with HP 10x57 stinger
	24-inch[3] with HP 12x53 stinger

[1]used where penetration is minimal and nominal capacity is large
[2]wall thickness is ½ inch for all pipe pile sizes
[3]prestressed concrete piles are square in section
[4]these sizes are only allowed with the written approval of SCDOT

Please note that the pipe piles are typically filled with concrete to improve seismic performance. Typically SCDOT uses pile bents for driven piles, with pile footings being used on a relatively limited basis. The piles are installed typically no closer than 3 diameters apart in the transverse direction. Driving criteria is based either on reaching a specified tip elevation or is based on achieving a specified nominal capacity. SCDOT also tries to indicate which loading condition controlled the design i.e. axial or lateral and static (strength) or seismic (extreme event). For drilled shafts, SCDOT typically uses a single drilled shaft supporting a single column with multiple columns supporting the bent (typically 3 to 5 columns) depending on the width of the bridge. We also have used hammer-head type foundations before as well as drilled shaft footings [e.g. The Cooper River Bridge (Arthur Ravenel, Jr. Bridge) in Charleston, SC].

3. SCDOT has adopted the use of the Idriss and Boulanger (2008) procedure. We both screen the site for potential SSL as well as conduct a full SSL analysis. These procedures are contained in Chapter 13 of the SCDOT Geotechnical Design Manual (GDM) v. 1.1 (SCDOT 2010). A copy of this Chapter, as well as the entire GDM, is available at the SCDOT website. Please note that we are in the process of revising our GDM and would be willing to provide ALDOT a draft copy of our GDM for reference.

4. First, SCDOT does not retrofit bridges to meet seismic performance. Second, if SCDOT reviews the project, we do not allow deep foundations to be founded in liquefiable or soft clays that may undergo SSL during seismic shaking. Finally, we account for the movement of the end slope into the bridge either through acceptable movements and the necessary loads being applied to the bridge or through ground improvement. If slope stability is not an issue we would typically design the bridge to accommodate the downdrag on the piles by checking the pile capacity. If slope instability is an issue, we start using the cheapest and easiest ground improvement method we can (i.e. geogrid) and then proceed toward the most expensive ground improvement method e.g. DSM or some other in-situ modification. Our number one rule is no collapse of the bridge.

5. The designers use L-pile, CSiBridge (CSI 2013), Leap Bridge (RC-Pier). Dynamic analysis is run using CSiBridge; this program allows performing the response spectral analysis and the push-over analysis. The designer shall meet the requirements of the Seismic Design Specifications. (Please note that this last answer was prepared by our Seismic Design Support Section).

9.5 State DOT Survey Summary

1. All states use driven piles for seismic design, but seismic hazard may not necessarily be the controlling factor in foundation selection and design. Arkansas primarily uses driven piles for seismic bridges. Kentucky generally uses driven piles as well; however, it is usually due to other considerations other than seismic hazard, and considers other foundation types is the it is warranted by the site conditions. SC exclusively uses driven piles and/or drilled shafts to support bridges in seismic hazard.

2. Each state uses a variety of driven piles. Most of the time, the selection of foundation type is dependent upon site conditions. Arkansas uses steel H-piles when significant depth of sand or clay to bedrock is present; concrete piles are used for seismic zone 2 (SDC B) or less, and steel pipe piles filled with concrete can be used for all seismic zones. Kentucky typically uses steel (H or pipe) piles when using driven piles. SC uses steel, concrete, or combination piles depending on local site conditions and are typically pile bents (not pile footings). Group spacing is typically what is recommended by design standards for all DOTs. SC did state that in the transverse direction, pile spacing is no less than three diameters. Arkansas decreased their typical batter slope (1.5H:12V) when in a seismic zone and Kentucky usually avoids battered piles all together in seismic areas. SC did not comment. Driving criteria is determined by WEAP analysis for Arkansas; Kentucky uses statnamic or dynamic (most likely Pile Driving Analyzer [PDA]); and SC uses a specified tip elevation that must be reached or achieving a specified nominal capacity.

3. Liquefaction assessments are handled differently by all three states. Arkansas uses the Youd and Idriss (2001) procedure; whereas Kentucky generally conducts a

preliminary assessment based on SPT and CPT testing, water table elevation and fines content. If further evaluation is needed, they perform analysis based on the NCEER workshop published in the ASCE Journal (2001) (Youd and Idriss 2001). SC adopted the Idriss and Boulanger (2008) procedure. They have also documented in the SCDOT GDM, a standardized procedure for the department to use (SCDOT 2010).

4. Remedial measures are generally not taken by any of the DOTs. Kentucky did order DSM to be done based on a 2500 year seismic event, but was eventually not economically feasible because the seismic event was lowered to 1000 year. SC makes an interesting point in that it does not allow deep foundations to be founded in soft clay or liquefiable sands if it was reviewed by the SCDOT. They did not expound on how they determine a suitable foundation selection and design for a site given those characteristics.

5. All three DOTs use computer programs to determine seismic response. SC's approach is very similar to part of this research project's scope. It uses LPILE to determine the foundation response, and then inputs the foundation springs into CSiBridge to perform a response spectral analysis as well as a static pushover analysis.

Chapter 10: Conclusion and Recommendations

10.1 Introduction

This objective of this study was to update the seismic standards for bridge design in the state of Alabama. With the transition of design from the Standard Specification to the new LRFD Specification, ALDOT wanted to know the changes that would occur in bridge design as a result, specifically in four major areas. These changes are due mainly to the research in seismic hazard mapping and earthquake engineering that have been incorporated into the LRFD Specifications, but not the Standard Specifications. The seismic hazard maps in the Guide Specifications have a higher return period than the maps in the Standard Specifications, meaning that bridges must be designed to experience larger seismic forces. This increase in forces must be dealt with by the designer. The first task established standard design procedures and details for bridges in low to moderate seismic regions, SDC A and SDC B. The second task investigated the current superstructure-to-substructure connection and proposed a new connection design. The third task studied the effects of using the Guide Specifications displacement based design procedures for bridges classified as “Critical” or “Essential.” The fourth task developed design methods for driven pile foundations under seismic loads.

10.2 Superstructure-to-Substructure Connection

The second task will be discussed first because its results will be included in the design standards for SDC A and B. The superstructure-to-substructure connection was analyzed because it was unknown if the current connection was adequate to resist the expected horizontal

design forces. In this study, it was assumed that the current connection used by ALDOT did not provide a complete load path in the longitudinal direction, so a new connection was designed that would provide the load path. However, it was eventually decided to continue using the original connection and allow the girders to move after the connection slipped. The connection needed to be analyzed in both orthogonal directions to ensure that it was acceptable. The results from this study include the following:

- Using Equation 10.1 to determine the minimum seat width was found to be acceptable for estimating the minimum seat width in the longitudinal direction and ensuring the girders had enough room to "ride out" the design earthquake.
- It was determined that for bridges in SDC B, the S_{D1} value used in Equation 9.1 should be taken as 0.3 in order to provide a greater seat width than that provided by the Guide Specifications.
- The connection was determined adequate in the transverse connection because the steel clip angles and anchor bolts were designed to resist the largest horizontal loads from the SDC B bridges studied.
- The anchor bolts were recommended to be designed for each bridge, since the diameter of the bolts depended on the expected horizontal force.

Equation 9.1 can be seen below. This equation was created through research conducted by the Applied Technology Council and Multidisciplinary Center for Earthquake Engineering Research (ATC/MCEER Joint Venture, 2003) that resulted in a better estimation of the seat width demand for girders.

$$N = \left(4 + 0.02L + 0.08H + 1.09\sqrt{H}\sqrt{1 + (2\frac{B}{L})^2}\right) * \left(\frac{1+1.25S_{D1}}{\cos(\alpha)}\right) \qquad \text{Equation 10.1}$$

10.3 Bridge Design Standards

Once the superstructure-to-substructure connection was analyzed, design standards were developed for bridges in SDC A and B. These standards were developed by re-designing multiple bridges in each SDC and observing the differences in the final design between the two specifications. SDC A was split into two categories representative of the expected spectral accelerations, A1 and A2. The design standards for bridges in SDC A1 included only designing the connection for the horizontal design forces, supplying the minimum seat width using Equation 5.1, and designing the transverse reinforcement for the column. Once these standards were met, the design for bridges in SDC A1 was completed. Bridges in SDC A2 were still expected to experience low seismic forces, but had the possibility of experiencing plastic forces, and thus required to satisfy the minimum detailing requirements of SDC B. The design standards for bridges in SDC A2 included designing the connection for the horizontal design forces, determining the plastic hinge length, calculating the spacing of reinforcement within the hinge, supplying the minimum seat length using Equation 5.1, designing the transverse reinforcement outside of the plastic hinge length. Standard design details for bridges in SDC A2 were developed to aid the designer with these calculations. Bridges in SDC A did not require any structural analysis.

However, for SDC B, a computer model and structural analysis were required to be completed in order to determine the bridge displacement capacity and column design forces. These bridges were expected to experience plastic forces, so the columns were designed to allow plastic hinges to form in order to dissipate the energy from the expected design earthquakes. The other design standards included calculating the plastic hinge length using the LRFD

Specifications, detailing the transverse reinforcement inside this length using the minimum ratios of the Guide Specifications, supplying the minimum seat length calculated from Equation 9.1 and designing the transverse reinforcement outside of the plastic hinge length. Standard design details for bridges in SDC B were developed to aid the designer with these calculations. One additional recommendation was made for bridges in SDC B: to use the extension length suggested in the LRFD Specifications to promote the formation of plastic hinges.

Other recommendations that were made concerning the seismic design of bridges include the following:

- Use a soil shear wave velocity test to verify soil site class of A or B at a bridge site to decrease the SDC of a bridge.
- The live load factor from the LRFD Specifications should not be used when calculating the horizontal design force in SDC A. However, it should be considered for high traffic bridges that constantly experience a full live load, such as in a major city center.
- The plastic hinge length should be determined using the LRFD Specifications because it results in a smaller hinge length, which allows a greater length of the column over which splicing can occur. For extremely tall columns, however, the length in the Guide Specifications should be checked.
- Cross-ties should be used to increase the spacing of transverse reinforcement outside of the plastic hinge length if it is determined that using only one tie around the perimeter of the longitudinal reinforcement results in very tight spacing.
- Smaller struts should be used in bridges with very tall columns to allow the struts to yield first and protect the columns.

10.4 Task 3 Conclusions

Based on the analysis performed in this project, the following conclusions regarding the performance and implementation of the Guide Specification design on Alabama bridges were reached:

- Ground Motions that represent the hazard for northern Alabama are difficult to acquire, and scaling of worldwide ground motions is required in order to simulate this hazard.
- The two largest seismic hazards locations in Alabama each control different natural period bridges. One hazard controls longer period bridges, and the other controls shorter period bridges.
- Current connection details at end span locations of highway bridges exhibit adequate strength and ductility for design level seismic events. Failures of these connections were only observed in cases of excessive bent and span displacements, indicating structural collapse of bridge bents.
- Highway bridges designed with stiffer substructures using the Guide Specification should behave in a manner that is considered safe and result in usability after a seismic event.
- Bridges with flexible substructures may require additional design provisions regarding column diameter.
- Bridges resting on weaker or scour-able soils will require additional analysis in order to determine lateral foundation and soil capacities, as well as capacities of substructure displacement. Increase in foundation and column diameters may be required if soil cannot provide adequate lateral resistance.

- Bridges with tall substructures will require additional p-delta analysis for larger displacements.
- Critical and Essential bridges can be designed using the ASSHTO guide specification in the state of Alabama, with minor additional analysis.

10.5 Task 4 Conclusions

Based on the research in Task 4, the following conclusions were made on the response of deep foundations to seismic and dynamic loads.

- The drilled shaft case histories with drilled shafts embedded in shallow bedrock performed well, overall. If structural failure occurred (plastic hinge zones developed), they typically developed at the rock line (longitudinal direction) or column/pier cap connection (transverse).
- Based on the Chambers County case histories, that the 25% scour case was more detrimental to the performance of the drilled shaft foundations than the 100% scour case. Plastic hinge zones seemed to be developing below the ground surface in the 25% scour case due to the low lateral resistance provided by the soil layers above the bedrock.
- The driven pile case histories performed well when founded in competent soil (Lee County case history). However, the Etowah case history suggested that pile performance is poor when thick layers of soft clay are present, even in a moderate seismic hazard. Buckling, due to the lack of lateral resistance by the soil is most likely the cause of failure.
- Plastic hinge zones typically formed at the rock line in the longitudinal direction and at the pier cap in the transverse direction when the bed rock was shallow.

- If soft soils are present over rock, plastic hinges may form below the ground surface, but above the rock line.
- If driven piles are founded through soil that provides adequate lateral resistance, plastic hinges would most likely form at the base of the column or at the top of the pier cap for longitudinal and transverse directions, respectively.
- Deep foundations should be evaluated for buckling using the recommendation ($P_{des}/P_{cr} < 50$) made by Bhattacharya (2003).
- An alternative (or adaptive) foundation design should be considered for sites that have liquefiable or soft clay soils present.
- If seismic design is required, a detailed site investigation as well as laboratory tests should be conducted to more accurately estimate the soil parameters. This could potentially lead to a more efficient foundation design and reduce construction costs.
- DOTs responding do not retrofit existing structures for on the basis seismic conditions. Soil improvement may be considered for new construction, but may be cost prohibitive. The most common method for improving seismic performance was driving foundations deeper and avoiding soft soil layers. Remedial measures are typically not taken by any of the states that responded to the survey.

10.6 Overall Conclusions

- The existing connection used by ALDOT is sufficient for seismic design in the higher seismic zone of Alabama provided that the larger seat length is used and the anchor bolts are designed based on the horizontal forces required by analysis.

- Critical and essential bridges can be designed according to the Guide Specification provided that the foundations and connections are designed to account for the lateral forces prescribed by the code and the foundation is capacity protected.
- It is not recommended to use pile foundations in the high seismic zones in soil with weak soils or liquefiable soils. Current drilled shaft designs appear sufficient to resist seismic loads.

10.7 Recommendations

- Though the likelihood of liquefaction occurring in Alabama is very low for most parts of the state, the potential for liquefaction should always be considered especially in regard to bridges near waterways in the northern part of the state.
- Soil data compiling of recent, past sites and future sites or bridge projects should be done to map site class and the SDC throughout the state. This can possibly expedite the design phase of future projects.
- In high seismic areas (relative to Alabama), shear wave velocity testing should be done. This could possibly lead to higher site classifications (A being the highest) which would lessen the seismic design requirements.

References

AASHTO. (2007). AASHTO Ground Motion Parameters Calculator Version 2.1. Washington DC.

AASHTO. (2010). *AASHTO LRFD Bridge Design Specifications, 5th Edition.* Washington, D.C.

AASHTO. (2009). *Guide Specifications for LRFD Seismic Bridge Design* (1st ed.). Washington DC: American Association of State Highway and Transportation Officials.

AASHTO. (2011). *Guide Specifications for LRFD Seismic Bridge Design* (2nd ed.). Washington DC: American Association of State Highway and Transportation Officials.

AASHTO. (2007). *LRFD Bridge Design Specifications* (4th ed.). Washington DC: American Association of State Highway and Transportation Officials.

AASHTO. (2009). *LRFD Bridge Design Specifications* (4th ed.). Washington DC: American Association of State Highway and Transportation Officials.

AASHTO. (2002). *Standard Specifications for Highway Bridges* (17th ed.). Washington DC: American Association of State Highway and Transportation Officials.

ACI 318. (2008). *Building Code Requirements for Structural Concrete and Commentary.* Farmington Hills, Michigan: American Concrete Institute.

ACI Committee 224. (2001). *Control of Cracking of Concrete Structures.* Farmington Hills, MI: American Concrete Institute.

AISC. (2005). *Steel Construction Manual* (13th ed.). United States: American Institute of Steel Construction.

Alabama Department of Transportation. (2008). *Bridge Bureau Structures Design and Detail Manual.* Montgomery, AL.

Alabama DOT. (2012). *ALDOT Standard Details.* Alabama Department of Transportation.

Alaska DOT. (2008). *Tanana River Bridge: Alaska Highway Bearings.* Alaska Department of Trasnportation and Public Facilities.

ALDOT. (1971). Hold Down and Anchorage Devices for Roadway Slabs: I-10 East Tunnel Interchange.

American Society for Testing and Materials. (1998). *ASTM D 6275 - Standard Practice for Laboratory Testing of Bridge Decks* . West Conshohocken, PA: ASTM International .

American Society of Civil Engineers. (2009). *Report Card for America's Infrastructure.* Retrieved June 2012, from Infrastructure Report Card: http://www.infrastructurereportcard.org/fact-sheet/bridges

American Welding Society. (2008). *AASHTO D1.5M Bridge Welding Code 5th Edition.* Washington, D.C.

ATC/MCEER Joint Venture. (2003). *Recommended LRFD Guidelines for the Seismic Design of Highway Briges.* Federal Highway Administration.

Badie, S. S. (2008). *NCHRP Report 584 - Full-Depth Precast Concrete Bridge Deck Panel Systems.* Washington, D.C.: Transportation Research Board.

Barker, R. M., & Puckett, J. A. (2007). *Design of Highway Bridges An LRFD Approach.* Hoboken, NJ: John Wiley & Sons.

Caltrans. (1994, June). Bridge Bearings. *Memo to designers 7-1* , pp. 1-12.

Caltrans. (2011, October). *Bridge Design Specifciations: Chapter 1.* Retrieved February 18, 2013, from California Department of Transportation: http://www.dot.ca.gov/hq/esc/techpubs/manual/bridgemanuals/bridge-design-practice/pdf/bdp_1.pdf

Chen, W.-F., & Duan, L. (2000). *Bridge Engineering Seismic Design.* Boca Raton: CRC Press.
Chopra, A. K. (2007). *Dynamics of Structures.* Upper Saddle River, NJ: Pearson Prentice Hall.
Colson, P. J., & Marshall, J. D. (2011). *Influence of the LRFD Bridge Design Specifications on Seismic Design in Alabama.* Auburn University, Auburn, AL.
Computer and Structures Inc. (2012). *CSI Bridge 15.* Berkely, CA: Computer and Structures, Inc.
Computers & Structures inc. (2012, August 02). Caltrans vs. fiber hinge. Berkley, California, United States of America.
Corporation, P. T. (2007). *Mathcad 14.* Needham, MA: Parametric Technology Corporation.
Coulston, P. J., & Marshall, J. D. (2011). *Influence of the LRFD Bridge Design Specifications on Seismic Design in Alabama.* Auburn University, Auburn, AL.
Culmo, M. P. (2011). *Accelerated Bridge Construction - Experience in Design, Fabrication, and Erection of Prefabricated Bridge Elements and Systems.* McLean, VA: Federal Highway Administration - Office of Bridge Technology.
EERI. (2001, November). Preliminary Observations on the Southern Peru Earthquake of June 23, 2001. *Learning from Earthquakes* , pp. 3-11.
Georgia DOT. (2012, November 30). *Basic Drawings.* Retrieved January 28, 2013, from GDOT: http://www.dot.ga.gov/doingbusiness/PoliciesManuals/roads/Pages/BasicDrawings.aspx
Kane, K. M. (2013). *Response of Deep Foundations to Seismic Loads in Alabama.* Auburn University, Auburn.
Law, J. D., & Marshall, J. D. (2013). *Update of Bridge Design Standards in Alabama for AASHTO LRFD Seismic Design Requirements.* Auburn, AL: Auburn University.
Missouri DOT. (2002). *Bridge Design Manual Section 6.1.* Missouri Department of Transportation.
Missouri DOT. (2009, January). *Bridge Standard Drawings - Bearings.* Retrieved January 28, 2013, from MoDOT: Business with MoDOT: http://www.modot.org/business/standard_drawings2/documents/brg05_ptfe_psi_4stp.pdf
North Carolina DOT. (2012, October 16). *TFE Bearing Details.* Retrieved January 31, 2013, from Connect NCDOT: https://connect.ncdot.gov/resources/Structures/Pages/Design-Manual.aspx
Oliver, R. S. (1999). *Rapid Replacement/Rehabilitation of Bridge Decks.* Auburn, AL: Auburn University.
Oregon DOT. (2012, December). *Bridge Design and Drafting Manual.* Retrieved January 28, 2013, from OREGON.gov: http://www.oregon.gov/ODOT/HWY/BRIDGE/docs/bddm/dec-2012_finals/section_1-2004_rev_dec-2012.pdf
PEER. (2010). *PEER Ground Motion Database*. Retrieved September 20, 2013, from PEER Ground Motion Database: http://peer.berkeley.edu/peer_ground_motion_database/spectras/21713/unscaled_searches/new
PTC. (2007). Mathcad. Needham, Massachusetts, USA.
Rodriguez-Marek, A. (2007). *DYNAMIC RESPONSE OF BRIDGES TO NEAR-FAULT, FORWARD DIRECTIVITY GROUND MOTIONS.* Pullman: Washington State Transportation Center.
South Carolina DOT. (2005, November 4). *Seismic Restrainer Details*. Retrieved January 28, 2013, from SCDOT: http://www.scdot.org/doing/technicalPDFs/bridgeDrawings/SeismicRestrainer.pdf

South Carolina DOT. (2006, April). *South Carolina Bridge Design Manual.* Retrieved January 28, 2013, from SCDOT:
http://www.scdot.org/doing/technicalPDFs/structuralDesign/Files/Chapter_21.pdf
South Carolina DOT. (2006, April). *South Carolina Bridge Design Manual.* Retrieved January 28, 2013, from SCDOT:
http://www.scdot.org/doing/technicalPDFs/structuralDesign/Files/Chapter_21.pdf
Steelman, J. S., Fahnestock, L. A., Filipov, E. T., LaFave, J. M., Hajjar, J. F., & Foutch, D. A. (2012, April 24). Shear and Friction Response of Non-Seismic Laminated Elastomeric Bridge Bearings Subject to Seismic Demands. *Journal of Bridge Engineering* , pp. 1-15.
Steelman, J. S., Fahnestock, L. A., Filipov, E. T., LaFave, J. M., Hajjar, J. F., & Foutch, D. A. (2012, April 24). Shear and Friction Response of Non-Seismic Laminated Elastomeric Bridge Bearings Subject to Seismic Demands. *Journal of Bridge Engineering* , pp. 1-15.
StructurePoint. (2012). *spColumn.* StructurePoint, LLC.
Tennessee DOT. (2010, November 1). *Standard Seismic Details*. Retrieved January 28, 2013, from Tennessee Department of Transportation:
http://www.tdot.state.tn.us/Chief_Engineer/engr_library/structures/stdenglishdrawings.htm
Tobias, D. H., Anderson, R. E., Hodel, C. E., Kramer, W. M., Wahab, R. M., & Chaput, R. J. (2008, August). Overview of Earthquake Resisting System Design and Retrofit Strategy for Bridges in Illinois. *Practice Periodical on Structural Design and Construction* , pp. 148-152.
USGS. (2013, May 17). *2008 Interactive Deaggregations*. Retrieved September 17, 2013, from USGS: https://geohazards.usgs.gov/deaggint/2008/
Utah Department of Transportation. (2010). *Full Depth Precast Concrete Deck Panel Manual.* UDOT.
Wight, J. K., & MacGregor, J. G. (2009). *Reinforced Concrete Mechanics and Design.* Saddle Bridge: Prentice Hall.
Wight, J. K., & MacGregor, J. G. (2009). *Reinforced Concrete: Mechanics and Design.* Upper Saddle River, NJ: Pearson Prentice Hall.